

**MODELING AND OPTIMIZATION OF
SYSTEMS FOR NUTRIENT RECOVERY FROM
LIVESTOCK WASTE**

EDGAR MARTÍN HERNÁNDEZ

A dissertation submitted for the degree of
DOCTOR IN CHEMICAL SCIENCE AND TECHNOLOGY

at the
UNIVERSIDAD DE SALAMANCA



**VNiVERSiDAD
D SALAMANCA**

CAMPUS OF INTERNATIONAL EXCELLENCE

Academic advisor: Mariano Martín Martín

Programa de Doctorado en Ciencia y Teconología Química

Departamento de Ingeniería Química y Textil

Universidad de Salamanca

February 2022



El Dr. D. Mariano Martín Martín, Profesor Titular de Universidad del Departamento de Ingeniería Química y Textil de la Universidad de Salamanca

Informa:

Que la memoria titulada: "Modeling and optimization of systems for nutrient recovery from livestock waste", que para optar al Grado de Doctor en Ciencia y Tecnología Química con Mención Internacional presenta **D. Edgar Martín Hernández**, ha sido realizada bajo nuestra dirección dentro del Programa de Doctorado Ciencia y Tecnología Químicas (RD 99/2011) de la Universidad de Salamanca, y que considerando que constituye un trabajo de tesis.

Autoriza:

Su presentación ante la Escuela de Doctorado de la Universidad de Salamanca, mediante el formato de compendio de publicaciones.

Y para que conste a los efectos oportunos, firmo la presente en Salamanca, a 01 de diciembre de 2021.

Fdo: Mariano Martín Martín

A mi familia, y a todos los que por mi vida pasaron.

*Non exiguum temporis habemus, sed multum perdimus.
Satis longa vita et in maximarum rerum consummationem
large data est, si tota bene collocaretur;
sed ubi per luxum ac neglegentiam difflit,
ubi nulli bonae rei impenditur,
ultima demum necessitate cogente quam ire non
intelleximus transisse sentimus.*

— Lucius Annaeus Seneca, De brevitate vitae.

*No tenemos un tiempo escaso, sino que perdemos mucho.
La vida es lo bastante larga para realizar las mayores empresas,
pero si se desparrama en la ostentación y la dejadez,
donde no se gasta en nada bueno, cuando al final
nos acosa el inevitable trance final, nos damos cuenta
de que ha pasado una vida que no supimos que estaba pasando.*

— Lucius Annaeus Seneca, De la brevedad de la vida.

ACKNOWLEDGMENTS / AGRADECIMIENTOS

El desarrollo de esta tesis ha sido un proceso emocionante del que han formado parte muchas personas. Le estoy enormemente agradecido a todas ellas, a las que intentaré mencionar en las siguientes líneas. Sin embargo, si me olvido de alguien, le ruego que acepte mis más sinceras disculpas, pero que tenga por seguro que le estoy tan agradecido como a las que aquí se mencionan.

Me gustaría comenzar por mi director de tesis, el Dr. Mariano Martín, por haber hecho posible desarrollar este trabajo que no solamente se compone de los documentos que aquí se presentan, si no también de múltiples experiencias, viajes y encuentros cuyo valor es incommensurable. Igualmente, me gustaría agradecer al Dr. Gerardo Ruiz Mercado, de la U.S. Environmental Protection Agency, y al Prof. Victor M. Zavala, de la Universidad de Wisconsin-Madison, por haber contribuido en gran medida al desarrollo de este trabajo.

No puedo dejar de mencionar a los miembros (y sobre todo amigos) del grupo PSEM3 de la Universidad de Salamanca que me han acompañado durante este emocionante camino, Antonio, Manu, Borja, Lidia, Guillermo, y a nuestras nuevas (y no tan nuevas) incorporaciones, Carlos, Sofía y Elena. De manera especial, también me gustaría agradecer a Clara y Enrique, pues sus propios trabajos han contribuido a desarrollar esta tesis. Y por su puesto, a todos aquellos que nos visitaron a lo largo de estos años, y que espero encontren en Salamanca un lugar acogedor al que volver cuando lo deseen, César, Juan, Salvador, Gabriel, Valentina, Thalles y Javier.

An important piece of this thesis is the collaboration with Dr. Gerardo Ruiz Mercado, to whom I am very grateful for the opportunity of collaborate with him and the U.S. Environmental Protection Agency, and for welcoming me during my time in Cincinnati. During this time I could meet some of the most kind people, who were a great support and became good friends, Marco, Gulizhaer, Jose, and Jessica. I also want to show my gratitude to Apoorva and Yicheng, who were graduate students at UW-Madison at the same time as I was, for the wonderful works I could collaborate with you, and for your contributions to this thesis and to my Ph.D. journey. También quiero mostrarle mi agradecimiento a Rodrigo y Claudio, que me recibieron cálidamente en el CIPA durante mi viaje a Chile en los albores de esta tesis.

Tan importante como los agradecimientos a aquellos que forman parte de la academia son aquellos dirigidos a aquellos que desde fuera apoyan

esta empresa y, sean conscientes de ello o no, también dejan su huella en este trabajo, particularmente a Cristina G., Ana, Cristina M., Joaquín, Dani, y Blanca, y a Teresa y a Cristina. También he de mencionar a Luismi, Miky y Tom, con los que junto a Cris pude compartir una gran estancia en Bélgica en los primeros pasos de esta tesis, y a Camila y Gonzalo, con los que poco después me encontré en Chile.

No puede faltar un especial agradecimiento a mis padres y a mi hermano, que son los que me han permitido estar aquí en el día de hoy. Finally, I feel the need to show a special appreciation to Evelyne, who appeared on this journey, and is part of it ever since.

Halifax (Canadá), 30 de octubre de 2021

ABSTRACT

Nutrient pollution of waterbodies is a major worldwide water quality problem. Excessive use and discharge of nutrients can lead to eutrophication of fresh and marine waters, resulting in environmental problems associated with algal blooms and hypoxia, public health issues related to the release of toxins, and freshwater scarcity.

Agricultural activities are one of the main contributors to anthropogenic nutrient releases. Focusing on the livestock industry, the nutrient releases, mainly phosphorus and nitrogen, result from the production of large amounts of organic waste. Particularly, the manure generated in the concentrated animal feeding operations(CAFOs) is a considerable challenge due to the high rates and spatial concentration of the organic waste generated. The abatement of nutrient releases from livestock facilities is a step to address the environmental problem of nutrient pollution.

This thesis aims at the holistic assessment of waste treatment processes and management practices for the effective recovery of nutrients from livestock waste. We have performed techno-economic assessments of phosphorus and nitrogen recovery technologies for livestock facilities to determine the systems which implementation in CAFOs is more viable, as well as the potential integration of nutrient recovery technologies with biogas production systems. Based on the information obtained in these studies, a geospatial evaluation of the impact of phosphorus recovery by deploying phosphorus recovery systems at CAFOs in the watersheds of the United States has been carried out. In addition, after establishing the most suitable type of processes for phosphorus recovery, a decision-making support tool for the selection of commercial phosphorus recovery technologies based on technical, economic, and environmental criteria of each CAFO has been developed. Finally, this tool has been used for the design and analysis of incentive policies to promote de deployment of phosphorus recovery processes at CAFOs, including the fair allocation of incentives in limited budget scenarios.

These studies are intended to contribute to the development and implementation of sustainable nutrient management strategies at livestock facilities, addressing one of the major water quality problems around the globe, and promoting the transition to a more sustainable paradigm for food production.

RESUMEN

La contaminación por nutrientes de las masas de agua es uno de los principales problemas de calidad del agua en todo el mundo. El uso excesivo de nutrientes da lugar a la eutrofización de aguas dulces y marinas, resultando en problemas medioambientales relacionados con la proliferación de algas y la hipoxia de las aguas, así como problemas de salud pública y escasez de agua potable. Las actividades agrícolas son uno de los principales contribuyentes a las emisiones antropogénicas de nutrientes. Si nos centramos en la industria ganadera, las liberaciones de nutrientes (principalmente fósforo y nitrógeno) son el resultado de la producción de grandes cantidades de residuos orgánicos. En particular, las deyecciones ganaderas provenientes de grandes instalaciones de ganadería intensiva son un reto de considerable importancia debido a las grandes cantidades de residuo generadas y su alta concentración espacial.

Esta tesis tiene como objetivo llevar a cabo una evaluación holística de los procesos de tratamiento y los procedimientos de gestión de residuos para la recuperación efectiva de nutrientes de los residuos ganaderos. Se han realizado estudios tecno-económicos de las tecnologías de recuperación de fósforo y nitrógeno con el fin de determinar los sistemas cuya implementación en las instalaciones ganaderas es más viable, así como la posible integración de estos sistemas con procesos de producción de biogás. A partir de la información obtenida en estos estudios, se ha realizado una evaluación geoespacial del impacto de la recuperación de fósforo en instalaciones ganaderas en las diferentes cuencas hidrográficas de Estados Unidos. Además, tras establecer el tipo de procesos más adecuados para la recuperación de fósforo, se ha desarrollado una herramienta de soporte a la toma de decisiones para la selección de tecnologías comerciales de recuperación de fósforo acorde a criterios técnicos, económicos y ambientales de cada instalación ganadera. Por último, esta herramienta se ha utilizado para el diseño y análisis de políticas de incentivos para promover la implementación de estos procesos en instalaciones de ganadería intensiva, incluyendo la distribución equitativa de incentivos en escenarios de presupuesto limitado.

Se pretende que estos estudios contribuyan al desarrollo y aplicación de estrategias de gestión de los nutrientes liberados por la industria ganadera, abordando uno de los principales problemas globales relacionados con la calidad del agua, y promoviendo la transición hacia un paradigma para la producción de alimentos más sostenible.

PUBLICATIONS

This thesis is based on the following publications:

CONTENTS

1	INTRODUCTION	1
1.1	Rationale: Overview of the nutrient pollution challenge	1
1.2	Approaches for processes modeling	7
1.2.1	Short-cut methods	7
1.2.2	Rules of thumb	7
1.2.3	Dimensionless analysis	7
1.2.4	Mechanistic models	8
1.2.5	Surrogate models	8
1.2.6	Experimental correlations	9
1.3	Approaches for decision-support systems	9
1.3.1	Multi-Attribute Decision Analysis (MADA)	10
1.4	Fairness metrics	16
1.5	Approaches for geospatial environmental assessment	17
1.6	Thesis outline	18
1.6.1	Part I - Phosphorus management and recovery	18
1.6.2	Part II - Nitrogen management and recovery	19
1.6.3	Part III - Nitrogen management and recovery	19
	Bibliography	20
2	OBJECTIVE	21
2.1	Scope and objectives of the thesis	21
2.1.1	Main objective	21
2.1.2	Specific objectives	21
I	PHOSPHORUS MANAGEMENT AND RECOVERY	
3	TECHNOLOGIES FOR PHOSPHORUS RECOVERY	25
3.1	Introduction	27
3.2	Process description	28
3.3	Modelling issues	29
3.3.1	Biogas production	30
3.3.2	Biogas purification	31
3.3.3	Electricity generation	31
3.3.4	Digestate conditioning	32
3.3.5	Solution procedure	52
3.4	Results	56
3.4.1	Mass and energy balances	57
3.4.2	Economic evaluation	59

3.4.3	Effect on the power, operating conditions and digestate treatment	62
3.5	Conclusions	63
	Nomenclature	64
	Acknowledgments	68
	Bibliography	68
4	GEOSPATIAL ASSESSMENT OF PHOSPHORUS RECOVERY THROUGH THE DEPLOYMENT OF STRUVITE PRECIPITATION SYSTEMS	69
4.1	Introduction	71
4.2	Methods	73
4.2.1	Spatial resolution	73
4.2.2	Assessment of anthropogenic phosphorus from agricultural activities	74
4.2.3	Thermodynamic model for precipitates formation	76
4.3	Results and discussion	84
4.3.1	Surrogate models to estimate the formation of precipitates from livestock organic waste	84
4.3.2	Phosphorus releases from cattle leachate potentially avoided via struvite formation	87
4.4	Conclusions	92
	Nomenclature	93
	Acknowledgments	94
	Bibliography	95
5	GEOSPATIAL ENVIRONMENTAL AND TECHNO-ECONOMIC FRAMEWORK FOR SUSTAINABLE PHOSPHORUS MANAGEMENT AT LIVESTOCK FACILITIES	97
5.1	Introduction	99
5.2	Methods	101
5.2.1	Environmental geographic information model	102
5.2.2	Techno-economic model	105
5.2.3	Multi-criteria decision model	111
5.2.4	Framework limitations	115
5.2.5	Case study	115
5.3	Results	117
5.3.1	Implementation of phosphorus recovery systems in the Great Lakes area	117
5.3.2	Economic results	120
5.4	Discussion	123
5.4.1	Economic implications	123
5.4.2	Phosphorus use efficiency	125
5.5	Conclusion	127

Acknowledgments	128
Bibliography	128
6 ANALYSIS OF INCENTIVE POLICIES FOR PHOSPHORUS RECOVERY	129
6.1 Introduction	131
6.2 Incentive policy assessment framework	132
6.2.1 Assessment of nutrient management systems	134
6.2.2 Environmental vulnerability to nutrient pollution . .	135
6.2.3 Multi-criteria decision analysis model for the assess- ment of nutrient management systems	136
6.2.4 Types of incentives considered	137
6.2.5 Scenarios description	138
6.2.6 Study Region - The Great Lakes area	138
6.3 Results and discussion	139
6.3.1 Single incentives	139
6.3.2 Combined effect of incentives for phosphorus and renewable electricity recovery	141
6.3.3 Environmental cost-benefit analysis	145
6.3.4 Fair distribution of incentives	147
6.4 Conclusions	150
Acknowledgments	151
Bibliography	151
II NITROGEN MANAGEMENT AND RECOVERY	
7 MULTI-SCALE TECHNO-ECONOMIC ASSESSMENT OF NITRO- GEN RECOVERY SYSTEMS FOR SWINE OPERATIONS	155
7.1 Introduction	157
7.2 Methods	158
7.2.1 Livestock waste	158
7.2.2 Nitrogen management systems assessment framework	159
7.2.3 Economic assessment	174
7.3 Results and discussion	175
7.3.1 Nitrogen flows and recovery efficiency	175
7.3.2 Economic assessment and scale-up	176
7.4 Conclusions	180
Acknowledgments	181
Bibliography	181
III INTEGRATION OF ANAEROBIC DIGESTION AND NUTRIENT MANAGEMENT SYSTEMS	
8 OPTIMAL TECHNOLOGY SELECTION FOR THE BIOGAS UP- GRADING TO BIOMETHANE	185
8.1 Introduction	187

8.2	Methodology for process design	189
8.3	Process design	190
8.3.1	Technology screening	190
8.3.2	Mathematical modelling	192
8.3.3	Selection of optimal configurations	195
8.3.4	Superstructure configuration	197
8.3.5	Economic evaluation	197
8.4	Results	198
8.4.1	Biogas composition	198
8.4.2	Selection of technology	199
8.4.3	Estimation of production and investment costs	199
8.4.4	Comparison with renewable-based hydrogenation processes	202
8.4.5	Plant scale-up study	204
8.5	Conclusions	206
	Nomenclature	208
	Acknowledgments	211
	Bibliography	211
9	CONTRIBUTIONS AND FUTURE DIRECTIONS	213
9.1	Contributions	213
9.2	Directions for future work	216

IV APPENDIX

A	APPENDIX A: SUPPLEMENTARY INFORMATION OF CHAPTER 3	221
A.1	Biogas production	222
A.2	H ₂ S removal	225
A.3	CO ₂ , NH ₃ and H ₂ O removal (PSA)	225
A.4	Brayton cycle	225
A.5	Rankine cycle	226
	Bibliography	229
B	APPENDIX B: SUPPLEMENTARY INFORMATION OF CHAPTER 4	231
B.1	Cattle organic waste composition	231
B.2	Distribution functions of elements from cattle waste	231
B.3	Thermodynamic modeling of the carbonates system	235
B.4	Surrogate models to estimate precipitates formation from livestock waste	238
B.4.1	Influence of magnesium	238
	Bibliography	241
C	APPENDIX C: SUPPLEMENTARY INFORMATION OF CHAPTER 5	243
C.1	Environmental geographic information model	243
C.1.1	Trophic State Index	243
C.1.2	Balance of anthropogenic phosphorus releases	244

C.1.3	Phosphorus in soils	245
C.2	Framework development	247
C.2.1	Data entry	247
C.2.2	Techno-economic model	247
C.3	Multi-criteria decision model	259
C.4	Description of the Great Lakes area	260
	Bibliography	261
D	APPENDIX D: SUPPLEMENTARY INFORMATION OF CHAPTER 7	263
D.1	Modeling details of nitrogen recovery processes	263
D.1.1	Anaerobic digestion	263
D.1.2	Biogas conditioning	264
D.1.3	Digestate solid-liquid separation	266
D.1.4	Struvite production: Multiform system	268
D.1.5	MAPHEX	270
D.1.6	Transmembrane chemisorption	270
D.1.7	Ammonia evaporation	275
D.1.8	Stripping in packed tower	276
D.1.9	Acidic scrubbing	278
D.2	Capital and operating expenses	281
D.3	Processing cost	283
	Bibliography	285
E	APPENDIX E: SUPPLEMENTARY INFORMATION OF CHAPTER 8	287
E.1	Literature review	287
E.2	Modelling approach	288
E.2.1	Amines	288
E.2.2	PSA	292
E.2.3	Membranes	294
E.3	Economic evaluation	296
E.4	Scaling-up study	297
	Bibliography	298

LIST OF FIGURES

Figure 1.1	Main flows of nutrients released by anthropogenic activities.	2
Figure 1.2	Main topics covered in this work.	6
Figure 1.3	Classification of MCDA methods.	10
Figure 3.1	Flowsheet for the production of power and fertilizers.	28
Figure 3.2	Scheme of the filter.	33
Figure 3.3	Scheme of the coagulation process.	37
Figure 3.4	Scheme for the centrifugation treatment.	43
Figure 3.5	Scheme for the FBR system.	47
Figure 3.6	Scheme for the CSTR based struvite production system.	47
Figure 3.7	Units cost distributions for cattle, pig, poultry and sheep manure treatment (ST: steam turbine, GT: gas turbine, HX: heat exchangers, FBR: fluidized bed reactor).	61
Figure 3.8	Operation cost distribution for cattle, pig, poultry and sheep manure treatment.	62
Figure 4.1	Flowchart of the proposed algorithm to solve the thermodynamic model for the formation of precipitates in cattle organic waste.	82
Figure 4.2	A solution procedure to evaluate the influence of the cattle waste composition variability in the formation of struvite.	83
Figure 4.3	Comparison between experimental results reported by Zeng and the results provided by the model developed in this work.	83
Figure 4.4	Influence of magnesium and calcium in struvite precipitation.	88
Figure 4.5	Techno-ecological synergy (TES) metric values for HUC8 watersheds. Red indicates watersheds with unbalanced agricultural phosphorus releases, and blue indicates watersheds with balanced agricultural phosphorus releases. White indicates watersheds with not available data.	89
Figure 4.6	Phosphorus releases avoided through struvite production for the different scenarios considered. Darker colors represent larger phosphorus recovery	90

Figure 5.1	Structure of the COW2NUTRIENT decision support framework for the assessment and selection of phosphorus recovery systems.	102
Figure 5.2	Process flowsheet for manure management and phosphorus recovery stages included in COW2NUTRIENT.	106
Figure 5.3	Flowsheet for the MCDA model.	113
Figure 5.4	Distribution of the phosphorus recovery systems selected for the CAFOs in the Great Lakes area. The boxplots represent the distribution of CAFO sizes in each studied state.	119
Figure 5.5	Capital expenses for deploying phosphorus recovery systems in the studied CAFOs. The dots represent the P recovery technologies installed in the studied CAFOs.	122
Figure 5.6	Operating expenses for deploying phosphorus recovery processes in the studied CAFOs. The dots represent the P recovery technologies installed in the studied CAFOs.	123
Figure 5.7	Net revenue from the phosphorus recovery processes selected in the studied CAFOs. The dots represent the P recovery technologies installed in the studied CAFOs.	124
Figure 6.1	Flowchart of the models for selection, sizing, and evaluation of nutrient recovery systems at livestock facilities.	133
Figure 6.2	Flowchart of the processes evaluated for livestock waste management.	134
Figure 6.3	States of the Great Lakes region studied in this work.	139
Figure 6.4	Distribution of profitable phosphorus recovery processes in the Great Lakes area for the scenarios considering phosphorus credits and renewable energy credits. The box-plots represent the distribution of CAFOs size in each state.	142
Figure 6.5	Economic evaluation of P recovery processes for the different incentives scenarios studied	144

Figure 6.6	Comparison of the total cost of phosphorus recovery for each scenario assessed and the environmental remediation cost due to phosphorus releases. REC denotes the electricity incentive values considered in USD/MWh, and PC denotes the value of phosphorus credits in USD/kg _P recovered. The red dotted line represents the economic losses due to phosphorus releases to the environment.	146
Figure 6.7	Allocation of incentives for achieving the economic neutrality of nutrient recovery systems minimizing the total cost of incentives.	148
Figure 6.8	Distribution of incentives considering the Nash allocation scheme. Scenarios assuming available incentives equal to the 10%, 30%, 50%, 70%, and 100% of the incentives needed to cover the economic losses of unprofitable P recovery systems in the Great Lakes area are illustrated.	149
Figure 7.1	Flowchart of the processes assessed for the processing of livestock waste	160
Figure 7.2	Nitrogen recovery systems assessed in the techno-economic assessment.	164
Figure 7.3	Tower flooding capacity correlation considering packing pressure drop.	171
Figure 7.4	Relative flows of inorganic nitrogen in the studied processes. Since a fraction of organic nitrogen in swine manure is mineralized after the anaerobic digestion of the waste, the 100% refers to the inorganic nitrogen in digestate.	177
Figure 7.4	Relative flows of inorganic nitrogen in the studied processes. Since a fraction of organic nitrogen in swine manure is mineralized after the anaerobic digestion of the waste, the 100% refers to the inorganic nitrogen in digestate.	178
Figure 7.5	Processing cost for different livestock facility sizes, including the cost of pretreatment and AD stages. .	179
Figure 8.1	Scheme of the methodology followed to determine the optimal biogas upgrading technology.	190
Figure 8.2	Scheme of the proposed superstructure for biogas upgrading into biomethane.	198
Figure 8.3	Breakdown of biomethane production costs for each residue analyzed.	201

Figure 8.4	Relation between population and food waste produced in Spain.	206
Figure 8.5	Scale-up in the investment costs for municipal food waste.	207
Figure 8.6	Scale-up in the investment costs for cattle manure. .	208
Figure B.1	Kernel density estimation (red dashed line) and probability density distribution (blue solid line) for the evaluated components in cattle organic waste. .	234
Figure B.2	Evolution phosphorus as phosphate fraction recovered as struvite and calcium fraction recovered as precipitates along Mg^{2+}/PO_4^{3-} molar ratio values considering 50 different composition data sets. . . .	238
Figure B.3	Evolution of phosphorus as phosphate fraction recovered as struvite and calcium fraction recovered as precipitates along Ca^{2+}/PO_4^{3-} molar ratio values considering 50 different composition data sets. . . .	239
Figure B.4	Evolution of phosphorus as phosphate fraction recovered as struvite and calcium fraction recovered as precipitates among alkalinity values considering 50 different composition data sets.	240
Figure C.1	Trophic State Index in the contiguous US HUC8 watersheds	244
Figure C.2	Balance of anthropogenic phosphorus releases in the contiguous US at a HUC8 spatial resolution . .	245
Figure C.3	Soil Fertility Level in the contiguous US at a HUC8 spatial resolution	247
Figure C.4	Adequate manure properties for anaerobic digestion. Adapted from AgSTARHandbook	248
Figure C.5	Correlations between AD capital and O&M costs, and the number of cattle in the livestock facility. .	250
Figure C.6	Estimated screw press investment costs (USD) as a function of the size.	252
Figure C.7	Estimated capital and operating costs for screw press units.	253
Figure C.8	Flowsheets of the nutrient recovery systems considered in the proposed framework. a: Multiform, b: Crystalactor, c: Ostara Pearl, d: Nuresys, e: P-RoC, f: MAPHEX.	254
Figure C.9	Estimated investment costs for a non-jacketed vessel, based on data from CAPCOST (CAPCOST).	257
Figure C.10	Estimated investment costs for conveyor dryer unit.	258

Figure C.11	Example of feasible weights space for a three criteria problem considering ranking of criteria. Figure adapted from tervonen_implementing_2007	259
Figure D.1	Correlations between AD capital and O&M costs, and the number of cattle in the livestock facility. Data from USDA_OM	265
Figure D.2	Estimated screw press investment costs (USD) as a function of the size.	267
Figure D.3	Estimation of Liquid-Cel TM 14x40 membrane module cost.	271
Figure D.4	CAPEX and OPEX of the assessed nitrogen recovery technologies, including the cost of anaerobic digestion stage.	281
Figure D.5	CAPEX and OPEX of the assessed nitrogen recovery technologies, excluding the cost of anaerobic digestion stage.	282
Figure D.6	Processing cost for different livestock facility sizes, excluding the cost of anaerobic digestion stage.	283
Figure E.1	Scheme of the proposed superstructure for biogas upgrading into biomethane.	289

INTRODUCTION

1.1 RATIONALE: OVERVIEW OF THE NUTRIENT POLLUTION CHALLENGE

Human population is experiencing a continuous growth since the end of the Black Death in the XIV century (**biraben1980essay**), which is at 7.8 billion as of 2020, and it is estimated to be at 9.7 billion and 10.9 billion by 2050 and 2100 respectively (**UNPopulationProspects**). Population growth demands increasing amounts of food, which in turn requires an efficient food production system to ensure global food security. In this context, the development of different technical advancements has been a key factor to increase the productivity of the food production system. Notably, crucial developments were achieved in the late modern period¹, including the commercial production of phosphate in 1847 (**Samreen2019**), the development of the Haber-Bosch process for the production of synthetic nitrogen-based fertilizers in 1913 (**smil1999detonator**), the mechanization of agriculture, and the development of the modern intensive farming in the XX century (**constable2003century; nierenberg2005happier**).

Despite these advancements have increased the productivity of agriculture and farming industries, multiple environmental impacts associated with them emerge, including water scarcity, greenhouse gases emissions, nutrient pollution of waterbodies, and soil degradation, among others. These threats must be carefully addressed in order to avoid the depletion of natural resources and reach a sustainable food production system.

Focusing on the impacts derived from agriculture and farming on the nutrient cycles, it can be observed that the natural cycles of phosphorus and nitrogen have been altered by these activities (**Bouwman2009**). Large amounts of nutrients are released into the environment in the form of synthetic fertilizers and livestock manure. Nitrogen and phosphorus are accumulated in soils, creating a nutrient legacy that is further transported to waterbodies by runoff. This process results in the eutrophication of waterbodies, which can lead to algal bloom episodes. Algal blooms are events resulting from the rapid growth of algae in a water system which

¹ The terminology used in this dissertation for the periodization of human history follows the English-language historiographical approach. It should be noted that the late modern period is referred to as the contemporary period in the European historiographical approaches.

can be promoted by an excess of nutrients in water. These episodes alter the normal functioning of aquatic ecosystems, since they cause hypoxia as a consequence of the aerobic degradation of algal biomass by bacteria. Moreover, some species of algae that cause algal blooms can release toxins into the water systems. The main flows of nutrient releases into the environment by anthropogenic activities are shown in Figure 1.1.

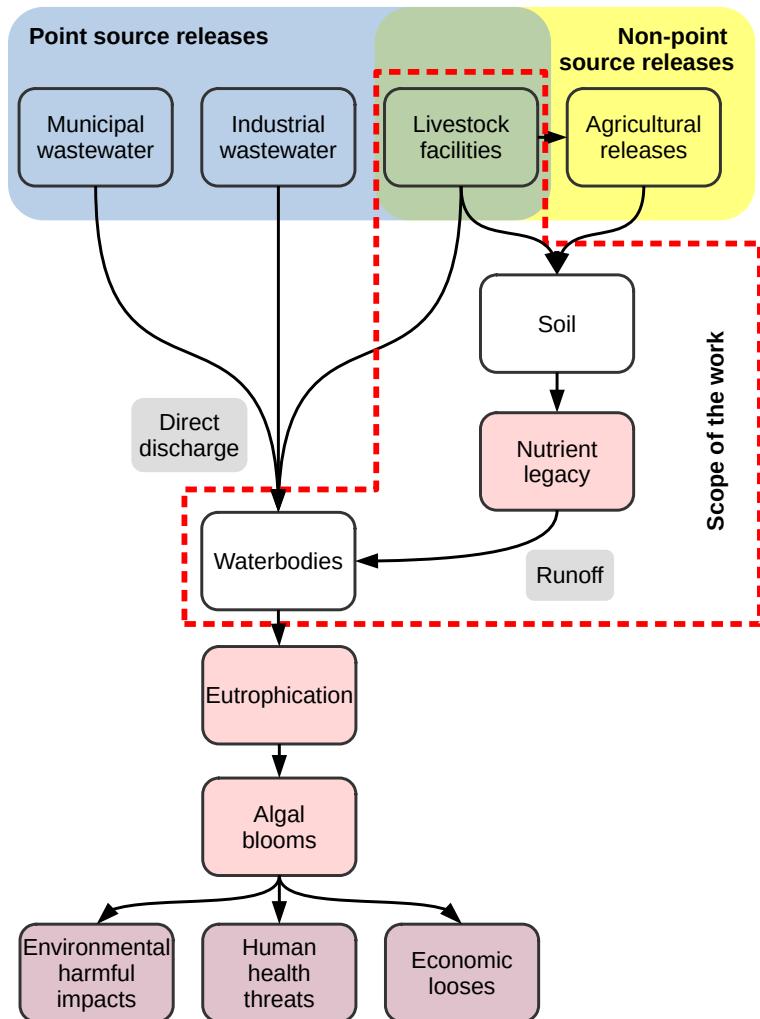


Figure 1.1: Main flows of nutrients released by anthropogenic activities.

In addition to the environmental problems, the use of nutrients for food production also raises geopolitical concerns since phosphorus is one of the most sensitive elements to depletion. Phosphorus is a non-renewable material whose reserves are expected to be depleted in the next 50 to 100 years. Moreover, no substitute material is currently known ([cordell2009story](#)). Conversely, synthetic nitrogen can be produced using the atmospheric N_2

as raw material through the Haber-Bosh process. However, nowadays this process relies on non-renewable energy sources, and therefore the production of synthetic nitrogen-based fertilizers is dependent on non-renewable resources as well.

Considering the two challenges described, i.e., nutrient pollution of waterbodies as a consequence of agricultural and farming activities, and the current dependency on non-renewable resources for the production of synthetic fertilizers, nutrient recovery and recycling is not only a desirable but also a necessary approach to develop a sustainable agricultural paradigm and ensure the global food security.

Attending to the nutrient releases from intensive livestock farming facilities, known as concentrated animal feeding operations (CAFOs)², several manure management techniques are currently used. The land application of manure is a common technique that allows the recycling of nutrients as fertilizers for crops (**Kellogg 2010**). However, the increase of intensive livestock farming generates vast amounts of waste generated by CAFOs, e.g., each adult cow generates between 28 and 39 kg of manure per day, and each adult pig generates around 11.5 kg of manure per day (**USDA Handbook**). Manure processing is commonly based on the separation of liquid and solid phases. The liquid phase can be treated in anaerobic and/or aerobic lagoons for organic matter and pathogens removal, as well as odor control (**tilley2014compendium**). The obtained liquid effluent can be used for irrigation and nutrient supplementation of crops. The solid phase can be composted for the degradation of organic matter and pathogens removal, resulting in a solid material called compost with a larger amount of nitrogen and phosphorus available for plants, which is the result of the mineralization of nutrients previously contained in organic compounds. Since compost is also a good source of organic matter for crops, it is a valuable material suitable for sale (**tilley2014compendium**). However, both materials, the liquid effluent obtained from the lagoons and compost, are too bulky to be economically transported to nutrient deficient locations (**burns2002phosphorus**). As a result, livestock waste is usually spread in the surroundings of livestock facilities, at a detrimental cost of environment. This results in the gradual build-up of nutrients in soils, which might lead to the harmful environmental impacts previously described.

A promising alternative for abating nutrient releases and reducing the environmental footprint of livestock industry is the implementation of processes for the recovery of phosphorus and nitrogen at CAFOs. At the

² CAFO is a regulatory term defined by the U.S. Environmental Protection Agency for large facilities where animals are kept and raised in confined situations (**animal_unit_definition**). This term is used in this dissertation to denote the intensive livestock farming facilities studied.

time, that valuable nutrient-rich materials are obtained for the redistribution of phosphorus and nitrogen to nutrient-deficient areas. There exist a number of processes for nutrient recovery from livestock waste, which can be differentiated into those technologies oriented to phosphorus recovery, including struvite precipitation, calcium-based precipitates production, coagulation-flocculation, electrochemical processes, and systems based on solid-liquid separation; and processes focused on nitrogen recovery, such as stripping, membrane separation, waste drying coupled with ammonia scrubbing, and solid-liquid separation processes. We note that anaerobic digestion is an additional process that can be integrated for manure treatment if the generation of biomethane is pursued, and for increasing the amount of recoverable nutrients through the partial mineralization of nutrients contained in organic compounds. It must be noted that only phosphorus and nitrogen in inorganic compounds can be taken by plants, and therefore the recovery of inorganic nutrients will be the target of the processes studied in this thesis.

The multiple processes for the recovery of phosphorus and nitrogen from livestock waste differ in aspects such as recovery efficiency, processing capacity, capital and operating costs, and products obtained. Therefore, a detailed analysis of each CAFO must be performed in order to select the optimal nutrient recovery system attending to type factors such as the type and amount of waste to be processed, the environmental vulnerability to eutrophication of each region, the current or potential installation of anaerobic digestion systems, etc. Additionally, in the decision-making process these factors have to be prioritized, i.e., sorted by relevance, to select the most suitable nutrient recovery system for each particular facility. As an example, more economical processes for nutrient recovery, whose recovery efficiencies are typically lower, could be installed in regions with a low risk of eutrophication. Conversely, regions at severe eutrophication risk require highly efficient nutrient recovery systems that may incur in larger investment and operating expenses.

Attending to the regulatory aspect, nowadays most of the efforts for abating of nutrient releases into the environment and mitigating the eutrophication of waterbodies are focused on the limitation of fertilizer application in croplands. The application of fertilizer and manure for nitrogen supplementation in the European Union (EU) is currently regulated by the Nitrates Directive (91/676/EEC) (**GRIZZETTI2021102281**). Regarding the limitations for phosphorus application, these are defined at national level. Several European countries have implemented phosphorus application standards based on the different crops and materials used as fertilizers, being generally more restrictive in Northwestern Europe (**amery2014agricultural**).

In sum, it can be observed that nutrient application is limited either in the form of synthetic fertilizers or manure application. However, at present there is a lack of regulation regarding livestock waste treatment (**Piot_Lepetit2012**). In this regard, new efforts to promote the production and adoption of bio-fertilizers obtained from organic waste are being performed through the development of the "Integrated Nutrient Management Plan" (INMAP), which is part of the EU Farm-to-Fork strategy and part of the Circular Economy Action Plan. INMAP should propose actions to promote the recovery and recycling of nutrients, as well as the development of markets for recovered nutrients (**ESSP2021; CircularEconomyActionPlan**). In this regard, a new regulation for fertilizer products has been released in 2019 (EU 2019/1009), moving struvite and other biofertilizers from the category of waste to fertilizers, establishing a regulatory framework for their use and trade.

In the United States, CAFOs are regulated under the Clean Water Act as point source waste discharges. This regulation sets the need of permits for discharging pollutants to water, which are called National Pollutant Discharge Elimination System (NPDES) permits, including nitrogen and phosphorus releases. These permits must include the necessary provisions for avoiding the harmful effects of the discharges on water and human health (**NPDE_basics**). The development and implementation of a Nutrient Management Plan (NMP) is a required element to obtain an NPDES permit. This document must identify the management practices to be implemented at each CAFO to protect natural resources from nutrient pollution. Land spreading of manure can also be regulated by the NPDES permits, establishing soil nutrient concentration limits and the yearly schedule for manure application. However, no specific methods or processes for waste treatment are defined under federal regulation (**NPDESforCAFO**). Regarding the use of the recovered nutrients, products obtained from nutrient recovery processes could be classified as waste by the Clean Water Act, preventing the application of these materials on croplands (**NACWA503**). However, the U.S. Environmental Protection Agency (US EPA) determined that, although these products could not be directly applied to land under the current regulation, they can be sold as a commodity to be outside of the Clean Water Act restrictions coverage (**CNP503**). Moreover, US EPA acknowledges that highly refined and primarily inorganic products (such as struvite) could be outside of the scope of these restrictions (**CNP503**). Nevertheless, further regulation is needed for defining the products obtained from nutrient recovery processes and to clearly state the conditions for their use as fertilizers on croplands.

Considering the previously described aspects, we note that the regulation of the products obtained from nutrient recovery systems is not

totally developed yet either in the European Union and the United States, although important efforts are being performed in order to set a comprehensive regulatory framework for the recycling of phosphorus and nitrogen. Furthermore, no regulation regarding the implementation of nutrient recovery processes has been developed. However, both regions have developed previous programs to study and promote the implementation of other technologies for the treatment of livestock and other organic waste. Particularly, the deployment of anaerobic digestion systems have received a considerable support from governmental agencies, resulting in programs such as AgSTAR in the US (**AgSTARProgram**), and BiogasAction (**BiogasAction**) and BIOGAS³ (**BIOGAS₃PROJECT**) in Europe, among many others. These programs could be a guideline for the development of nutrient recovery plans at CAFOs.

An overview of the main topics studied in this thesis can be observed in Figure 1.2. This work pretends to analyze strategies for promoting effective nutrient recycling addressing studies on the technical, environmental and economic dimensions involved, pursuing the development of sustainable food production paradigm.

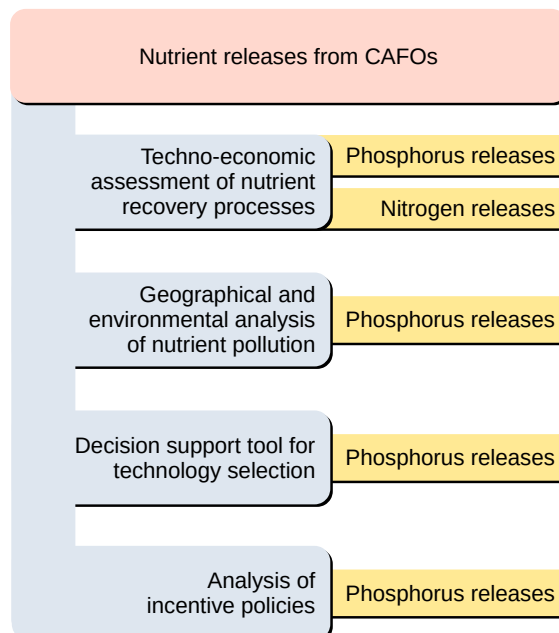


Figure 1.2: Main topics covered in this work.

1.2 APPROACHES FOR PROCESSES MODELING

Process modeling, defined as the mathematical modeling and simulation of systems, falls under the scope of the Process System Engineering (PSE) discipline. These systems include physical, chemical, and/or biological operations. Process modeling forms the foundation for other activities involved in the scope of PSE, including process design, optimal scheduling and planning of the systems operations, and process control (**STEPHANOPOULOS20114272**).

Different modeling techniques have been developed to mathematically describe and represent systems from different domains, including but not limited to the chemical, biochemical, agrochemical, food, and pharmaceutical domains of engineering (**PISTIKOPOULOS2021107252**). An overview of the main modeling techniques is shown in the next sections based on the classification proposed by **MARTIN201216**.

1.2.1 *Short-cut methods*

These types of models are the most basic approach to process modeling. They are based on mass, energy, and momentum balances, and can be embedded in other models, such as supply chain models.

1.2.2 *Rules of thumb*

This approach is based on industrial operational data. It provides typical ranges for operating and design values, reflecting the actual parameters of the systems modeled. However, the use of these models is constrained by the availability of data. Compendiums of rules of thumb for different systems can be found in **copper2005chemical; hall2012rules; sadhukhan2014biorefineries**.

1.2.3 *Dimensionless analysis*

This methodology is based on dimensionless groups that describe the performance of a particular system. These models are able to capture the physical meaning of the modeled processes, and they are specially useful to capture scale-up and scale-down issues (**szirtes2007applied**).

1.2.4 Mechanistic models

This approach relies on first principles for systems modeling, as short-cut models. However, mechanistic models rely in more detailed first principles such as the underlying chemistry, physics or biology that governs the behavior of a particular system. Chemical ([loeppert1995chemical](#)) and phase ([brignole2013phase](#)) equilibrium models, kinetic models ([buzzi2009kinetic](#)), population balances ([ramkrishna2000population](#)), and computer fluid dynamics (CFD) ([anderson1995computational](#)) fall under this category.

1.2.5 Surrogate models

These models aim at developing simplified models from data obtained from rigorous mechanistic models. This approach is widely used for embedding system models into other applications such as process control or supply chain design. Surrogate models building has been systematized into four steps, i.e., design of experiments (DOE), running the rigorous models at the sampling points designated by the DOE, construction of the surrogate model, and validation of the model obtained ([queipo2005surrogate](#)).

Polynomial regression models, in which the relationship between the variables is expressed using a polynomial function, are one of the most basic types of surrogate models. In the case of polynomial regression models involving multiple variables, the optimal variables to be addressed within the pool of variables considered can be determined by using machine learning-based tools such as ALAMO ([wilson2017alamo](#)), ensuring an optimal trade-off between model accuracy and complexity. Other types of surrogate models are Kriging models, which estimate the relationship between variables as a sum of a linear model and a stochastic Gaussian function representing the fluctuations of data ([quirante2015rigorous](#)), and artificial neural networks (ANN), which are based on generating an input signal as the summation of all the weighted inputs, which is through nodes containing a transfer function. Nodes are connected by edges with assigned weights that adjust the signals transmitted between nodes. Nodes are structured in layers, in a way that nodes receive signals from nodes of the preceding layer, and if the output of the node is above a threshold value defined by the transfer function, sends the output signal to the next layer ([himmelblau2000applications](#)).

1.2.6 *Experimental correlations*

As the surrogate models, experimental correlations are models built using data of the systems represented, but conversely to those one, experimental correlations are built using data from experimental results. Similarly to the rules of thumb, the accuracy of these models is limited by the availability of data, and they are only applicable to the range of operating conditions of the data used for constructing the model.

1.3 APPROACHES FOR DECISION-SUPPORT SYSTEMS

Decision-making activities require to analyze multiple relevant criteria for each course of action. Since criteria often conflict each other, each decision-making process requires the balancing of criteria, prioritizing some criteria over another through the use of some criteria weighting scheme. This procedure requires managing a vast amount of information of conflicting nature, leading to a complex decision-making process. Therefore, different approaches generally called multiple-criteria decision analysis (MCDA) have been developed to explicitly structure and solve decision problems. MCDA aim is to integrate criteria assessment with value judgment to analyze and compare the different available alternatives, identifying the best solution for the specific decision-making context studied. However, it must be highlighted that a certain degree of subjectivity might exist in several steps of the MCDA, such as the choice of the set of criteria considered relevant for a particular problem. Therefore, the solution proposed by any MCDA approach must be analyzed considering the assumptions made for building the problem. In sum, MCDA seeks to structure problems with multiple conflicting criteria, and providing justifiable and explainable solutions to guide decision-makers facing such problems. The solution of a multiple-criteria decision-making problem can be defined as a unique solution representing the most suitable alternative from the set of potential alternatives, or as a subset of satisfactory alternatives (**belton2002multiple**).

An MCDA problem can be articulated in different stages, starting with the problem definition and structuring. At this stage, the goals, constraints, and stakeholders comprising the problem are defined, as well as the different solution alternatives. Based on this information, a model can be built for the assessment and comparison of alternatives. This stage includes the definition of the relevant criteria used for alternatives comparison, their relative priority, and the system for criteria evaluation. Finally, the

information retrieved by the model can be used for making informed decisions.

Multi-criteria decision-making problems can be classified into Multi-Attribute Decision Analysis (MADA), which are discrete choice problems where the number of alternatives is finite, and Multi-Objective Decision Analysis (MODA), that are mathematical programming problems that consider infinite number of alternatives, as shown in Figure 1.3. However, we note that mathematical programming techniques are not limited to formulating and solving problems with infinite alternatives, but they can also be used for dealing with discrete decision-making problems ([giove2009decision](#)).

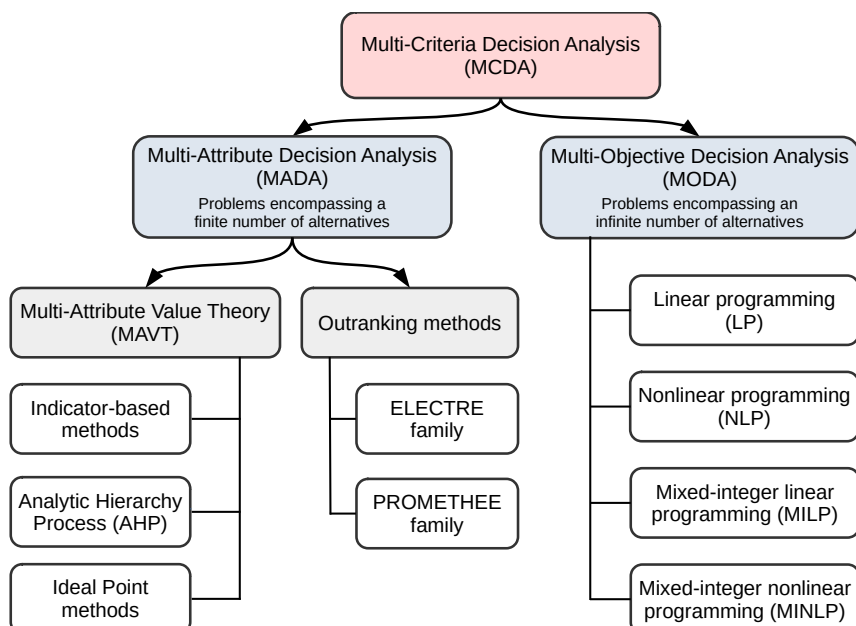


Figure 1.3: Classification of MCDA methods.

1.3.1 Multi-Attribute Decision Analysis (MADA)

In the case of problems consisting of a finite number of alternatives, the suitability of each alternative to the problem given can be measured through its performance according to the multiple criteria considered. A large number of MCDA approaches have been (and are currently being) developed for discrete choice problems, including methods based on value functions (Multi-Attribute Value Theory methods, MAVT) and outranking methods.

1.3.1.1 *Multi-Attribute Value Theory (MAVT)*

INDICATOR-BASED METHODS Multi-Attribute Value Theory (MAVT) approaches are based on an indicator-based methodology for alternatives comparison. The relevant criteria considered in the decision-making process are normalized to a common scale to allow criteria comparison using an utility or value function. A number of utility functions have been proposed in the literature, including standardization, min-max, and target utility functions (**HandbookCompositeIndicators**). The normalized criteria are weighted and aggregated to build a composite index, prioritizing some criteria over others. Different aggregation schemes have been proposed, providing different degrees of compensability between indicators, i.e. a deficit in one criteria can be fully, partially, or not compensated by a surplus in other criteria (**MarcoCinelli2020**). Additive weighting aggregation is a full compensatory method, while geometric and harmonic aggregation methods are partial compensation schemes. Other aggregation schemes include geometric averaging, which is a non-compensatory method, and the Choquet integral (**marichal2000determination**). The composite index obtained is a single numerical value that can be used to score and rank the proposed alternatives based on their suitability to the criteria considered.

A major source of uncertainty in indicator-based methods is the value of criteria weights. This issue can be addressed using the stochastic multi-criteria acceptability analysis (SMAA) method. SMAA is a sensitivity analysis method that addresses the uncertainty of criteria weights value exploring the feasible space of weights through the Monte Carlo method. Further, details about the SMAA approach can be found in **tervonen_implementing_2007**.

ANALYTIC HIERARCHY PROCESS (AHP) Analytic Hierarchy Process (AHP) decomposes the decision problem into multiple simpler sub-problems. These sub-problems are hierarchized and independently analyzed. The sub-problems are solved through the pairwise comparison of alternatives, obtaining numerical indexes that can be used to compare their performance. Finally a numerical weight (priority) is assigned to each element of the hierarchy, and they are used for aggregating the indexes obtained by each alternative at each element of the hierarchy in a final numerical value that can be used to score the overall performance of each alternative accordingly to the set of criteria considered (**saaty2000fundamentals**).

IDEAL POINT METHODS Ideal Point methods set an optimal solution, that represent a utopia point where all criteria values are optimal. The

performance of each alternative is evaluated through a composite index, that can be constructed using the MAVT approach. The alternatives are ranked based on their relative distance relative to the optimal solution. One of the most common Ideal Point methods is TOPSIS (**hwang1995multi**).

1.3.1.2 Outranking methods

Outranking methods are based on the pairwise comparison of the alternatives for each criterion considered, determining the preferred alternative for each of the criteria. Preference information about all criteria is aggregated to establish evidence for selecting one alternative over another. These methods indicate the dominance of one alternative over another, but they do not quantify the performance gap between the alternatives compared (**giove2009decision**). Some of the most popular outranking methods are ELECTRE I (**roy1968classement**), II (**roy1973methode**), and III (**roy1978electre**), and PROMETHEE (**vincke1985preference**).

1.3.1.3 Multi-Objective Decision Analysis (MODA)

Problems consisting of an infinite number of solutions require multi-objective mathematical programming (optimization) techniques to be solved. These problems are subjected to a number of equality and/or inequality constraints restricting the solutions that are feasible. The multiple conflicting criteria are combined in an objective function. This objective function represents the improving level of the criteria, and it will be minimized or maximized for selecting the best solution that represents the optimal trade-off between the different conflicting criteria (**giove2009decision**). Other approach for solving multi-objective mathematical programming problems is to set a priori targets for different criteria, or combinations of criteria, that are considered satisfactory, obtaining the problem solution by minimizing the deviations from these goals. Mathematical programming problems can be also classified according to the use of linear or nonlinear equations, and continuous and/or discrete variables (**giove2009decision**).

LINEAR PROGRAMMING (LP) Linear programming (LP) refers to those mathematical programming problems based on linear equations and continuous variables. A linear programming problem can be expressed as shown in Eq. 1.1, where x is a vector of dimension n , A is a mxn matrix, c is the n dimension vector of cost coefficients, and the right-hand side b is a vector of dimension m (**grossmann2021advanced**).

$$\begin{aligned}
 \min \quad & Z = c^T x \\
 \text{s.t.} \quad & Ax \leq b \\
 & x \geq 0
 \end{aligned} \tag{1.1}$$

The two most widely used methods to solve LP problems are the Simplex algorithm (**Dantzig1990**) and interior-point methods (**kantorovich1948newton**; **POTRA2000281**). The Simplex method is more efficient for solving problems with thousands of variables and constraints, while interior-point is more efficient on very large scale and sparse problems (**grossmann2021advanced**). These methods are implemented in solvers such as CPLEX (**cplex2009v12**), Gurobi (**gurobi**), or XPRESS (**xpress**).

NONLINEAR PROGRAMMING (NLP) Nonlinear programming (NLP) refers to those mathematical programming problems containing nonlinear equations, either in the constraints or in the objective function, and continuous variables. A nonlinear programming problem can be expressed as shown in Eq. 1.2, where x is an n dimension vector, $f(x)$ is the objective function of the problem, $h(x)$ is the set of equality constraints and $g(x)$ is the set of inequality constraints (**floudas1995nonlinear**).

$$\begin{aligned}
 \min \quad & f(x) \\
 \text{s.t.} \quad & h(x) = 0 \\
 & g(x) \leq 0 \\
 & x \in X \subseteq \Re^n
 \end{aligned} \tag{1.2}$$

Some of the most common algorithms to solve NLP problems are successive quadratic programming (SQP), reduced gradient algorithms, and interior point methods.

SQP algorithms are based on the solution of quadratic programming subproblems. Each subproblem optimizes a quadratic model of the objective function subject to linearized constraints. In each of the iterations a search direction is determined reducing some merit function to ensure problem convergence (**gill2005snopt**). SNOPT is a solver based on this method (**gill2005snopt**).

Reduced gradient methods consider a linear approximation of the constraints and eliminate variables to reduce the dimension of the problem. The resulting problem is solved by applying the Newton's method. In each of the iterations, the reduced gradient is calculated, the search direction is determined, and finally a line search is performed minimizing the objective

function. MINOS ([murtagh1983minos](#)) or CONOPT ([drud1985conopt](#)) are solvers based on this algorithm.

Interior point methods reformulate the original NLP problem by means of slack variables to replace the inequalities by equalities and the log-barrier function to handle the non-negativity of the x variables. The new problem is solved applying the Newton's method. IPOPT ([wachter2006implementation](#)) and KNITRO ([waltz2004knitro](#)) are solvers based on this approach.

MIXED-INTEGER LINEAR PROGRAMMING (MILP) Mixed-integer linear programming (MILP) refers to those mathematical programming problems based on linear equations and containing discrete variables. A mixed-integer linear programming problem can be expressed as shown in Eq. [1.3](#), where x are continuous variables and y are discrete variables. Typically, discrete variables are binary variables ([grossmann2021advanced](#)).

$$\begin{aligned} \min \quad & Z = a^T x + b^T y \\ \text{s.t.} \quad & Ax + By \leq d \end{aligned} \tag{1.3}$$

$$\begin{aligned} & x \geq 0 \\ & y \in \{0, 1\}^m \end{aligned} \tag{1.4}$$

A number of methods have been proposed to solve MILP problems, including cutting planes, Benders decomposition, branch and bound search, and branch and cut methods.

Cutting planes consist of a sequence of LP problems in which different cutting planes are generated to cut-off the solution of the relaxed LP. They reduce the feasible region of the linear relaxation of the original problem excluding those solutions that are feasible in the linear relaxation but not in the original MILP problem.

Benders decomposition is based on the generation of a lower and an upper bound of the solution of the MILP problem in each iteration. The upper bound is calculated from the primal problem, which corresponds with the original problem where the binary variables have been fixed. Conversely, the lower bound is determined through a master problem, which is a LP problem derived from the original problem by means of the duality theory. Branch and bound method structure the problem in form of a binary tree that includes all possible combinations of binary variables. The tree is explored by solving the relaxed versions of the original problem. If the relaxation does not result in an integer solution (0 or 1), it is necessary to go deeper into the solution tree to explore further combinations of the binary variables. If the result obtained is an integer, the next step is to return to the previous subproblem to explore

the alternative branch. However, diverse procedures have been developed to discard certain branches, avoiding the need of exploring the whole tree and reducing the problem (**floudas1995nonlinear**).

Branch and cut methods combine branch and bound methods with cutting planes targeting a tighter lower bound. In the different nodes, the relaxed problem is solved. If the solution is not integer, a subsequent relaxed problem is solved by adding cutting planes in order to strengthen the lower bound (**grossmann2021advanced**). Gurobi (**gurobi**) and CPLEX (**cplex2009v12**) are solvers based on this approach.

MIXED-INTEGER NONLINEAR PROGRAMMING (MINLP) Mixed-integer nonlinear programming (MINLP) refers to those mathematical programming problems containing nonlinear equations and discrete variables, typically, binary variables. A mixed-integer nonlinear programming problem can be expressed as shown in Eq 1.5, where x represents a vector of continuous variables, y is the vector of binary variables, $h(x, y)$ and $g(x, y)$ denote the equality and inequality constraints respectively. $f(x)$ represents the objective function (**grossmann2021advanced**).

$$\begin{aligned} \min \quad & f(x, y) \\ \text{s.t.} \quad & h(x, y) = 0 \\ & g(x, y) \leq 0 \\ & x \in X \subseteq \Re^n \\ & y \in \{0, 1\}^m \end{aligned} \tag{1.5}$$

Some algorithms for solving MINLP problems are the generalized Benders decomposition, outer approximation, and generalized cross decomposition.

Generalized Benders decomposition (GBD) is based on the generation of a lower and an upper bound of the solution of the MINLP minimization problem in each iteration. Similarly to the Benders decomposition, the upper bound is calculated from the primal problem, which correspond with the original problem where the binary variables have been fixed. The lower bound is determined through a master problem, which is a MILP problem derivated from the original problem by means of the duality theory. In addition, the master problem provides information about the binary variables to be fixed in the next iteration (**Geoffrion1972237**).

Outer approximation (OA) provides a lower and an upper bound in each iteration. As the previous case, the upper bound is calculated from the primal problem. The lower bound is calculate from a master problem obtained based on an outer approximation, i.e., the nonlinear objective

function and the constraints are linearized around the primal solution. Additionally, the master problem provides information about the binary variables to be fixed in the next iteration (**duran1986outer**).

Generalized cross decomposition (GCD) is based on the generation of a primal problem that provides an upper bound of the solution and also the Lagrange multipliers for the dual subproblem. The dual problem is used to determine the lower bound of the problem, and provides a vector of binary variables to be fixed in the primal problem. The solution of the primal and dual problems go through convergence tests. If any of these test fails, a master problem is solved. This approach seeks to minimize the number of master problems to be solved since the computational requirements of the this problem are higher. This procedure is repeated at each iteration of the algorithm (**holmberg1990convergence**).

1.4 FAIRNESS METRICS

The fair allocation of limited resources among multiple stakeholders is key issue in resource management. This distribution can be guided through the individual utilities associated with the allocation of a certain resource to each stakeholder. Several utility allocation schemes have been proposed in the literature in order to address different issues, including the different scales of stakeholders, the existence of a unique solution fairness, and the Pareto optimality, which indicates that no utility is wasted. A brief description of different fairness measures is provided below. A more detailed analysis of multiple fairness measures and their properties can be found in **sampat2019fairness**.

SOCIAL WELFARE APPROACH The social welfare scheme seeks to maximize the sum of the individual utilities, i.e., the total utility of the community comprised by the stakeholders. This is an intuitive scheme that satisfies the Pareto optimality, but it has some deficiencies. Particularly, this approach is very sensitive to the difference of stakeholders scales, favoring the large stakeholders over the small ones. In addition, the social welfare scheme can result in multiple allocation solutions that result in the same total utility (i.e., the solution is non-unique), leading to ambiguous solutions (**sampat2019fairness**).

NASH SCHEME The Nash scheme (**Nash1950; roth1979impossibility**) maximizes the product of the individual utilities, which is equivalent to maximize the sum of the logarithms of the individual utilities. Therefore, this approach is able to capture the different scales of stakeholders.

In addition, this scheme satisfies the Pareto optimality and has unique solution.

Some variations of the Nash scheme have been proposed in the literature such as the proportional fairness scheme, which is based on a logarithmic transformation of the Nash utility function ([bertsimas2011price](#)).

RAWLSIAN JUSTICE The Rawlsian justice ([Rawls2020](#)) seeks to prioritize the smallest stakeholders (i.e., the stakeholders with the last utility) over the largest ones. This schemes presents significant deficiencies: it does not consider the large stakeholders, the Pareto optimality is not satisfied, and solution provided can be non-unique.

PARAMETRIC SCHEMES There exist a number of parametric schemes whose properties are defined through a set of parameters. Notable parametric schemes are the α -Fair scheme ([lan2010axiomatic](#)), the superquantile scheme ([dowling2016framework](#)), and the generalized entropy scheme ([cowell1981additivity](#)). Some of these schemes can be reduced to the social welfare, Nash, and Rawlsian schemes for certain values of their parameters ([sampat2019fairness](#)).

1.5 APPROACHES FOR GEOSPATIAL ENVIRONMENTAL ASSESSMENT

The development of mitigation measures to reduce the environmental footprint of anthropogenic activities requires the previous understanding and quantification of the environmental impacts associated to each sector. This process, called environmental impact assessment (EIA), involves the analysis of multi-disciplinary information, including environmental, physical, geological, ecological, economic, and social data ([gharehbaghi2018gis](#)). Since EIA aims to evaluate the environmental impact of an activity on a particular geographical location, all these data have a common geographic component, becoming geospatial data.

Geospatial data can be managed and analyzed through specific systems denoted as geographic information system (GIS). GIS is a key tool for EIA that uses the geographic component of geospatial data as an integrative framework that provides the ability to analyze and map the descriptive information of the locations studied. The geographic component of data is the key element of GIS systems, since the spatial (or spatio-temporal) location is used as a key to relate other descriptive information. From the perspective of EIA, this information can be analyzed, interpreted, and mapped in order to determine the vulnerability level to a particular environmental threat at each location, find relationships between human activities

and environmental damages, measure the performance of mitigation and remediation processes, etc.

As a result, the combination of GIS, EIA, and methods for the analysis of multi-dimensional information, such as MCDA, provides tools for the development of strategies to promote the transition to a sustainable paradigm for human growth. In this regard, the development of a sustainable, reliable, and resilient water, energy and food nexus is a major issue for food security and environmental protection.

1.6 THESIS OUTLINE

This dissertation is structured in three parts. Part I is devoted to the study of phosphorus management and recovery, Part II addresses a techno-economic assessment of the technologies for nitrogen recovery, and Part III conducts a techno-economic analysis for determining the optimal biomethane production process in order to integrate biogas production and nutrient recovery processes.

1.6.1 *Part I - Phosphorus management and recovery*

CHAPTER 3 - TECHNOLOGIES FOR PHOSPHORUS RECOVERY. This chapter evaluates the main processes for phosphorus recovery from livestock waste, identifying the most promising processes to be deployed at CAFOs through the techno-economic assessment of the technologies under evaluation embedded in a mixed-integer nonlinear programming model.

CHAPTER 4 - GEOSPATIAL ASSESSMENT OF PHOSPHORUS RECOVERY THROUGH STRUVITE PRECIPITATION. This chapter studies the mitigation of phosphorus releases through the deployment of struvite precipitation systems in the watersheds of the contiguous United States. Specific surrogate models to predict the production of struvite and calcium precipitates from cattle leachate were developed based on a detailed thermodynamic model. In addition, the variability in the organic waste composition is captured through a probability framework based on the Monte Carlo method.

CHAPTER 5 - GEOSPATIAL ENVIRONMENTAL AND TECHNO-ECONOMIC FRAMEWORK FOR SUSTAINABLE PHOSPHORUS MANAGEMENT AT LIVESTOCK FACILITIES. This chapter presents a decision support framework, COW2NUTRIENT (Cattle Organic Waste to NUTRIent and ENergy Technologies), for the assessment and selection of phosphorus recovery

technologies at CAFOs based on environmental information on nutrient pollution and techno-economic criteria. This framework combines eutrophication risk data at subbasin level and the techno-economic assessment of six state-of-the-art phosphorus recovery processes in a multi-criteria decision analysis (MCDA) model. An indicator-based methodology has been used to assess and select phosphorus recovery technologies based on technical, environmental, and economic criteria combined in a composite index. We aim to provide a useful framework for the selection of the most suitable P recovery system for each particular CAFO, and for designing and evaluating effective GIS-based incentives and regulatory policies to control and mitigate nutrient pollution of waterbodies.

CHAPTER 6 - ANALYSIS OF INCENTIVE POLICIES FOR PHOSPHORUS RECOVERY. This chapter conducts a research on the design and analysis of incentive policies using the COW2NUTRIENT framework. The goal is to implement phosphorus recovery technologies at CAFOs minimizing the negative impact in the economic performance of CAFOs. The Great Lakes area is used as case study, analyzing the economic impact of the implementation of nutrient recovery systems either considering the deployment of standalone nutrient recovery processes, or integrated systems combining nutrient recovery with anaerobic digestion for the production of electricity and biomethane. Moreover, the fair allocation of monetary resources when the available budget is limited is studied using the Nash allocation scheme.

1.6.2 *Part II - Nitrogen management and recovery*

CHAPTER 7 - MULTI-SCALE TECHNO-ECONOMIC ASSESSMENT OF NITROGEN RECOVERY SYSTEMS FOR SWINE OPERATIONS. This chapter evaluates the main processes for nitrogen recovery at intensive swine operations. A multi-scale techno-economic analysis is performed to estimate the capital and operating costs for different treatment capacities, identifying the most promising processes.

1.6.3 *Part III - Nitrogen management and recovery*

CHAPTER 8 - OPTIMAL TECHNOLOGY SELECTION FOR THE BIOGAS UPGRADING TO BIOMETHANE. This chapter performs a systematic study of different biogas upgrading to biomethane processes by means of mathematical programming. The goal is to identify the optimal upgrading process attending to the particular characteristics of the biogas produced from livestock manure. Food waste and wastewater sludge are

also included for comparison. The information obtained on the optimal biomethane production processes is used to evaluate the potential combination of biomethane production and nutrient recovery processes into an integrated resources recovery facility.

BIBLIOGRAPHY

2

OBJECTIVE

2.1 SCOPE AND OBJECTIVES OF THE THESIS

2.1.1 *Main objective*

This thesis seeks to promote the recovery and recycling of nutrients contained in livestock waste by identifying the most appropriate technologies for phosphorus and nitrogen recovery at cattle and swine CAFOs, assessing the potential nutrient releases abatement that could be achieved by the deployment of these systems and analyzing incentive policies for their effective implementation at livestock facilities. Moreover, we introduce a systematic framework for evaluating and selecting the most suitable nutrient recovery system at CAFOs considering geospatial environmental vulnerability to nutrient pollution.

2.1.2 *Specific objectives*

OBJECTIVE I: To identify the role of intensive farming activities on nutrient pollution, including the main sources of nutrient releases, as well as potential processes and systems for nutrient recovery.

OBJECTIVE II: To identify environmental indicators for nutrient pollution, and use them to assess the potential for the abatement of phosphorus releases by deploying the processes previously selected at livestock facilities at subbasin spatial resolution.

OBJECTIVE III: To develop a decision-support system for the evaluation and selection of nutrient recovery systems at livestock facilities integrating techno-economic data of the nutrient recovery technologies and environmental vulnerability to nutrient pollution information determined through a tailored geographic information system (GIS) in order to select the most suitable system for each particular livestock facility.

OBJECTIVE IV: To design and analyze potential incentive policies for the deployment of phosphorus recovery technologies at livestock facilities, as well as to study the fair allocation of limited monetary resources.

Part I

PHOSPHORUS MANAGEMENT AND RECOVERY

3

TECHNOLOGIES FOR PHOSPHORUS RECOVERY

ABSTRACT

A mixed-integer nonlinear programming strategy is proposed to design integrated facilities to simultaneously recover power and nutrients from organic waste. The facilities consider anaerobic digestion of different types of manure (cattle, pig, poultry, and sheep). The products from this step are biogas and a nutrient-rich effluent. The biogas produced is cleaned and used in a gas turbine to produce power while the hot flue gas obtained from combustion produces steam that is fed to a steam turbine to produce additional power. The nutrient-rich effluent is processed to recover the nutrients using different technologies that include filtration, coagulation, centrifugation, and struvite precipitation in stirred and fluidized bed reactors. This processing step provides a mechanism to prevent phosphorus or nitrogen release to the environment and to avoid the development of eutrophication processes. It is found that struvite production in fluidized beds is the technology of choice to recover nutrients from all manure sources. Furthermore, power production depends strongly on manure composition and exhibits high cost variability (from 4,000 €/kW in the case of poultry manure to 25,000 €/kW in the case of cattle and pig manure).

Keywords: Biogas; Digestate; Anaerobic digestion; Manure; Power production; Mathematical optimization

RESUMEN

Se propone una estrategia de programación mixta entera no lineal para diseñar instalaciones integradas de recuperación simultánea de energía y nutrientes contenidos en residuos orgánicos. Las instalaciones propuestas consideran la digestión anaeróbica de diferentes tipos de deyecciones ganaderas (vacuno, porcino, avícola y ovino). Los productos de este proceso son biogás y un efluente rico en nutrientes. El biogás producido es purificado y es utilizado en una turbina de gas para producir energía eléctrica, mientras que los gases de combustión calientes resultantes de la combustión se emplean en la generación de vapor que se alimenta a una turbina de vapor para producir energía adicional. El efluente rico en nutrientes se procesa para recuperar los nutrientes utilizando diferentes tecnologías que incluyen filtración, coagulación, centrifugación y precipitación de estruvita en reactores de mezcla completa y en reactores de lecho fluidizado. Este tratamiento proporciona un mecanismo para prevenir la liberación de fósforo o nitrógeno al medio ambiente y evitar el desarrollo de procesos de eutrofización. Se ha comprobado que la producción de estruvita en reactores de lecho fluidizado es la tecnología seleccionada para recuperar los nutrientes de todas las fuentes de estiércol. Además, la producción de energía depende en gran medida de la composición del estiércol y presenta una gran variabilidad de costes (desde 4.000 euros/kW en el caso del estiércol de aves de corral hasta 25.000 euros/kW en el caso del estiércol de vacuno y de cerdo).

Palabras clave: Biogás; Digestato; Digestión anaerobia; Deyecciones ganaderas; Producción de electricidad; Optimización matemproduccióntica

3.1 INTRODUCTION

Countries across the globe generate large amounts of organic waste that include urban residues and sludge and manure from livestock activities. While many of these waste streams can be used as a source for power and chemical products, identifying suitable cost-effective technologies is challenging. Anaerobic digestion (AD) is a promising technology to treat these residues to produce biogas, which can be used as a source for thermal energy and electrical power ([Leon](#)) or chemicals ([hernandez2016optimal](#)). However, AD technologies also generate a nutrient-rich residual stream called digestate, that must be further processed to prevent waste and soil contamination. In particular, nutrient management is needed to prevent losses of phosphorous and nitrogen to surface and underground water bodies which leads to eutrophication processes ([Sampat2017](#); [GarciaSerrano](#)). There are a number of technologies that can be used to process the digestate that range from simple mechanical separations such as filters ([gustafsson2008phosphate](#)) and centrifugation units ([meixner2015effect](#)) to chemical processing such as struvite precipitation ([bhuiyan2008phosphorus](#)). Recent studies have analyzed the production of highly concentrated nutrient products such as struvite ([lin2015phosphorus](#)). The variability in the recovered product quality, selling price, and production cost presents complex trade-offs for the optimal use of the digestate. Existing studies have only addressed the performance of various treatment mechanisms and lack a systematic design perspective that evaluates the performance of coupled biogas and nutrient recovery technologies ([drosg2015nutrient](#)). This is necessary, for instance, to assess economic performance of nutrient recovery in the face of strong variations in the digestate content obtained from AD ([AlSeadi2008](#)).

In this work we propose a systematic design framework to optimize the simultaneous production of energy from the biogas obtained by anaerobic digestion of cattle, sheep, poultry and pig manure, along with the recovery of nitrogen and phosphorous from the digestate. The proposed framework determines the optimal technology configuration, equipment sizing, and operational conditions for various compositions of manure and digestate and revenues for biogas, electricity, and fertilizer.

The paper is organized as follows. In Section [3.2](#) we present a brief description of the process and the flowsheet. In Section [3.3](#) we focus on the modelling of the digestate processing technologies and costing. Section [3.4](#) presents the results for various feedstocks, and Section [3.5](#) draws conclusions.

3.2 PROCESS DESCRIPTION

The proposed process consists of four sections: biogas production, biogas purification (biogas generation), electrical power generation, and nutrient recovery from digestate. This is illustrated in Figure 3.1.

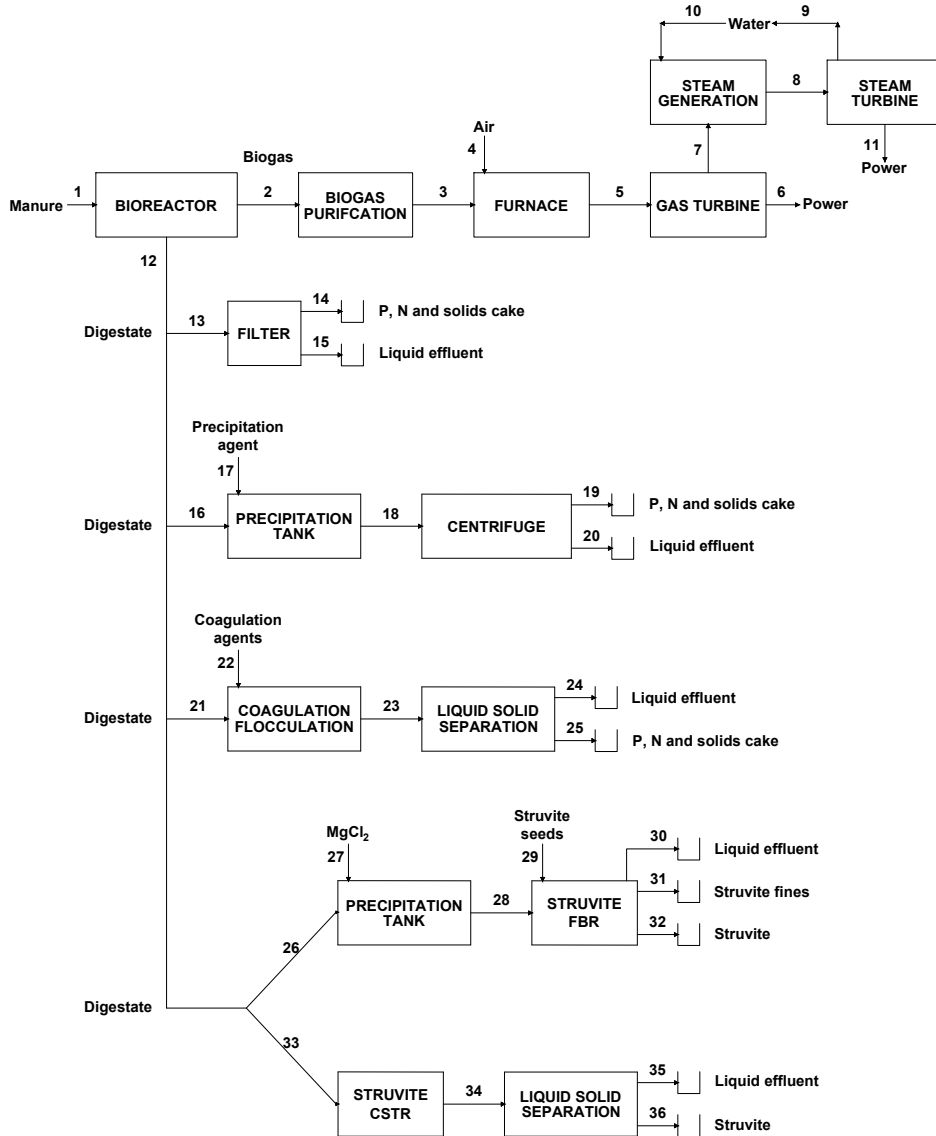


Figure 3.1: Flowsheet for the production of power and fertilizers.

The biomass together with water and nutrients (manure slurry) are fed to a bioreactor through stream 1, where the mixture is anaerobically digested to produce biogas and a decomposed substrate (digestate). The

Table 3.1: Manure composition and properties (kowalski2013changes; Lorimor2004; AlSeadi2008; martins2009biogas).

Manure/ element	Dry matter		N		P		K		VS		V_{biogas} ($\frac{\text{m}^3_{\text{gas}}}{\text{kg vs}}$)	Density ($\frac{\text{kg}}{\text{m}^3}$)	
	(% wt)		(% dry mass)		(% dry mass)		(% dry mass)		(% dry mass)				
	Max	Min	Max	Min	Max	Min	Max	Min	Max	Min	Max	Min	
Cattle	10	2	8	4.7	1.3	0.8	10	3.3	0.8	0.8	0.3	0.2	1041.2
Pig	6	2	15	13	2.2	1.9	8.3	3.9	0.8	0.7	0.5	0.25	1000.0
Poultry	60	30	5.4	5.4	1.7	1.7	1.2	2.3	0.8	0.8	0.6	0.35	1009.2
Sheep	28	28	2.9	2.9	0.78	0.78	2.9	2.9	0.8	0.8	0.61	0.37	1009.2

biogas, composed of methane, carbon dioxide, nitrogen, hydrogen sulfide, ammonia and moisture leaves the bioreactor through stream 2, and it is then sent to the purification section to remove H₂S in a fixed-bed reactor and to eliminate CO₂ and traces of NH₃ in a second step by using a pressure swing adsorption (PSA) system. The purified biogas (stream 3) is used in a Brayton cycle, modelled as a furnace and an expansion, producing power. Air is fed via stream 4 and the exhaust gases (stream 7) are fed to a regenerative Rankine cycle, where it produces high pressure overheated steam extracted in stream 8. This overheated steam is fed to a steam turbine, where it is expanded to produce power. The exhaust steam from the turbine is recovered in stream 9 and reused in the Rankine cycle through stream 10. Between streams 9 and 10 hot flue gases from the gas turbine reheat and produced overheated steam from the recycled water (**Leon**).

The digestate is released from the digester through stream 12, and it can be processed through a number of technologies to remove nitrogen and phosphorous. We consider filtration, centrifugation, coagulation, and struvite production using either a fluidized bed reactor (FBR) or a continuous stirred tank reactor (CSTR). These technologies are described in detail in Section 3.3.4.

Four manure types have been considered as raw material for the process: cattle, pig, poultry and sheep manure. Table 6.1 shows the composition and properties of each type of manure.

3.3 MODELLING ISSUES

We evaluate the performance of the different unit operations in the process by using detailed models that comprise mass and energy balances, thermodynamics, chemical and vapor–liquid equilibria, and product yield calculations. The global process model comprises total mass flows, component mass flows, component mass fractions, temperatures and pressures of

Table 3.2: Set of components.

Number of component	Component	Number of component	Component	Number of component	Component	Number of component	Component
1	Wa	12	O	23	K ₂ O	34	Cl
2	CO ₂	13	N	24	CaCO ₃	35	Struvite
3	CO	14	Norg	25	FeCl ₃	36	K-Struvite
4	O ₂	15	P	26	Antifoam	37	MgCl ₂ (CSTR)
5	N ₂	16	K	27	Fe ₂ (SO ₄) ₃	38	NaOH (CSTR)
6	H ₂ S	17	S	28	Al ₂ (SO ₄) ₃	39	Mg (CSTR)
7	NH ₃	18	Rest	29	AlCl ₃	40	Cl (CSTR)
8	CH ₄	19	Cattle slurry	30	MgCl ₂	41	Struvite (CSTR)
9	SO ₂	20	Pig slurry	31	NaOH	42	K-Struvite (CSTR)
10	C	21	Poultry slurry	32	Struvite seeds	43	FeCl ₃ Coag
11	H	22	P ₂ O ₅	33	Mg		

the streams in the process network. The components that are considered in our calculations belong to the set shown in Table 3.2.

In the following subsections, we briefly present the main equations used to characterize the operation of the different units. For the sake of brevity, simpler balances based on removal efficiency or stoichiometry and equations connecting units are omitted. The power production system is described in detail in previous work (**Leon**) and we thus only provide a brief description.

The cost estimation for the alternatives and for the entire process is based on the estimation of the unit costs from different sources using the factorial method. From the units cost, the facility cost is estimated using the coefficients in **rk1999coulson**, so that the total physical plant cost involving equipment erection, piping instrumentation, electrical, buildings, utilities, storage, site development, and ancillary buildings is 3.15 times the total equipment cost for processes which use fluids and solids. On the other hand, the fixed cost, which includes design and engineering, contractor's fees, and contingency items is determined as 1.4 times the total physical plant cost for the fluid and solid processes. In the subsequent cost estimation procedures these parameters are denoted as f_i for the total physical plant parameter and f_j for the fixed cost parameter.

3.3.1 Biogas production

AD is a complex microbiological process that decomposes organic matter in the absence of oxygen. It produces a gas mixture following hydrolysis, acidogenesis, acetogenesis, and methanogenesis steps, consisting mainly of methane and carbon dioxide (biogas), and decomposed substrate (digestate). The anaerobic reactor is modeled using mass balances of the species

involved in the production of biogas and digestate. Inorganic nitrogen, organic nitrogen, sulfur, carbon, and phosphorus balances are formulated by using the composition of volatile solids in manure, see Table 6.1 ([kowalski2013changes](#); [Lorimor2004](#); [AlSeadi2008](#); [martins2009biogas](#)). Typical bounds for the biogas composition are provided. The reactor operates at 55 °C. We refer the reader to the Supplementary Material and [Leon](#) for details on the modelling of the digester.

3.3.2 Biogas purification

This system consists of a number of stages to remove H₂S, CO₂ and NH₃. Here we highlight some basics about the operation of these stages. For further details we refer the reader to previous work ([Leon](#)).

The removal of H₂S is carried out in a bed of Fe₂O₃, that operates at 25–50 °C producing Fe₂S₃. The regeneration of the bed uses oxygen to produce elemental sulfur and Fe₂O₃.

CO₂ is adsorbed using a packed bed of zeolite 5A. The typical operating conditions for PSA systems are low temperature (25 °C) and moderate pressure (4.5 bar). The recovery of the PSA system is assumed to be 100% for NH₃ and H₂O (because of their low total quantities in the biogas, in general), 95% for CO₂, and 0% for all other gas of the mixture.

In both cases the system is modelled as two beds in parallel so that one bed is in adsorption mode while the second one is in regeneration mode, to allow for continuous operation of the plant. Further details can be found in the Supplementary Material.

3.3.3 Electricity generation

We consider two stages for the generation of power. The initial one consists of the use of a gas turbine, a common alternative for using any gas fuel. However, the flue gas that exits the gas turbine is at high temperature. We can either produce steam as a utility or use that steam within a regenerative Rankine cycle to enhance the production of power. The details for the process appear in [Leon](#) or in the Supplementary Material.

3.3.3.1 Brayton cycle

We model the Brayton cycle as a double-stage compression system (one for the air and one for the fuel) with intercooling with variable operating pressure for the gas turbine. The compression is assumed to be polytropic with a coefficient equal to 1.4 and an efficiency of 85% ([Moran2003](#)).

The combustion of methane from the biogas is assumed to be adiabatic, heating up the mixture. We consider the combustion chamber as an adiabatic furnace. We use an excess of 20% of air with respect to the stoichiometry and 100% conversion of the reaction:



The hot flue gas is expanded in the gas turbine to generate power and the expansion is assumed polytropic. In this case, a value of 1.3 is used based on an offline simulation using CHEMCAD®, with an efficiency of 85% (**Moran2003**). Finally, the exhaust gas is cooled down and used to generate high-pressure steam to be fed to the Rankine cycle.

3.3.3.2 *Rankine cycle*

We use the hot flue gas from the turbine to generate steam following a scheme that consists of using the hot gas in the order that follows. First, the hot flue gas is used for the superheating stage of the steam that is to be fed to the turbine. Next, the hot gas is used in the regenerative stage of the Rankine cycle, reheating the steam from the expansion of the high pressure turbine. Subsequently, the flue gas is used in the evaporation and preheating of the condensed water, see Figure 3.1. The details of the modelling of the Rankine cycle can be seen in **martin2013optimal**. We assume an isentropic efficiency of 0.9 for each expansion.

3.3.4 *Digestate conditioning*

Four different alternatives are considered to process the digestate including filtration, centrifugation, coagulation, and struvite production. For struvite production, the performance of fluidized bed reactors (FBR) and stirred tanks reactors (CSTR) systems is compared. For filtration, centrifugation, and coagulation technologies, nutrients output is a cake composed of different solids and nutrients, with a complex composition. The credit that we can get from the cake has been estimated based on the amount of nutrients contained. The prices for the nutrients (N, P and K) are assumed as follows: 0.45 €/kg for N, 0.24 €/kg for K and 0.32 €/kg for P (**hernandez2017bio**).

3.3.4.1 *Filtration*

Filtration is a low-cost technology that is appropriate for small installations where the amount of P to be removed is moderate. This technology

consists of a filter that contains a reactive medium to help remove phosphorus. P removal using reactive filtration takes place through various mechanisms depending on the characteristics of the filter media. For instance, filter media made of compounds rich in cations under basic environments (usually containing calcium silicates at pH values above 9) form orthophosphate precipitates in the form of calcium phosphates, principally as hydroxyapatite ([pratt2012biologically](#)). Metallurgical slag captures P by adsorption over metal at pH close to 7 ([pratt2012biologically](#)). In this work we consider the use of five different types of filter media. Among them, we have studied wollastonite as a filter media rich in alkaline calcium silicates, dolomite Polonite® as calcium carbonate based components, and Filtra P as calcium hydroxide based product ([osterberg2012removal](#); [vohla2011filter](#)). For the metallurgical slag, we have considered the blast furnace slag described by [cucarella2008effect](#). These filters are used in wastewater treatment facilities ([gustafsson2008phosphate](#)) and further analysis can be found in [shilton2006phosphorus](#). Details on Ca-rich filters can be found in [koiv2010phosphorus](#). The removal yield of P and N for the different filter media is shown in Table 3. It is possible to combine this filter medium with nitrogen-philic filters to simultaneously remove nitrogen and phosphorous. An advantage of this technology is that the cake produced can be used as soil fertilizer ([hylander2006phosphorus](#)). The removal yield of nitrogen for Filtra P® has been considered similar to the limestone nitrogen removal yield, as Filtra P® is a limestone derived product.

The model for the filtration is based on the removal efficiency per filter media, see Fig. 3.2. It has been considered that materials such as total solids, carbon and potassium are forming solid compounds, so they will be retained by the filter media, Eqs. 3.4–3.7.

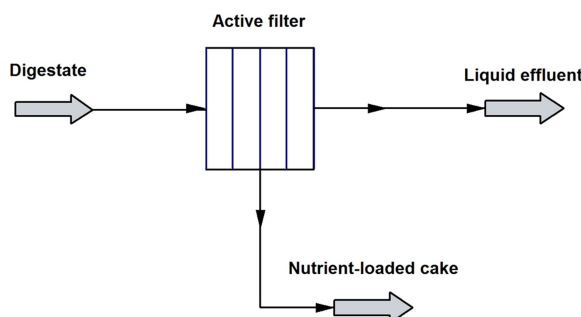


Figure 3.2: Scheme of the filter.

$$F_i^{cake} \geq F_i^{in} \cdot \eta_i^j - M \cdot (1 - y^j) \quad (3.2)$$

$i \in \{P, N\}$
 $j \in \{\text{filter media}\}$

Table 3.3: Recovered P and N yield for different filter media..

Media/nutrient	P (% recovered)	N (% recovered)
Polonite	96.7 ^a	18.0 ^c
Filtral P	98.2 ^a	50.0 ^e
Wollastonite	51.1 ^a	70.0 ^d
Dolomite	44.0 ^b	50.0 ^e
Metal slag	85.6 ^a	67.0 ^f

a: gustafsson2008phosphate

b: pant2001phosphorus

c: kielinska2005evaluation

d: lind2000onutrient

e: azizz2004removal

f: yang2009converter

$$\sum y^j = 1 \quad (3.3)$$

$$F_i^{liquid effluent} = F_i^{in} - F_i^{cake} \quad (3.4)$$

$$F_k^{cake} = F_k^{in}; k \in \{\text{TS, C ,K}\} \quad (3.5)$$

$$F_{Wa}^{cake} = \left(F_{TS}^{cake} + \sum_i F_i^{cake} \right) \cdot \frac{C_{Wa}^{cake}}{1 - C_{Wa}^{cake}} \quad (3.6)$$

$$F_{Wa}^{liquid effluent} = F_{Wa}^{in} - F_{Wa}^{cake} \quad (3.7)$$

To select among the five filter media, we use a Big M formulation to select one of them assigning a binary variable $y^{\text{filter media}}$ for each filter media, Eqs. 3.2 and 3.3. This variable takes a value of 1 for the selected

filter media and o for the rest, so that we are able to evaluate one filter media per time.

It is assumed that the cake obtained contains moisture with a value of 55% in weight basis (C_{Wa}^{cake}). The optimal filter media among the evaluated compounds is metal slag (li2015study).

The cost of each alternative has been estimated according to the number of filters, which depends on the maximum flow they can process. The maximum flow per filter unit, F_{max}^{filter} , is 1,300 ft³/min (loh2002process). To design the filter units we have taken the minimum value between the flow provided by mass balances and the maximum flow allowed per filter, Eqs. 3.8–3.10.

$$F \left(\frac{\text{ft}^3}{\text{min}} \right) = \frac{F_{in}}{\rho_{digestate}} \quad (3.8)$$

$$n_{filters} \geq \frac{F_{total}^{filter}}{F_{max}^{filter}} \quad (3.9)$$

$$F_{design}^{filter} \left(\frac{\text{ft}^3}{\text{min}} \right) = \min \left(F_{max}^{filter}, F_{total}^{filter} \right) \quad (3.10)$$

In fact, since the maximum flow for a cartridge filter is 1,300 ft³/min, for this facility the number of filters considered in this work will always be one and the design flow is equal to the flow provided by mass balances.

The correlation used to calculate the filter cost, Eq. 3.11, is obtained from data reported in loh2002process. This correlation provides the price in 1998 dollars, so we use the Chemical Engineering Index to update it.

$$FC_{filtration} (\text{USD}) = 4.7436 \cdot F_{design}^{filter} + 807.6923 \quad (3.11)$$

The operating cost is estimated using a simple correlation, Eq. 3.14, where we assume that the utilities contribute 20% of the total (vian1975pronostico). The other economical contributions considered are chemicals, estimated as in Eq. 3.12, labour, as per Eq. 3.13, and the contribution of the investment cost of the units given by Eqs. 3.10 and 3.11. The filter media are considered as chemicals that will be replaced annually.

$$ChemC_{filtration} \left(\frac{\text{EUR}}{\text{year}} \right) = \frac{F_p^{in} \cdot 3600 \cdot h \cdot d}{kg_{filter\ media}} \cdot Price_{filter\ media} \quad (3.12)$$

In Eq. 3.12, $kg_{filter\ media}$ are calculated as the P content in the inlet stream divided by the filter media P adsorption capacity.

$$\begin{aligned} \text{Labour cost} \left(\frac{\text{EUR}}{\text{year}} \right) = \\ \left(61.33 \cdot F_P^{recovered} \cdot 3.6 \cdot h^{(-0.82)} \right) \cdot \left(F_P^{recovered} \cdot 3.6 \cdot h \cdot d \right) \cdot \left(\frac{\text{Salary}}{h \cdot d} \right) \cdot n_{OP} \end{aligned} \quad (3.13)$$

The number of operations considered, n_{OP} , is equal to 1.

$$\begin{aligned} \text{Operating cost} \left(\frac{\text{EUR}}{\text{year}} \right) = \\ \frac{\text{ChemC} + 1.5 \cdot \text{Labour cost} + 0.3 \cdot \text{Fixed Cost} \cdot f_i \cdot f_j}{(1 - \text{Utilities})} \end{aligned} \quad (3.14)$$

Finally the credit obtained from the cake is computed as the weighted sum of each nutrient value, Eq. 3.15, (hernandez2017bio), and the benefits (or losses) are computed as the difference between the credit obtained from the cake and the operating costs of the facility, Eq. 3.16.

$$\begin{aligned} \text{Cost}_{cake} \left(\frac{\text{EUR}}{\text{year}} \right) = \\ \left(F_P^{recovered} \cdot Price_P + F_N^{recovered} \cdot Price_N + F_K^{recovered} \cdot Price_K \right) \\ \cdot 3600 \cdot h \cdot d \end{aligned} \quad (3.15)$$

$$\text{Benefits}_{Filtration} \left(\frac{\text{EUR}}{\text{year}} \right) = \text{Cost}_{cake} - \text{Operating cost} \quad (3.16)$$

3.3.4.2 Coagulation

Coagulation is a chemical treatment to process the digestate. The goal of this process is to destabilize colloidal suspensions by reducing the attractive forces, followed by a flocculation process to form flocs from the previously destabilized colloids and to subsequently precipitate them. The nutrients are then recovered with other sedimented solids by clarification. Both N and P can be removed from the influent through coagulation-flocculation, where phosphorus is removed primarily in the form of metal hydroxides, which is the dominant process at typical plant pH values (szabó2008significance). Nitrogen elimination is related to the removal of

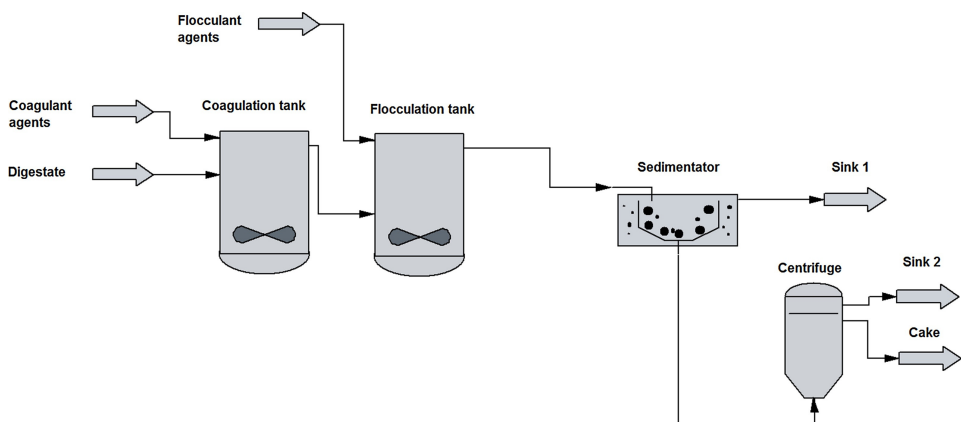


Figure 3.3: Scheme of the coagulation process.

the colloidal matter (**aguilar2002nutrient**). Different coagulation agents are considered aiming at selecting the optimal one: FeCl_3 , $\text{Fe}_2(\text{SO}_4)_3$, $\text{Al}_2(\text{SO}_4)_3$, and AlCl_3 . The flowsheet for the process of coagulation is presented in Fig. 3.3.

The removal efficiency achieved is similar for the different coagulant agents, with values up to 99% for phosphorus and 57% for nitrogen (**aguilar2002nutrient**). The main variables which influence the coagulation–flocculation process are the initial ratio of metal to phosphorus, pH, and chemical oxygen demand (COD). The initial metal-phosphorus molar ratio must be between 1.5 and 2.0, and the recommended pH range is from 5.5 to 7. COD has a negative impact on the removal efficiency when its value is increased (**szabó2008significance**).

To determine the amount of coagulant agent to be added to the system, it has been considered that a metal/phosphorus molar ratio of 1.75 must be achieved (**szabó2008significance**). Given the relationship between the P in the raw material stream, the metal added, and the metal concentration in the commercial presentation of the coagulant agent, we are able to compute the coagulant agent amount that should be added. In the coagulation and flocculation tanks the flocs are formed and nutrients are recovered in the sediment together with coagulation agents and organic solids contained in the raw material. In the decanter, it has been considered that the stream with solids has a water content of 50% ($C_{\text{Wa}}^{\text{sedimentator}}$) (**williams2011digestates**) and the water content of the centrifuge outlet solids stream is 60% ($C_{\text{Wa}}^{\text{centrifuge}}$) (**wakeman2007separation**).

Other elements present in the digestate, such as total solids, carbon, and potassium are assumed to be present in the solid forming compounds that sediment. Thus, they are among species that constitute the cake.

Taking into account the elements mentioned above mass balances have been formulated with the corresponding removal ratios. To select and evaluate the different coagulant agents, the problem has been modelled using a mixed-integer nonlinear programming (MINLP) formulation with Big-M constraints, Eqs. 3.17 and 3.18.

$$F_j^{\text{coag tank}} \geq \frac{F_P^{\text{in}}}{\text{MW}_P} \cdot \text{MeP}_{\text{ratio}} \cdot \frac{\text{MW}_j}{C_{\text{Me}}} - M \cdot (1 - y^j) \quad (3.17)$$

$j \in \{\text{coagulant agents}\}$

$$\sum y^j = 1 \quad (3.18)$$

where MeP is the metal/phosphorus ratio and M is a large value to formulate the Big-M constraint to select and evaluate the different coagulant agents. Mass balances are computed using Eqs. 3.19–3.28.

$$F_j^{\text{coag tank}} = F_j^{\text{floc tank}} = F_j^{\text{sedimentator}} = F_j^{\text{centrifuge}} = F_j^{\text{cake}} \quad (3.19)$$

$j \in \{\text{coagulants}\}$

$$F_i^{\text{in}} = F_i^{\text{coag tank}} = F_i^{\text{floc tank}} = F_i^{\text{sedimentator}} \quad (3.20)$$

$i \in \{\text{P, N}\}$

$$F_i^{\text{cake}} = F_i^{\text{centrifuge}} = F_i^{\text{sedimentator}} \cdot \eta_i^j \quad (3.21)$$

$$F_i^{\text{sink1}} = F_i^{\text{sedimentator}} - F_i^{\text{centrifuge}} \quad (3.22)$$

$$F_k^{\text{in}} = F_k^{\text{coag tank}} = F_k^{\text{floc tank}} = F_k^{\text{sedimentator}} = F_k^{\text{centrifuge}} = F_k^{\text{cake}} \quad (3.23)$$

$k \in \{\text{TS, C, K}\}$

$$F_{\text{Wa}}^{\text{in}} = F_{\text{Wa}}^{\text{coag tank}} = F_{\text{Wa}}^{\text{floc tank}} = F_{\text{Wa}}^{\text{sedimentator}} \quad (3.24)$$

$$F_{Wa}^{centrifuge} = \left(F_{TS}^{centrifuge} + \sum_i F_i^{centrifuge} + \sum_j F_j^{centrifuge} \right) \cdot \frac{C_{Wa}^{sedimentator}}{1 - C_{Wa}^{centrifuge}} \quad (3.25)$$

$$F_{Wa}^{sink1} = F_{Wa}^{sedimentator} - F_{Wa}^{centrifuge} \quad (3.26)$$

$$F_{Wa}^{cake} = \left(F_{TS}^{cake} + \sum_i F_i^{cake} + \sum_j F_j^{cake} \right) \cdot \frac{C_{Wa}^{centrifuge}}{1 - C_{Wa}^{centrifuge}} \quad (3.27)$$

$$F_{Wa}^{sink2} = F_{Wa}^{centrifuge} - F_{Wa}^{cake} \quad (3.28)$$

The estimation of the size and cost of both the coagulation and flocculation tanks has been carried out using a correlation developed by **almena2016technoeconomic** as a function of the weight of the vessels. To simplify the mass balances it is considered that the volume provided by the coagulant agents is negligible with respect to the processed stream of the digestate. The vessel size is computed from the residence time. The hydraulic retention time considered in the coagulation tank is 4 min (**zhou2008enhanced**). The vessel size is computed from the residence time, Eq. 3.29. Using these data, the diameter and length are computed using rules of thumb, Eqs. 3.30 and 3.31. Finally, a correlation for the thickness as a function of the diameters allows determining the mass of metal required for the vessel and its weight, Eqs. 3.32 and 3.33. Vessel cost estimation is provided by Eq. 3.34.

$$V_{Coagtank} (\text{m}^3) = HRT_{Coag\ tank} \cdot \frac{F_{digestate}^{in}}{\rho_{digestate}} \quad (3.29)$$

$$D_{Coag\ tank} (\text{m}) = \left(\frac{6 \cdot V_{Coag\ tank}}{7 \cdot \pi} \right)^{1/3} \quad (3.30)$$

$$L_{Coag\ tank} (m) = 4 \cdot D_{Coag\ tank} \quad (3.31)$$

$$e_{Coag\ tank} (\text{m}) = 0.0023 + 0.003 \cdot D_{Coag\ tank} \quad (3.32)$$

$$W_{Coag\ tank} (\text{kg}) = \rho_{SS316} \cdot \quad (3.33)$$

$$\left[\pi \cdot \left(\left(\frac{D_{Coagtank}}{2} + e_{Coag\ tank} \right)^2 - \left(\frac{D_{Prec\ tank}}{2} \right)^2 \right) \cdot L_{Coag\ tank} + \frac{4}{3} \cdot \pi \cdot \left(\left(\frac{D_{Coag\ tank}}{2} + e_{Coag\ tank} \right)^3 - \left(\frac{D_{Coag\ tank}}{2} \right)^3 \right) \right]$$

$$Cost_{Vessel} (\text{USD}) = 6839.8 \cdot V_{Coag\ tank} (\text{m}^3)^{0.65} \quad (3.34)$$

To estimate the power consumed by the agitator, Eq. 3.35, rules of thumb have been used; where the specific power consumed, $\kappa_{agitator}$, is tabulated in **walas1988chemical**. For our slurries a value of $\kappa_{agitator}$ equal to 10 HP per 1000 US gallons is the most appropriate.

$$P_{Agitator} (\text{HP}) = V_{Coag\ tank} (\text{US gallon}) \cdot \frac{\kappa_{agitator}}{1000} \quad (3.35)$$

The agitator cost is also estimated using a correlation from **walas1988chemical**, Eq. (36). For cost estimation purposes we have considered stainless steel 316 as construction material and a dual impeller operating at speed between 56 and 100 rpm depending on the tanks size. With these considerations the values for a , b and c are 8.8200, 0.1235 and 0.0818 respectively (**walas1988chemical**). This correlation provides the cost in 1985 dollars, so it is necessary to update the result using the Chemical Engineering Index as before.

$$Cost_{Agitator} (\text{USD}_{1985}) = e^{a+b \cdot \ln(P_{agitator}(\text{HP})) + c \cdot [\ln(P_{agitator}(\text{HP}))]^2} \quad (3.36)$$

The total cost of the coagulation tank is equal to the sum of the vessel cost and the agitator cost, Eq. 3.37.

$$Cost_{Coag\ tank} = Cost_{Vessel} + Cost_{Agitator} \quad (3.37)$$

The flocculation tank is designed similarly to that of the coagulation, using Eqs. 3.29–3.37. For this step the hydraulic retention time is 25 min (**zhou2008enhanced**).

The decanter is assumed to be circular because of its lower operating and maintenance costs. The area, Eq. 3.38, is computed using the parameter $A_{specific}$, which is the specific clarifier area in m^2 per ton of inlet flow

per day (**wef2005wef**). The typical value, $10 \text{ m}^2/(\text{t/day})$, is taken from **green2008perry**. The diameter of the clarifier, $D_{clarifier}$, is computed from the area value, Eq. 3.39.

$$A_{clarifier} (\text{m}^2) = \frac{A_{specific} \cdot F_{digestate}^{in} \left(\frac{\text{m}^3}{\text{day}} \right)}{1000} \quad (3.38)$$

$$D_{clarifier} (\text{m}) = \left(\frac{4 \cdot A_{clarifier}}{\pi} \right)^{1/2} \quad (3.39)$$

The number of clarifiers is an integer value that is computed as the minimum integer from the ratio between the clarifier diameter calculated before and the maximum clarifier diameter, $D_{max}^{clarifier}$, Eq. 3.40. The maximum clarifier diameter value considered is 40 m (**green2008perry**).

$$n_{clarifiers} \geq \frac{D_{clarifier}}{D_{max}^{clarifier}} \quad (3.40)$$

The diameter used in the final design will be the smallest between $D_{clarifier}$ and $D_{max}^{clarifier}$, Eq. 3.41.

$$D_{design}^{clarifier} (\text{m}) = \min(D_{max}^{clarifier}, D_{clarifier}) \quad (3.41)$$

To model the minimization function and compute $D_{design}^{clarifier}$, the following smooth function approximation, given by Eq. 3.42, is used based on previous work (**de2016characterization**) to avoid discontinuities within the problem formulation.

$$D_{design}^{clarifier} (\text{m}) = \frac{D_{max}^{clarifier}}{1 + e^{(-F_{digestate}^{in} + 0.342) \cdot 2.718}} \quad (3.42)$$

The cost estimation correlation has been developed from the data in **wef2005wef**, Eq. 3.43. It includes all the items involved in the operation of such an unit. The correlation must be updated to current prices using the Chemical Engineering Index.

$$Cost_{clarifier} (\text{USD}_{1979}) = \left(13060 \cdot D_{design}^{clarifier} - 58763 \right) \cdot n_{clarifiers} \quad (3.43)$$

Centrifuge sizing and costing is based on the data by **green2008perry**. We assume pusher type with a maximum diameter of 1250 mm. The modelling equation for sizing is given in Eq. 3.44.

$$D_{\text{Centrifuge}} \text{ (in)} = 0.3308 \cdot \frac{F_{\text{digestate}}^{\text{in}}}{1000} \cdot 3600 + 9.5092 \quad (3.44)$$

The number of centrifuges is calculated taking into account the maximum centrifuge diameter, Eq. 3.45, and the diameter used in the final design will be the minimum value between D Centrifuge and D Centrifuge max , Eq. 3.46.

$$n_{\text{centrifuges}} \geq \frac{D^{\text{centrifuge}}}{D_{\text{max}}} \quad (3.45)$$

$$D_{\text{design}}^{\text{centrifuge}} = \min(D_{\text{max}}^{\text{centrifuge}}, D^{\text{centrifuge}}) \quad (3.46)$$

As in the clarifier, we develop a smooth approximation, Eq. 3.47, to compute the design diameter avoiding discontinuities as follows:

$$D_{\text{design}}^{\text{centrifuge}} = \frac{D^{\text{centrifuge}}_{\text{max}}}{1 + e^{(-F_{\text{digestate}}^{\text{in}} + 35.369) \cdot 0.0395}} \quad (3.47)$$

The cost for the centrifuge is estimated based on the data by **green2008perry** as a function of its diameter, Eq. 3.48. Since the cost correlation is based on 2004 values, the Chemical Engineering Index it used to update the equipment cost.

$$\begin{aligned} \text{Cost}_{\text{centrifuge}} (\text{USD}_{2004}) = \\ (10272 \cdot D_{\text{design}}^{\text{centrifuge}} - 24512) \cdot n_{\text{centrifuges}} \end{aligned} \quad (3.48)$$

We estimate the operating cost of this system by accounting for the annualized equipment cost (fixed cost), chemicals and labor cost. A similar procedure as before is followed (**vian1975pronostico**) but for the clarifier fixed costs as the correlation to estimate its costs already includes the operating cost, Eq. 3.49.

$$\begin{aligned} FC_{\text{coagulation}} \left(\frac{\text{EUR}}{\text{year}} \right) = \\ (Cost_{\text{Coag tank}} + Cost_{\text{Floc tank}} + Cost_{\text{centrifuge}}) \cdot f_i \cdot f_j + Cost_{\text{clarifier}} \end{aligned} \quad (3.49)$$

The chemicals costs are estimated as Eq. 3.50.

$$\begin{aligned} ChemC_{coagulation} \left(\frac{\text{EUR}}{\text{year}} \right) = & \\ & \left(F_{Fe_2(SO_4)_3}^{in} \cdot Price_{Fe_2(SO_4)_3} + F_{Al_2(SO_4)_3}^{in} \cdot Price_{Al_2(SO_4)_3} + \right. \\ & \left. F_{FeCl_3}^{in} \cdot Price_{FeCl_3} + F_{AlCl_3}^{in} \cdot Price_{AlCl_3} \right) \cdot 3600 \cdot h \cdot d \end{aligned} \quad (3.50)$$

To estimate the price for the cake, as in the previous case, we assume the price of each of the nutrients contained (N, P, and K). The price for each nutrient is taken same as before. Thus, the cake price is computed as the weighted sum of each nutrient, as in Eq. 3.15 ([hernandez2017bio](#)).

Finally, the economic benefits or losses of operating this system are calculated as the difference between the credit obtained from the cake and the operating costs of section of the facility, as in Eq. 3.16.

3.3.4.3 Centrifugation

Centrifugation is a pretreatment that separates solid and liquid phases and that can be used to recover nutrients from the digestate. The advantage of this system is the simple equipment used. Precipitant agents can be added to improve the removal efficiency significantly. Previous studies show that an appropriate mixture of CaCO_3 and FeCl_3 promotes nutrients recovery. In particular, a ratio of 0.61 kg CaCO_3 per kilogram of total solids in the raw material inlet stream, and 0.44 kg of FeCl_3 per kilogram of total solids in the raw material inlet stream, achieves a removal efficiency up to 95% and 47% for P and N respectively ([meixner2015effect](#)). Fig. 3.4 presents a scheme of the process.

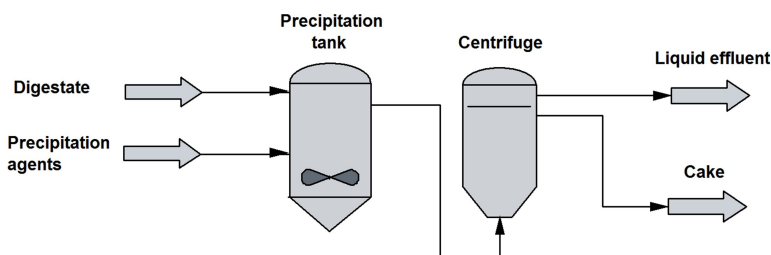


Figure 3.4: Scheme for the centrifugation treatment.

Centrifugation process consists of two units, a precipitation tank where CaCO_3 and FeCl_3 are added, and the centrifuge. These equipment have been modeled using mass balances and removal ratios for the precipitating species. Note that the total solids, carbon, and potassium are assumed to be present in the form of solid compounds, so they will be removed as part of

the cake. Moreover, the water content of the centrifuge outlet solids stream is assumed to be 60% ($C_{Wa}^{centrifuge}$) (wakeman2007separation). Mass balances for the process have been evaluated in Eqs. 3.51-3.59:

$$F_j^{in} = F_{TS}^{in} \cdot \frac{\varphi_j}{C_j} \quad (3.51)$$

$j \in \{\text{precipitation agents}\}$

$$F_j^{in} = F_j^{prec\ tank} = F_j^{centrifuge} = F_j^{cake} \quad (3.52)$$

$$F_i^{in} = F_i^{prec\ tank} = F_i^{centrifuge} \quad (3.53)$$

$i \in \{\text{P, N}\}$

$$F_i^{cake} = F_i^{centrifuge} \cdot \eta_i \quad (3.54)$$

$$F_i^{liquid\ effluent} = F_i^{centrifuge} - F_i^{cake} \quad (3.55)$$

$$F_k^{in} = F_k^{prec\ tank} = F_k^{centrifuge} = F_k^{cake} \quad (3.56)$$

$k \in \{\text{TS, C, K}\}$

$$F_{Wa}^{in} = F_{Wa}^{prec\ tank} = F_{Wa}^{centrifuge} \quad (3.57)$$

$$F_{Wa}^{cake} = \left(F_{TS}^{cake} + \sum_i F_i^{cake} + \sum_j F_j^{cake} \right) \cdot \frac{C_{Wa}^{centrifuge}}{1 - C_{Wa}^{centrifuge}} \quad (3.58)$$

$$F_{Wa}^{liquid\ effluent} = F_{Wa}^{centrifuge} - F_{Wa}^{cake} \quad (3.59)$$

where φ_j is the precipitation agent per total solids mass ratio (0.61 kg CaCO₃/kg TS and 0.44 kg FeCl₃ /kg TS).

These units have been designed using correlations as a function of the flow processed. For the design of the precipitation tank (volume, diameter, length, thickness, weight, and cost calculations) the equations provided by **almena2016technoeconomic** have been used as before, Eqs. 3.29-3.37, considering a hydraulic retention time of 2.5 min (**szabo2008significance**).

$$V_{prec\ tank} \left(\text{m}^3 \right) = HRT_{Prec\ tank} \cdot \left(\frac{F_{digestate}^{in}}{\rho_{digestate}} + \frac{F_{FeCl_3}^{in}}{\rho_{FeCl_3}} \right) \quad (3.60)$$

The volume of CaCO_3 added is assumed negligible compared to the volume of the liquid because it is added as a solid. Thus, the diameter of the tanks is computed using Eqs. 3.60 and 3.30 as in the previous unit. The cost of the vessel is given by the weight of the metal, using the correlations provided by (**almena2016technoeconomic**), Eqs. 3.31-3.34. The power required is computed, as in previous cases, using the rules of thumb in (**walas1988chemical**), Eq. 3.35, where the value of $\kappa_{agitator}$ agitator is equal to 10 HP per 1000 gal, in accordance with the data collected in the literature **walas1988chemical**. The cost correlation is given by Eq. 3.36 and updated to 2016 prices. The total cost of the precipitation tank included the vessel and the agitator costs, Eq. 3.37.

The centrifuge size is characterized by its diameter. We model it as in the previous technologies using Eqs. 3.44-3.48. The operating costs involve fixed, chemicals and labour costs. Fixed costs are estimated using Eq. 3.61. The labor cost is estimated in Eq. 3.13, where n_{OP} is equal to 1 (**vian1975pronostico**). Total operating cost is given by Eq. 3.14. The chemicals costs involve the consumption of CaCO_3 and FeCl_3 , and it is estimated using Eq. 3.62:

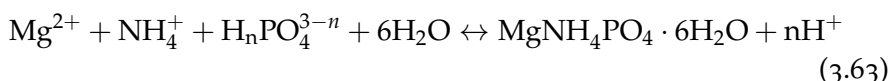
$$FC_{centrifugation} \left(\frac{\text{EUR}}{\text{year}} \right) = (Cost_{centrifuge} + Cost_{Prec\ tank}) \cdot f_i \cdot f_j \quad (3.61)$$

$$\begin{aligned} ChemC_{centrifugation} \left(\frac{\text{EUR}}{\text{year}} \right) &= \\ \left(F_{\text{CaCO}_3}^{in} \cdot Price_{\text{CaCO}_3} + F_{\text{FeCl}_3}^{in} \cdot Price_{\text{FeCl}_3} \right) \cdot 3600 \cdot h \cdot d \end{aligned} \quad (3.62)$$

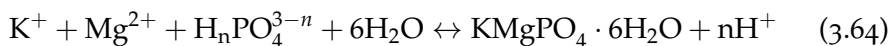
The cake recovered is the main asset of the process. Its price is estimated as the weighted sum of each nutrient, Eq. 3.15, (**hernandez2017bio**). Finally, the benefits or losses of operating this system are calculated as the difference between the revenue obtained from the cake and the operating costs of the facility, Eq. 3.16.

3.3.4.4 Struvite production

P and N can be recovered from digestate through the formation of struvite, which is a phosphate mineral with a chemical formula of $\text{MgNH}_4\text{PO}_4 \cdot 6\text{H}_2\text{O}$. The advantage of this technology is that struvite is a solid with a high nutrients density, it is easy to transport, and it can be used as slow-release fertilizer without any post-processing ([doyle2002struvite](#)). The removal of nutrients via struvite production follows the reaction below, requiring the addition of MgCl_2 , resulting in the production of struvite crystals that can be recovered as solid:



Due to the presence of potassium in the digestate, together with struvite, another product called potassium struvite or K-Struvite, is also produced. In this case the ammonia cation is substituted by the potassium cation ([wilsenach2007phosphate](#)).



Since the formation of struvite is favored over the formation of K-Struvite, it is considered that only 15% of the potassium contained in the digestate will react to form K-Struvite ([zeng2006nutrient](#)). The mass balance for the reactors is given by the stoichiometry of the reactions above.

Two different types of reactors can be used to obtain struvite, either a stirred tank (CSTR) or a fluidized bed reactor (FBR). Figs. [3.5](#) and [3.6](#) provide detailed flowsheets of each case. In case of the FBR, struvite is recovered from the bottoms and the liquid must be processed in a hydrocyclone to avoid discharging fines. In the case of CSTR tanks, we need to use a centrifuge to recover the struvite. We can help the crystal growth by seeding ([doyle2002struvite](#); [kumashiro2001pilot](#)). Due to the substantial increase in the struvite formation yield, we consider the addition of struvite seeds in both cases. The reaction takes place at about 27 °C, with the addition of MgCl_2 at a concentration of 57.5 mg/dm³ ([zhang2014phosphate](#)). A Mg:P molar ratio of 2 ([bhuiyan2008phosphorus](#)) is used.

The FBR system is composed of three elements: a mixer tank, a FBR reactor, and a hydrocyclone. The system operation consists of a digestate flow which is mixed with a stream of MgCl_2 in the mixing tank. The addition of MgCl_2 helps precipitate the struvite by increasing the concentration of the species inside the reactor. As the concentration of NH_4^+ is high due to

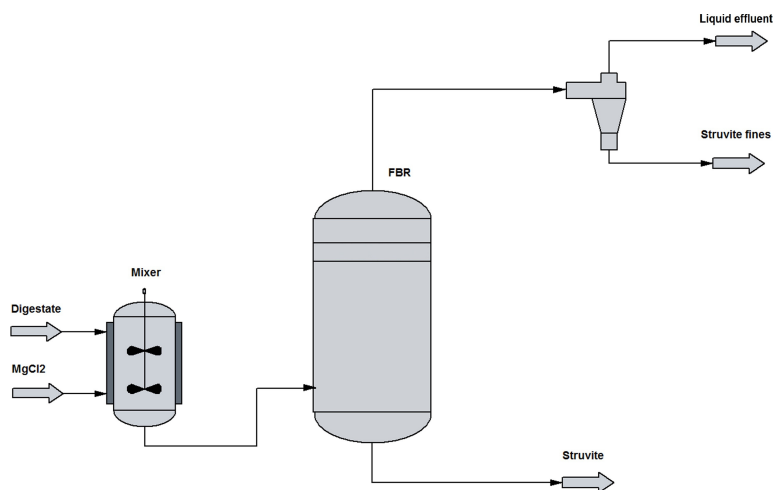


Figure 3.5: Scheme for the FBR system.

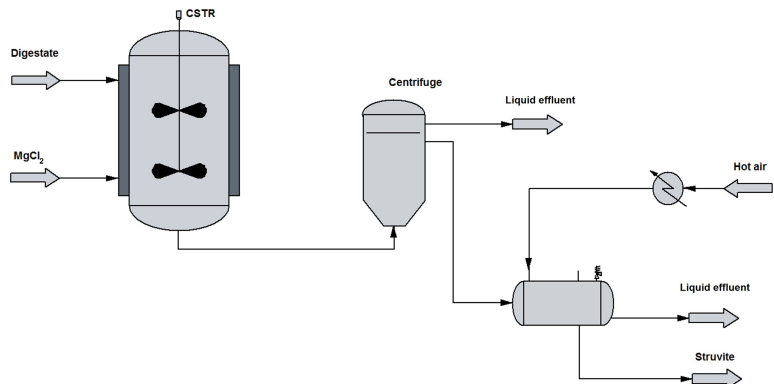


Figure 3.6: Scheme for the CSTR based struvite production system.

the pH, and the inorganic N and P are the elements we want to recover, the only element which is necessary to be added is Mg in form of $MgCl_2$.

In the tank there is a suspension of struvite seeds with a size of 0.8 mm which promote the precipitation of struvite. The solid struvite is evacuated from the reactor at the bottom and its moisture is low enough to avoid the use of a dryer. The other stream which leaves the reactor contains liquid water in a high proportion with the excess of Mg, the total solids from the digestate, and low amounts of nutrients and other components. This stream is introduced in a hydrocyclone to recover fines of struvite which can be removed by this stream. 100% of fines removal is assumed but no fines production is considered in the model.

To estimate the cost of this system we evaluate the effect of the following variables, whose operating values are shown between parenthesis:

- Digestate input mass and volume flow (between 1 and 100 kg/s)
- Recovered struvite humidity (5% in mass)
- Amount of phosphorus recovered (90%)
- Mg:P molar ratio with a value of 2

In an FBR there are some variables which influence in the design and hence the cost. The variables considered in this work are showed below with the typical values used in the present study between parenthesis:

- d_p : bed particle diameter, assumed to be 0.8 mm (**jordaan2011development**)
- Sphericity: 0.6 is a standard sphericity for particles used in fluidized bed reactors (**Fogler2005Elements**)

Furthermore, the reaction kinetics and equilibrium are considered to estimate the residence time in the reactor. A first order kinetics, developed by (**nelson2003struvite**), has been used, Eqs. 3.65 and 3.66. The kinetic constant is $3.42 \cdot 10^{-3} \text{ s}^{-1}$ for a pH of 9.

$$\frac{-dC}{dt} = k (C - C_{eq}) \quad (3.65)$$

$$\ln (C - C_{eq}) = -kt + \ln (C_0 - C_{eq}) \quad (3.66)$$

Struvite formation is an equilibrium reaction. We use the equilibrium ion activity product (IAP_{eq}) value of $7.08 \cdot 10^{-14}$ (**nelson2003struvite**) to calculate the equilibrium concentrations in the kinetic model, Eq. 3.67. We assumed that the values of ions concentration are equal to ions activity.

$$IAP_{eq} = (Mg^{2+})(NH_4^+)(PO_4^{3-}) = 7.08 \cdot 10^{-14} \quad (3.67)$$

Minimum fluidization velocity is calculated in the first step by considering that the fluid stream is a liquid (**mangin2004fluid**). This consideration is motivated because the liquid digestate works as fluidization agent (**le2006understanding**). The digestate density is 950 kg/m^3 (**rigby2011new**). The expression used to calculate u_{mf} through Reynolds and Archimedes numbers is given by Eq. 3.68, (**tisa2014basic**).

$$u_{mf} = \frac{Re_l \cdot mf \cdot \mu_{digestate}}{\rho_{digestate} - d_p} \quad (3.68)$$

Eq. 3.68 parameters are determined by Eqs. 3.69 and 3.70.

$$Re_{l,mf} = \sqrt{33.72 + 0.0404Ar_l(1 - \alpha_{mf})^3} - 33.7 \quad (3.69)$$

$$Ar_l = \rho_{digestate} (\rho_{struvite} - \rho_{digestate}) g \frac{d_p^3}{\mu_{digestate}^2} \quad (3.70)$$

If the flow has no gas phase, α_{mf} is equal to zero. The terminal velocity is computed using Eq. 3.71 ([tisa2014basic](#)).

$$u_t = \left(\frac{1.78 \cdot 10^{-2} \cdot \eta^2}{\rho_{digestate} \cdot \mu_{digestate}} \right)^{1/3} d_p \quad (3.71)$$

where the parameter η is given by Eq. 3.72:

$$\eta = g (\rho_{struvite} - \rho_{digestate}) \quad (3.72)$$

Finally, the fluid velocity u_0 must be between u_{mf} and u_t . A superficial velocity equal to five times the minimum fluidization velocity is selected ([tejero2004optimization](#)), Eqs. 3.73 and 3.74.

$$u_{mf} < u_0 < u_t \quad (3.73)$$

$$u_0 = 5 \cdot u_{mf} \quad (3.74)$$

Once the superficial velocity is computed, the area and diameter can be calculated from the mass flow Eqs. 3.75 and 3.76.

$$A_{FBR} = \frac{F_{digestate}^{in}}{u_0} \quad (3.75)$$

$$D_{FBR} = \sqrt{\frac{4A_{FBR}}{\pi}} \quad (3.76)$$

The length of the bed is determined by the residence time through the kinetics and the equilibrium ion activity product presented above. Consequently, the magnesium and ammonium concentrations can be calculated

from the digestate mass balance and the external magnesium added. Using the IAP_{eq} value, the phosphate concentration in equilibrium at the operational conditions can be determined. This equilibrium value will be used in kinetics, Eq. 3.77.

$$t = \frac{\ln(C_0 - C_{eq}) - \ln(C - C_{eq})}{k} \quad (3.77)$$

Thus, the bed length is computed as per Eq. 3.78. Typically, the length of the reactor must be 15% larger than the bed, Eq. 3.79.

$$L_{bed} = \frac{u_0}{t} \quad (3.78)$$

$$L_{FBR} = 1.15 \cdot L_{bed} \quad (3.79)$$

The estimation of the reactor cost is carried out assuming that it is a vessel as presented in the processes above, Eqs. 3.30-3.34 ([almena2016technoeconomic](#)). The cost of the mixer tank is also estimated as that of a vessel, using Eqs. 3.29-3.34, with a volume given by that to provide a hydraulic retention time of 150 s ([szab02008significance](#)). The impeller is also designed using the same procedure as before, Eqs. 3.35 and 3.36 ([walas1988chemical](#)).

Finally, to estimate the cost of the hydrocyclone, a surrogate model using data from Matche website has been developed ([Matche](#)) (www.matche.com). There is a maximum diameter, therefore, if a unit larger than the standard is required, we actually need to duplicate the equipment, Eq. 3.81. To estimate the diameter, we considered that there is a linear relationship between the diameter and the flow based on rules of thumb in design literature. A typical unit size of a 20 in diameter hydrocyclone can process 1,000 US gallons per min, Eq. 3.80 ([walas1988chemical](#)).

$$D_{hydrocyclone} (\text{in}) = F_{digestate}^{in} \left(\frac{\text{US gallon}}{\text{min}} \right) \cdot \frac{20}{1000} \quad (3.80)$$

$$n_{hydrocyclone} \geq \frac{D_{hydrocyclone}}{D_{max}} \quad (3.81)$$

where $n_{hydrocyclone}$ is an integer. The maximum diameter for a hydrocyclone, $D_{max}^{hydrocyclone}$, is 30 inch based on standard sizes (www.matche.com).

Thus, the design diameter is the lower diameter between $D_{hydrocyclone}^{hydrocyclone}$ and $D_{max}^{hydrocyclone}$, Eq. 3.82.

$$D_{design}^{hydrocyclone} = \min(D_{total}^{hydrocyclone}, D_{max}^{hydrocyclone}) \quad (3.82)$$

The estimation of the cost for the fines recovery equipment is computed using Eq. 3.83 and updated as explained above.

$$\begin{aligned} Cost_{hydrocyclone} (\text{USD}_{2014}) &= \\ n_{hydrocyclone} \cdot (2953.2 \cdot D_{design}^{hydrocyclone} - 34,131) \end{aligned} \quad (3.83)$$

The CSTR process consists of four elements: the CSTR reactor, a centrifuge, and a dryer with its corresponding heat exchanger. As the residence time in the CSTR is large enough, it is not necessary to use a mixing tank and MgCl² is added directly in the reactor. Thus, struvite is formed in one step in the CSTR. Since the digestate already contains NH₄⁺ and P, we need to add MgCl². As a result, struvite precipitates, and it is recovered from the bottoms of the reactor and dried in a two step process. The first step consists of a centrifuge that recovers struvite with 5% (on weight basis) water (**baasal1989preliminary**). Next, a drum dryer is implemented to remove the residual moisture to reach commercial standards and reduce transportation costs. Fig. 3.6 shows the details of the flowsheet.

The design of the units involved in this process and their cost estimation is based on the following variables:

- Digestate input mass and volume flow (between 1 and 100 kg/s)
- Recovered struvite humidity (5% in mass)
- Amount of phosphorus recovered (90%)
- Mg:P molar ratio with a value of 2

The CSTR is assumed to be a stirred vessel; consequently, it is designed as in the previous cases, Eqs. 3.29-3.37, with a residence of 471.05 s. The residence time is calculated from mass balances and the kinetics described in the FBR process, Eqs. 3.65 and 3.66.

The centrifuge size is characterized by its diameter. Both, the size and cost are computed using the data in **green2008perry**. We assume a pusher type for the centrifuge with a maximum diameter of 1250 mm as before, Eqs. 3.44-3.48.

The cost estimation for the dryer relies on the amount of water to evaporate, and the evaporation capacity. The evaporation capacity ($e_{capacity}$) is reported in the literature to be equal to $0.01897 \text{ (kg/(s · m²))}$ (**walas1988chemical**). Consequently, the dryer cost is computed using a correlation provided by **martin2011energy**, Eq. 3.84, updating the cost to current prices using the Chemical Engineering Index.

$$Cost_{dryer} (\text{USD}_{2007}) = 1.15 \cdot \left(6477.1 \cdot \frac{F_{water}^{in}}{e_{capacity}} + 102394 \right) \quad (3.84)$$

The operating cost of the CSTR and the FBR based processes is computed considering three items, fixed, chemicals and labor, and assuming that utilities account for 20% of the operating costs. The correlations for computing each of them are taken from **vian1975pronostico** and **sinnott1999chemical**, Eq. 3.13 for labour and Eq. 3.14 for total operating cost. Fixed cost for struvite processes is calculated using Eq. 3.85. We assume that the seeds required for the FBR process are internally produced in the startup of the facility.

$$FC_{struvite} \left(\frac{\text{EUR}}{\text{year}} \right) = (\sum Cost_{equipment}) \cdot f_i \cdot f_j \quad (3.85)$$

The revenue obtained from the struvite is determined assuming a selling price of 0.763D EUR/kg, Eq. 3.86, (**molinos2011economic**).

$$Cost_{struvite} \left(\frac{\text{EUR}}{\text{year}} \right) = \left(F_{struvite}^{recovered} \cdot Price_{struvite} \right) \cdot 3600 \cdot h \cdot d \quad (3.86)$$

Finally, the benefits or losses for CSTR and FBR are calculated as the difference between the credit obtained from the struvite and the operating costs of the facility, Eq. 3.16.

3.3.5 Solution procedure

The detailed models for each of the alternatives such as the five filter media or the number of different coagulants result in a large and complex MINLP when cost estimation is involved. We use a two-stage procedure to select the best technology. In the first stage we develop MINLP subproblems to select the appropriate filter media or coagulant. Next, using the detailed models for the best option, surrogate cost models are developed for the five alternative technologies used to process the digestate. However,

there are still binary decisions to account for the cost of the active alternative in the superstructure. Thus, the surrogate models are in the form of linear equations. For instance, the surrogate model for the filter to be implemented in the superstructure is given by a linear function as given by Eq. 3.87.

$$\begin{aligned} \text{Operating cost} \left(\frac{\text{EUR}}{\text{year}} \right) = & \\ 20,521 \cdot F_{\text{design}} \left(\frac{\text{ft}^3}{\text{min}} \right) - 33,488 \cdot a_{\text{Filter}} \end{aligned} \quad (3.87)$$

We avoid the use of binary variables within the formulation (due to highly non linear model of the entire superstructure) by using smooth approximations. We define a_{Filter} as a parameter that takes a value of 0 when $F_{\text{design}}^{\text{Filter}}$ is 0 and 1 if $F_{\text{design}}^{\text{Filter}}$ is not equal to 0. The smooth approximation for a_{Filter} is defined as follows, Eq. 3.88:

$$a_{\text{Filter}} = \frac{1}{1 + e^{(-F_{\text{design}} + 0.049) \cdot 361}} \quad (3.88)$$

Metal slag is selected as the best filter for the filtration process. For the case of the coagulants, the solution of the subproblem, Eqs. 3.17-3.50 selects the use of AlCl³. As in the previous case, a surrogate model is developed to be included in the superstructure so that we avoid including binary variables and allow for zero operating costs in case this technology is not selected, Eq. 3.89.

$$\begin{aligned} \text{Operating cost} \left(\frac{\text{EUR}}{\text{year}} \right) = & \\ 1,019,589.91 \cdot F_{\text{digestate}}^{\text{in}} \left(\frac{\text{kg}}{\text{s}} \right) - 368,838.56 \cdot a_{\text{Coag}} \end{aligned} \quad (3.89)$$

where the smooth approximation for the term a_{Coag} is given by Eq. 3.90.

$$a_{\text{Coag}} = \frac{1}{1 + e^{(-F_{\text{digestate}}^{\text{in}} + 0.068) \cdot 863}} \quad (3.90)$$

Similar to previous cases we develop a surrogate model to estimate the operating cost for the centrifugation as a function of the flowrate of digestate, Eq. 3.91:

$$\begin{aligned} \text{Operating cost} \left(\frac{\text{EUR}}{\text{year}} \right) = & \\ 458,498.29 \cdot F_{\text{digestate}}^{\text{in}} + 24,924.67 \cdot a_{\text{Centrifugation}} \end{aligned} \quad (3.91)$$

As before, $a_{\text{Centrifugation}}$ is approximated as follows, Eq. 3.92:

$$a_{\text{Centrifugation}} = \frac{1}{1 + e^{(-F_{\text{digestate}}^{\text{in}} + 0.068) \cdot 863}} \quad (3.92)$$

Finally, to include the operating costs for the production of struvite, we again develop surrogate models for the FBR, Eq. 3.93 and for the CSRT Eq. 3.95, where a smooth approximation is proposed for the fixed term, a_{FBR} and a_{CSTR} respectively, Eqs. 3.94 and 3.96.

$$\begin{aligned} \text{Operating Cost}_{\text{FBR}} \left(\frac{\text{EUR}}{\text{year}} \right) = & \\ 245,008 \cdot F_{\text{digestate}}^{\text{in}} + 1 \cdot 10^6 \cdot a_{\text{FBR}} \end{aligned} \quad (3.93)$$

$$a_{\text{FBR}} = \frac{1}{1 + e^{(-F_{\text{digestate}}^{\text{in}} + 0.06785) \cdot 862.9679}} \quad (3.94)$$

$$\begin{aligned} \text{Operating Cost}_{\text{CSTR}} \left(\frac{\text{EUR}}{\text{year}} \right) = & \\ 277,051 \cdot F_{\text{digestate}}^{\text{in}} + 1 \cdot 10^6 \cdot a_{\text{CSTR}} \end{aligned} \quad (3.95)$$

$$a_{\text{CSTR}} = \frac{1}{1 + e^{(-F_{\text{digestate}}^{\text{in}} + 0.06785) \cdot 862.9679}} \quad (3.96)$$

The benefits/losses in the superstructure for any of the technologies to process the digestate is computed as the difference between the revenue obtained from the nutrients and generated power, and the operating costs of the facility.

Finally, the whole superstructure is built (see Fig. 3.1). This superstructure contains models of the fermenter, biogas purification, gas cycle, steam cycle, and digestate treatment processes. The aim of this superstructure is to determine the optimal operating conditions and to select the best digestate treatment technology. Thus, digestate treatment processes have

been implemented in the superstructure through detailed mass balances including the solution to the kinetics of the fluidized bed reactors as well as the surrogate models developed in the previous stage to estimate the operating costs. It should be noted that in filtration, centrifugation, and coagulation processes we have included a benefits penalty, $F_{total}^{recovered}$, due to the fact that the product recovered is a mixture of nutrients and organic matter with a nutrients concentration lower than struvite. This penalty represents the concentration of nutrients in the recovered product given by the ratio between the nutrients recovered and the total recovered mass flow, Eq. 3.97.

$$\begin{aligned} Price \left(\frac{\text{EUR}}{\text{year}} \right) = & \\ & \left(F_P^{recovered} \cdot Price_p + F_N^{recovered} \cdot Price_N + F_K^{recovered} \cdot Price_K \right) \\ & \cdot \frac{1}{F_{total}^{recovered}} \cdot 3600 \cdot h \cdot d \end{aligned} \quad (3.97)$$

The total energy obtained in the system to be optimized is the sum of the one generated at the three sections of the turbine, high, medium and low pressure and that of the gas turbine. We use part of the energy produced to power the compressors used across the facility. The economic benefits or losses of each digestate treatment process are added to the energy benefits.

$$\begin{aligned} Z = & \left[\left(\sum_{i \in \text{Turbines}} W_{Turbine} + W_{Gas\ Turbine} - \sum_{j \in \text{Compressors}} W_{Compressors} \right) \right. \\ & \left. \cdot 3600 \cdot h \cdot d \cdot C_{Electricity} \right] + Benefits_{Filtration} + Benefits_{Centrif} + \\ & Benefits_{Coagulation} + Benefits_{FBR} + Benefits_{CSTR} \end{aligned} \quad (3.98)$$

Eq. 3.98 is the objective function that we maximize to determine the optimal operational conditions and to select the best digestate treatment process subject to the following constraints:

- Bioreactor and biogas composition model. Described in Section 3.3.1
- Digestate processing. Described in Section 3.3.4
- Biogas purification. Described in Section 3.3.2
- Brayton cycle. Described in Section 3.3.3.1

- Rankine cycle. Described in Section [3.3.3.2](#)

The main decision variables are related to the selection of the digestate processing technology, among filtration, centrifugation, coagulation and struvite production using CSTR or FBR. The decision variables are also associated with the selection of the type of filter and the coagulation agent. Furthermore, the biogas usage to produce steam requires the operating pressures and temperatures at the gas turbine, and the steam turbine as well as the extraction from the steam turbine to reheat the condensate before regenerating steam using the flue gas from the gas turbine. The superstructure consists of an NLP of approximately 4,000 equations and 5,000 variables solved using a multistart procedure with CONOPT 3.0 as the preferred solver. The computational time is around 60 min, although it varies for each problem as a consequence of the different data used in each case.

3.4 RESULTS

Following the optimization procedure presented in Section 3.4 we first decide on the filter media and the coagulant chemical. We solve MINLP subproblems leading to the selection of the filter media and the coagulant agent. We use the metal slag as the filter media and the AlCl_3 as the coagulant for all raw materials. Next, we developed surrogate models for the five technologies included in the superstructure and solve a reformulated NLP including smooth approximations for the cost functions of the digestate treatment so as to maximize the power produced and the treatment section. The plant size is assumed to be that which processes 10 kg/s of manure based on the typical amount of manure produced in cattle farms (**LeonMsc**). Four manures have been evaluated on the plant: cattle, pig, poultry and sheep, with the aim of determining, for each one, the power generated the composition of the biogas produced, the optimal digestate treatment technology to recover its nutrients and the biogas-manure and digestate-manure ratios. Section [3.4.1](#) summarizes the main operating conditions of the major units in the process and the selection of digestate processing technology. Section [3.4.2](#) presents the detail economic evaluation of the four optimal processes, one per manure type. Finally, in Section [3.4.3](#) an analysis of the effect of the manure composition on the power, operating conditions and digestate treatment is performed.

Table 3.4: Operating data of the optimal configuration for each raw material.

		T (°C)	P (bar)	Extractions																																																																									
Cattle	Bioreactor	55	1	–																																																																									
	Gas turbine	2430 (in)	8.2 (in)	–																																																																									
		1205 (out)	1 (out)	–																																																																									
	Steam turbine	1000 (T ₁)	125 (P ₁)	6.7% to HX7																																																																									
		568 (T ₂)	11 (P ₂)	–																																																																									
		442 (T ₃)	5 (P ₃)	–																																																																									
		41.8 (T ₄)	0.08 (P ₄)	–																																																																									
	FBR	25	1	–																																																																									
	Bioreactor	55	1	–																																																																									
	Gas turbine	2430 (in)	8.2 (in)	–																																																																									
		1205 (out)	1 (out)	–																																																																									
Pig	Steam turbine	1000 (T ₁)	125 (P ₁)	6.7% to HX7																																																																									
		568 (T ₂)	11 (P ₂)	–																																																																									
		442 (T ₃)	5 (P ₃)	–																																																																									
		41.8 (T ₄)	0.08 (P ₄)	–																																																																									
	FBR	25	1	–																																																																									
	Bioreactor	55	1	–																																																																									
	Gas turbine	2430 (in)	8.2 (in)	–																																																																									
		1205 (out)	1 (out)	–																																																																									
	Steam turbine	1000 (T ₁)	125 (P ₁)	6.7% to HX7																																																																									
		568 (T ₂)	11 (P ₂)	–																																																																									
Poultry		442 (T ₃)	5 (P ₃)	–		41.8 (T ₄)	0.08 (P ₄)	–	FBR	25	1	–	Bioreactor	55	1	–	Gas turbine	2430 (in)	8.2 (in)	–		1205 (out)	1 (out)	–	Steam turbine	1000 (T ₁)	125 (P ₁)	6.7% to HX7		568 (T ₂)	11 (P ₂)	–		442 (T ₃)	5 (P ₃)	–		41.8 (T ₄)	0.08 (P ₄)	–	Sheep	FBR	25	1	–	Bioreactor	55	1	–	Gas turbine	2337 (in)	15.6 (in)	–		896 (out)	1 (out)	–	Steam turbine	769.6 (T ₁)	95 (P ₁)	2.9% to HX7		439.1 (T ₂)	11 (P ₂)	–		329.6 (T ₃)	5 (P ₃)	–		73.0 (T ₄)	0.35 (P ₄)	–	FBR	25	1	–
		442 (T ₃)	5 (P ₃)	–																																																																									
		41.8 (T ₄)	0.08 (P ₄)	–																																																																									
	FBR	25	1	–																																																																									
	Bioreactor	55	1	–																																																																									
	Gas turbine	2430 (in)	8.2 (in)	–																																																																									
		1205 (out)	1 (out)	–																																																																									
	Steam turbine	1000 (T ₁)	125 (P ₁)	6.7% to HX7																																																																									
		568 (T ₂)	11 (P ₂)	–																																																																									
		442 (T ₃)	5 (P ₃)	–																																																																									
		41.8 (T ₄)	0.08 (P ₄)	–																																																																									
Sheep	FBR	25	1	–																																																																									
	Bioreactor	55	1	–																																																																									
	Gas turbine	2337 (in)	15.6 (in)	–																																																																									
		896 (out)	1 (out)	–																																																																									
	Steam turbine	769.6 (T ₁)	95 (P ₁)	2.9% to HX7																																																																									
		439.1 (T ₂)	11 (P ₂)	–																																																																									
		329.6 (T ₃)	5 (P ₃)	–																																																																									
		73.0 (T ₄)	0.35 (P ₄)	–																																																																									
	FBR	25	1	–																																																																									

3.4.1 Mass and energy balances

Table 3.4 shows the main operating conditions of major units for the four different manure types. Cattle, pig, and poultry show similar values among

them and to previous work (**Leon**). The gas in the gas turbine reaches a temperature of 2400 °C and a pressure of 8.2 bar before expansion for cattle, pig and poultry manure. However, sheep manure shows different values. While the temperature is similar, the pressure is 15.6 bar, almost twice the value found for the rest of the raw materials. Furthermore the flue gas exits the turbine 300 °C below that when the rest of the manure types are used. Furthermore while the high pressure of the steam turbine is 125 bar for cattle, pig, and poultry manure, in case of sheep manure the steam turbine operates at 95 bar at the high pressure section of the turbine. This is related to the lower gas temperature from the gas turbine since the overheated steam needs to be produced using that stream. Intermediate and low pressures are the same in the steam turbine using any of the manure types, but the exhaust pressure of the steam is higher in case of sheep manure. Table 3.5 shows the products obtained from the various manure types, power, biogas, and digestate. Poultry is the waste that is more efficient towards power production due to its higher concentration. In all cases an FBR reactor for the production of struvite is the selected technology to recover N and P. In the table we also see the effect of the fact that cattle and pig manure are mostly liquids, since most of the product is digestate, almost 98%, while the use of poultry or sheep manure reduces the production of digestate to 75% and 88% respectively, increasing the production of biogas and power. Finally in Table 3.6 the biogas composition for each manure considered are presented. The main purpose of the facility is the production of power. However, the biogas composition is typically within a range of values per component that have been imposed as bounds. As a result of maximizing the electricity production for all studied cases, the same biogas composition is obtained, 67.5% molar in CH₄ and the rest is mostly CO₂.

Table 3.5: Process optimization results for considered manures.

Manure	Power (kW)	Comp. biogas (CH ₄ /CO ₂ ratio)	Digestate treatment technology	Product recovered	Biogas/manure ratio	Digestate/manure ratio
Cattle	2,612	0.816	FBR struvite	Struvite	0.0208	0.9794
Pig	2,612	0.816	FBR struvite	Struvite	0.0208	0.9794
Poultry	31,349	0.818	FBR struvite	Struvite	0.2499	0.7526
Sheep	14,106	0.818 3.4	FBR struvite	Struvite	0.1217	0.8795

Table 3.6: Process optimization results for considered manures.

Manure	CH ₄ (%wt)	CO ₂ (%wt)	Water (%wt)	O ₂ (%wt)	N ₂ (%wt)
Cattle	0.385	0.470	0.120	0.006	0.020
Pig	0.385	0.470	0.120	0.006	0.020
Poultry	0.385	0.470	0.120	0.006	0.020
Sheep	0.385	0.470	0.120	0.006	0.020

3.4.2 Economic evaluation

This section is divided into the estimation of the investment cost, using a factorial method based on the cost of the units, and the estimation of the electricity production cost.

3.4.2.1 Investment cost

We use the factorial method to estimate the investment cost for this facility. This is based on the estimation of the equipment cost and several coefficients to account for pipes, installation, etc. (Sinnott and Towler, 2009). The cost for the different units has been estimated based on (**Matche**) website (www.matche.com), (**towler2009chemical**) and (**peters2003plant**), updating the cost of the units when required. We assume a plant that processes fluids and solids. Due to the different composition of each manure the specific production of biogas for each one is different, being larger for poultry and sheep than for cattle and pig. The reason for that could be that sheep and poultry manures have less water content while the water content in cattle and pig reaches 98% (<http://adlib.eversite.co.uk>). For cost estimation proposes the digester maximum size considered is 6,000 m³ per unit, since the larger units could face mixing and homogenization problems (**rohstoffe2010guia**). This result for the facility investment cost will be different for each raw material. Fig. 3.7 shows the equipment cost distribution where digester and gas turbine are the most important contributions:

- **Cattle manure:** a plant that processes 10 kg/s of this type of manure requires an investment of 69.1 M EUR, of which 14.9 M EUR represents the equipment cost. The larger cost is assumed by the digester units, with a 75% of the total units cost, followed by the heat exchanger network with a contribution of 12% while both turbines add up to 12%.

- **Pig manure:** a facility to process 10 kg/s of this manure requires an investment of 69.5 M EUR, with a cost of 14.9 M EUR in equipment. Since the digestate-manure and biogas-manure ratios between cattle and pig manure are very similar, the investment costs are analogous among them. The unit cost distribution is similar to the cattle manure case.
- **Poultry manure:** The investment for a plant that processes 10 kg/s of this manure is 208.0 M EUR. The units investment adds up to 44.7 M EUR. In this case the units cost distribution is more homogeneous among different items: 60% to digester units, 20% to gas turbine, 10% to heat exchanger network and 9% to steam turbine. It should be noted that, as poultry manure has a high content of dry matter (around 60% on a weight basis), it is necessary to add additional water to decrease the dry matter content to reach 25% with the aim of avoid mixing problems in the digester due to an excessive solids concentration inside.
- **Sheep manure:** The facility to treat 10 kg/s of this manure requires an investment of 105.0 M EUR, where 22.5 M EUR represents the equipment cost. For this plant the main units cost distribution is as follows: 50% for the digester, 25% for gas turbine, 17% for heat exchanger network and 7% for steam turbine.

It is clear that the digester shows the largest share in the investment cost and therefore the concentration of the manure highly determines the cost of the facility. **Iantzz2012economic** presented the investment cost of a facility for heat and power production as a function of its scale. Actually, our plant does not produce steam as a final product but only power. Thus, it is interesting to see that the raw material determines the investment per kW from the 4,000 EUR/kW in case of poultry manure or the 7,500 EUR/kW in case of sheep manure, to the more than 25,000 EUR/kW in case of pig and cattle.

3.4.2.2 *Production cost*

To calculate the production cost, 20 years of plant life is considered, with a capacity factor of 98%. Apart from the equipment amortization, other items are also taken into account such as salaries, administrative fees, chemicals cost, maintenance cost, utilities and contingency costs. Thus, apart from the annualized equipment cost, 1.5 M EUR are spent in salaries, 0.25 M EUR in Administration, 2 M EUR in Maintenance, 0.25 M EUR in other expenses (**Leon**) while chemicals are computed as described in

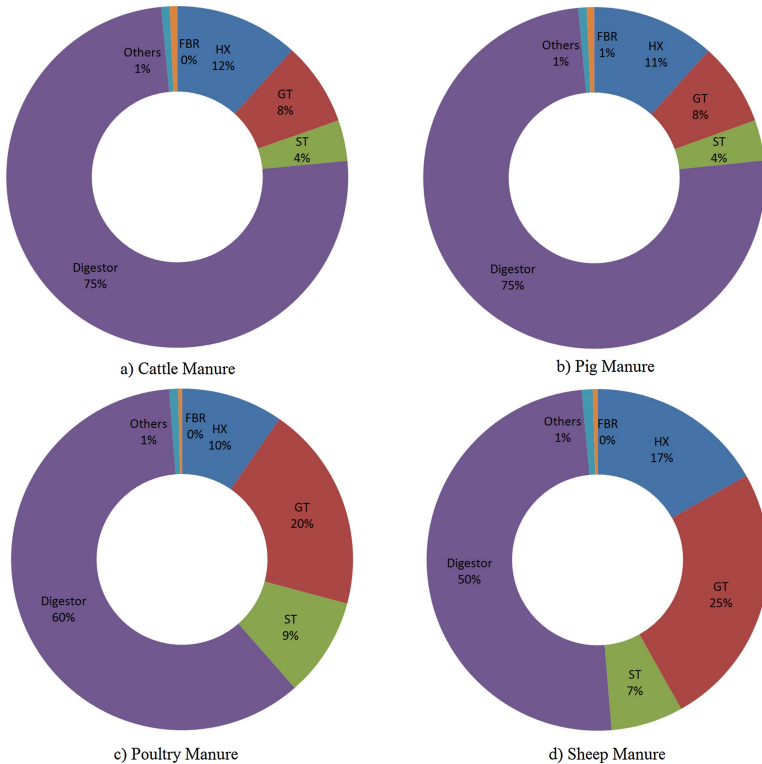


Figure 3.7: Units cost distributions for cattle, pig, poultry and sheep manure treatment (ST: steam turbine, GT: gas turbine, HX: heat exchangers, FBR: fluidized bed reactor).

Section 3.2. The cost of utilities adds up to 0.08 M EUR, accounting for the cooling water and the steam needed to maintain the operation of the digester and to condition the digestate for its use as a fertilizer. Finally, we assume that the livestock manure is for free. Fig. 3.8 shows the distribution of the production costs for each of the manure types. We see that the figures are very similar. The equipment amortization represents at least 43% of the production costs. This share increases up to 60% for the case of the use of poultry. As the investment is lower, the annual cost for other items is almost constant and their contribution to the electricity cost plays a more important role. Chemicals is the second most important contribution to the cost of electricity with a share of up to 23% for the use of cattle or pig manure and down to 16% in the case of sheep manure. We assume in all cases that waste is for free. Under these considerations the electricity production costs obtained are presented in Table 3.7.

The Net Profit Value has also been calculated as a measure of the project profitability, considering an electricity price of sale of 0.06 EUR/kWh. To compare the profitability of this project a secure investment as the inversion

in Spanish national debt has been chosen, considering a discount rate of 3% (**TesoroSpain**). The results obtained are presented in Table 3.7, and it should be noted that facilities for poultry and sheep manures obtain positive NPV while those which use cattle and pig manure as raw material show negative NPV, so from the point of view of NPV as an indicator to decide the project viability, those ones would be disregarded.

Table 3.7: Electricity production cost and NPV for the facility considering different raw materials.

Raw material	Annual production costs (M EUR /year)	Electricity production cost (EUR/kWh)	NPV (EUR /year)
Cattle manure	12.04	0.45	$-1.93 \cdot 10^7$
Pig manure	12.07	0.45	$-1.96 \cdot 10^7$
Poultry manure	25.51	0.03	$2.85 \cdot 10^8$
Sheep manure	15.53	0.10	$5.40 \cdot 10^7$

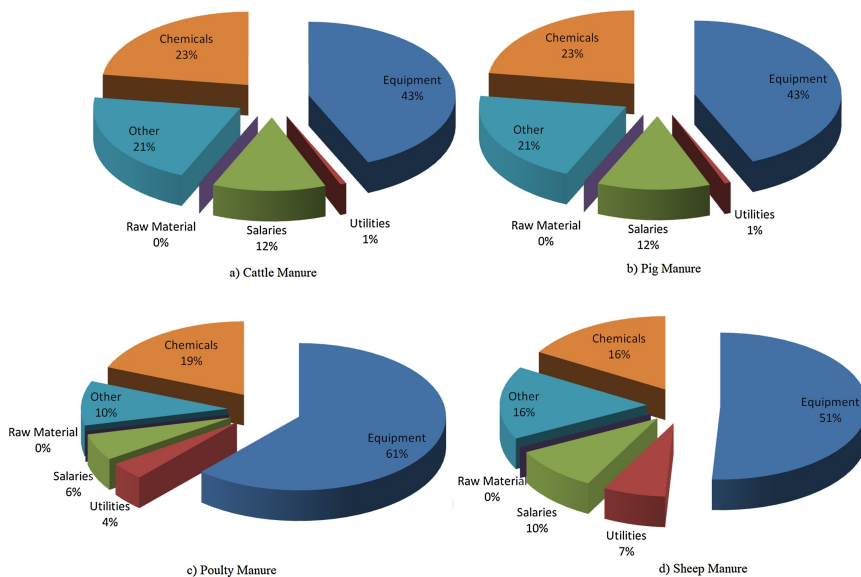


Figure 3.8: Operation cost distribution for cattle, pig, poultry and sheep manure treatment.

3.4.3 Effect on the power, operating conditions and digestate treatment

The results obtained from the treatment of different manure streams show the influence of the manure composition in the amount produced and the composition of biogas and digestate obtained. Struvite production

using FBR is the best choice for digestate treatment. This can be explained by the advantages in recovering nutrients in solid form since they can be easily transported and stored. Furthermore the material is highly concentrated in nutrients with a relatively high selling price. Biogas production is similar for cattle and pig manures, but is significantly higher in the poultry and sheep cases. The investment cost when processing cattle and pig manure is dominated by the digester, resulting in similar investment and production costs for facilities using either of the two types of manure. However, the higher concentration in organic matter in sheep and poultry manure does not only result in higher power production capacities, but the fact that the contribution to the cost of the turbines is also larger and so is the investment cost of these facilities. On the other hand, the electricity production cost is lower in the last two cases as result of the economies of scale between the investment cost and the biogas produced and the higher amount of struvite produced, with the extreme case of poultry manure where the struvite selling benefits are capable to cover the electricity production costs. Note that the availability of poultry and or sheep manure should be less than for cattle and pig manure.

3.5 CONCLUSIONS

In this work, we have designed optimal integrated facilities for the production of biogas-based electrical power and fertilizers from manure. Detailed equation based models for the anaerobic digestion, the Brayton and regenerative Rankine cycles and different technologies for digestate treatment have been developed. To solve the model a two-step procedure has been performed. First, the individual detailed models for each digestate treatment technology are used to formulate a MINLP model aiming at selecting the best configuration for that technology: the best precipitation agent, filter media, etc. In the second step, the best configuration of each technology has been implemented in the entire superstructure. Due to the fact that only one digestate processing technology is allowed and the highly non-linear nature of the model, surrogate models for the cost of each alternatives with a smooth approximations have been developed. For the optimal selection a detailed economic evaluation is performed. The results show that FBR technologies are preferred to recovery nutrients. Furthermore, in some cases this process can produce electricity at a competitive price (in case of poultry and sheep manure). The investment cost is highly dependent on the water and organic content of the manure type, ranging from 70 M EUR to 208 M EUR when a large energy production is possible and large gas and steam turbines are to be installed. However, for

these cases of higher investment cost, the production cost of power is the most competitive due to the large production capacity. Biogas power plants show a wide range of values of power per kW installed depending on the manure concentration. Competitive values of 4,000 EUR/kW for poultry manure are obtained, due to the highly concentrated manure, while large values of 25,000 EUR/kW installed are reported in case of the diluted cattle or pig manure.

NOMENCLATURE

Sets

- a $\in \{\text{H}_2\text{O}, \text{CH}_4, \text{CO}_2, \text{NH}_3, \text{H}_2\text{S}, \text{O}_2, \text{N}_2\}$
- a' $\in \{\text{CH}_4, \text{CO}_2, \text{NH}_3, \text{H}_2\text{S}, \text{O}_2, \text{N}_2\}$
- d $\in \{\text{C}, \text{N}_{\text{organic}}, \text{N}_{\text{NH}_3}, \text{P}, \text{K}, \text{H}_2\text{O}, \text{Rest}\}$
- e $\in \{\text{CH}_4, \text{NH}_3, \text{H}_2\text{S}\}$
- h $\in \{\text{CH}_4, \text{CO}_2, \text{O}_2, \text{N}_2\}$
- i $\in \{\text{P}, \text{N}\}$
- j $\in \{\text{filter media}\}$
- k $\in \{\text{TS}, \text{C}, \text{K}\}$

Parameters

- $A(i)$ Antoine A coefficient for vapor pressure of component i
- A_{specific} specific clarifier area ($\text{m}^2 / (\text{ton}\cdot\text{day})$)
- $B(i)$ Antoine B coefficient for vapor pressure of component i
- $C(i)$ Antoine C coefficient for vapor pressure of component i
- HRT_{unit} hydraulic retention time of *unit* (s)
- IAP_{eq} ion activity product equilibrium
- $MW_{\text{component}}$ molecular weight of *component* (kg/kmol)
- MeP_{ratio} metal/phosphorus molar ratio in coagulation process
- P_{atm} atmospheric pressure (1 bar)
- $Price_{\text{component}}$ price of *component* (EUR/kg)
- R ideal gas constant (8.314 J/mol·K)
- T_{atm} room temperature (25 °C)
- η_c compressors efficiency (0.85)
- η_i^j separation yield of component i in inprocess j

η_s	isentropic efficiency (0.9)
$\kappa_{agitator}$	agitator specific power consumed (HP / 1000 US gallon)
φ_j	precipitation agent j : total solids (mass ratio)
c_{pH_2O}	specific heat capacity of water (4.18 kJ/kg °C)
c_{psat}	specific heat capacity of flue gas
d	working days per year
d_p	particle diameter (m)
g	gravity acceleration (m^2/s)
h	working hours per day
k	kinetic constant (s^{-1})

Variables

A_{unit}	area of unit (m^2)
Ar_l	Arquimedes number for liquid
$Benefits_{technology}$	benefits or losses obtained with <i>technology</i>
$C : N$	carbon to nitrogen molar ratio
C_0	initial concentration (kmol/m ³)
$C_{component}^{unit}$	concentration of <i>component</i> in the <i>unit</i> inlet stream ($kg_{component}/kg_{total}$)
C_{eq}	equilibrium concentration (kmol/m ³)
$ChemC_{technology}$	cost of chemicals for <i>technology</i>
$Cost_{unit}$	cost of <i>unit</i>
D_{unit}	diameter of <i>unit</i>
$E_{cj}(T)$	equilibrium constant of component j at temperature T
$FC_{technology}$	fixed cost of <i>technology</i>
$F_{unit,unit1}$	mass flow from stream from <i>unit</i> to <i>unit1</i> (kg/s)
$F_{component}^{unit}$	mass flow of <i>component</i> in the <i>unit</i> inlet stream (kg/s)
F_{design}^{unit}	mass inlet flow used in the design of <i>unit</i> (kg/s)
F_{max}^{unit}	maximum mass inlet flow admitted by a single <i>unit</i> (kg/s)
$F_{recovered}^{total}$	recovered matter total mass flow (kg/s)
$H_b^{unit,unit1}$	enthalpy of the stream at state b from <i>unit</i> to <i>unit1</i> (kJ/kg)
$H_{steam(isoentropy)}$	isentropic expansion enthalpy of steam (kJ/kg)
K_{index}	potassium index of fertilizer
L_{unit}	length of <i>unit</i>

N_{NH_3}	nitrogen contained in ammonia
N_{index}	nitrogen index of fertilizer
N_{org}	nitrogen contained in organic matter
$P_j^*(T)$	saturation pressure of pure component j at temperature T (bar)
P_v	vapor pressure (bar)
$P_{in/compressor}$	inlet pressure to compressor (bar)
P_{index}	phosphorous index of fertilizer
$P_{out/compressor}$	outlet pressure of compressor (bar)
P_{unit}	power of unit
$Q_{(unit)}$	heat exchanged in <i>unit</i> (kW)
$R_{C-N/fertilizer}$	carbon to nitrogen ratio in fertilizer
$R_{C-N/k}$	carbon to nitrogen ratio in <i>k</i>
$R_{V-F/i}$	rate of evaporation in equilibrium system <i>i</i>
$Re_{l,mf}$	Reynolds number for liquid in minimum fluidization conditions
<i>Rest</i>	rest of the elements contained in the biomass
$T_{(unit,unit1)}$	temperature of the stream from <i>unit</i> to <i>unit1</i> (°C)
$T_{bubble/i}$	bubble point temperature of equilibrium system <i>i</i> (°C)
$T_{in/compressor}$	inlet temperature to compressor (°C)
$T_{m/i}$	average temperature in equilibrium system <i>i</i> (°C)
$T_{out/compressor}$	outlet temperature of compressor (°C)
$T_{turb,i,min}^*$	saturated temperature at exit of body <i>i</i> (°C)
$V_{biogas,k}$	biogas volume produced per unit of volatile solids (VS) associated to waste <i>k</i> ($m^3_{biogas}/kg_{VS/k}$)
V_{unit}	volume of <i>unit</i>
W_{unit}	weight of <i>unit</i>
W_{unit}	power produced or consumed in <i>unit</i> (kW)
$Y_{a',biogas-dry}$	molar fraction of component <i>a</i> in the dry biogas
Z	objective function
$\Delta H_{comb,digestate-dry}$	heat of combustion of dry digestate (kW)
$\Delta H_{comb,e}$	heat of combustion of component <i>e</i> (kW)
$\Delta H_{comb,k}$	heat of combustion of component <i>k</i> (kW)
$\Delta H_{f,h}(T)$	heat of formation of component <i>h</i> at temperature T (kW)
$\Delta H_{reaction(bioreactor)}$	reaction heat of anaerobic digestion (kW)

α_{mf}	parameter dependent of the number of phases in the FBR
$\mu_{component}$	viscosity of component ($\text{kg}/(\text{m}\cdot\text{s})$)
$\rho_{component}$	density of <i>component</i> (kg/m^3)
$a_{technology}$	selection parameter which takes value 0 when $F_{design}^{technology}$ is 0 and 1 if $F_{design}^{technology}$ is not equal to 0
e_{unit}	thickness of <i>unit</i>
$fc_j^{unit,unit1}$	mass flow of component <i>j</i> from <i>unit</i> to <i>unit1</i> (kg/s)
l_{j-i}	molar fraction of component <i>j</i> in the liquid phase of equilibrium system <i>i</i>
$n_{(unit,unit1)}$	total mol flow from stream from <i>unit</i> to <i>unit1</i> (kmol/s)
n_{unit}	number of units used in the process
$p_{turb,i}$	inlet pressure to body <i>i</i> in the turbine (bar)
$s_{b,(unit,unit1)}$	entropy the stream at the state <i>b</i> for the stream from <i>unit</i> to <i>unit1</i> ($\text{kJ}/\text{kg}\cdot\text{K}$)
t	time (s)
u_0	fluid velocity (m/s)
u_t	terminal velocity (m/s)
u_{mf}	minimum fluidization velocity (m/s)
v_{j-i}	molar fraction of component <i>j</i> in the vapor phase of equilibrium system <i>i</i>
$w'_{C/k}$	dry mass fraction of C in <i>k</i> ($\text{kg}_{C/k}/\text{kg}_{DM/k}$)
$w'_{DM/k}$	dry mass fraction of <i>k</i> ($\text{kg}_{DM/k}/\text{kg}$)
$w'_{K/k}$	dry mass fraction of K in <i>k</i> ($\text{kg}_{K/k}/\text{kg}_{DM/k}$)
$w'_{NH_3/k}$	dry mass fraction of NH_3 in <i>k</i> ($\text{kg}_{NH_3/k}/\text{kg}_{DM/k}$)
$w'_{N_{org}/k}$	dry mass fraction of N_{org} in <i>k</i> ($\text{kg}_{N_{org}/k}/\text{kg}_{DM/k}$)
$w'_{P/k}$	dry mass fraction of P in <i>k</i> ($\text{kg}_{P/k}/\text{kg}_{DM/k}$)
$w'_{Rest/k}$	dry mass fraction of the rest of the elements contained in <i>k</i> ($\text{kg}_{Rest/k}/\text{kg}_{DM/k}$)
$w'_{Rest/k}$	dry mass fraction of the rest of the elements contained in <i>k</i> ($\text{kg}_{Rest/k}/\text{kg}_{DM/k}$)
$w'_{Rest/k}$	dry mass fraction of the rest of the elements contained in <i>k</i> ($\text{kg}_{Rest/k}/\text{kg}_{DM/k}$)
$w'_{VS/k}$	dry mass fraction of volatile solids out of the dry mass of <i>k</i> ($\text{kg}_{VS/k}/\text{kg}_{DM/k}$)
$x_{a/biogas}$	mass fraction of component <i>a</i> in the biogas

y^j	binary variable to evaluate the element j
y_{biogas}	specific saturated moisture of biogas

ACKNOWLEDGMENTS

We acknowledge funding from the National Science Foundation (under grant CBET-1604374) and MINECO (under grant DPI2015-67341-C2-1-R) and E.M. also acknowledges an undergraduate research grant.

BIBLIOGRAPHY

GEOSPATIAL ASSESSMENT OF PHOSPHORUS RECOVERY THROUGH THE DEPLOYMENT OF STRUVITE PRECIPITATION SYSTEMS

ABSTRACT

Nutrient pollution is one of the major worldwide water quality problems, resulting in environmental and public health issues. Agricultural activities are the main source of nutrient release emissions, and the livestock industry has been proven to be directly related to the presence of high concentrations of phosphorus in the soil, which potentially can reach water-bodies by runoff. To mitigate the phosphorus pollution of aquatic systems, the implementation of nutrient recovery processes allows the capture of phosphorus, preventing its release into the environment. Particularly, the use of struvite precipitation produces a phosphorus-based mineral that is easy to transport, enabling redistribution of phosphorus to deficient locations. However, livestock leachate presents some characteristics that hinder struvite precipitation, preventing extrapolation of the results obtained from wastewater studies to cattle waste. Consideration of these elements is essential to determine the optimal operating conditions for struvite formation, and for predicting the amount of struvite recovered. In this work, a detailed thermodynamic model for precipitates formation from cattle waste is used to develop surrogate models to predict the formation of struvite and calcium precipitates from cattle waste. The variability in the organic waste composition, and how it affects the production of struvite, is captured through a probability framework based on the Monte Carlo method embedded in the model. Consistent with the developed surrogate models, the potential of struvite production to reduce the phosphorus releases from the cattle industry to watersheds in the United States has been assessed. Also, the more vulnerable locations to nutrient pollution were determined using the techno-ecological synergy sustainability metric (TES) by evaluating the spatial distribution and balance of phosphorus from agricultural activities. Although only struvite formation from cattle operations is considered, reductions between 22% and 36% of the total phosphorus releases from the agricultural sector, including manure releases and fertilizer application, can be achieved.

Keywords: Organic waste; Phosphorus; Nutrient pollution; Struvite; Thermodynamics

RESUMEN

La contaminación por nutrientes es uno de los principales problemas de calidad del agua en todo el mundo, lo que provoca problemas medioambientales y de salud pública. Las actividades agrícolas son la principal fuente de emisión de nutrientes, y se ha demostrado que la industria ganadera está directamente relacionada con la presencia de altas concentraciones de fósforo en el suelo, que potencialmente pueden llegar a las masas de agua por escorrentía. Para mitigar la contaminación por fósforo de los sistemas acuáticos, la implementación de procesos de recuperación de nutrientes permite la captura de fósforo, evitando su liberación al medio ambiente. En particular, el uso de la precipitación de estruvita produce un mineral a base de fósforo que es fácil de transportar, lo que permite la redistribución del fósforo a lugares deficientes. Sin embargo, los lixiviados ganaderos presentan algunas características que dificultan la precipitación de estruvita, impidiendo la extrapolación de los resultados obtenidos en los estudios de aguas residuales a los residuos ganaderos. La consideración de estos elementos es esencial para determinar las condiciones óptimas de operación para la formación de estruvita, y para predecir la cantidad de estruvita recuperada. En este trabajo, se utiliza un modelo termodinámico detallado para la formación de precipitados a partir de residuos ganaderos con el fin de desarrollar modelos sustitutos para predecir la formación de estruvita y precipitados de calcio a partir de residuos ganaderos. La variabilidad en la composición de los residuos orgánicos, y cómo afecta a la producción de estruvita, se capta a través de un marco probabilístico basado en el método de Monte Carlo integrado en el modelo. En consonancia con los modelos sustitutos desarrollados, se ha evaluado el potencial de la producción de estruvita para reducir las emisiones de fósforo de la industria ganadera a las cuencas hidrográficas de Estados Unidos. Asimismo, se determinaron los lugares más vulnerables a la contaminación por nutrientes utilizando la métrica de sostenibilidad de la sinergia tecno-ecológica (TES) mediante la evaluación de la distribución espacial y el equilibrio del fósforo procedente de las actividades agrícolas. Aunque sólo se tiene en cuenta la formación de estruvita procedente de las explotaciones ganaderas, se pueden conseguir reducciones de entre el 22% y el 36% del total de las emisiones de fósforo procedentes del sector agrícola, incluidas las emisiones de estiércol y la aplicación de fertilizantes.

Palabras clave: Residuos orgánicos; Fósforo; Contaminación por nutrientes; Estruvita; Termodinámica

4.1 INTRODUCTION

Livestock farming and other agricultural activities have altered the natural nutrient cycles. Phosphorus, one of the three plant-grow macronutrients, enters to the global cycle as phosphate rock, which through erosion and chemical weathering is transferred to soils and waterbodies. Also, phosphorus deposited in soils will reach fresh and marine waterbodies by runoff. Phosphorus in rivers is transported to stagnant waterbodies (such as lakes) and oceans, reaching the bottom of lakes and oceans as sediments. The cycle is closed when the buried phosphorus is uplifted again by tectonic processes. Along the cycle, phosphorus can be taken by plants and algae, but after the death of living organisms it returns to the cycle (**RUTTENBERG2001401**). This global natural cycle is largely altered by human activities through the mining and shipping of phosphate rock, mainly for fertilizer production, resulting in unbalanced phosphorus releases to the environment.

Nutrient pollution from anthropogenic sources has become as a critical worldwide water quality problems. Nutrient contamination results in environmental and public health issues as a result of the exponential growth of algae, cyanobacteria, and the occurrence of harmful algal blooms (HABs), which turns into dead zones and hypoxia due to the aerobic degradation of the algal biomass by bacteria; shifting the distribution of aquatic species and releasing toxins in drinking water (**Sampatz2**). In addition, the development of HABs and eutrophication processes contributes to climate change through the emission of large amounts of strong greenhouse gases such as CH₄ and N₂O (**Beaulieu**).

However, phosphorus is a limited non-renewable resource, essential nutrient to support life, and widely used as fertilizer to increase crop yields. Actually, phosphorus is one of the most sensitive elements to depletion, as it is a key agricultural fertilizer that has no known substitute. Current global reserves of phosphate rock could be depleted in the next 50 to 100 years (**Cordell**). Therefore, the development of a circular economy around phosphorus capable of recovering the nutrient and reintegrating it into the productive cycle is not only desirable but also a necessary measure to reach sustainable development. Agricultural activities are the main source of nutrients in waterbodies (**Dzombak**), and among them, livestock industry is one of the largest economic sectors. Additionally, the increasing income-spending potential of the middle class in developing countries has increased the demand for dairy and beef products, resulting in the generation of large amounts of livestock organic waste. Considering that an average dairy cow generates 51.19 kg of raw manure per day (**USDAWaste**), the total phosphorus excreted is 11.02 kg per year per

animal, equivalent to 5.96 kg of phosphorus as phosphate per year per animal. In the U.S. as of January 2020, a total of 94.4 million head has been reported (**USDAcattle2020**). Thus, this shows potential phosphate U.S. releases of $562.6 \cdot 10^6$ kg/yr. **Sampat** presented the link between the presence of livestock facilities and larger concentrations of phosphorus in soil, which potentially can be lost as runoff reaching waterbodies. For animals on pasture, organic waste should not be a resource of concern if stocking rates are not excessive. However, for concentrate animal feeding operations (CAFOs), manure should be correctly managed due to the high rates and spatial concentration of the organic waste generated, representing potential environmental issues. Usually, manure is collected in the animal living zones, and stored as liquid or slurry to be further spread in croplands as nutrient supplementation; or as solid in dry stacking or composting facilities to be sold as compost. Liquid fraction of manure can be also treated in aerobic or anaerobic ponds. However, these approaches do not allow a correct nutrient management since nutrients concentration is variable and not well defined, and nitrogen and phosphorus are unbalanced regarding the nutrient necessities of plants, i.e., if nitrogen demand is covered, there is a surplus in the phosphorus supply which can runoff to waterbodies, and if phosphorus demand is covered, there is a deficit in the nitrogen supply, being necessary to apply additional fertilizers. In addition, during rainy periods the applied manure can runoff, dragging the nutrients contained in it. Nonetheless, phosphorus from liquid cattle waste, either processed in an anaerobic digestion stage or raw waste, can be potentially recovered through different processes (**muhmood2019formation**), reducing the nutrient inputs to waterbodies and its consequential environmental, economic, and social impacts. Among these, it is found that struvite production is one of the most promising cost-effective choices for the recovery of nutrients from cattle waste (**Martin**). Struvite is a phosphate-based mineral, which can be applied as a slow release fertilizer (**Richards**), allowing the redistribution of phosphorus from livestock facilities to nutrient-deficient locations.

Previous studies report struvite formation from different sources of waste, such as municipal wastewater treatment plants (**Battistoni**), mineral fertilizer industry (**Matynia**), or agricultural industry (**Shashvatt**). Thermodynamic models representing the formation of struvite and other precipitates have been also developed for various wastes including liquid swine manure (**celen_using_2007**), human urine (**Harada; ronteltap_struvite_2007**), and municipal wastewater (**rahaman_modeling_2014**). Additionally, some complex approaches considering the hydrodynamic and kinetic effects in the formation of struvite have been studied but limited to wastewater treatment (**rahaman_modeling_2014; mangin2004fluid**). However, the results

obtained from those studies cannot be extrapolated to struvite formation from cattle organic waste, since these residues have some characteristics that hinder struvite formation, including high ionic strength, which reduces the effective concentration of ions; the presence of calcium ions competing for phosphate ions (Yan), which inhibits a selective recovery by nutrient precipitation techniques; and the high variability in the manure composition, as a function of the geographical area, the animal feed, etc. (Tao). Other controlling factors are the pH level, the magnesium-phosphorus ratio, and the alkalinity of the leachate. Therefore, for an accurate prediction of struvite formation from this waste, it is necessary to include within the thermodynamic model structure for precipitates formation the specific features of cattle waste described above.

In this work, specific surrogate models to predict the production of struvite and calcium precipitates from cattle leachate are developed based on a detailed and robust thermodynamic model. In addition, the variability in the organic waste composition is captured through a probability framework based on Monte Carlo method. The reduced models obtained are used to evaluate the potential of struvite production from cattle waste to mitigate phosphorus releases in watersheds of the United States. Future applications of the developed surrogate models include the development of applications for environmental assessment and the design of policies to prevent nutrient releases, among others.

4.2 METHODS

4.2.1 *Spatial resolution*

A watershed is an area of land which drains all the streams and rainfall to a common drainage, defining the spatial boundaries for the collection of lost elements as runoff. The surface water drainages of the U.S. are identified by the U.S. Geological Survey through the Hydrologic Unit Code system (HUC). The HUC system is a hierarchical system indicated by the number of digits in groups of two, with six levels identified by codes from 2 to 12 digits (i.e., HUC₂ to HUC₁₂). These levels refer to regions, subregions, basins, subbasins, watersheds, and subwatersheds. The spatial resolution of this study is the continental United States at watershed scale, considering the boundaries defined by the Hydrologic Unit Code system at 8 digits (HUC8), representing the subbasin level (**HUC8**).

4.2.2 Assessment of anthropogenic phosphorus from agricultural activities

4.2.2.1 Phosphorus releases

Agricultural emissions are one of the main sources of anthropogenic P releases due to the excessive use of commercial fertilizers and livestock manure for cropland nutrients needs and the uncontrolled nutrient runoff to waterbodies, although for some areas urban source releases can contribute significantly to the total P releases to the environment. However, this analysis is limited to the evaluation of phosphorus releases from agricultural activities (**Dzombak; Alexander_2008; SPARROW_report_1999**).

Watershed phosphorus releases (E_x) are computed as the sum of the phosphorus releases from fertilizer applications to croplands and from the manure generated by livestock facilities. The releases of phosphorus to each watershed by manure emissions, accounting cattle, swine and poultry, and by fertilizers application, is reported by the IPNI NuGIS project. This is consistent with the most recent data available (year 2014) for fertilizers sales provided by the Association of American Plant Food Control Officials (AAPFCO), fitting the data to HUC8 watershed boundaries. More information about the methodology used for the estimation of agricultural phosphorus releases can be found in (**NuGIS**). Phosphorus content for several commercial phosphate fertilizers and different manure types can be found in **OSU2017** and **OSU2005** respectively.

4.2.2.2 Phosphorus uptakes

The elements considered for phosphorus uptake are the crops sown and managed by humans in each watershed. Additionally, the phosphorus retained by wetlands has been considered in the phosphorus balance. The phosphorus uptake by each type of vegetation at watershed level is computed as the product of the land area occupied, the grow yields per area unit and the phosphorus uptake per plant mass unit. Therefore, the total watershed phosphorus uptake (U_x) is computed as the sum of the phosphorus uptake by each type of plant, Eq. 4.1.

$$U_x = \sum^i \text{Area}_i \cdot \text{Yield}_i \cdot P_{\text{uptake } i} \quad \forall i \in \text{Plant varieties} \quad (4.1)$$

Since different crops have different phosphorus uptakes and yield rates, the amount of each type of crop is estimated for each watershed. To determine the land cover uses, accounting croplands, pasturelands, wetlands and developed areas (urban areas), information available for the most recent year (2011) from the U.S. Environmental Protection Agency's (U.S.

EPA) EnviroAtlas database is used (**EnviroAtlas**). Data from EnviroAtlas is provided with higher spatial resolution, at HUC12 level. To ensure spatial consistency, the data is reconciled at HUC8 level. Once the land uses of each watershed are known, data from the 2017 U.S. Census of Agriculture is used to determine the distribution of crops on croplands, considering corn, soybeans, small grains, cotton, rice, vegetables, orchards, greenhouse and other crops (namely oil crops, sugar crops, and fruits) (**2017CensusofAgriculture**). The data provided by the U.S. Census of Agriculture have a spatial resolution of HUC6. Therefore, it is reconciled at HUC8 level scaling by the area fraction represented by each HUC8 watershed over the total HUC6 hydrologic unit. If two or more crops were harvested from the same land during the year (double cropping), the area was counted for each crop. To determine the nutrients uptake of each type of crop, data from the U.S. Department of Agriculture (USDA) Waste Management field Handbook is considered (**USDAWaste**). For croplands, the specific nutrient uptake values are used for corn, soybeans, cotton, rice and orchards, while average values including the most representative species are used for small grains, vegetables, greenhouse crops, pasture crops, and forest. For pasture lands the average nutrient uptake and crop yield including the main pasture crops: alfalfa, switchgrass and wheatgrass; for forests lands the nutrient uptake and crop yield of Northern hardwoods is considered, and for developed areas null nutrient uptake is considered. The wetlands phosphorus uptake value considered is $0.77 \text{ gP m}^{-2} \text{ year}^{-1}$, based in the data reported by **Kadlec**.

4.2.2.3 Phosphorus balance

To reach environmental sustainability of a productive activity, the releases of phosphorus should be balanced with the phosphorus uptakes from that activity, reducing the impact over the original ecosystems as much as possible. To evaluate the balance of phosphorus releases involved in agricultural activities throughout the U.S. watersheds, the techno-ecological synergy (TES) sustainability metric proposed by **TESmetric** has been considered, Eq. 5.1. A negative value of V_x indicates that the emissions, (E_x), are larger than the uptake capacity of the agricultural activities, (U_x), impacting the ecosystems, while positive values reflect that the releases are lower than the uptake capacity.

$$V_x = \frac{(U_x - E_x)}{E_x} \quad (4.2)$$

4.2.3 *Thermodynamic model for precipitates formation*

The behavior of cattle leachate system has been evaluated through a thermodynamic model, evaluating the formation of different precipitates through chemical equilibrium and material balances, capturing the mutual dependencies based on the competition for the same ions. Four aqueous chemical systems have been considered, water, ammonium, phosphoric acid, and carbonates systems. Moreover, the formation of seven possible precipitates is evaluated: struvite, K-struvite, magnesium hydroxide, calcium hydroxide, calcium carbonate, hydroxyapatite, dicalcium phosphate, and tricalcium phosphate.

4.2.3.1 *Uncertainty in livestock organic waste composition*

The variability in the composition of raw material creates operational difficulties that any material recovery process must deal with. The composition of cattle organic waste depends on multiple factors, among which are livestock feed, geographical area, climate, and other local factors of the livestock operation (**Tao**). Several elements of cattle manure composition play an active role in the formation of struvite and other precipitates. These include the high ionic strength, which reduces the effective concentration of ions; and the distribution ratios between calcium, ammonia and phosphate; and the leachate alkalinity, affecting the chemical equilibrium. To capture the uncertainty generated by the variability in the composition of cattle leachate, 37 data sets of 20 literature references containing the mass fraction of different elements comprising organic livestock waste are evaluated. To estimate feasible cattle leachate compositions, the probability density distribution of each element is calculated by fitting it to the kernel density estimate (KDEs). The selected probability density distributions are normal distribution, as shown in Eq. 4.3, for the distribution of nitrogen, nitrogen as ammonia/total nitrogen ratio, and phosphorus; and lognormal distribution, as defined by Eq. 4.4, for phosphorus as phosphate/total phosphorus ratio, calcium, and potassium. The probability density distribution parameters for each evaluated compound are collected in Table 4.1, where σ is the standard deviation, σ^2 is the variance, μ is the mean of the distribution, M is equal to e^μ , and γ is a displacement parameter. Kernel density estimations and probability density distributions for each element evaluated can be found in the Supplementary Material.

The uncertainty in the composition of cattle waste is addressed through the evaluation of the thermodynamic model described in the following sections for multiple cattle waste compositions generated including the

probability density distribution of each elements in a Monte Carlo model (**Thomopoulos**).

$$f(x) = \frac{1}{\sqrt{2\pi}\sigma} e^{-\frac{(x-\mu)^2}{2\sigma^2}} \quad (4.3)$$

$$f(x) = \frac{\frac{1}{\frac{x-\gamma}{M}\sigma\sqrt{2\pi}} e^{-\frac{\ln(\frac{x-\gamma}{M})^2}{2\sigma^2}}}{M} \quad (4.4)$$

Table 4.1: Probability density distributions parameters for cattle organic waste elements.

Param.	Normal distribution			Param.	Lognormal distribution		
	N	N-NH ₄ ⁺ : N _{total}	P		P-PO ₄ ³⁻ : P _{total}	Ca	K
μ	0.3841	0.6200	0.04000	M	42.15	0.08000	0.2600
σ	0.1309	0.1250	0.03684	σ	0.0040	0.4500	0.8000
				γ	-41.53	0.04044	0.03389

4.2.3.2 Initial conditions

A set of initial conditions must be defined to establish the physico-chemical characteristics of the livestock organic material (**Tao**), see Table 4.2. Please note that pH refers the adjusted pH for optimal struvite precipitation (**Tao; Zeng**).

4.2.3.3 Activities

Since the cattle waste is a highly non-ideal media due to the high concentrations of dissolved ions, activities instead of molar concentrations are used in the model. Activity coefficients (γ_x) for a element x are calculated using the Debye-Hückel relationship, Eq. 4.6, which relates activity coefficient, temperature, and ionic strength, calculated using Eq. 4.5. Eq. 4.7 is employed to estimate the parameter A (**Tao; Metcalf**). Finally, activities for each compound are calculated using Eq. 4.8

Table 4.2: Initial conditions of the livestock organic material system

Variable	Value	Unit
Temperature	298	K
pH	9	-
Electrical conductivity (<i>EC</i>)	18,800	$\frac{\mu\text{S}}{\text{cm}}$
Alkalinity	3000-14500	mg of CaCO_3
$[\text{Ca}^{2+}]$	0.075-0.175 (determined by Monte Carlo model)	% wt wet
$[\text{K}^+]$	0.10-0.65 (determined by Monte Carlo model)	% wt wet
$[\text{P-PO}_4^{3-}]$	0.001-0.024 (determined by Monte Carlo model)	% wt wet
$[\text{N-NH}_4^+]$	0.015-0.64 (determined by Monte Carlo model)	% wt wet
$[\text{Mg}^{2+}]$	0-10	$\text{Mg}^{2+}/\text{PO}_4^{3-}$ molar ratio

$$I = 1.6 \cdot 10^{-5} \cdot EC, \quad I(M), \quad EC \left(\frac{\mu\text{S}}{\text{cm}} \right) \quad (4.5)$$

$$\log_{10}(\gamma_x) = -A \cdot z_x^2 \cdot \left(\frac{\sqrt{I}}{1 + \sqrt{I}} \right) - 0.3 \cdot I \quad (4.6)$$

$$A = 0.486 - 6.07 \cdot 10^{-4} \cdot T + 6.43 \cdot 10^{-6} \cdot T^2, \quad T(K) \quad (4.7)$$

$$\{x\} = [x] \cdot \gamma_x \quad (4.8)$$

4.2.3.4 Distribution of species in aqueous phase

The distribution of species for ammonia, water, phosphoric acid, and carbonate systems in cattle leachate is determined by chemical equilibria:

$$\sum_j n_j \text{Reactant}_j \leftrightarrow \sum_k m_k \text{Product}_k \quad (4.9)$$

where n_j and m_k are the stoichiometric coefficients of the reactants and products respectively, and defining J as the set of chemical systems described in Table 4.3 for water, ammonia, and phosphoric acid systems, the thermodynamic equilibrium is defined for all the elements of the set as shown in Eq. 4.10. In combination with the material balances, Eq. 4.11, these define the chemical equilibrium for all the elements of the set. The description of the model for carbonate system is detailed in the Supplementary Material, and pK values are collected in Table 4.3.

$$K_J = \frac{\left(\prod_k \{Products\}_k^{m_k}\right)_J}{\left(\prod_j \{Reactants\}_j^{n_j}\right)_J} \quad (4.10)$$

$$[i]_J^{initial} = \sum_J [Compounds]_J \quad (4.11)$$

Table 4.3: pK_{sp} values for the considered aqueous phase chemical systems.

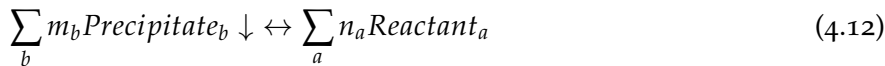
Name	Chemical system	pK	Source
Ammonia	$\text{NH}_4^+ \leftrightarrow \text{NH}_3 + \text{H}^+$	9.2	(Bates)
Water	$\text{H}_2\text{O} \leftrightarrow \text{OH}^- + \text{H}^+$	14	(Skoog)
Phosphoric acid	$\text{H}_3\text{PO}_4 \leftrightarrow \text{H}_2\text{PO}_4^- + \text{H}^+$	2.1	(Ohlinger)
	$\text{H}_2\text{PO}_4^- \leftrightarrow \text{HPO}_4^{2-} + \text{H}^+$	7.2	(Ohlinger)
Carbonic acid	$\text{HPO}_4^{2-} \leftrightarrow \text{PO}_4^{3-} + \text{H}^+$	12.35	(Ohlinger)
	$\text{H}_2\text{CO}_3 \leftrightarrow \text{HCO}_3^- + \text{H}^+$	6.35	(Skoog)
	$\text{HCO}_3^- \leftrightarrow \text{CO}_3^{2-} + \text{H}^+$	10.33	(Skoog)

4.2.3.5 Precipitates formation

Table 4.4: Solids species considered in this work.

Name	Chemical system	pK_{sp}	Source
Struvite	$\text{MgNH}_4\text{PO}_4 \cdot 6\text{H}_2\text{O} \leftrightarrow \text{Mg}^{2+} + \text{NH}_4^+ + \text{PO}_4^{3-}$	13.26	(Ohlinger)
K-struvite	$\text{MgKPO}_4 \cdot 6\text{H}_2\text{O} \leftrightarrow \text{Mg}^{2+} + \text{K}^+ + \text{PO}_4^{3-}$	10.6	(TaylorAW)
Hydroxyapatite	$\text{Ca}_5(\text{PO}_4)_3\text{OH} \leftrightarrow 5\text{Ca}^{2+} + 3\text{PO}_4^{3-} + \text{OH}^-$	44.33	(Brezonik)
Calcium carbonate	$\text{CaCO}_3 \leftrightarrow \text{Ca}^{2+} + \text{CO}_3^{2-}$	8.48	(Morse)
Tricalcium phosphate	$\text{Ca}_3(\text{PO}_4)_2 \leftrightarrow 3\text{Ca}^{2+} + 2\text{PO}_4^{3-}$	25.50	(Fowler)
Dicalcium phosphate	$\text{CaHPO}_4 \leftrightarrow \text{Ca}^{2+} + \text{HPO}_4^{2-}$	6.57	(Gregory)
Calcium hydroxide	$\text{Ca}(\text{OH})_2 \leftrightarrow \text{Ca}^{2+} + 2\text{OH}^-$	5.19	(Skoog)
Magnesium hydroxide	$\text{Mg}(\text{OH})_2 \leftrightarrow \text{Mg}^{2+} + 2\text{OH}^-$	11.15	(Skoog)

The precipitates that can be potentially formed from cattle waste have been selected based on the precipitates reported by previous studies (**Tao; Harada; gadekar2010validation**). A general solubility equilibrium, where n_a and m_b are the stoichiometric coefficients of the reactants and solid products respectively, can be written as:



The solid species considered in this study and their corresponding pK_{sp} values are shown in Table 4.4. These are the main precipitates that can be formed from the ions found in the cattle leachate. Considering the activity of solid species is equal to 1, and defining L as the set of chemical systems described in Table 4.4, the solubility equilibrium is defined for all the elements of the set as shown in Eq. 4.13.

The supersaturation index (Ω) is defined as the ratio between the ion activity product and the solubility product (K_{sp}), as shown in Eq. 4.14 (**Tao**). Therefore, the value of Ω determines if a compound precipitates. A saturation index $\Omega > 1$ indicates supersaturated conditions where precipitate may form, $\Omega = 1$ indicates equilibrium between solid and liquid phases, and $\Omega < 1$ indicates unsaturated conditions where no precipitate can form.

The higher value of the supersaturation index, the larger formation potential of a precipitate. Therefore, the sequence for the precipitation of different species can be set by comparing the supersaturation index values. The amount of solid species generated is computed through material balances, Eq. 4.15.

$$K_{sp_L} = (\prod \{\text{Reactants}\}_a^{n_a})_L \quad (4.13)$$

$$\Omega_L = \frac{(\prod \{\text{Reactants}\}_a^{n_a})_L}{K_{sp_L}} \quad (4.14)$$

$$[i]_L^{initial} = \sum_L [\text{Compounds}]_L \quad (4.15)$$

$$i \in \{\text{NH}_4^+, \text{Ca}^{2+}, \text{Mg}^{2+}, \text{PO}_4^{3-}, \text{CO}_3^{2-}\}$$

4.2.3.6 Thermodynamic model algorithm

Figure 4.1 shows a flowchart describing the proposed algorithm to solve the thermodynamic model of solid compound formation in cattle organic waste. In step *a*, the operating conditions and the initial molar

concentrations of Ca^{2+} , K^+ , Mg^{2+} , NH_4^+ , and PO_4^{3-} in cattle leachate are defined as described previously. In step *b*, ionic strength and activity coefficients are computed. Next, in steps *c* and *d*, two parallel problems are solved, the equilibrium of the aqueous species, and the alkalinity problem to determine the distribution of carbonates. After determining the concentration of all species in the organic waste, the supersaturation index for all species is computed in step *e*. The compound with the maximum supersaturation index is assumed to precipitate first. The amount of formed precipitate is computed by solving the solubility equilibrium and the material balance. As a result of the precipitate formation, the concentration of some species in aqueous phase is reduced. Therefore, the equilibrium of the aqueous species and the alkalinity problem must be recalculated, to obtain the new concentration values of the different compounds in the waste, and the iterative process, starts again.

The iterative process runs until each component saturation index is equal or less than one, and the formation of the precipitates stops.

4.2.3.7 *Integration of waste composition uncertainty and precipitates formation thermodynamic models*

The evaluation of livestock waste variability in the formation of struvite and other precipitates, consists of 5 steps, as shown in Fig. 4.2. First, cattle waste composition data are collected from literature. Using these data, probability density distributions for the compounds of cattle leachate are estimated, and they are used in the Monte Carlo model to obtain feasible composition data sets of cattle organic waste. Random points are generated for each chemical compound and species ratios (i.e. N, P, K, Ca, $\text{N-NH}_4^+ : \text{N}_{\text{total}}$, and $\text{P-PO}_4^{3-} : \text{P}_{\text{total}}$). Finally, the thermodynamic model is solved for the composition data sets generated, obtaining the precipitated compounds formed.

The thermodynamic model has been implemented in the algebraic modeling language JuMP, embedded in the programming language Julia ([DunningHuchetteLubin2017; bezanson2017julia](#)). The statistical study of cattle waste composition data, the Monte Carlo framework, result analysis, and data visualization were made in Python language ([Python; Numpy; Matplotlib; Pandas](#)).

4.2.3.8 *Model validation and limitations*

The developed model was validated using the data provided by [Zeng](#). Their work was carried out under similar operational conditions to which this work intends to evaluate. In Fig. 4.3 experimental and model results

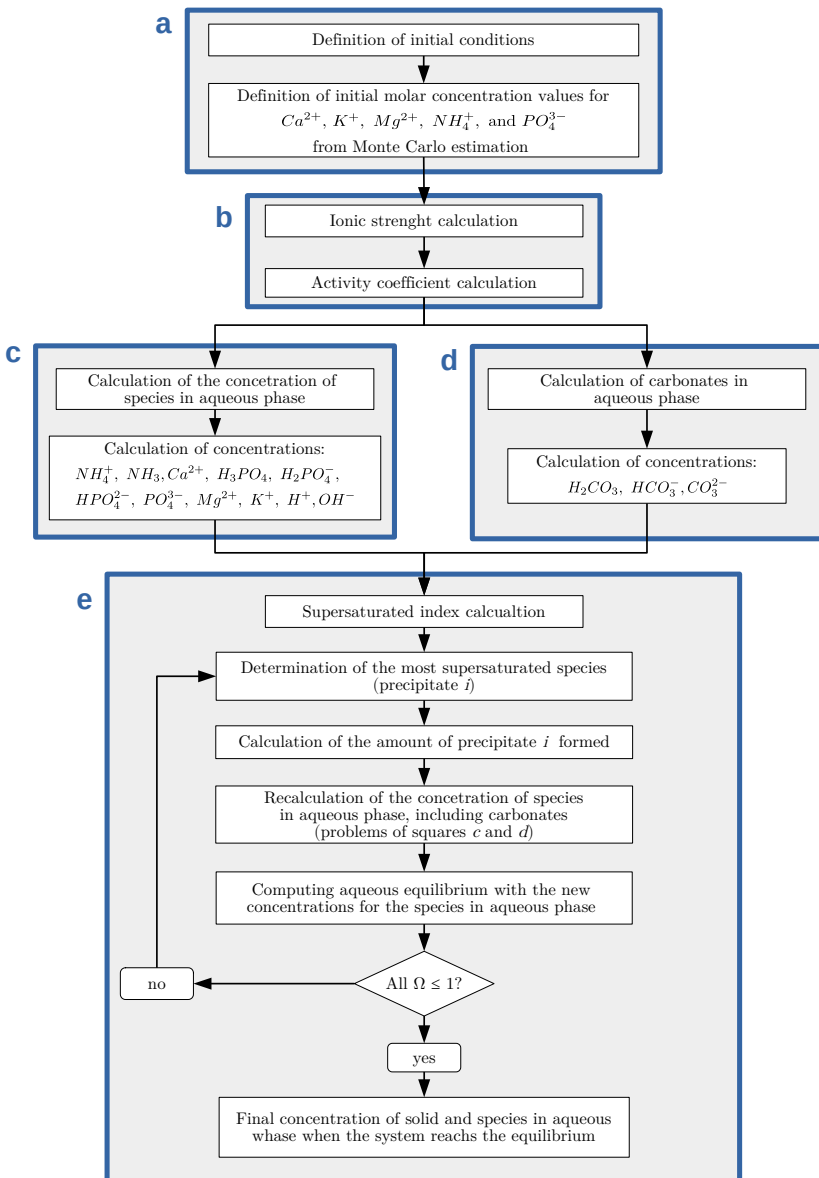


Figure 4.1: Flowchart of the proposed algorithm to solve the thermodynamic model for the formation of precipitates in cattle organic waste.

are compared. The values at high Mg^{2+} molar ratio, when the largest supersaturation values are reached and the formation of struvite is close to the maximum allowed by the thermodynamic equilibrium, match the experimental data. However, at lower ratios, differences between results of the thermodynamic model proposed and experimental data can be observed. As the authors of the article indicate, this differences can be due

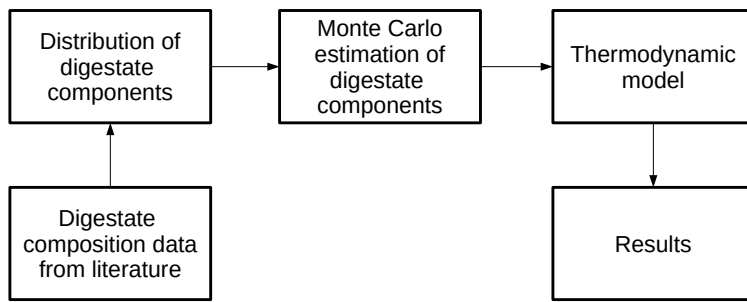


Figure 4.2: A solution procedure to evaluate the influence of the cattle waste composition variability in the formation of struvite.

to the presence of many suspended solids which interfere in the struvite formation process. Note that this work is focused on the thermodynamic aspect, without considering other aspects such as chemical kinetics or transport phenomena. The scarcity of data is an impediment to further validate the model.

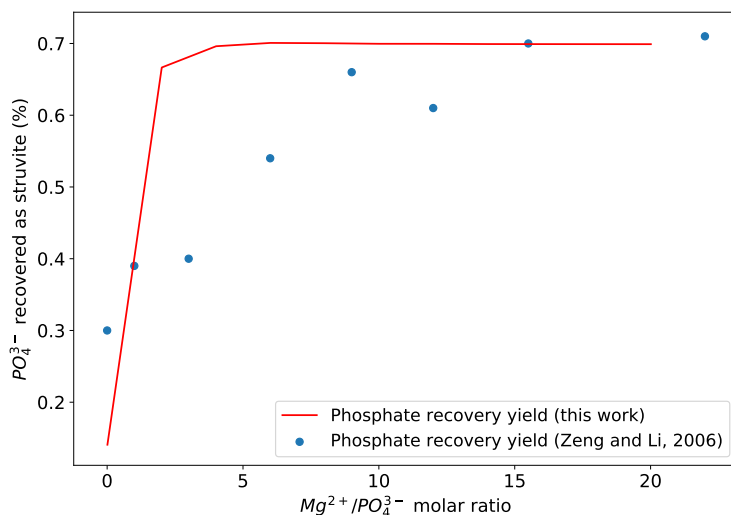


Figure 4.3: Comparison between experimental results reported by Zeng and the results provided by the model developed in this work.

In addition to the lack of previous studies and data availability to evaluate the effects of kinetics and transport phenomena in the formation of precipitates from cattle leachate, another improvement of the proposed model can be achieved by the experimental determination of pK_{sp} values for the potential precipitates formed from cattle leachate. For struvite, the selected pK_{sp} value is taken from the work of Ohlinger, as they determined

the pK_{sp} value for struvite formation in digestate, a medium with high organic load and dissolved elements like cattle leachate. Otherwise, when pK_{sp} data for cattle waste is unavailable from previous studies, the reported values for water are used. A limitation in the use of the obtained surrogate models is that the formation of struvite and calcium precipitates can only be determined for cattle waste. Although a general formulation for the thermodynamic model is used, and the methodology proposed to include the effect of the uncertainty is not restricted to the use of a specific waste, only cattle leachate has been considered in this study. However, if data on the composition is available, surrogate models to predict the formation of struvite and calcium precipitates from other waste sources can be easily developed.

4.3 RESULTS AND DISCUSSION

4.3.1 Surrogate models to estimate the formation of precipitates from livestock organic waste

The influence of the main controllable parameters for struvite production at industrial scale operation was evaluated: the presence of magnesium and calcium, and the alkalinity. Surrogate models were developed to allow the analytical estimation of precipitates formation. pH value for the struvite precipitation process has been considered as a fixed variable, since there is a wide consensus about a pH value of 9, at which struvite solubility is minimum, is optimal, enhancing the phosphorus and nitrogen conversion to struvite and its eventual precipitation (**Tao; Zeng**).

4.3.1.1 Influence of magnesium

In phosphorus recovery processes through struvite formation, magnesium is usually added to increase the saturation of struvite, enhancing its precipitation. This is especially important for cattle leachate due to the high presence of calcium ions competing with other cations for phosphate anions, and the high ionic strength of livestock leachate, reducing the effective concentration of ions. If the supplementation of magnesium provides enough magnesium ions, struvite will reach higher supersaturation ratio than calcium precipitates, leading the formation of struvite over calcium compounds. To estimate the performance of struvite precipitation from cattle leachate, the developed thermodynamic model was solved for 50 different composition data sets. The average alkalinity value of the range reported by **Tao** is considered, 8770.5 mg of CaCO_3 . The plots showing evolution of precipitates formation in function of the $\text{Mg}^{2+}/\text{PO}_4^{3-}$ molar ratio

are collected in the Supplementary Material. Analyzing the average fraction of PO_4^{3-} recovered in form of struvite as a function of the $\text{Mg}^{2+}/\text{PO}_4^{3-}$ molar ratio, a tentative value for $\text{Mg}^{2+}/\text{PO}_4^{3-}$ molar ratio between 2 and 4 can be set as a compromise effectiveness-cost solution. Higher values result in a considerable consumption of magnesium returning lower improvements in phosphate recovery as struvite. The surrogate model obtained to evaluate performance of struvite precipitation in function of the magnesium supplied is a Monod type equation, as shown in Eq. 4.16, where $x_{\text{Mg}^{2+}:\text{PO}_4^{3-}}$ is referred to the $\text{Mg}^{2+}/\text{PO}_4^{3-}$ molar ratio.

$$x_{\text{struvite}(\text{PO}_4^{3-})} = \frac{0.957 \cdot x_{\text{Mg}^{2+}:\text{PO}_4^{3-}}}{0.996 + x_{\text{Mg}^{2+}:\text{PO}_4^{3-}}} \quad (4.16)$$

The evolution in the formation of calcium precipitates as a function of the $\text{Mg}^{2+}/\text{PO}_4^{3-}$ molar ratio was also studied. Hydroxyapatite and calcium carbonate are the only calcium precipitates produced. Both hydroxyapatite and CaCO_3 patterns can be related to the increment of struvite formation along the increase of $\text{Mg}^{2+}/\text{PO}_4^{3-}$ molar ratio values, which reduces the presence of phosphate ions, and consequently decreases the supersaturation of hydroxyapatite. Therefore, there are more calcium ions available to form calcium carbonate. Surrogate models fit to first order polynomial equations for hydroxyapatite, Eq. 4.18, and for calcium carbonate, Eq. 4.17.

$$x_{\text{hydroxyapatite}(\text{Ca}^{2+})} = -1.299 \cdot 10^{-2} \cdot x_{\text{Mg}:\text{PO}_4^{3-}} + 0.248 \quad (4.17)$$

$$x_{\text{CaCO}_3(\text{Ca}^{2+})} = 1.296 \cdot 10^{-2} \cdot x_{\text{Mg}:\text{PO}_4^{3-}} + 0.749 \quad (4.18)$$

4.3.1.2 Influence of calcium

One of the hindrances of cattle leachate for struvite precipitation is the presence of calcium ions competing with other cations for phosphate to form different precipitates. To study the inhibitory influence of calcium in cattle leachate for struvite precipitation, the thermodynamic model was evaluated for the same 50 different composition data sets used in the previous study along $\text{Ca}^{2+}/\text{PO}_4^{3-}$ molar ratio values from 0 to 5. To exclude the influence of magnesium concentration, the study was carried out fixing the $\text{Mg}^{2+}/\text{PO}_4^{3-}$ molar ratio at 2. The plots showing evolution of precipitates formation in function of the $\text{Ca}^{2+}/\text{PO}_4^{3-}$ molar ratio are collected in the Supplementary Material.

The phosphorus as phosphate fraction recovered as struvite exhibits a steep descent at $\text{Ca}^{2+}/\text{PO}_4^{3-}$ values between 0 and 2, followed by an

asymptotic behavior tending to 0. The dispersion of the values has slight variations along with the evaluated Mg^{2+}/PO_4^{3-} values. For hydroxyapatite and calcium carbonate, the higher Ca^{2+}/PO_4^{3-} value, the greater dispersion for the obtained values. This is due to the increase in the supersaturation values for both calcium precipitates because of the presence of a higher number of calcium ions in the leachate.

The surrogate models obtained for struvite and calcium carbonate fit pseudo-sigmoidal equations, Eqs. D.11 and 4.21 respectively; while for hydroxyapatite (HAP) is a second polynomial function, Eq. 4.20. In all cases, $x_{Ca^{2+}:PO_4^{3-}}$ is referred to Ca^{2+}/PO_4^{3-} molar ratio.

$$x_{\text{struvite}}(PO_4^{3-}) = \frac{0.798}{1 + (x_{Ca^{2+}:PO_4^{3-}} \cdot 0.576)^{2.113}} \quad (4.19)$$

$$\begin{aligned} x_{\text{hydroxyapatite}}(Ca^{2+}) &= \\ &- 4.321 \cdot 10^{-2} \cdot x_{Ca^{2+}:PO_4^{3-}}^2 + 0.313 \cdot x_{Ca^{2+}:PO_4^{3-}} - 3.619 \cdot 10^{-2} \end{aligned} \quad (4.20)$$

$$x_{CaCO_3}(Ca^{2+}) = \frac{1.020}{1 + (x_{Ca^{2+}:PO_4^{3-}} \cdot 0.410)^{1.029}} \quad (4.21)$$

4.3.1.3 Influence of alkalinity

Alkalinity is a parameter which can be used to control the production of calcium precipitates. When the presence of carbonates is low, the competition between hydroxyapatite and calcium carbonate tends to benefit the first compound because the limited availability of carbonate ions reduces the supersaturation of calcium carbonate. However, the predominance of hydroxyapatite reduces the formation of struvite since both elements compete for phosphate ions. Therefore, the presence of significant amounts of carbonates (performing at alkaline conditions) reduces the formation of hydroxyapatite and promotes the formation of struvite.

The results for the formation of struvite, hydroxyapatite and calcium carbonate considering the same 50 different composition data sets used in the previous studies in function of the alkalinity are collected in the Supplementary Material. It can be observed that the behavior of struvite formation and calcium carbonate are related, with an abrupt change for both elements at alkalinity values between 3,000 and 4,000 mg of $CaCO_3$, reaching plateaus beyond these values. The dispersion of values follow a similar pattern for both struvite and calcium carbonate, being lower at low

alkalinity values, and progressively growing until reaching a value of 4,000 mg of CaCO_3 . Beyond this value, the dispersion of values remains constant. Hydroxyapatite formation decrease continuously along the alkalinity values, being complementary with the formation of calcium carbonate.

Therefore, struvite formation from livestock leachate can be enhanced inhibiting hydroxyapatite formation by controlling the alkalinity level, increasing the formation of calcium carbonate and reducing the concentration of calcium ions competing for phosphate. Pseudo-sigmoidal fits are shown in Eq. 4.22 for $x_{\text{struvite}}(\text{PO}_4^{3-})$, Eq. 4.23 for the case of hydroxyapatite, and Eq. 4.24 for calcium carbonate, where x_{Alk} is referred to alkalinity (mg | CaCO_3).

$$x_{\text{struvite}}(\text{PO}_4^{3-}) = \frac{0.695}{1 + (x_{\text{Alk}} \cdot 4.229 \cdot 10^{-4})^{-2.638}} \quad (4.22)$$

$$x_{\text{hydroxyapatite}}(\text{Ca}^{2+}) = \frac{0.260}{1 + (x_{\text{Alk}} \cdot 6.460 \cdot 10^{-5})^{3.390}} \quad (4.23)$$

$$x_{\text{CaCO}_3}(\text{Ca}^{2+}) = \frac{0.847}{1 + (x_{\text{Alk}} \cdot 4.646 \cdot 10^{-4})^{-1.870}} \quad (4.24)$$

4.3.1.4 Interactions between calcium and magnesium to phosphate ratios

Interactions between calcium and magnesium to phosphate ratios were evaluated to determine a target operational area for optimal struvite production performance. In Fig. 4.4 the formation of struvite as function of $\text{Mg}^{2+}/\text{PO}_4^{3-}$ and $\text{Ca}^{2+}/\text{PO}_4^{3-}$ molar ratios is shown, where the area with the highest phosphate recovery in form of struvite has been shaded. It can be observed that struvite formation depends strongly on the $\text{Ca}^{2+}/\text{PO}_4^{3-}$ molar ratio. For $\text{Ca}^{2+}/\text{PO}_4^{3-}$ values less than 3 struvite formation reaches the maximum values, even for low $\text{Mg}^{2+}/\text{PO}_4^{3-}$ molar ratio values. For high calcium/phosphate ratios, struvite formation decreases abruptly, obtaining low increases in struvite formation even for large supplies of magnesium.

4.3.2 Phosphorus releases from cattle leachate potentially avoided via struvite formation

Phosphorus pollution of waterbodies, followed by eutrophication and hypoxia scenarios, represents a major environmental problem for the current

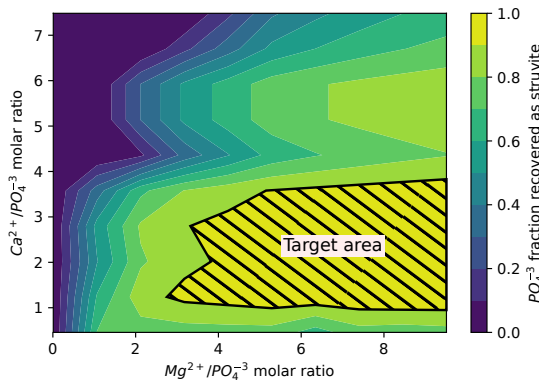


Figure 4.4: Influence of magnesium and calcium in struvite precipitation.

societies. Considering the United States, the Census of Agriculture reports more than 93 million of cattle heads ([2017 Census of Agriculture](#)), generating an estimated amount of 1,144 million of tons of organic waste per year. The phosphorus contained in the organic waste can be lost as runoff, reaching waterbodies, and polluting the surrounding aquatic ecosystems. Actually, several outstanding cases of eutrophication have taken place in the U.S. in recent times, such as the events occurred in Lake Erie since 1990, and the dead zone in the Gulf of Mexico because of in-excess nutrients discharges collected along the Mississippi River basin. Therefore, nutrient recovery strategies must be implemented to capture phosphorus (and nitrogen) before reaching the waterbodies. Additionally, phosphorus recovery as struvite allows its redistribution to nutrient deficient areas ([Martin](#)). The surrogate models developed are used to estimate the potential phosphorus emissions avoided in each watershed through phosphorus recovery from cattle leachate as struvite.

4.3.2.1 Balance of phosphorus involved in agricultural activities throughout the U.S. watersheds

To reach environmental sustainability and reduce the impact over the original ecosystems as much as possible, the releases of phosphorus should be balanced with a coordinated network of phosphorus uptakes. To determine the balance between the releases and uptakes of phosphorus from the agricultural sector, the TES sustainability metric is computed for each watershed in the U.S., showing the watersheds where the phosphorus releases are unbalanced and impacting the environment, Fig. 4.5. For a total of 2,104 HUC8 watersheds, data is unavailable for 6 watersheds, the phosphorus releases and uptakes are balanced in 1,410 watersheds, and 691 exhibit unbalanced phosphorus releases, representing the 33.12% of

total watersheds. It can be observed a larger concentration of unbalanced watersheds along the Mississippi River basin and around the Lake Erie, areas currently affected by eutrophication issues.

For studies requiring higher spatial resolution, more accurate values for the TES metric can be estimated through the use of local inventories for phosphorus releases and uptakes. A dataset with the phosphorus releases and uptakes, the phosphorus balance, and the TES metric computed for each watershed are available in the Supplementary Material. A dataset with the phosphorus releases and uptakes, the phosphorus balance, and the TES metric computed for each watershed are available in the Supplementary Material.

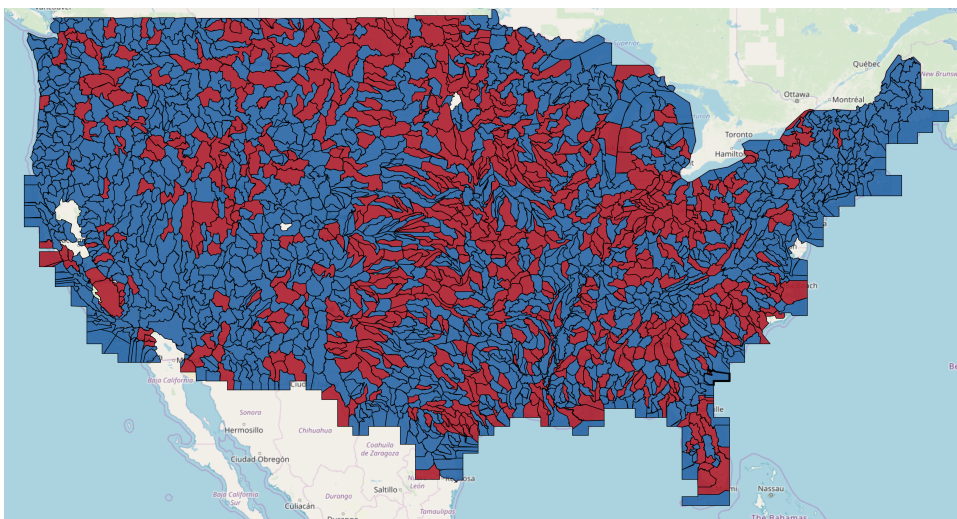


Figure 4.5: Techno-ecological synergy (TES) metric values for HUC8 watersheds. Red indicates watersheds with unbalanced agricultural phosphorus releases, and blue indicates watersheds with balanced agricultural phosphorus releases. White indicates watersheds with not available data.

4.3.2.2 Phosphorus recovered from cattle leachate through struvite precipitation

Since the scope of the surrogate models developed is limited to the treatment of cattle leachate, only P releases from cattle organic waste will be considered for recovery. Additionally, as it is mentioned in the description of the model, only the phosphate fraction of phosphorus can be recovered through struvite precipitation. Data provided by IPNI NuGIS (**NuGIS**) report total manure generated, but do not report the breakdown of manure generated by different livestock sources. Therefore, the inventory of cattle for each HUC6 watershed reported by the U.S. Census of Agriculture

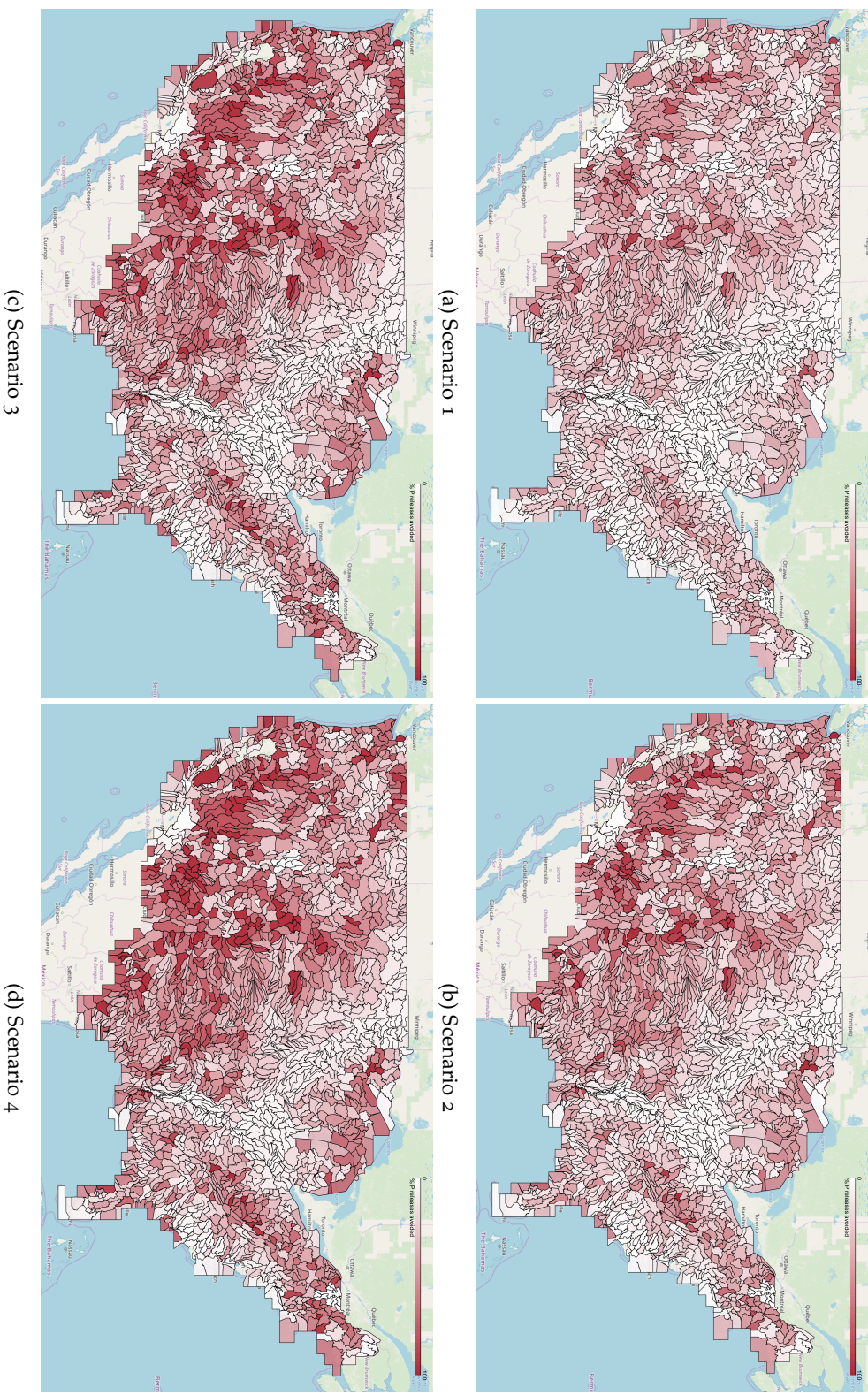


Figure 4.6: Phosphorus releases avoided through struvite production for the different scenarios considered. Darker colors represent larger phosphorus recovery

is used ([2017 Census of Agriculture](#)). To keep spatial consistency between data, the inventory of cattle was aggregated from HUC6 to HUC8 watershed level scaling by the fraction of area represented by each HUC8 basin over the total HUC6 area. The breakdown of cattle types in the U.S. Census of Agriculture is not available at watershed level, but it is available at state level. Therefore, the number of cattle heads is weighted by the fraction of milk and beef animals in the corresponding state. Finally, the animals number for each type of cattle is calculated using the normalization values provided by Kellogg et al. (2010) ([Kellogg2000](#)). If the watershed is shared among several states, the average of the represented states is considered.

Since the supply of magnesium is the easiest controllable variable in the struvite precipitation process, the scenarios evaluated to determine the phosphorus emissions avoided through struvite precipitation were defined through the use of different amounts of magnesium using the surrogate model shown in Eq. [4.16](#). The different supplies of magnesium have a direct influence on the economy of the process, being one of the highest operating costs items. A summary of the scenarios evaluated and the results obtained is presented in Table [4.5](#). The fraction of phosphorus releases avoided is computed over the total phosphorus releases from agricultural activities, including manure releases and fertilizer application, as described in Section [4.2.2.1](#).

Table 4.5: Scenarios considered and results for cattle leachate phosphorus recovery

Scenario	1	2	3	4
Mg ²⁺ /PO ₄ ³⁻ molar ratio	1	2	4	6
Total P releases avoided (total watersheds) (tons)	422,104	562,430	674,556	722,573
Average P releases avoided (total watersheds) (%)	22.63	30.16	36.17	38.75
Average P releases avoided (unbalanced watersheds) (%)	18.07	24.08	28.88	30.94
kg Mg/kg P _{recovered}	2.68	4.02	6.71	9.40

The results for each scenario considered at watershed scale are shown in Fig. [6.6](#), where darker colors represent larger phosphorus releases avoided. It can be observed that struvite production can contribute to reducing phosphorus emissions around Lake Erie and the Great Lakes region, one of the most severely affected areas by eutrophication problems. Additionally, other areas where the phosphorus emissions avoided are especially significant are the upper basin of the Mississippi River, and the basins located in the south-central region of the United States, such

as the areas of some tributaries rivers to the Mississippi River basin, the Rio Grande river and the Colorado River basin. At national level, struvite production can contribute to reduce the agricultural phosphorus releases by 22% for most conservative case where the lowest amount of magnesium is added. The phosphorus fraction recovered raises until a 30% and 36% when the amount of magnesium added is multiplied by 2 and by 4 respectively. However, for the scenario 4 the increase in the supply of magnesium only increases the phosphorus recovered in 2 percentual points compared with the previous scenario. Therefore, the implementation of struvite production processes for phosphorus recovering in cattle facilities can contribute significantly to the reduction in the phosphorus emissions from agricultural operations, reducing the runoffs to waterbodies and mitigating the nutrient pollution of the aquatic ecosystems. However, when only unbalance watersheds are considered, the average fraction of phosphorus releases avoided decreases, suggesting that, from a global overview, the phosphorus releases due to fertilizers play a major role in these watersheds than when balance and unbalance watersheds are evaluated altogether. Data at watershed level are collected in the Supplementary Material.

Therefore, the phosphorus recovered from livestock facilities have a significant impact in the reduction of phosphorus releases to the environment. However, to achieve a successful implementation of nutrient management strategies, coordinated network management efforts to mitigate nutrient pollution of aquatic systems including point and non-point sources, should be performed for optimizing nutrient management programs that minimize the capital and operating costs while maximizing the environmental benefits. Proposals for the development of coordinated management systems for organic wastes have been presented by **Sharara, Sampat³, and hu_logistics_2019**.

4.4 CONCLUSIONS

To estimate the potential phosphorus releases avoided through struvite precipitation from cattle waste, a thermodynamic framework has been developed to evaluate struvite production from cattle organic waste as a technology for nutrient management and recovery. A set of practical numerical correlations is developed to help predict the struvite recovery. Cattle waste treatment and nutrient recovery through struvite formation is a feasible process from a thermodynamic perspective, reaching phosphate recovery efficiencies up to 80% with the addition of considerable amounts of magnesium. Additionally, the results show that alkaline conditions can control the calcium ions when their presence in the medium is high and

these can interfere in the formation of struvite by precipitating the calcium ions as calcium carbonate, and enhancing the recovery of phosphate as struvite. However, the variability in the organic waste composition is an important parameter that has a high impact on the efficiency of the process. Therefore, an individual composition analysis of the treated cattle waste should be the ideal procedure to achieve the optimal performance of the process by adjusting the operating conditions, particularly the amount of magnesium added and the alkalinity of the medium. Nevertheless, there are opportunities for improving the proposed model by the experimental determination of pK_{sp} values for all potential precipitates from cattle leachate, and by including the effects from kinetics and transport phenomena.

The techno-ecological synergy sustainability metric (TES) is a useful tool for visualizing the spatial distribution of environmental problems, making it possible to determine what areas are more sensible to nutrient pollution, and allowing an adequate distribution of efforts to mitigate phosphorus releases and achieved better nutrient management practices. In the U.S., struvite production has large potential for reducing the phosphorus losses from livestock facilities, avoiding between the 22% and the 36% of the phosphorus releases from the agricultural sector at national level, reducing the phosphorus runoff and mitigating the nutrient pollution of waterbodies. In addition, it can be observed how struvite production can significantly contribute to reducing phosphorus emissions around Lake Erie and the Great Lakes region, some of the most severely affected areas by eutrophication problems. It should be remarked that the production of struvite from cattle leachate allows the redistribution of phosphorus to nutrient deficient areas reducing the phosphorus runoff to waterbodies and mitigating the nutrient pollution of aquatic ecosystems. However, future research is needed to consider temporal aspects, transportation logistics, and coordinated management strategies for achieving global solutions to global problems.

NOMENCLATURE

Variables

<i>A</i>	parameter of the Debye-Hückel relationship
<i>EC</i>	electrical conductivity $\left(\frac{\mu\text{S}}{\text{cm}} \right)$
<i>E_x</i>	emissions of component <i>x</i>
<i>I</i>	ionic strength (M)

K	thermodynamic equilibrium constant
K_{sp}	solubility product
M	equal to e^μ
T	temperature (K)
U_x	uptakes of component x
V_x	techno-ecological synergy sustainability metric for component x
Ω	supersaturation ratio
γ	displacement parameter
γ_x	activity coefficient for element x
μ	mean of the distribution
σ	standard deviation
σ^2	variance
m	stoichiometric coefficient
n	stoichiometric coefficient
x_{Alk}	alkalinity (mg $CaCO_3$)
x_{CaCO_3}	fraction of calcium recovered as calcium carbonate
$x_{Ca^{2+}:PO_4^{3-}}$	Ca^{2+}/PO_4^{3-} molar ratio
$x_{Mg^{2+}:PO_4^{3-}}$	Mg^{2+}/PO_4^{3-} molar ratio
$x_{hydroxyapatite(Ca^{2+})}$	fraction of calcium recovered as hydroxyapatite
$x_{struvite(PO_4^{3-})}$	fraction of phosphorus as phosphate recovered as struvite
z_x	integer charge of ion x

Abbreviations

AAPFCO	Association of American Plant Food Control Officials
CAFO	Concentrated Animal Feeding Operation
HAB	Harmful Algal Bloom
HUC	Hydrologic Unit Code
KDE	Kernel Density Estimation
USDA	United States Department of Agriculture

ACKNOWLEDGMENTS

We acknowledge funding from the Junta de Castilla y León, Spain, under grant SAo26G18 and grant EDU/556/2019, and by an appointment for E.

Martín-Hernández to the Research Participation Program for the Office of Research and Development, U.S. EPA, administered by the Oak Ridge Institute for Science and Education.

Disclaimer: The views expressed in this article are those of the authors and do not necessarily reflect the views or policies of the U.S. EPA. Mention of trade names, products, or services does not convey, and should not be interpreted as conveying, official U.S. EPA approval, endorsement, or recommendation.

BIBLIOGRAPHY

GEOSPATIAL ENVIRONMENTAL AND TECHNO-ECONOMIC FRAMEWORK FOR SUSTAINABLE PHOSPHORUS MANAGEMENT AT LIVESTOCK FACILITIES

ABSTRACT

Nutrient pollution of waterbodies is a major worldwide water quality problem. Excessive use and discharge of nutrients can lead to eutrophication and algal blooms in fresh and marine waters, resulting in environmental problems associated with hypoxia, public health issues related to the release of toxins and freshwater scarcity. A promising option to address this problem is the recovery of nutrient releases prior to being discharged into the environment. Driven by the sustainable materials management concept, the COW₂NUTRIENT (Cattle Organic Waste to NUTRIent and ENergy Technologies) framework is developed for the techno-economic evaluation and selection of nutrient recovery systems at livestock facilities. Environmental vulnerability to nutrient pollution determined through a geographic information system (GIS)-based model and techno-economic information of different state-of-the-art nutrient management technologies are combined in a multi-criteria decision analysis (MCDA) model, resulting in the selection and economic analysis of the most suitable process for each studied livestock facility. This framework has been employed for studying the implementation of sustainable phosphorus management systems at 2,217 livestock facilities in the Great Lakes area, resulting in capital expenses of 2.5 billion USD if only phosphorus recovery technologies are installed, and up to 5.2 billion USD if nutrient management is combined with biogas and power production. However, considering potential economic incentives for the recovery of phosphorus, net revenues up to 230 million USD per year can be achieved. Therefore, the framework presented reveals the potential of implementing nutrient management systems at regional scale for the abatement of phosphorus releases from livestock facilities.

Keywords: Organic waste; Harmful algal blooms; Nutrient pollution; Livestock waste; Phosphorus recovery

RESUMEN

La contaminación por nutrientes de las masas de agua es uno de los principales problemas de calidad del agua en todo el mundo. El uso y el vertido excesivos de nutrientes pueden provocar la eutrofización y la proliferación de algas en las aguas dulces y marinas, lo que da lugar a problemas medioambientales relacionados con la hipoxia, cuestiones de salud pública relacionadas con la liberación de toxinas y escasez de agua dulce. Una opción prometedora para abordar este problema es la recuperación de los vertidos de nutrientes antes de ser vertidos al medio ambiente. Impulsado por el concepto de gestión sostenible de materiales, se ha desarrollado el marco COW2NUTRIENT (Cattle Organic Waste to NUTRIent and ENergy Technologies) para la evaluación y selección tecnoeconómica de sistemas de recuperación de nutrientes en instalaciones ganaderas. La vulnerabilidad ambiental a la contaminación por nutrientes, determinada a través de un modelo basado en un sistema de información geográfica (SIG), y la información tecno-económica de diferentes tecnologías de gestión de nutrientes de última generación se combinan en un modelo de análisis de decisiones multicriterio (MCDA), dando como resultado la selección y el análisis económico del proceso más adecuado para cada instalación ganadera estudiada. Este marco se ha empleado para estudiar la implantación de sistemas de gestión sostenible del fósforo en 2.217 instalaciones ganaderas de la zona de los Grandes Lagos, lo que supone unos gastos de capital de 2.500 millones de dólares si sólo se instalan tecnologías de recuperación de fósforo, y de hasta 5.200 millones de dólares si la gestión de nutrientes se combina con la producción de biogás y energía. Sin embargo, si se tienen en cuenta los posibles incentivos económicos para la recuperación de fósforo, se pueden conseguir ingresos netos de hasta 230 millones de dólares al año. Por lo tanto, el marco presentado revela el potencial de la aplicación de sistemas de gestión de nutrientes a escala regional para la reducción de las emisiones de fósforo de las instalaciones ganaderas.

Palabras clave: Residuos orgánicos; Florecimiento de algas; Contaminación por nutrientes; Residuos ganaderos; Recuperación de fósforo

5.1 INTRODUCTION

Phosphorus is a source of concern for modern societies. On the one hand, nutrient pollution of waterbodies is one of the major water quality problems worldwide, resulting in environmental issues as a consequence of the eutrophication of waterbodies, and the occurrence of cyanobacteria and harmful algal blooms (HABs). Surveys reveal that eutrophication is a global problem, reporting that 54% of lakes in Asia, 53% in Europe, 48% in North America, 41% in South America, and 28% in Africa are eutrophic ([ansari_eutrophication_2010](#)). In addition to eutrophication, hypoxia of aquatic ecosystems is associated with the aerobic degradation of the algal biomass by bacteria, shifting the distribution of aquatic species and releasing toxins in drinking water sources ([sampat_economic_2018](#)). Although eutrophication is affected by several factors, such as temperature and the self-purification capacity of waterbodies, the primary limiting factor for eutrophication is often the phosphate concentration ([Ullmanns](#)). Aside from disturbing aquatic ecosystems, eutrophication also contributes to climate change, emitting large amounts of strong greenhouse gases as a consequence of the biomass degradation, such as CH₄ and N₂O ([beaulieu_eutrophication_2019](#)). On the other hand, phosphorus is an essential nutrient for living organisms, and a key element for maintaining agricultural productivity. However, phosphorus is a resource very sensitive to depletion, since extractable deposits of phosphorus rock are limited and there is no known substitute or synthetic replacement. Projections estimate limited availability of phosphate over the next century ([cordell_story_2009](#)). Therefore, in addition to the environmental perspective, the search for phosphorus recycling processes is a major driving force for the development of nutrient recovery systems ([reijnders2014phosphorus](#)).

Agricultural activities are one of the main contributors to human-based phosphorus releases ([Dzombak](#)), including non-point source releases by over-use of fertilizers in croplands, point source releases originated from the disposal of livestock waste, and nutrient legacy that have accumulated in watersheds due to historical phosphorus releases. Focusing on the point source releases generated by the cattle industry, these result from the production of large amounts of livestock organic waste, containing substantial amounts of phosphate and ammonia. [Sampat2017](#) presented the link between the presence of livestock facilities and higher concentrations of phosphorus in soil, resulting in increased nutrient runoff to waterbodies. While for animals on pasture, organic waste should not be a source of concern if stocking rates are not excessive, for concentrated animal feeding operations (CAFOs) manure should be properly managed due to the high rates and spatial concentration of the organic waste gener-

ated. A common practice to recycle the nutrients contained in the organic waste is the land application of the manure. However, since the high-water content of manure makes its transportation to nutrient deficient locations difficult and expensive, it is usually spread in the surroundings of the CAFOs, leading to surplus of nutrients in soils and phosphorus runoff to waterbodies (**USDAHandbook**).

The implementation of nutrient recovery technologies at livestock facilities to recover phosphorus from cattle manure is a promising approach to recycle and leverage nutrients more efficiently, mitigating the nutrient pollution of waterbodies (**li2021toward**). However, the technologies that can be implemented at CAFOs differ widely in aspects such as phosphorus recovery performance, final products obtained, capital expenses, and operational costs. Additionally, different levels of environmental vulnerability to eutrophication may require the use of different P recovery processes, searching for the most effective balance between P recovery efficiency and cost. Previous efforts for the technical evaluation of different phosphorus recovery technology have been performed, resulting in processes with proven technical feasibility for phosphorus recovery. Particularly, there exists a considerable body of literature on the production of struvite (**muhmood2019formation**). Other mature processes for the recovery of phosphorus are the formation of calcium precipitates (**berg2006phosphorus**), and systems based on physical separations (**church_novel_2016**). Additionally, novel processes are currently under development, such as membrane separation processes (**li2020application**), microalgae-based processes (**robles2020new**), adsorption using biochar (**wang2020phosphorus**), and electrochemical processes (**belarbi2020bench**). Moreover, a decision-making framework has been developed for the selection and implementation of phosphorus recovery systems in urban areas (**pearce2015phosphorus**). However, to the best of the authors knowledge, there are no specific frameworks to study the implementation of phosphorus recovery systems at livestock facilities considering GIS environmental and techno-economic dimensions.

In this work, we propose a novel framework, COW2NUTRIENT (Cattle Organic Waste to NUTRIent and ENergy Technologies), for the assessment and selection of phosphorus recovery technologies at CAFOs based on environmental and techno-economic criteria. This framework combines eutrophication risk data at subbasin level and the techno-economic assessment of six state-of-the-art phosphorus recovery processes in a multi-criteria decision analysis (MCDA) model. This information is normalized and aggregated for the selection of the most suitable technology for each analyzed CAFO. The goal is to develop a flexible framework able to balance the operating cost of the systems and P recovery efficiency as a function

of the environmental vulnerability to eutrophication of each region. The minimization of operating costs is prioritized in regions with low eutrophication risk, while the efficiency of P recovery is the most relevant criteria in regions affected by nutrient pollution. Also, COW2NUTRIENT aims to provide a useful framework for designing and evaluating effective GIS-based incentives and regulatory policies to control and mitigate nutrient pollution of waterbodies. The practicability of the proposed framework is assessed by studying and designing the implementation of P recovery systems at 2,217 current livestock facilities in the Great Lakes area.

5.2 METHODS

COW2NUTRIENT framework is comprised by three models, i.e. environmental geographic information, techno-economic, and multi-criteria decision analysis models, in order to integrate the geographic data on vulnerability to nutrient pollution, and the technical and economic information of the nutrient recovery systems through an MCDA model, as shown in Figure 6.1. First, the geographic location of the individual facilities (longitude and latitude) is supplied to the environmental GIS model to determine the vulnerability level to nutrient pollution of the region where the studied CAFOs are located. Secondly, data regarding the number and type of animals at the facility (i.e., beef and dairy cattle, adult animals, heifers, and calves) are entered into the techno-economic model to capture the characteristics of the livestock facility evaluated. Data reported by the US Department of Agriculture were considered for manure generation ratios (**Kellogg2010**) and composition (**USDAHandbook**). These values are collected in Table 3S of the Supplementary Material. In addition, economic data are fed into the techno-economic model for economic performance evaluation purposes, including the value of incentives received for phosphorus recovery (in the form of P credits), and for the generation of bio-based methane or electricity (in form of Renewable Energy Certificate (REC) and Renewable Identification Number (RIN) respectively). The output data from the techno-economic and environmental geographic information models are imported in the MCDA model. In this module, the data is normalized and aggregated, returning a composite index for each technology. This composite index is used to score and rank the nutrient recovery systems based on their performance. All models have been developed using Python (**Python**).

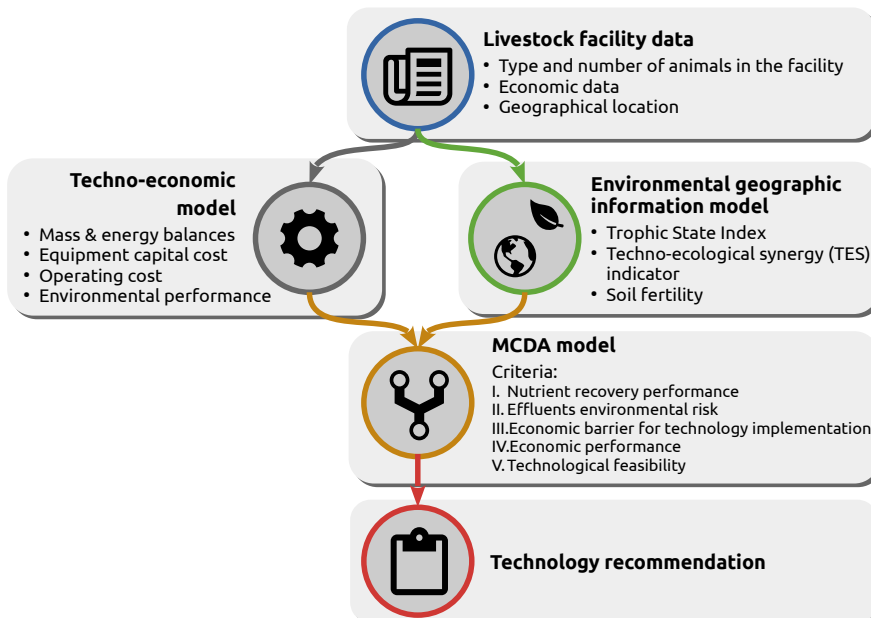


Figure 5.1: Structure of the COW2NUTRIENT decision support framework for the assessment and selection of phosphorus recovery systems.

5.2.1 *Environmental geographic information model*

The environmental vulnerability to nutrient pollution of the area where the livestock facilities are located determines the preference (i.e., ranks the importance) of each criterion. Three indicators are used to evaluate the eutrophication risk of each region studied at subbasin spatial resolution. The trophic state of waterbodies is evaluated through the Trophic State Index (**carlson_trophic_1977**), determining their eutrophication level. The phosphorus saturation of soils, which can result in the transport of phosphorus to waterbodies by run-off, is evaluated through Mehlich 3 phosphorus concentration (**Espinoza2006**). Finally, the balance between phosphorus releases and uptakes from anthropogenic activities is assessed through the techno-ecological synergy metric (**TESmetric**), determining if there is a net accumulation or depletion of phosphorus in a region over time. The use of these three indicators makes it possible to determine if there exist an immediate risk of eutrophication in the region studied (eutrophized waterbodies), a long-term risk (moderate value of TSI, soils saturated by phosphorus, or phosphorus releases and uptakes from anthropogenic activities unbalanced), or if there is no risk of eutrophication (phosphorus uptakes and releases are balanced). Detailed descriptions of

the performed data analysis, and maps for the contiguous US are provided in Section 1 of the Supplementary Material.

5.2.1.1 *Spatial resolution*

A watershed is defined as the region draining all the streams and rainfall to a common waterbody, defining the geographic limits for the collection of runoff elements. US watersheds are designated by the US Geological Survey through the Hydrologic Unit Code (HUC) system. The HUC system divides the US into regions, subregions, basins, subbasins, watersheds, and subwatersheds. Each hydrologic unit of these six levels is identified hierarchically by a unique numeric code from 2 to 12 digits (i.e., HUC₂ to HUC₁₂). The spatial resolution of this study is the contiguous United States at the subbasin level, defined by the HUC system at 8 digits (HUC8) (**HUC8**).

5.2.1.2 *Trophic State Index*

The Trophic State Index (TSI) is a metric proposed by **carlson_trophic_1977** to determine the trophic status of waterbodies (**QAPP2012**). The TSI of a waterbody is scored in a range from 0 to 100 representing its trophic state, as shown in Table 5.1. Oligotrophic and mesotrophic states denote low and intermediate biomass productivities, while eutrophic and hypereutrophic states are referred to waterbodies with high biological productivity and frequent algal blooms. Combined data for chl- α and total phosphorus concentrations retrieved from the National Lakes Assessments conducted by the US EPA in 2007 and 2012 (**NLA2012; NLA2007**) is used to determine the Trophic State Index of lentic waters in the contiguous US. No TSI values were assigned to the watersheds without reported data. Correlations to estimate the TSI from chlorophyll- α and total phosphorus concentrations are collected in Section 1 of Supplementary Material.

Table 5.1: Relation between TSI value and trophic class.

TSI	<40	40-50	50-70	>70
Trophic Class	Oligotrophic	Mesotrophic	Eutrophic	Hypereutrophic

5.2.1.3 *Techno-ecological synergy sustainability metric*

The techno-ecological synergy sustainability metric (TES) is an indicator proposed by **TESmetric** to evaluate the fraction of net anthropogenic phosphorus releases, Eq. 5.1.

$$V_x = \frac{(U_x - E_x)}{E_x} \quad (5.1)$$

A negative value for TES indicator (V_x) indicates that the releases (E_x) are larger than the uptake capacity of the evaluated system, (U_x), and thus impacting in the ecosystems; while positive values reflects that the releases can be absorbed by the system without any harm.

Phosphorus releases from agricultural activities have been estimated from data reported by the Nutrient Use Geographic Information System project. Since this work is limited to the assessment of agricultural phosphorus releases, other possible sources of phosphorus releases are not considered. Further information about the methodology used for the estimation of human-based phosphorus releases can be found in **NuGIS**. Anthropogenic phosphorus uptakes are those due to the crops grown in each watershed, including corn, soybeans, small grains, cotton, rice, vegetables, orchards, greenhouse and other crops (i.e., fruits, sugar crops, and oil crops). The estimation of the phosphorus uptakes is performed considering the different phosphorus requirements and yield rates of each crop, as well as the land cover and the crops distribution in each watershed. Data retrieved from **2017 Census of Agriculture, USDA Handbook**, and **EnviroAtlas** is used for this purpose.

5.2.1.4 Phosphorus saturation of soils

Phosphorus concentration in soil is used for the evaluation of the phosphorus legacy that is continuously built up in soils, providing a metric of soil quality. However, only a fraction of phosphorus is available for plants. To measure this phosphorus fraction available for plants, several standardized phosphorus soil tests have been proposed, including Olsen, Bray 1, and Mehlich 3 tests. Among them, Mehlich 3 (M₃P) has been selected as a measure of the concentration of P in soils since it is a widely used metric, and it is the P soil test least affected by changes in soil pH. To estimate the fraction of phosphorus available for plants from total phosphorus concentration data, a correlation developed by **AllenMallarino2006** has been used, Eq. 5.2. It must be noted that this correlation has been developed for agricultural soils in Iowa, but due to the lack of studies in this topic, it has been used for soils throughout the contiguous US. Therefore, it must be considered as an exploratory effort to determine the phosphorus saturation in the US soils. Data reported by **SoilsUSGS** is used to evaluate the concentration of total phosphorus along the contiguous US.

$$M_3P \text{ (% over TP)} = \frac{4.698 \cdot 10^{-1}}{1 + (\text{TotalP (mg/kg)} \cdot 1.336 \cdot 10^{-3})^{-2.148}} \quad (5.2)$$

The relationship between M₃P test value and the quality of soil is shown in Table 5.2. Soil fertility levels below optimum indicate that nutrient supplementation is needed to enhance the yield of crops, optimum values indicates that no nutrient supplementation is needed, and excessive soil fertility level indicate over-saturation of phosphorus in soil that can reach waterbodies by runoff (Espinoza2006).

Table 5.2: Relationship between Mehlich 3 phosphorus and soil fertility level (Espinoza2006).

Soil Fertility Level	M ₃ P soil phosphorus concentration (ppm)
Very Low	<16
Low	16-25
Medium	26-35
Optimum	36-50
Excessive	>50

5.2.2 Techno-economic model

COW2NUTRIENT framework evaluates all the stages involved in the processing of manure for P recovery, from organic waste collection to the recovery of nutrients and other by-products such as electricity or biomethane, as represented in Fig 5.2. In addition to the assessment of nutrient recovery systems, the framework is flexible to include anaerobic digestion, and the subsequent biogas valorization, for the production of methane or electricity. The techno-economic model is based on mass balances, thermodynamics, and chemical equilibria for each possible stage of the manure treatment process, i.e. manure conditioning, anaerobic digestion, biogas purification, biogas valorization, and phosphorus recovery. Preliminary design and sizing of equipment is performed to estimate the capital and operating expenses when no specific costs data are available. A detailed description of equipment design and sizing, as well as the correlations used for costs estimation, can be found in Section 2 of the Supplementary Material.

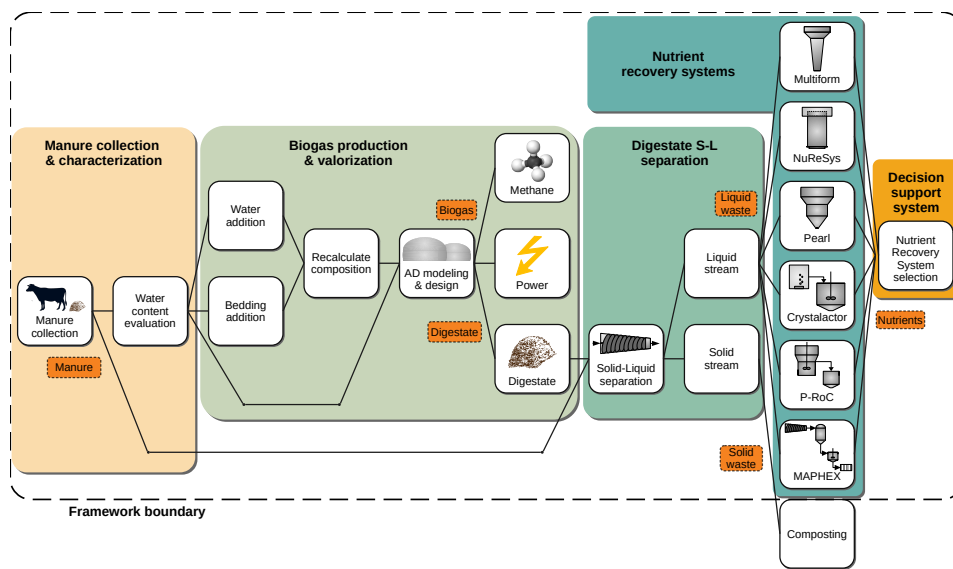


Figure 5.2: Process flowsheet for manure management and phosphorus recovery stages included in COW2NUTRIENT.

5.2.2.1 Manure conditioning

It is considered that the collection of manure does not involve any cost, since CAFOs have manure collection systems already installed. All manure produced is assumed to be collected. If the anaerobic digestion (AD) stage is implemented, a preconditioning stage is considered to adjust the water content of the waste. US EPA determines that the content of total solids in manure should be less than 15% (**AgSTARHandbook**), as shown in Figure 6S of the Supplementary Material. Therefore, additional water may be added to reduce the solids content in manure before the AD stage.

5.2.2.2 Anaerobic digestion

Anaerobic digestion is a microbiological process that breaks down organic matter in the absence of oxygen. It involves four stages, hydrolysis, acidogenesis, acetogenesis, and methanogenesis; producing a mixture of gases mainly composed of methane and carbon dioxide (biogas), and a decomposed organic substrate (digestate). The model of the anaerobic digester is formulated through the mass balances of the species involved in the production of biogas and digestate. A detailed description of the digester modeling can be found in **Leon**. As a result of the AD process, a fraction of organic phosphorus and nitrogen are transformed in their inorganic forms. To evaluate the amount of organic nutrients transformed into inorganic phosphorus and nitrogen, data available in literature was

considered, resulting in an increase of 24% and 16% over the original inorganic ammonia and phosphate respectively, as shown in Table 5S of the Supplementary Material. Correlations to estimate the capital cost and operating and management costs (O&M) as a function of the animal population of CAFOs were developed using data from the US EPA AgSTAR program (**AgSTAR2003**) and the USDA (**USDA_OM**) respectively. We refer the reader to the Supplementary Material for further information.

5.2.2.3 Biogas purification

Before transforming biogas into marketable products, a purification stage has to be carried out to remove H_2S , H_2O , and NH_3 . The removal of H_2S is performed in a bed of ferric oxide through the production of Fe_2S_3 operating at a temperature range of 25-50°C. The bed regeneration is carried out using oxygen to produce elemental sulfur and ferric oxide (Fe_2O_3). Water and ammonia are adsorbed using a pressure swing adsorption system (PSA) with zeolite 5A as adsorbent material, operating at low temperature (25°C) and moderate pressure (4.5 bar). The assumed recovery for NH_3 and H_2O is 100%. For further details about the modeling of the biogas purification stage, we refer the reader to previous works (**Leon; MartinHernandez**).

5.2.2.4 Biogas valorization

Two final added value products have been considered, methane and electricity, since they can be obtained through relatively simple processes and there exists developed markets for them.

METHANE PRODUCTION The process considered for methane production is the removal of CO_2 using a PSA system with a bed of zeolite 5A, since this process was demonstrated as the optimal biogas upgrading process by **MartinHernandez2020**, where further details about the modeling of the PSA system can be found.

ELECTRICITY PRODUCTION Electricity is produced from biogas through a gas turbine. A Brayton cycle consisting of double-stage compression system, one for the air stream and one for the biogas stream, is considered. Polytropic compression is assumed, with a polytropic index of 1.4 and an efficiency of 85% (**moran2010fundamentals**). The adiabatic combustion of methane contained in the biogas is assumed, with a pre-heating of the biogas-air mixture, considering the combustion chamber as an adiabatic furnace. An air excess of 20% with respect to the stoichiometric needs, and

100% conversion of the reaction are assumed. Further details for electricity production can be found in **MartinHernandez**.

5.2.2.5 Solid-liquid separation

Nutrients contained in organic waste (manure or digestate, depending on whether AD is carried out or not) are present in both organic and inorganic forms. Organic nutrients are chemically bonded to carbon, and they have to be converted into their inorganic forms through a mineralization process to be available for the vegetation to grow. Organic nutrients are mainly contained in the solid phase of organic waste. Inorganic nutrients are water soluble, and they are mostly present in the liquid phase, or bounded to soluble minerals. They are immediately available to plants, including algae involved during the occurrence of HABs. To recover the inorganic fraction of nutrients, a solid-liquid separation stage is implemented, keeping the inorganic nutrients in the liquid stage, which will be further processed, and the organic nutrients in the solid phased, which can be composted to mineralize nitrogen and phosphorus and be further used as fertilizers. The study of organic waste composting is out of the scope of this work.

Based on the evaluation reported by **MollerSLsep**, a screw press is the technology selected to carry out the solid-liquid separation stage since it is the most cost-efficient equipment. The partition coefficients for the different components are shown in Table 6S of the Supplementary Material. Assuming the discretization of units due to the commercial sizes available, the investment and operating costs for the screw press equipment are presented in Figure 9S of the Supplementary Material.

5.2.2.6 Phosphorus recovery

The technologies to recover inorganic phosphorus can be classified in three categories: struvite-based phosphorus recovery, calcium precipitates-based phosphorus recovery, and physical separation systems. Table 6.1 shows the classification and characteristics of the evaluated technologies. Regarding struvite-based systems, the formation of struvite has been widely described in the literature, mainly focused on phosphorus recovery from wastewater (**rahaman_modeling_2014; Battistoni**). However, cattle organic waste shows some characteristics that hinder struvite formation, including high ionic strength, which reduces the effective concentration of ions; and the presence of calcium ions competing for phosphate ions (**Yan2016**), which inhibits a selective recovery by phosphorus precipitation. The high variability in the manure composition, as a function of the geographic area, the animal feed, etc., represents an additional challenge for

nutrient recovery (**Tao**). Therefore, specific correlations for livestock waste to estimate the molar fraction of PO_4^{3-} and Ca^{2+} recovered as struvite as a function of the amount of calcium contained in the waste were developed in a previous work (**MartinStruvite**).

Among the different products obtained by the different processes, only struvite generates income. Calcium precipitates lacks of a well-established market as fertilizer, and therefore no sales of this product are considered. MAPHEX produces an organic solid rich in nutrients, but with a lower nutrient density compared with struvite, hindering transportation of this product and decreasing its market value. Therefore, we have assumed that no income is obtained from this product. Nevertheless, the recovered products allow phosphorus distribution from CAFO releases to phosphorus-deficient areas.

All technologies considered are at or near commercial stage. We note that, for all the technologies evaluated, the installation of several P recovery units in parallel arrangement is considered if the amount of waste to be processed exceeds the treatment capacity of the system. The description of the processes, and the correlations used to estimate the struvite formed, equipment cost, and operating costs are collected in the Section 2.2.4 of the Supplementary Material.

5.2.2.7 *Incentives for the installation of nutrient recovery systems*

COW2NUTRIENT can evaluate the effect of different kinds of incentives on the economic performance of the nutrient recovery systems. These incentives can be received as a result of the recovery of phosphorus, in the form of P-credits, or for the generation of electricity or biomethane, in form of Renewable Energy Certificates (REC) and Renewable Identification Numbers (RIN) respectively. Renewable Energy Credits are a mechanism implemented in the US which guarantees that energy is generated from renewable sources, providing a system for trading produced renewable electricity. Each produced renewable megawatt-hour generates one REC, that can be sold separately from the electricity commodity itself and can be used to meet regulatory requirements by generators, trades, or end-users. On the other hand, RINs are identification numbers assigned to batches of biofuel, allowing their tracking through the production, purchase, and final usage. The allocation of RINs is associated with the allocation of incentives for the generation bio-fuels. The considered values for the different incentives are listed in Table 4S of the Supplementary Material.

Table 5.3: Description of phosphorus recovery technologies systems by COW2NUTRIENT framework. $\chi_{Ca^{2+}:PO_4^{3-}}$ refers to the Ca^{2+}/PO_4^{3-} molar ratio. n_i denotes the number of units of the technology i installed.

Technology	Company	Technology type	Technology readiness level	Phosphorus recovery efficiency (%)	Treatment capacity ($\frac{kg_{P-PO_4}}{day-unit}$)	CAPEX ($\frac{MM\ USD}{unit}$)	OPEX ($\frac{USD}{kg_{P-PO_4}}$)	Reference
Multiform	Multiform Harvest	Struvite-based	9	$\frac{1 + \left(\chi_{Ca^{2+}:PO_4^{3-}} - 0.576 \right)}{0.798.100}^{2.113}$	38.5	1.1	154.42	1
CrystaLactor	Royal Haskoning DHV	Struvite-based	9	$\frac{1 + \left(\chi_{Ca^{2+}:PO_4^{3-}} - 0.576 \right)}{0.798.100}^{2.113}$	137.7	$2.3 + 0.71 \cdot n_{CrystaLactor}$	2.12	2
NuReSys	Nutrient Recovery Systems	Struvite-based	9	$\frac{1 + \left(\chi_{Ca^{2+}:PO_4^{3-}} - 0.576 \right)}{0.798.100}^{2.113}$	204.0	1.38	6.22	1
Pearl 500	Ostara	Struvite-based	9	$\frac{1 + \left(\chi_{Ca^{2+}:PO_4^{3-}} - 0.576 \right)}{0.798.100}^{2.113}$	65.0	2.3	7.54	3
Pearl 2K	Ostara	Struvite-based	9	$\frac{1 + \left(\chi_{Ca^{2+}:PO_4^{3-}} - 0.576 \right)}{0.798.100}^{2.113}$	250.0	3.1	7.54	1
Pearl 10K	Ostara	Struvite-based	9	$\frac{1 + \left(\chi_{Ca^{2+}:PO_4^{3-}} - 0.576 \right)}{0.798.100}^{2.113}$	1250.0	10.0	7.54	4
P-Roc	Karlsruhe Institute of Technology	Calcium precipitates-based	6	60	24.3	Tailored design based on waste flow processed. See Section 2.2.4.4 of Supplementary Material.	23.22 - 167.8	5
MAPHEX	University of Pennsylvania and USDA	Modular phases separation system	7	90	18.5	0.3	110.8	6,7

- 1: PearlKcost2
- 2: egle_phosphorus_2016
- 3: Pearl500cost1
- 4: Pearl10Kcost1
- 5: ebrecht_p_recovery_2011
- 6: church_novel_2016
- 7: church_versatility_2018

5.2.3 Multi-criteria decision model

The determination of the most suitable nutrient management process is not a trivial procedure since multiple criteria play a critical role at the decision-making stage. COW₂NUTRIENT performs the selection of P recovery technologies considering information concerning environmental, economic, and technology readiness dimensions. The integration of these dimensions is justified by the need to find the most suitable system for each CAFO by balancing operating cost and efficiency in the mitigation of nutrient pollution according to the local environmental vulnerability to eutrophication. Finally, the technical maturity of each system is also considered to assess the development level of the different processes. Therefore, a multi-criteria decision analysis (MCDA) model was developed to address the selection of the most suitable phosphorus recovery systems for each studied CAFO. The workflow of the MCDA model is summarized in Figure 5.3.

Five criteria are combined in a composite index for the assessment of the environmental, economic, and technology maturity dimensions of the different technologies. Two environmental criteria are studied to assess the performance of the different technologies to mitigate phosphorus releases from CAFOs, i.e., the fraction of phosphorus recovered, and the potential environmental threat for the local ecosystem of the effluents containing the non-recovered phosphorus evaluated through the eutrophication potential of the effluents. The economic aspect is considered by means of two criteria, the economic barrier for the implementation of P recovery processes, measured in terms of capital cost, and the overall economic performance of the systems, which is evaluated through the net present value (NPV) (**sinnott2014chemical**). Finally, the technological maturity of the different technologies is considered through the technology readiness level (TRL) index. The construction of a composite index integrating these criteria is composed of three steps: criteria normalization, weighting, and aggregation (**MarcoCinelli2020**).

5.2.3.1 Data normalization

Since each criteria has a different range of potential values, they must be normalized to a common scale to allow each criteria to be compared with the others. However, the composite index can be affected by the normalization technique used. In order to study the robustness of the composite index obtained, and to address the uncertainty originated by data normalization, normalized data using standardization, min-max, and target normalization methods is calculated (**HandbookCompositeIndicators**).

Table 5.4: Criteria preference as a function of the GIS-based environmental indicators for nutrient pollution.

Local environmental indicators values	Criteria ranking	Description
Condition 1: TES > TSI and TES > Soil fertility	TRL > NPV > Capital cost > TP recovered > Eutrophication potential	Unbalanced phosphorus releases but no immediate threat to soil and water bodies.
Condition 2: TES = Unbalanced		Prevalence of economic criteria for nutrient recovery system selection.
Condition 1: TSI \geq TES or TSI \geq Soil fertility	TRL > Eutrophication potential > NPV > TP recovered > Capital cost	High Trophic State Index. Immediate environmental risk due to potential algal blooms.
Condition 2: TSI = Eutrophic or Hypereutrophic		Prevalence of environmental criteria for nutrient recovery system selection.
Condition 1: Soil fertility \geq TES and Soil fertility > TSI	TRL > TP recovered > NPV > Eutrophication potential > Capital cost	Excessive P in soil. Immediate environmental risk due to potential P runoff.
Condition 2: Soil fertility = Excessive		Prevalence of environmental criteria for nutrient recovery system selection.
Condition: TES \neq Saturated and TSI \neq Eutrophic or Hypereutrophic and Soil fertility \neq Excessive	TRL > NPV > Capital cost > TP recovered > Eutrophication potential	No environmental risk. Prevalence of economic criteria for nutrient recovery system selection.

TRL: Technology Readiness Level

TSI: Trophic State Index

TES: Techno-Ecological Synergy sustainability metric

NPV: Net Present Value

TP: Total Phosphorus

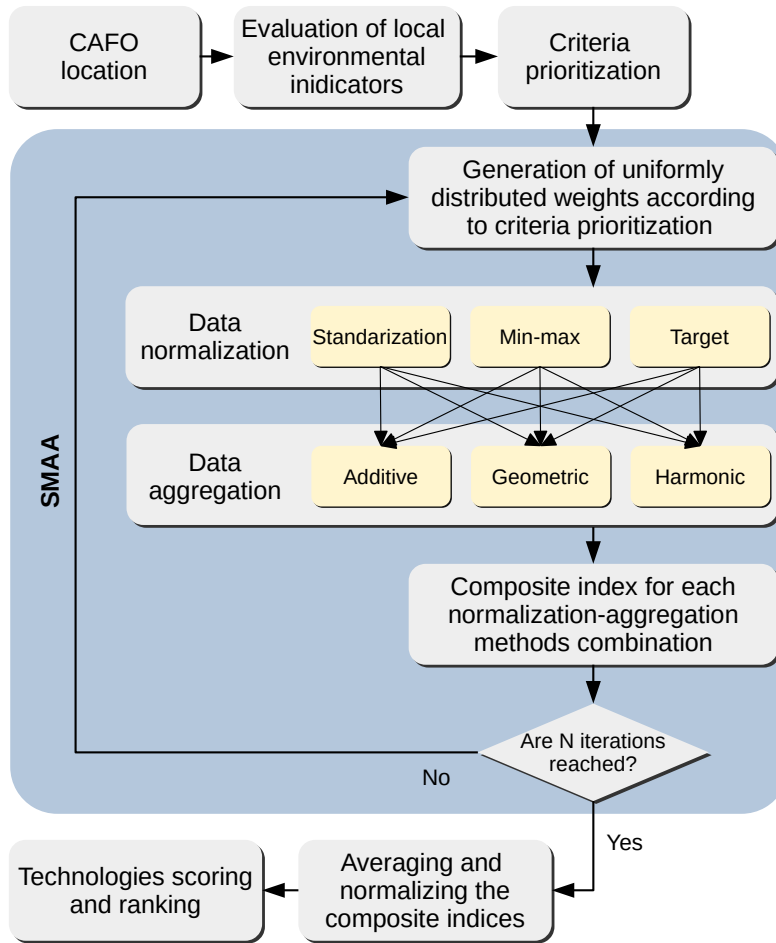


Figure 5.3: Flowsheet for the MCDA model.

5.2.3.2 Criteria weighting

The normalized criteria are weighted to set the relative importance of each criterion, prioritizing some criteria over others. This is needed in order to obtain a flexible decision method able to balance the operating cost of the systems and the P recovery efficiency as a function of the environmental vulnerability to eutrophication of each region. The minimization of the operating costs is prioritized in regions with low eutrophication risk, while the efficiency of P recovery is more relevant in regions affected by nutrient pollution. Therefore, the criteria are dynamically weighted according to the values of TSI, TES and Mehlich 3 phosphorus concentration in each region studied. The preference of criteria as a function of the environmental

vulnerability to eutrophication is shown in Table 5.4. On the one hand, if there is immediate environmental risk by nutrient pollution (i.e., high values for TSI or soil fertility), phosphorus recovery efficiency is prioritized over economic performance. Conversely, if there is environmental risk in the long run due to the unbalance between anthropogenic phosphorus releases and uptakes (negative value of TES indicator), or there is no potential environmental risk, the economic performance is prioritized over the phosphorus recovery efficiency. Finally, since the objective of this framework is to select P recovery systems that are feasible to install and operate in CAFOs, the TRL index is set as the criteria with highest preference in all cases in order to minimize the risk of selecting non-full-scale processes. As a result, the selection of processes with low TRL will be hampered unless they have good economic or environmental performance.

The procedure described above sets the prioritization of criteria, i.e., they can be sorted in order of importance. However, it does not provide an specific value for the weights, which values are unknown. In order to avoid the risk of biasing the decision-making procedure setting arbitrary values for the weights, a stochastic multi-criteria acceptability analysis (SMAA) is used to explore the weights space ([tervonen_implementing_2007](#)). Through this approach, the feasible space of each weight (i.e., the space delimited by the previous and the subsequent weights) is explored through the Monte Carlo method, retrieving a set of weights for all criteria according to the assigned order. The SMAA is formulated by defining the set of n weights (ω) as a non-negative set which elements must sum 1, as shown in Eqs. 5.3 and 5.4.

$$\omega_j \geq 0 \quad \forall j \in n \quad (5.3)$$

$$\sum_{j=1}^n \omega_j = 1 \quad (5.4)$$

$$\omega_{j1} \geq \omega_{j2} \geq \dots \geq \omega_{jn} \quad (5.5)$$

The preference information of the criteria, defined through the ranking of the criteria shown in Table 5.4, is expressed as a sequence of inequality constraints, Eq. 5.5. A detailed description of the SMAA method can be found in [tervonen_implementing_2007](#). A number of Monte-Carlo simulations (N) of 100 is assumed as a trade-off between computational cost and MCDA model performance.

5.2.3.3 Criteria aggregation

The aggregation stage merges the weighted criteria, resulting in the composite index. Similarly to the normalization stage, different aggregation methods are evaluated to improve the robustness of the solutions retrieved by the framework. Different aggregation schemes denote different degrees of compensability between indicators, i.e. a deficit in one criteria can be fully, partially, or not compensated by a surplus in other criteria (**MarcoCinelli2020**). Three aggregation functions are evaluated including full compensation (additive aggregation) and partial compensation schemes (geometric and harmonic aggregation methods). Nine composite indexes are obtained for each P recovery technology combining normalization and aggregation techniques, as shown in Figure 5.3. Finally, the composites indexes are normalized in a range from 0 to 1 and ranked to determine the most suitable P recovery process for the CAFO under study.

5.2.4 Framework limitations

The main limitations of the proposed framework lie in the uncertainty of the input data. On the one hand, since the data regarding the animal number, type of animals, and location of CAFOs are reported by the state environmental protection agencies of each state, they are considered reliable. On the other hand, to estimate the local vulnerability to phosphorus pollution throughout the contiguous US, HUC8 spatial resolution has been chosen as a trade-off solution between spatial accuracy and data uncertainty. However, more accurate results can be obtained if reliable data for phosphorus level in soils, fertilizer application rates, etc. are available for higher spatial resolution. Particularly, further studies for developing more accurate correlations to estimate the fraction of phosphorus available to plants based on soil type and climate conditions in each region would improve the accuracy of the assessment of local risk to phosphorus pollution. Additionally, since the proposed framework is focused on phosphorus recovery for freshwater nutrient pollution prevention and control, the recovery of other resources contained in livestock manure (such as organic carbon and nitrogen) is not considered in this study.

5.2.5 Case study

5.2.5.1 Study region

The Great Lakes area, located in North America, is selected in order to demonstrate the implementation of nutrient management systems at

CAFOs using the COW2NUTRIENT framework. This region is selected because its high concentration of CAFO facilities, resulting in significant nutrient releases that contribute to frequent HABs and eutrophication episodes, as well as to the nutrient legacy accumulated over time ([sayers2019satellite](#); [han2012historical](#)). The evaluation and implementation of phosphorus recovery systems at CAFOs already in operation at the US states of Pennsylvania (**Pennsylvania_CAFOS**), Ohio (**Ohio_CAFOS**), Indiana (**Indiana_CAFOS**), Michigan (**Michigan_CAFOS**), Wisconsin (**Wisconsin_CAFOS**), and Minnesota (**Minnesota_CAFOS**) are performed using the criteria prioritization based on the GIS indicators describing the environmental impact of nutrient pollution shown in Table 5.4. The states of Illinois and New York, and the Canadian province of Ontario, which are also part of the Great Lakes area, are not included due to the unavailability of reliable information about their CAFOs. A description of the studied states listing the animal units, annual manure generation, and annual phosphorus releases by the year 2019, disaggregated for dairy and beef cattle, is collected in Table 10S of the Supplementary Material.

It should be noted that, accordingly to the US regulatory definition of CAFOs, only intensive livestock facilities with 300 animal units or more are considered in this study (**CAFO_definition**), resulting in the evaluation of 2,217 CAFOs. An animal unit is defined as an animal equivalent of 1,000 pounds (453.6 kg) live weight (**animal_unit_definition**). Animal units is used as a unit to measure the size of CAFOs due to the presence of different types of animals in the CAFOs, i.e. beef or dairy cows, and animals of different age, including heifers, calves, and adult animals. Different types of animals result in different manure generation rates and composition. Therefore, the different types of animals within each studied CAFO are normalized using the definition of animal units to estimate the amount and composition of the manure generated.

5.2.5.2 Scenarios description

Two scenarios have been evaluated, the deployment of only phosphorus recovery systems, and the integration of these processes with AD and electricity production processes. Incentives for the recovery of phosphorus based on the work of [sampat_economic_2018](#) are considered, assuming a phosphorus credit value of 22 USD/kg_P recovered for both scenarios. We note that this value is significantly lower than the economic impact of P release from livestock waste, valued in 74.5 USD/kg_P released ([sampat2021valuing](#)). Additionally, in the scenario considering the production biogas-based electricity, a value of Renewable Energy Certificates (fixed electricity selling

price) of 60 USD per MWh generated is assumed. Finally, a discount rate of 7% is considered in both scenarios.

5.3 RESULTS

5.3.1 *Implementation of phosphorus recovery systems in the Great Lakes area*

Table 5.5 summarizes the results of the phosphorus recovery process selection in the Great Lakes area. It can be observed that only three out of the six commercial processes evaluated are selected to be installed. All selected processes recover P in the form of struvite, which is a valued product that can be sold, generating income. Although the Ostara Pearl process also produces struvite, it results in larger operating costs than the technologies selected. Conversely, P-RoC recovers phosphorus in the form of calcium-based precipitates. This product lacks a well-established market, and therefore it does not generate income. In addition, P-RoC is the technology with the lowest TRL, which hampers the selection of this process. The selection of modular phosphorus recovery systems, such as MAPHEX, which due to economies of scale are especially suitable for small livestock facilities, is largely prevented by the absence of small-scale CAFOs. Therefore, a sub-set of three technologies is obtained. Therefore, it can be concluded that the selection of this pool of three technologies amongst the six systems evaluated is mainly driven by economic factors. Additionally, the low TRL of P-RoC also hampers the selection of this process.

The selection of the most suitable technology for each studied CAFO among the sub-set comprised by Multiform, Nuresys, and Crystalactor systems is based on the CAFO scale and local eutrophication risk, as it is discussed in the following sections.

5.3.1.1 *Effect of CAFOs scale on selecting P recovery systems*

A relationship between CAFOs size and the selected technologies can be observed in Table 5.5. This relationship is also observed in Figures 5.4 and 5.5. Multiform is the predominant phosphorus recovery process. Furthermore, we observe that in those states with smaller CAFOs (Minnesota and Indiana) the selection of Multiform is more predominant than in states with larger CAFOs. On the contrary, in the states with large CAFOs or with outliers representing large facilities, (such as Ohio and Wisconsin) Crystalactor is selected for some facilities. Additionally, NuReSys is a technology also selected for medium-size CAFOs.

Table 5.5: Distribution and characteristics studied CAFOs, and phosphorus recovery processes selected. Only selected technologies are included in the table.

State	CAFO average size (animal units)	Number of CAFOs	Manure generated (ton/year)	P recovered (ton/year, (%))	Number of phosphorus recovery systems installed					
					Multiform		NuReSys		Crystalactor	
					S1	S2	S1	S2	S1	S2
Indiana	1,574.41	119	$2.48 \cdot 10^6$	1558.8 (78.7)	116	113	0	0	3	6
Michigan	2,461.52	144	$4.76 \cdot 10^6$	3004.4 (79.0)	127	113	16	30	1	1
Minnesota	634.23	1,487	$1.13 \cdot 10^7$	6938.1 (76.9)	1,477	1,476	0	0	10	11
Ohio	2,415.24	53	$1.68 \cdot 10^6$	1055.8 (78.6)	50	47	1	3	2	3
Pennsylvania	1,495.94	131	$2.59 \cdot 10^6$	1633.2 (78.9)	124	119	6	11	1	1
Wisconsin	2,628.19	283	$1.02 \cdot 10^7$	6510.5 (79.4)	262	255	6	7	15	21

S1: Phosphorus recovery systems only.

S2: Phosphorus recovery systems coupled with AD and electricity production.

The integration of biogas production and upgrading affects the selection of P recovery processes as a consequence of the high investment expenditures associated to the installation of AD processes. These large costs blur the capital investment differences between different P recovery processes. As a result, the MDCA model promotes the implementation of technologies with better long-term economic performance (lower operating costs), such as NuReSys and Crystalactor, in spite of the fact that they involve larger investments costs than other technologies like Multiform, as shown in Figure 5.4b.

Based on the data illustrated in Figures 5.5 to 5.7, a preliminary screening of P recovery systems can be performed based on the size of the CAFOs. If the installation of only nutrient recovery systems is considered, Multiform can be selected for CAFOs with sizes up to 5,000 animal units, NuReSys can be selected for CAFOs with a size between 2,000 and 5,000 animal units, and Crystalactor is selected for CAFOs larger than 5,000 animal units. For the scenario integrating anaerobic digestion and phosphorus recovery processes, Multiform is mostly selected for CAFOs up to 4,000 animal units, although it is also selected in some larger CAFOs, NuReSys are mostly selected for CAFOs between 2,000 and 6,000 animal units, while the size range for the selection of Crystalactor is similar to the previous case. The operating costs are shown in Figure 5.6. It can be observed that the operating cost of Multiform is larger than NuReSys, and in turn the operating cost of this one is larger than Crystalactor, showing an opposite pattern than capital costs.

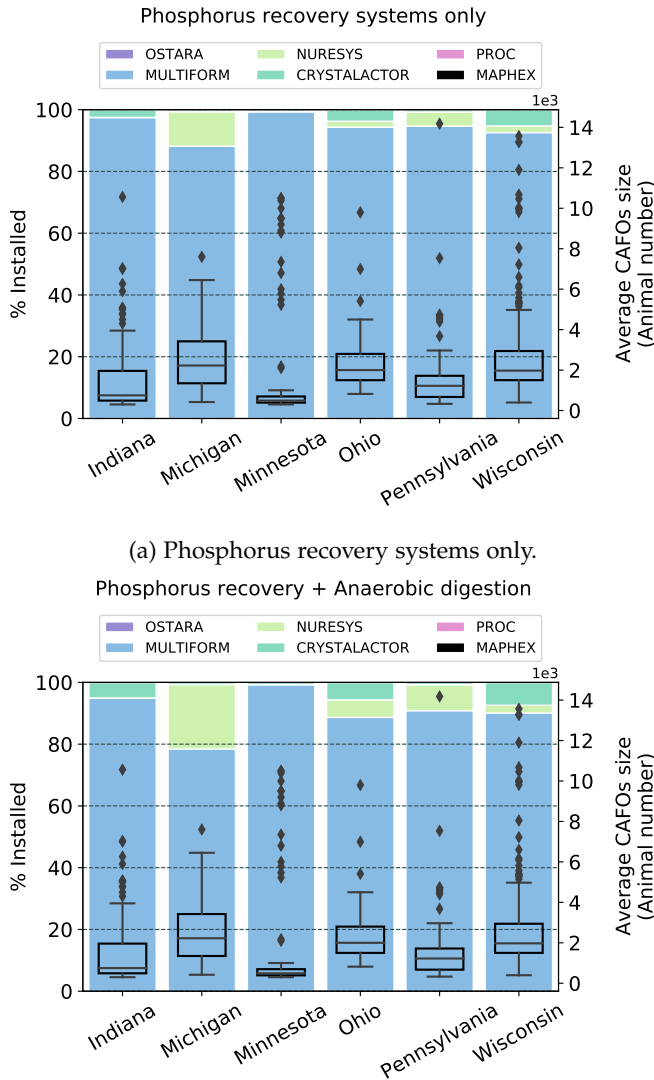


Figure 5.4: Distribution of the phosphorus recovery systems selected for the CAFOs in the Great Lakes area. The boxplots represent the distribution of CAFO sizes in each studied state.

5.3.1.2 Effect of local eutrophication risk on the selection of P recovery systems

The results obtained reveal that CAFOs scale is the main driver for the selection of phosphorus recovery technologies. However, the role of the environmental vulnerability to eutrophication can be appreciated in those CAFOs where two different systems show similar economic performance.

From the results illustrated in Figure 5.7, it can be observed that Multi-form and NuReSys technologies are selected for CAFOs with similar size. However, the economic performance of the second technology is better as consequence of the lower operating expenses and larger net revenues of this technology. Although both technologies have similar phosphorus recovery yield, Multiform shows better environmental performance since the eutrophication potential of its output streams is lower than NuReSys effluents. This difference in eutrophication potential between both technologies is mainly driven by the higher nitrogen recovery of Multiform. Therefore, in those locations that are highly vulnerable to nutrient pollution, the solution proposed by the COW2NUTRIENT framework is driven more by environmental criteria than by economic criteria, resulting in the selection of the Multiform process.

Table 5.6: Economic results per state for installing phosphorus recovery systems in the studied states of the Great Lakes area.

State	CAPEX (MM USD)		OPEX (MM USD/year)		Net revenue (MM USD/year)	
	S1	S2	S1	S2	S1	S2
Indiana	145.58	325.00	21.18	34.16	19.32	11.88
Michigan	191.09	480.19	36.74	55.92	41.00	32.15
Minnesota	1,591.40	2,866.31	140.74	251.58	39.61	-46.15
Ohio	68.30	179.29	12.95	20.32	14.46	10.80
Pennsylvania	148.16	332.03	21.46	35.03	20.82	12.95
Wisconsin	396.24	1,009.47	73.55	117.80	95.44	74.14

S1: Phosphorus recovery systems only.

S2: Phosphorus recovery systems coupled with AD and electricity production.

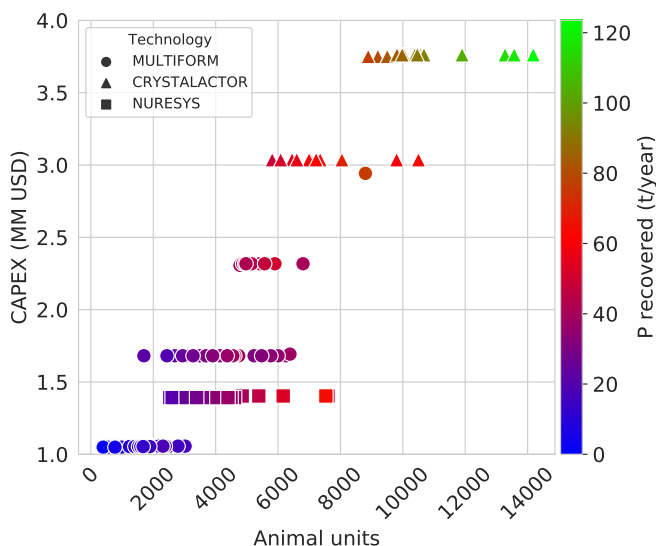
5.3.2 Economic results

The capital expenditures (CAPEX), operating expenses (OPEX), and net revenues (difference between incomes and operating expenses) associated with the deployment of the nutrient management systems are listed per state in Table 5.6. For the scenario considering the installation of only phosphorus recovery processes, the CAPEX and OPEX are 2,540.77 MM USD and 185.65 MM USD per year respectively. If the integration of biogas production and upgrading to power with phosphorus management is considered, the CAPEX and OPEX increase up to 5,192.29 MM USD and

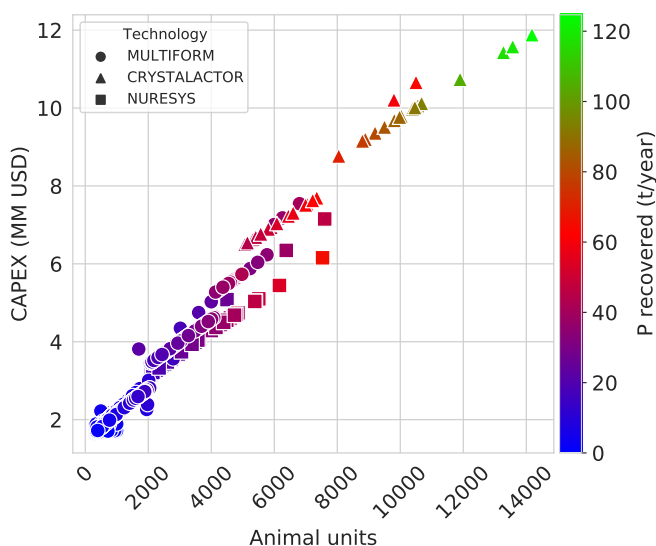
267.51 MM USD per year respectively. It can be observed that, due to the high CAPEX of biogas production and upgrading stages, the net revenues decrease from 230.65 MM USD per year for the scenario considering only phosphorus recovery systems to 95.77 MM USD per year if the processes for phosphorus recovery and AD are combined.

Figures 5.5 and 5.6 show the evolution of CAPEX and OPEX of the P recovery technologies installed at the livestock facilities studied as a function of CAFOs scale. Figure 5.5a shows the CAPEX when the implementation of only P recovery systems is considered. We observe that CAFOs are grouped in sets selecting the same P recovery technology. This is because the manufacturers standardize the size of each P recovery technology, which in turn determines the maximum waste processing capacity of each technology (as shown in Table 6.1). This results in the use of the same P recovery equipment, and thus the same CAPEX, for all the CAFOs generating waste below the maximum processing capacity. Likewise, we note different CAPEX values for the implementation of the same P recovery technology. This is a consequence of installing of multiple in-parallel P recovery units to increase the processing capacity of such technology, since the waste generated in that CAFO exceeds its maximum processing capacity. It can also be appreciated that CAFOs with similar size might result in the installation of different technologies, or a different number of units of the same technology. This is because, although CAFOs can have a similar number of animal units, the type of the animals can be different, resulting in the generation of different amounts of manure. In the case of considering biogas production and upgrading, illustrated in Figure 5.5b, the required CAPEX increases significantly, blurring the differences in the capital investment between different P recovery processes observed in Figure 5.5a into the cost of the whole system. The integration of AD and electricity production also results in the increase of the OPEX, as shown in Figure 5.6.

The net revenue of the installed nutrient management systems according with the economic parameters described at the beginning of the section is shown in Figure 5.7. We observe a pattern characterized by the increase of the net revenues with the increase of CAFOs size. However, the implementation of P recovery technologies in CAFOs below 1,000 animal units, and below 2,000 animal units if biogas production and upgrading is also considered, result in economic losses. Additionally, the integration of these processes slightly decreases the net revenues of the systems installed for phosphorus recovery.

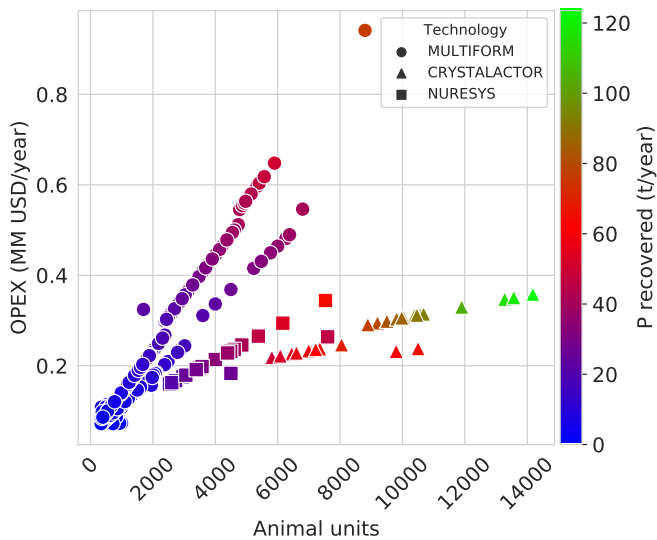


(a) Phosphorus recovery systems only.

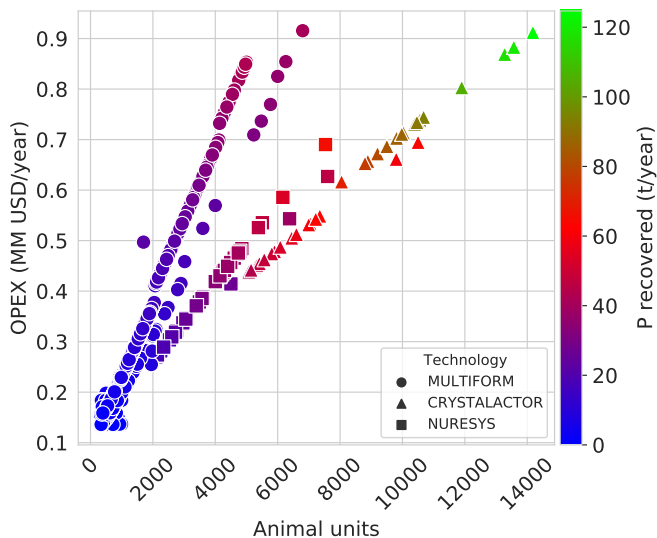


(b) Phosphorus recovery systems coupled with AD and electricity production.

Figure 5.5: Capital expenses for deploying phosphorus recovery systems in the studied CAFOs. The dots represent the P recovery technologies installed in the studied CAFOs.



(a) Phosphorus recovery systems only.



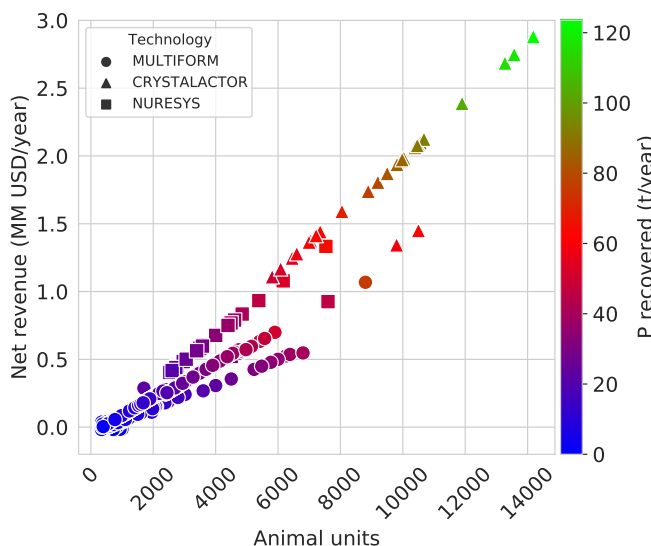
(b) Phosphorus recovery systems coupled with AD and electricity production.

Figure 5.6: Operating expenses for deploying phosphorus recovery processes in the studied CAFOs. The dots represent the P recovery technologies installed in the studied CAFOs.

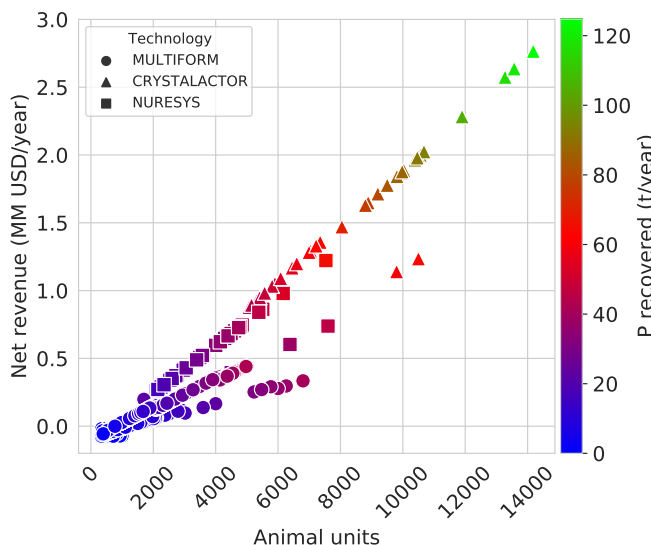
5.4 DISCUSSION

5.4.1 Economic implications

In this work, fixed incentives for P recovery and biogas-based electricity generation have been considered as starting point to explore the



(a) Phosphorus recovery systems only.



(b) Phosphorus recovery systems coupled with anaerobic digestion and electricity production.

Figure 5.7: Net revenue from the phosphorus recovery processes selected in the studied CAFOs. The dots represent the P recovery technologies installed in the studied CAFOs.

effect of the application of incentives in the implementation of P recovery technologies, either standalone or integrated with biogas production and upgrading processes. The results shown in Figure 5.7 reveal the effect of the economies of scale in the net revenues from the implementation of P

recovery technologies in the Great Lakes area are highly dependent on the economies of scale, i.e., the larger the amount of waste to be treated, the larger the net revenues obtained. However, while for the largest CAFOs significant profits are obtained, negative revenues (i.e., economic losses) are obtained for the smallest CAFOs, even for large P credits prices such as 22 USD/kg_P recovered. This suggests that the implementation of fixed incentives is not a fair policy, since the small CAFOs are not profitable while they increase the profits of the largest CAFOs. Therefore, alternative incentive policies must be explored. **sampat2019coordinated** studied the development of a coordinated management system for the treatment of cattle manure and P recovery. That framework captures the geographical phosphorus imbalance by proposing different prices for manure treatment that capture the regional remediation cost caused by P releases. They found that economic drivers are needed for a cost-effective recovery and redistribution of phosphorus, considering fixed incentives for P recovery up to 50 USD/kg_P for this purpose. Therefore, further research about the effect of implementing dynamic incentives for P recovery is needed. These incentive policies can follow different schemes, such as progressive incentives for P recovery based on the amount of manure treated, or cooperative schemes where the profits from P recovery obtained by the largest livestock facilities are redistributed to the smallest CAFOs. This is a concept that has been studied for minimizing the costs of meeting greenhouse gases emission targets (**galan2018time**), and could be adopted for the reduction of P releases.

Furthermore, consideration should be given to the fair allocation of incentives in those scenarios where the available incentives budget is not enough to avoid economic losses in all CAFOs. In this regard, the fairness measure considered for budget allocation must be carefully selected among the existing schemes (**sampat2019fairness**).

5.4.2 *Phosphorus use efficiency*

Currently, manure or digestate in liquid phase is usually supplied as nutrient supplementation in croplands, or it is treated in either aerobic or anaerobic ponds. Solid phase processing is based on composting or drying. However, the high density of manure and digestate and low concentration of nutrient prevent an efficient redistribution of the phosphorus released from CAFOs to phosphorus-deficient areas (**burns2002phosphorus**). Therefore, the implementation of phosphorus recovery processes is a desirable measure for sustainable phosphorus management. We find that implementing struvite production processes considering incentives for P

recovery of 22 USD/kg_P recovered is economically feasible for CAFOs larger than 1,000 animal units if standalone P recovery technologies are implemented, and for CAFOs larger than 2,000 animal units if they are integrated with biogas production and upgrading processes. The requirement of large incentives to produce profit in most of the P recovery systems installed at CAFOs might raise the debate of whether it is worthwhile to implement P recovery systems; or if the economic resources should be allocated to simpler phosphorus management alternatives, such as the redistribution of either raw or pond-stored manure. In this regard, **sampat2019coordinated** studied the separation of manure in liquid and solid phases, and their further transport to demanding allocations, considering a coordinated management system in Upper Yahara watershed (Wisconsin, United States). In addition, that study considered the implementation of economic incentives from 0 to 50 USD/kg_P. However, the results showed that manure redistribution is not an economically viable technique for phosphorus recycling in this range of incentives. The main drawback of manure redistribution is the large transportation cost of both liquid and solid raw manure because of the high volume of these materials and their low phosphorus concentration. Therefore, the results reveal that on-site manure processing to generate valuable products (struvite) is more beneficial than manure redistribution.

The replacement of phosphorus from synthetic fertilizers by the recovered P, mitigating the dependency on fertilizers from non-renewable resources (phosphate rock), is an interesting alternative towards the sustainability of the agri-food sector. However, phosphorus availability for plants depends on several factors, including the P product used as fertilizer and soil pH level. Since struvite is the product recovered in all studied CAFOs, we will focus the discussion on this product. **vaneeckhaute2015efficiency** compared the bio-availability of several bio-based fertilizers, including struvite, to synthetic triple super phosphate (TSP). This study shows that P available in soil (measured as Prhizon) was a 45% higher than TSP in acidic soils (pH=5.0), but 60% lower in slightly basic soils (pH=7.9). Based on these data, one kilogram of manure processed for P recovery by struvite production can replace from $1.53 \cdot 10^{-3}$ to $3.71 \cdot 10^{-3}$ kg of TSP ($5.02 \cdot 10^{-3}$ kg of struvite are recovered per kilogram of manure processed). However, it must be noted that currently the cost of recovered P from manure (2.12–15.42 USD/kg_P recovered, see Table 6.1) is considerable larger than the cost of phosphorus from synthetic TSP (1.23 USD/kg_P) (**fertilizers_price**). As a result, from an economic perspective the complete substitution of phosphate rock is currently hindered by the large recovery costs, in addition to a limited availability of resources recovered from waste, and henceforth further exploration on resource recovery from different wastes is required to achieve P circularity reducing the recovery costs, and increasing the

amount of phosphorus from organic waste, including but not limited to livestock manure.

5.5 CONCLUSION

We presented a framework for the techno-economic evaluation and selection of phosphorus recovery systems considering the local vulnerability to phosphorus pollution through a GIS environmental model. A multi-criteria decision analysis model is used for the comparison and selection of phosphorus recovery systems based on the economic performance and technological readiness level of the processes, and the eutrophication risk of the watershed where the studied CAFOs are located. Technologies for P recovery in the form of struvite are selected in all CAFOs studied. The selection of P recovery technologies is mainly driven by economic criteria, and the effect of the economies of scale is very significant. However, environmental criteria (P recovery efficiency, eutrophication potential of process effluents) are the decision criteria at some CAFOs where different technologies show similar economic performances. The results show that a preliminary screening of P recovery systems can be performed based on the size of CAFOs. Multiform can be selected for CAFOs with sizes up to 5,000 animal units, NuReSys can be selected for CAFOs with a size between 2,000 and 5,000 animal units, and Crystalactor is selected for CAFOs larger than 5,000 animal units. The implementation of these systems in the Great Lakes area involves capital expenditures of 2.5 billion USD and operating costs of 186 million USD per year if only phosphorus recovery technologies are installed, and 5.2 billion USD and 268 million USD per year respectively if biogas production and upgrading are also considered. The implementation of fixed incentives of 22 USD/kg_P recovered is considered to avoid economic losses due to P recovery costs impact in the economy of CAFOs. However, we find that the implementation of fixed incentives is not a fair policy, since the small CAFOs are not profitable while they increase the profits of the largest CAFOs. The phosphorus recovered in the form of struvite from one kilogram of manure processed can replace from $1.53 \cdot 10^{-3}$ to $3.71 \cdot 10^{-3}$ kg of synthetic triple super phosphate, but incurring in significantly larger production costs (2.12-15.42 USD/kg_P recovered) than synthetic fertilizer (1.23 USD/kg_P).

As part of future work, customized incentive policies adapted to the particularities of each livestock facility can be proposed in order to optimize the allocation of limited monetary resources. Additionally, it would be interesting to analyze the potential of crop-livestock integration as an alternative for phosphorus recycling to the implementation of physico-

chemical P recovery processes. Another interesting research line is the integration of multiple processes in order to recover additional valuable products from organic waste (such as biochar), adapting the concept of refinery to resource recovery from organic waste.

ACKNOWLEDGMENTS

This research was supported in part by an appointment for E. Martín-Hernández to the Research Participation Program for the Office of Research and Development, US EPA, administered by the Oak Ridge Institute for Science and Education through Interagency Agreement No. DW-89-92433001 between the US Department of Energy and the US Environmental Protection Agency. PSEM3 research group acknowledge funding from the Junta de Castilla y León, Spain, under grant SA026G18 and grant EDU/556/2019.

Disclaimer: The views expressed in this article are those of the authors and do not necessarily reflect the views or policies of the US EPA. Mention of trade names, products, or services does not convey, and should not be interpreted as conveying, official US EPA approval, endorsement, or recommendation.

BIBLIOGRAPHY

6

ANALYSIS OF INCENTIVE POLICIES FOR PHOSPHORUS RECOVERY

ABSTRACT

Livestock operations have been highly intensified over the last decades, resulting in the advent of large concentrated animal feeding operations (CAFOs). Intensification decreases production costs but also leads to substantial environmental impacts. Specifically, nutrient runoff from livestock waste results in eutrophication, harmful algal blooms, and hypoxia. The implementation of nutrient recovery systems in CAFOs can abate nutrient releases and negative ecosystem responses, although they might negatively affect the economic performance of CAFOs. We design and analyze potential incentive policies for the deployment of phosphorus recovery technologies at CAFOs considering the geospatial vulnerability to nutrient pollution. The case study demonstration consists of 2,217 CAFOs in the U.S. Great Lakes area. The results reveal that phosphorus recovery is more economically viable in the largest CAFOs due to economies of scale, although they also represent the largest eutrophication threats. For small and medium-scale CAFOs, phosphorus credits progressively improve the profitability of nutrient management systems. The integration of biogas production does not improve the economic performance of phosphorus recovery systems at most of CAFOs, as they lack enough size to be cost-effective. Phosphorus recovery proves to be economically beneficial by comparing the net costs of nutrient management systems with the negative economic impact derived from phosphorus releases. The incentives necessary for avoiding up to $20.7 \cdot 10^3$ ton/year phosphorus releases and achieve economic neutrality in the Great Lakes area are estimated at \$223 million/year. Additionally, the fair distribution of limited incentives is studied using a Nash allocation scheme, determining the break-even point for allocating monetary resources.

Keywords: Organic waste; Incentive policy; Environmental policy; Livestock industry; Phosphorus recovery; Circular economy

RESUMEN

Las explotaciones ganaderas se han intensificado mucho en las últimas décadas, lo que ha dado lugar a la aparición de grandes explotaciones concentradas de alimentación animal (CAFO). La intensificación disminuye los costes de producción, pero también provoca importantes impactos ambientales. En concreto, la escorrentía de nutrientes procedente de los residuos ganaderos provoca eutrofización, floraciones de algas nocivas e hipoxia. La implantación de sistemas de recuperación de nutrientes en las CAFO puede reducir las emisiones de nutrientes y las respuestas negativas del ecosistema, aunque podría afectar negativamente a los resultados económicos de las CAFO. Diseñamos y analizamos posibles políticas de incentivos para la implantación de tecnologías de recuperación de fósforo en las CAFO teniendo en cuenta la vulnerabilidad geoespacial a la contaminación por nutrientes. El caso de demostración consiste en 2.217 CAFO en la zona de los Grandes Lagos de Estados Unidos. Los resultados revelan que la recuperación de fósforo es más viable económicamente en las CAFO más grandes debido a las economías de escala, aunque también representan las mayores amenazas de eutrofización. Para las CAFO de pequeña y mediana escala, los créditos de fósforo mejoran progresivamente la rentabilidad de los sistemas de gestión de nutrientes. La integración de la producción de biogás no mejora el rendimiento económico de los sistemas de recuperación de fósforo en la mayoría de las CAFO, ya que carecen del tamaño suficiente para ser rentables. La recuperación de fósforo demuestra ser económicamente beneficiosa al comparar los costes netos de los sistemas de gestión de nutrientes con el impacto económico negativo derivado de las emisiones de fósforo. Los incentivos necesarios para evitar hasta $20.7 \cdot 10^3$ toneladas/año de vertidos de fósforo y lograr la neutralidad económica en la zona de los Grandes Lagos se estiman en 223 millones de dólares/año. Además, se estudia la distribución justa de los limitados incentivos mediante un esquema de asignación de Nash, determinando el punto de equilibrio para la asignación de los recursos monetarios.

Palabras clave: Residuos orgánicos; Políticas de incentivos; Políticas ambientales; Industria ganadera; Recuperación de fósforo; Economía circular

6.1 INTRODUCTION

In the context of continuous human population growth, an efficient and sustainable food production system becomes a key factor to guarantee social welfare. Currently, intensive livestock farming produces most of the meat and dairy products worldwide, and the demand is expected to double by 2050 compared to 2007 ([livestock_projection](#)). To meet this increasing demand, the development of intensive farming practices has resulted in the concentrated animal feeding operations (CAFOs) ([animal_unit_definition](#)), which allows larger and cheaper productivity than traditional systems. However, concerns in terms of food safety, animal health, and environmental impacts are associated with intensive livestock farming. Focusing on environmental impacts, livestock industry needs large amounts of water, represents 14.5% of the anthropogenic-based GHG emissions ([eisler_agriculture:_2014](#)), and is a source of nutrient releases which lead to high concentrations of phosphorus in soil and waterbodies ([Sampat2017](#)). Focusing on nutrient pollution, phosphorus releases by improper organic waste management from livestock facilities contribute largely to the eutrophication of fresh and marine waters, promoting harmful algal blooms (HABs) which can release toxins and cause the hypoxia of waterbodies as a result of algae biomass decomposition.

Therefore, the development of sustainable agricultural intensification techniques is not only a desirable but also a necessary measure to reduce the environmental impact of livestock industry while meeting the current and future food demand. In this regard, the implementation of integrated systems for manure management can recover valuable components contained in livestock waste, including phosphorus and biogas-based products, and the environmental footprint of CAFOs is decreased.

From a technical perspective, the adoption of nutrient management systems in CAFOs is feasible, but their practical implementation has to overcome several other logistical and economic barriers. Therefore, developing effective incentive policies to support the economic sustainability of livestock facilities plays a critical role in the successful adoption of phosphorus recovery technologies. This is especially relevant because, despite the additional capital and operating costs these processes entail for the CAFOs, long-term remediation expense up to 74.5 USD per kg of released phosphorus ([Sampat2020](#)) can be avoided by recovering phosphorus before it reaches soil and waterbodies. Remediation costs are believed to not affect the owners of livestock facilities directly; however, environmental remediation costs are usually covered by public budgets funded by taxpayers, and may lead to the eventual application of specific taxes on livestock products for their environmental footprint. Different incentive

schemes can be considered to promote the adoption of sustainable nutrient management systems, including phosphorus releases allowances in the form of P credits and renewable electricity certificates (REC) for energy recovery.

In this work, a systematic analysis of different incentive schemes is performed through a computational framework for the techno-economic analysis of nutrient and energy recovery technologies for livestock facilities. Suitable nutrient and energy recovery technologies are determined for each studied CAFO among the state-of-the-art processes for organic waste management. The effect of different incentive policies on the economic performance of nutrient management technologies is studied considering the environmental vulnerability to nutrient pollution in the Great Lakes area. Additionally, the combination of incentives for the recovery of both phosphorus and electricity has been considered to identify potential synergies between the different technologies involved in the processing of livestock waste. The results obtained allow for the identification of the optimal incentive policies for the implementation of sustainable nutrient management systems at CAFOs as a function of their size, type of animals, and the environmental vulnerability of the area where each studied CAFO is located. In addition, we study the allocation of limited monetary resources using a Nash scheme; this determines the break-even point for the allocation of monetary resources based on the availability of incentives.

6.2 INCENTIVE POLICY ASSESSMENT FRAMEWORK

A two-stage framework is proposed for the evaluation of incentive policies, as shown in Figure 6.1. In the first stage, the size and geographical location of the studied CAFOs are analyzed, selecting the most suitable P recovery process for each CAFO assessed from a pool of six P recovery technologies. We note that these technologies can be implemented either standalone, or integrated with anaerobic digestion (AD) for biogas production. In a second stage, the effect of incentives on the economic performance of the P recovery system recommended is evaluated.

The P recovery selection stage is composed of different models that are fed with data regarding the type and number of animals in the studied CAFO, as well as its geographical location (box *a*). The techno-economic assessment of the different phosphorus recovery technologies, and biogas production in those cases where this process is considered, is performed based on the characteristics of the CAFO (box *b*). Additionally, the assessment of the regional environmental vulnerability to nutrient pollution is carried out in a parallel stage (box *c*). The information returned by these

models is normalized and aggregated in a multi-criteria decision analysis (MCDA) model to select the most suitable nutrient management technology for the evaluated livestock facility (box *d*). The stage analyzing the impact of incentives on the economic performance of the nutrient management systems is comprised by an economic model that estimates the profit of the P recovery systems implemented and the total cost of phosphorus recovery. Additionally, a cost-benefit analysis comparing the recovery cost and the economic losses due to nutrient pollution is performed (box *e*).

For the sake of brevity, a brief description of the processes is provided in this section. A detailed description of the framework employed for incentives assessment can be found in **Tool**.

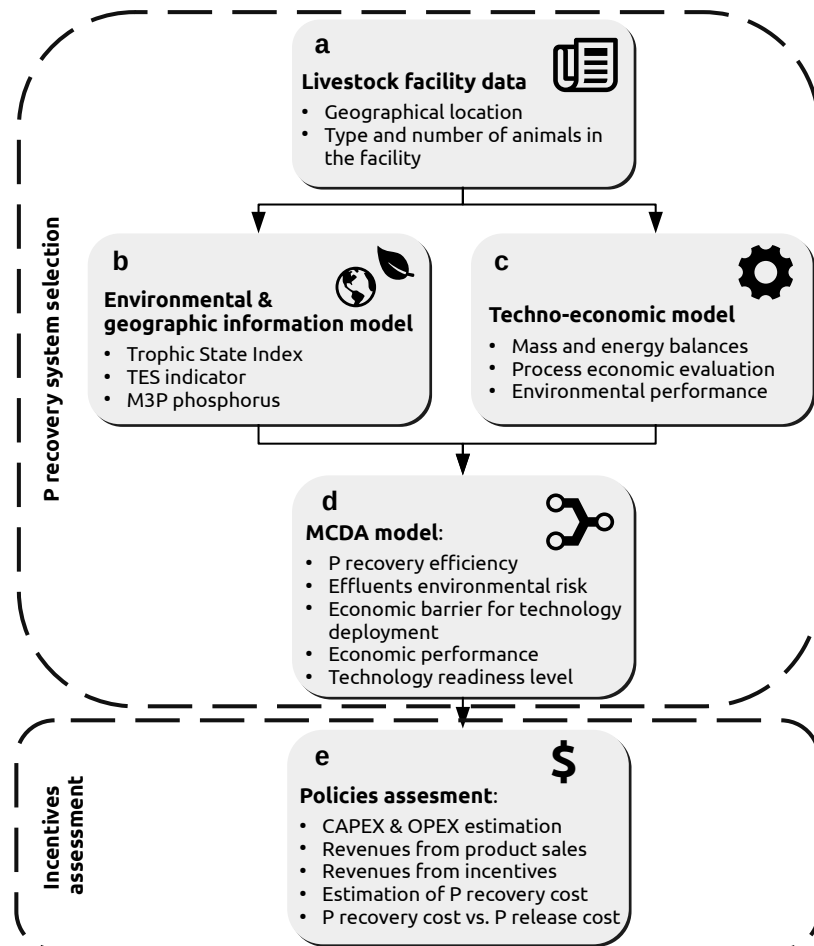


Figure 6.1: Flowchart of the models for selection, sizing, and evaluation of nutrient recovery systems at livestock facilities.

6.2.1 Assessment of nutrient management systems

Figure 7.1 illustrates the processes considered for livestock waste management. These processes comprise all manure treatment stages from waste collection to phosphorus recovery, including the optional biogas production stages.

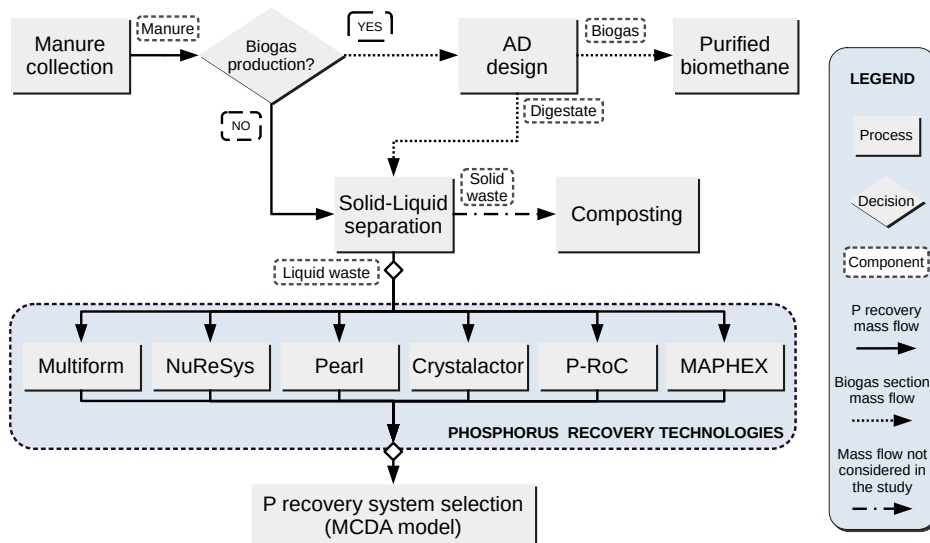


Figure 6.2: Flowchart of the processes evaluated for livestock waste management.

6.2.1.1 Phosphorus recovery systems

Six state-of-the-art technologies are assessed for phosphorus recovery at CAFOs. These technologies can be classified into three categories, i.e. struvite-based phosphorus recovery (Multiform, Crystalactor, Ostara Pearl, and NuReSys), calcium precipitates-based phosphorus recovery (P-RoC), and physical separation systems (MAPHEX). Table 6.1 summarizes the main parameters of the P recovery technologies assessed. The different processes, including solid-liquid separation, biogas production, and phosphorus recovery systems, are modeled based on first principles, which include mass and energy balances, thermodynamics, and product yield calculations. Additionally, data from manufacturers have been considered when available, particularly for the estimation of capital expenses (CAPEX) and operating expenditures (OPEX). A review and modeling details of the technologies considered can be found in **Tool**.

Table 6.1: Description of phosphorus recovery technologies considered in this work. $x_{Ca^{2+}:PO_4^{3-}}$ refers to the Ca^{2+}/PO_4^{3-} molar ratio.

P recovery process	Technology readiness level	Technology type	Phosphorus recovery efficiency (%)	Reference
Multiform	9	Struvite	$\frac{0.798 \cdot 100}{1 + \left(\frac{x_{Ca^{2+}:PO_4^{3-}} - 0.576}{0.798 \cdot 100} \right)^{2/113}}$	(Pearl2Kcost2)
Crystalactor	9	Struvite	$\frac{0.798 \cdot 100}{1 + \left(\frac{x_{Ca^{2+}:PO_4^{3-}} - 0.576}{0.798 \cdot 100} \right)^{2/113}}$	(egle_phosphorus_2016)
NuReSys	9	Struvite	$\frac{0.798 \cdot 100}{1 + \left(\frac{x_{Ca^{2+}:PO_4^{3-}} - 0.576}{0.798 \cdot 100} \right)^{2/113}}$	(Pearl2Kcost2)
Pearl	9	Struvite	$\frac{0.798 \cdot 100}{1 + \left(\frac{x_{Ca^{2+}:PO_4^{3-}} - 0.576}{0.798 \cdot 100} \right)^{2/113}}$	(Pearl2Kcost2)
P-RoC	6	Calcium precipitates	60	(ehbrecht_p-recovery_2011)
MAPHEX	7	Modular system based on phases separation	90	(church_novel_2016)

6.2.1.2 Biogas production and upgrading

Nutrient management technologies can be implemented either as standalone systems, or integrated with biogas production and upgrading processes, being both scenarios considered in this work. In scenarios in which the integrated nutrient-energy recovery processes are considered, biogas is produced through AD of cattle waste. In a second stage, biogas impurities (mainly H_2S , NH_3 , and moisture) are eliminated, and carbon dioxide is removed using a pressure swing adsorption (PSA) unit. A detailed description for the modeling of AD and biogas purification processes can be found in **Leon**. A comprehensive description for the PSA system and its modeling is shown in **MartinHernandez**.

6.2.2 Environmental vulnerability to nutrient pollution

A geographic information system (GIS) model is developed to estimate the environmental vulnerability to nutrient pollution of the area where each studied CAFO is located. We have considered three dimensions of phosphorus pollution to determine the eutrophication risk in each studied watershed, (i) the average Trophic State Index (TSI) of the waterbodies in the studied area (**carlson_trophic_1977**), (ii) the legacy of phosphorus in soils measured by the Mehlich 3 phosphorus (M_3P) concentration (**Espinoza2006**), and (iii) the balance between phosphorus releases and uptakes derived from human activities using the the techno-ecological synergy (TES) metric (**TESmetric**). These parameters have been evaluated at a sub-basin spatial scale, which corresponds to the HUC8 level defined in the Hydrologic Unit Code (HUC) system (**HUC8**). The information retrieved by this environmental GIS-based model is used to set the priority

of environmental and economic criteria, as described in the next section. A detailed description of the GIS model used to estimate the vulnerability to nutrient pollution can be found in **Tool**.

6.2.3 Multi-criteria decision analysis model for the assessment of nutrient management systems

The model developed for the evaluation of on-site processes for the treatment of livestock waste is based on a multi-criteria decision analysis (MCDA) framework. This framework combines the information from the techno-economic assessment and the local environmental vulnerability to nutrient pollution. Five parameters which can be classified in three dimensions are evaluated to select the most suitable P recovery process for each CAFOs; i.e., (i) environmental dimension assessing the performance of the different technologies to mitigate phosphorus releases from CAFOs, which measured through the fraction of phosphorus recovered by each technology (criterion 1), and the eutrophication potential of its effluents (criterion 2), (ii) the economic performance of the P recovery systems, including the economic barrier for the implementation of P recovery processes measured in terms of capital cost (criterion 3), and the net present value (NPV) of each process (criterion 4), and (iii) the technical maturity of each system, measured through the technology readiness level (TRL) index (criterion 5).

We developed a flexible criteria aggregation method able that balances the operating cost of the systems and the P recovery efficiency as a function of the environmental vulnerability to eutrophication of each region through criteria prioritization. In order to promote the implementation of proven P recovery processes, the TRL index is set as the criteria with highest preference in all cases. Regarding the environmental and economic aspects, environmental criteria are prioritized in the MCDA module if high values for TSI or M₃P are reported for the area of study, which result in severe environmental risk of phosphorus pollution. As a consequence, the selection of phosphorus recovery technologies with larger recovery efficiencies is prioritized even if they incur in larger capital or operating expenses. On the other hand, economic criteria are prioritized for technology selection either of the following situations happens, (a) if the trophic state of waterbodies is oligotrophic or mesotrophic and therefore there is no immediate eutrophication risk, but phosphorus emissions and uptakes are unbalanced, or (b) no environmental risk is reported.

For each studied CAFO, the normalized criteria are combined following the preference method described above. As a result, we obtain a composite index for each P recovery technology that collects the information

of the criteria considered. Based on the value of this composite index, these processes can be compared and ranked, selecting the most suitable system for each studied CAFO. Detailed descriptions for the construction of composite indexes can be found in **HandbookCompositeIndicators**.

In order to achieve a robust decision for the selection of the most adequate phosphorus recovery process, a sensitivity analysis considering different methods for the normalization and aggregation of economic and environmental information is performed (**MarcoCinelli2020**). A comprehensive description of the MCDA model for the selection of phosphorus recovery systems according to the economic and environmental parameters of each CAFO is collected in **Tool**.

6.2.4 Types of incentives considered

The implementation of nutrient recovery incentives in the form of phosphorous credits (P credits) has been studied in this work. In addition, in those scenarios where biogas production is integrated, renewable electricity certificates (REC) are also considered.

P credits can provide a mechanism to promote the recovery of phosphorus that is similar to the carbon credit scheme used in the context of carbon emissions, leading to the development of a credits market around phosphorus releases. The acquisition of P credits can bring allowances for phosphorus releases. Conversely, an entity can obtain income by recovering phosphorus releases, which is the P credits definition considered in this work. Previous efforts to determine the impact of implementing phosphorus recovery incentives for livestock waste management supply chain networks have been addressed by **sampat_economic_2018**. An optimal value of 22 USD per kg of phosphorus recovered is proposed to ensure the profitability of nutrient management systems implemented at CAFOs. Additionally, since the deployment of phosphorus recovery systems results in marketable nutrient-rich products in the form of struvite, incomes from the sale of these products are included in the calculation of revenues.

REC incentives for energy recovery provide a fixed remuneration for the electricity produced, which can result in a higher transaction price of electricity to cover the extra production costs and guarantee long-term price stability. Many different REC values have been proposed by governmental organizations worldwide based on geographical factors and power production capacity (**Deremince**). Therefore, similar to the electricity market price, a value of 60 USD/MWh, has been considered as baseline price.

6.2.5 Scenarios description

A total of 36 scenarios combining incentives in the form of phosphorus credits (0, 1, 3, 5, 11, and 22 USD/kg_P recovered) and for the production of electricity (considering final electricity prices of 30, 60, 75, 90, and 120 USD/MWh) are evaluated for the implementation of nutrient management systems at 2,217 CAFOs in the Great Lakes area. The base value assumed for P credits is 22 USD per kg of phosphorus recovered, based on the work of **sampat_economic_2018**. Although this reference value is comparatively large with respect to the price of phosphorus in commercial fertilizer, 1.23 USD/kg P (**fertilizers_price**), we note that it is significantly lower than the economic losses due to the environmental and social impact of nutrient pollution, estimated to be 74.5 USD per kg of P released (**Sampat2020**). Regarding RECs, an average electricity market price of 60 USD/MWh has been selected as the base-scenario. An electricity price below this value, 30 USD/MWh, and three values above the electricity market price, 75, 90, and 120 USD/MWh have been considered. These high REC values are studied due to the need of large incentives for biogas facilities to be economically viable reported by **sampat_economic_2018**.

We note that there are two special cases among the scenarios assessed. For those scenarios where P credits are 0, the only income of phosphorus recovery is from the sales of marketable nutrient-rich products in the form of struvite, in addition to the incomes from electricity generated if the corresponding technologies are selected. For those scenarios with an electricity price of 0 USD/MWh, no biogas production and upgrading process is implemented, considering only incomes associated with P credits and struvite sales are considered.

6.2.6 Study Region - The Great Lakes area

The Great Lakes area, shown in Figure 6.3, is considered to study the effect of different incentive policies on P recovery processes. This region collects several factors which make it specially vulnerable to nutrient pollution originated from livestock waste. First, it has a considerable amount of CAFOs, resulting in the generation of large amounts of organic waste. Second, the fresh waterbodies in the region are key resources, accounting for 21% of the global freshwater supply (**freshwater_Great_Lakes**), providing habitat to a wide range of fauna, and contributing to the local economy through recreational activities. Finally, there exists a continuous increase of cyanobacteria and HABs since the 1960s, especially in the Lake Erie, which is the shallowest lake.

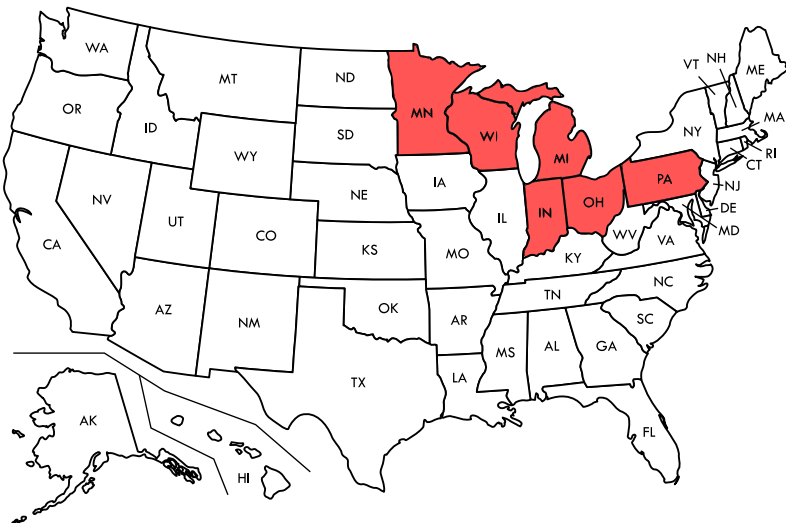


Figure 6.3: States of the Great Lakes region studied in this work.

The CAFOs considered for the deployment of livestock waste treatment processes are those livestock facilities with more than 300 animal units (**CAFO_definition**) reported in the National Pollutant Discharge Elimination System (NPDES) by the US EPA in the Great Lakes area (i.e. Minnesota, Indiana, Ohio, Pennsylvania, Wisconsin, and Michigan). An animal unit is defined as an animal equivalent of 1,000 pounds live weight (**animal_unit_definition**). There are 2,217 CAFOs considered in total. The states of Illinois and New York, as well as the Ontario province in Canada, are not part of this study due to the lack of reliable data about CAFOs. The animal number, manure generated, and phosphorus releases by CAFOs in the studied states are reported in Table 6.2.

6.3 RESULTS AND DISCUSSION

6.3.1 Single incentives

In this section, the effect of the implementation of single P credits or REC incentives is studied. The capital and operating costs associated with the installation of P recovery systems if no incentives are considered are reported **Tool**.

6.3.1.1 Effect of P credits

The effect of applying P credits on the economic performance of nutrient management systems has been studied. Revenues from struvite sales are

Table 6.2: Livestock residues and phosphorus releases by CAFOs in the Great Lakes area.

	Pennsylvania	Ohio	Indiana	Michigan	Minnesota	Wisconsin
Number of CAFOs	131	53	119	144	1,487	283
Total animal units	196,617	128,008	187,355	354,460	943,094	744,015
Dairy animal units (%)	85.06	79.17	81.93	87.90	45.43	98.38
Beef animal units (%)	14.94	20.83	18.07	12.10	54.57	1.62
Manure generated (kt/year)	$2.60 \cdot 10^3$	$1.68 \cdot 10^3$	$2.48 \cdot 10^3$	$4.76 \cdot 10^3$	$1.13 \cdot 10^4$	$1.03 \cdot 10^4$
Phosphorus releases (t/year)	$2.08 \cdot 10^3$	$1.34 \cdot 10^3$	$1.98 \cdot 10^3$	$3.80 \cdot 10^3$	$9.02 \cdot 10^3$	$8.20 \cdot 10^3$
Reference	1	2	3	4	5	6

¹ Pennsylvania_CAFOS

² Ohio_CAFOS

³ Indiana_CAFOS

⁴ Michigan_CAFOS

⁵ Minnesota_CAFOS

⁶ Wisconsin_CAFOS

also considered in those CAFOs installing struvite production technologies. Since in this first scenario only the effect of P credits is studied, incomes from electricity production are excluded; and therefore, the nutrient management systems are not integrated with biogas production. The effect of the value of P credits over the profitability of the nutrient recovery systems is shown in Fig 6.4a, where the distribution of CAFOs size is shown using boxplots. It can be observed that, for P credits values strictly below 11 USD per kg of recovered phosphorus, the proportion of profitable P recovery processes (those installed processes whose incomes are larger than the operating expenses) is small and constant. However, when the value of the incentive is set at 11 USD per kg of recovered phosphorus, the increase in the number of profitable processes is very significant for all states except Minnesota, which CAFOs median size is the smallest. For states with large CAFOs, i.e. Michigan, Ohio and Wisconsin, the percentage of profitable processes can reach around 80% under high P credits; while for Indiana and Pennsylvania, with medium-size CAFOs, around 40% are profitable. For P credits of 22 USD per kg of recovered phosphorus, there is an additional 25% increase of profitable nutrient recovery systems in those states with large CAFOs. In the states with medium size CAFOs the increase of profitable processes is also very significant, reaching approximately 80% of the studied CAFOs. Finally, for the case of Minnesota, there is a large

increase in the profitable P recovery systems installed as well, reaching near the 60% of the CAFOs studied.

6.3.1.2 Effect of renewable energy certificates

The effect of REC in the implementation of P recovery systems is studied in this section. Integration of biogas production with P recovery processes is considered in all the cases studied in this scenario. In addition to revenues obtained from RECs, incomes from the sales of struvite produced by the phosphorus recovery processes have been considered as well. The effect of P credits is excluded in this scenario.

Figure 6.4b shows the percentage of profitable P recovery processes for each studied state together with the distribution of the size of CAFOs. As it can be observed, the impact of the incomes from electricity in the economic performance is much less significant than the effect of P credits given the incentive ranges considered. Only the largest CAFOs, most of which represent outliers in the distribution of CAFOs size, are profitable when prices equal to or above 75 USD/MWh are considered. The large CAPEX prevent the economic feasibility of biogas production in small and medium CAFOs. Therefore, only large-scale CAFOs can benefit from the operation of biogas processes to cover the cost of P recovery systems via biogas-based electricity production.

6.3.2 Combined effect of incentives for phosphorus and renewable electricity recovery

Synergies derived from the combination of P credits and RECs might be obtained when integrating phosphorus recovery technologies with biogas production and upgrading processes. However, since the deployment of the biogas processes involves large investments and considerable operating costs, a detailed analysis must be conducted to identify the most cost-effective incentives policy.

The results obtained from combining the incentive schemes described in previous sections are shown in Figure 6.5. The fraction of profitable processes is shown in Figure 6.5a, which are defined as those CAFOs with positive net incomes. It can be observed that, if the value of P credits and RECs are set similar to the market prices (i.e. 1 USD/kg_{P recovered} and 60-75 USD/MWh respectively), the fraction of profitable processes is very low. Wisconsin is the state with the largest share of profitable P recovery processes under this scenario, which is 4-5% of the total CAFOs.

Phosphorus credits have a larger impact on the profitability of nutrient management systems, near to 100% for P credits of 22 USD/kg_{P recovered}

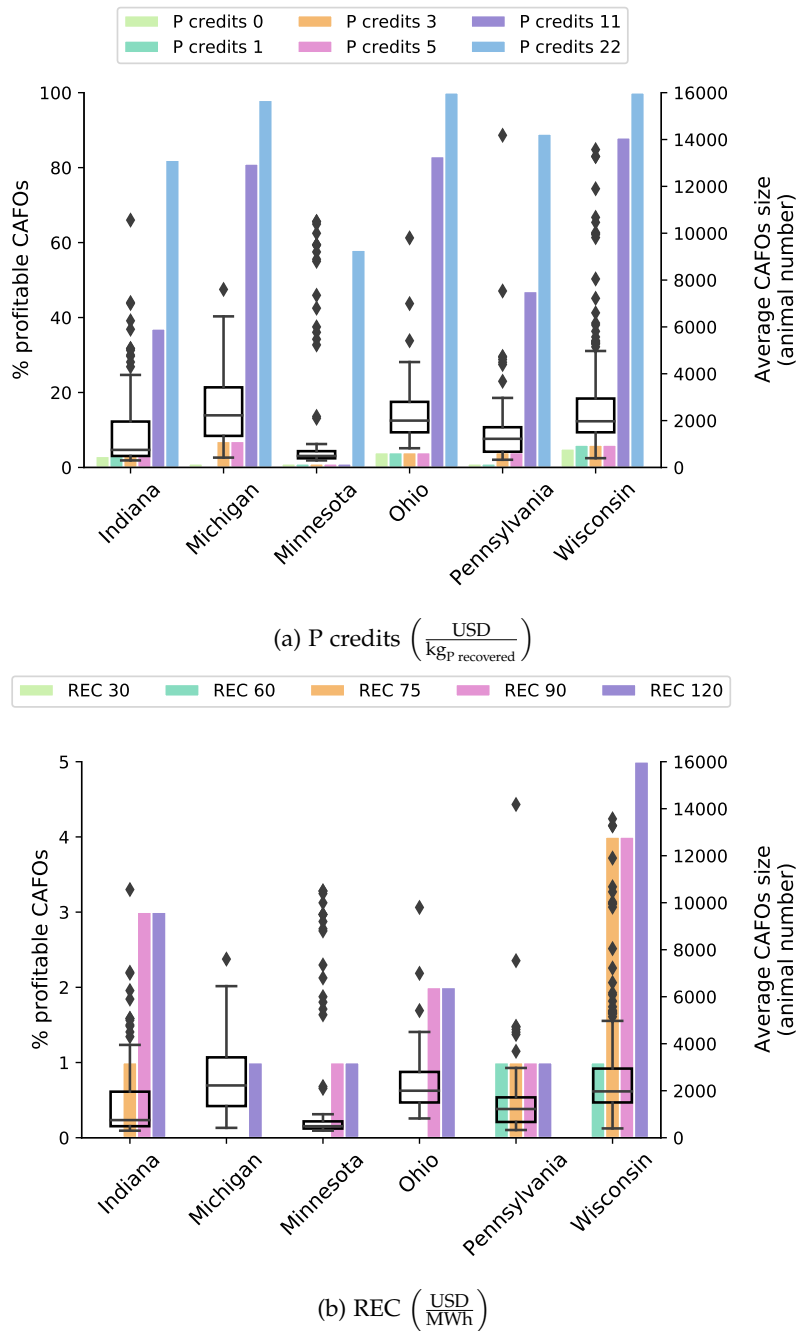


Figure 6.4: Distribution of profitable phosphorus recovery processes in the Great Lakes area for the scenarios considering phosphorus credits and renewable energy credits. The box-plots represent the distribution of CAFOs size in each state.

for states with large CAFOs (i.e. Michigan, Ohio and Wisconsin). The price of electricity has a weak influence on the profitability of the deployed systems in these scenarios. For states with medium-size CAFOs, Indiana and Pennsylvania, the share of profitable processes is around 80-85%. For Minnesota, which is the state with the smallest median CAFOs size, the share is 58%. Therefore, the installation of AD processes has a significantly negative impact in the states with small and medium size CAFOs due to the lack of economies of scale. A similar behavior is found when the value of phosphorus credits is reduced to 11 USD/kg_{P recovered}.

This pattern is reverted when P credits of 3-5 USD/kg_{P recovered} are considered. For these scenarios the share of profitable processes is considerably reduced compared to the previous scenarios. Actually, for Indiana, Minnesota, and Ohio, there is no difference between setting phosphorus credits incentives below 5 USD/kg_{P recovered} and the case considering no P credits (where the only income of phosphorus recovery is from the sales of nutrient-rich products obtained). However, in all states except Minnesota, the amount of profitable systems increases for electricity prices larger than 60 USD/MWh, reaching a share of P recovery processes with positive net incomes up to 22 % for Michigan. For the scenario considering P credits of 1 USD/kg_{P recovered}, only Ohio shows a slight improvement in the fraction of profitable facilities if the production of electricity is also considered. Therefore, there is a threshold for P credits between 1 and 3 USD/kg_{P recovered} below which no improvement in the fraction of profitable P recovery systems is observed. For those scenarios where no incentive for phosphorus recovery is considered, the results obtained have been previously described in Section 6.3.1.2. It is interesting to note, as a consequence of the large capital and operating expenses of AD processes, the economic performance of the scenarios considering only P recovery systems is at least as profitable as the profitability of the scenarios considering biogas generation associates the largest REC incentives.

The net treatment cost per ton of manure processed captures the perspective of CAFOs owners on P recovery. It is defined as the difference between the revenues (sum of struvite sales, R_c (USD/year), and incentives, I_c (USD/year)) and the operating expenditures of livestock treatment processes, $OPEX_c$ (USD/year), as shown in Eq. 6.1. F_{manure_c} denotes the mass flow of manure processed in ton/year.

$$\text{Net treatment cost}_c \left(\frac{\text{USD}}{\text{t}_{\text{manure}}} \right) = \frac{R_c + I_c - OPEX_c}{F_{\text{manure}_c}} \quad (6.1)$$

The results obtained in terms of net treatment cost are illustrated in Figure 6.5b. These show a base cost for the recovery of phosphorus

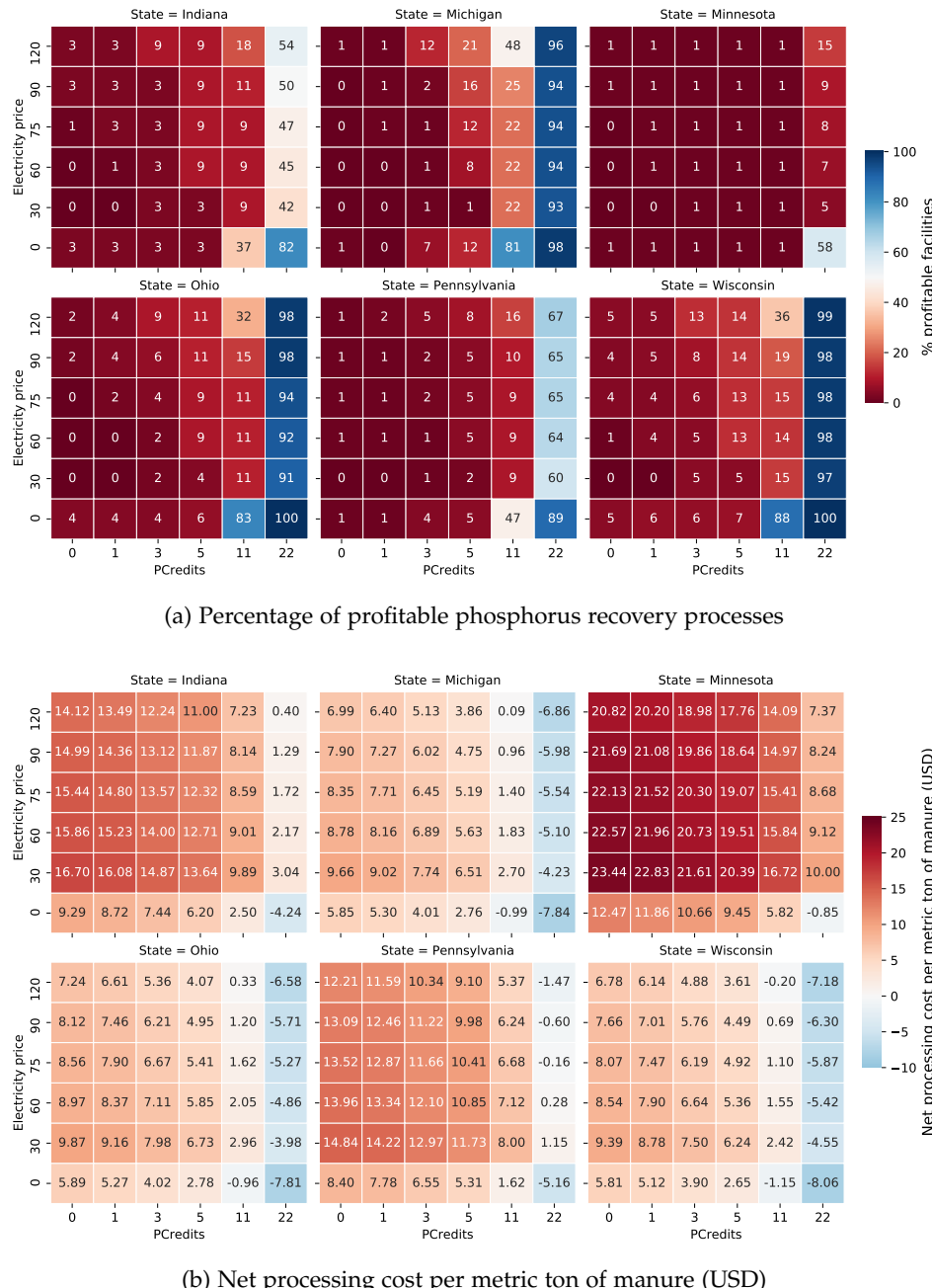


Figure 6.5: Economic evaluation of P recovery processes for the different incentives scenarios studied

between 5.81 and 12.47 USD per ton of processed manure if no incentives or anaerobic digestion stages are considered. From this base case, it can be observed that the costs vary following the same pattern as the fraction

of profitable processes described previously. The installation of biogas processes is not profitable by itself, increasing the processing costs by 1.2-1.9 times over the base case if no P credits are considered, and it is only beneficial for specific scenarios which have large size CAFOs, and moderate P credits (>3 USD/kg_{P recovered}) and electricity incentives (>60 USD/MWh). The scenarios combining states with large CAFOs and high value for P credits, and the optional production of renewable energy from biogas result in negative processing costs. This means that phosphorus recovery results in profits for the CAFO. We note that, as the analysis of the different scenarios is carried out at the state level, a negative processing cost indicate that, under certain schemes for incentives, the profitable P recovery processes are able to balance out the non-profitable ones in the state.

It is worth noting that the results reveal that in the largest CAFOs the recovery of phosphorus is more feasible, due to the economies of scale. At the same time, however, these large-scale CAFOs also represent the major environmental threats due to the release of larger amounts of phosphorus.

6.3.3 Environmental cost-benefit analysis

CAFOs are an environmental concern in terms of nutrient pollution as a consequence of the high spatial concentration of animals, resulting in large releases of phosphorus. The long-term environmental impact of phosphorus releases result in large economic losses, accounting for the remediation cost of environmental degradation and the economic impact on the local population affected by HABs. Therefore, an analysis for the cost-effectiveness of the total cost involved in phosphorus recovery, including the amortization of the investment, operating costs, and total cost of incentives, can show the economic advantages of phosphorus recovery.

$$\text{Total treatment cost}_c \left(\frac{\text{USD}}{\text{kg}_P \text{ recovered}} \right) = -R_c + I_c + OPEX_c \quad (6.2)$$

Figure 6.6 shows the total cost of phosphorus recovery under different policies, defined in Eq. 6.2, compared with the economic losses due to phosphorus releases into the environment. It can be observed that all scenarios studied result in a phosphorus recovery cost lower than the economic losses due to phosphorus releases, estimated in 74.5 USD per kg of phosphorus released by Sampat2020. Phosphorus recovery is, therefore, more cost-effective than its release to the environment. The lowest total cost for phosphorus recovery is obtained in the scenario not involving any incentive (REC: 0 - PC: 0), resulting in costs between 3 and 5 times lower

than the economic cost of phosphorus release to the environment. The application of incentives increases the total monetary cost of phosphorus recovery, mainly driven by the application of phosphorus credits. However, since incentives are an income for the owners of livestock facilities, the economic cost of nutrient management systems for the owners of CAFOs is progressively reduced, increasing the number of profitable P recovery systems, and reducing the recovery cost of phosphorus, as it is shown in Fig. 6.5.

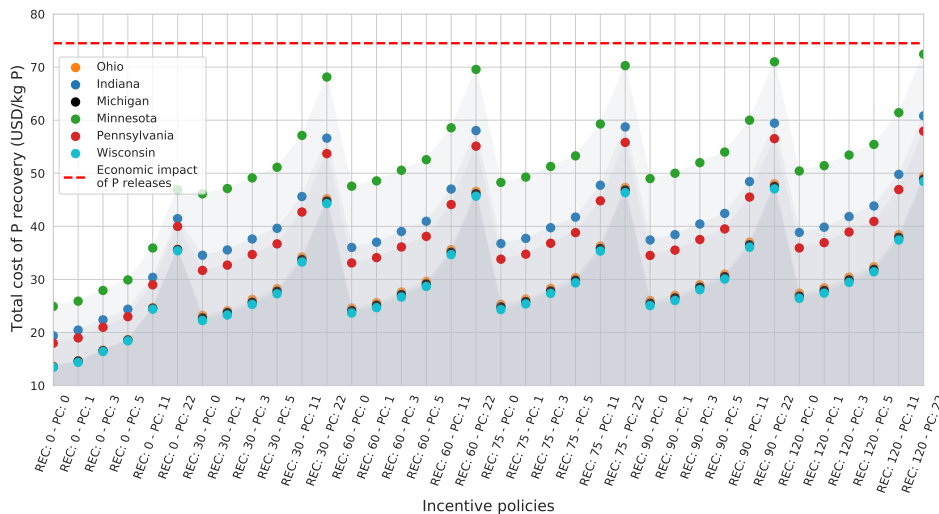


Figure 6.6: Comparison of the total cost of phosphorus recovery for each scenario assessed and the environmental remediation cost due to phosphorus releases. *REC* denotes the electricity incentive values considered in USD/MWh, and *PC* denotes the value of phosphorus credits in USD/kg_P recovered. The red dotted line represents the economic losses due to phosphorus releases to the environment.

The role of the size of CAFOs in the cost of phosphorus recovery can be also observed in this study. Accordingly with the results shown in previous sections, those states with larger average size of CAFOs, such as Wisconsin, Ohio, and Michigan, have recovery costs significantly lower than the states where medium and small size CAFOs are predominant. It is worth noting that the total cost of phosphorus recovery is lower than the economic losses due to the release of phosphorus to the environment for all the evaluated states and policies.

6.3.4 Fair distribution of incentives

The effect of different incentive schemes has been previously discussed, revealing that the P recovery systems in small CAFOs require significant economic support in the form of incentives to balance the monetary losses, while in the largest CAFOs these systems can be self-profitable. This situation leads to the problem of the fair distribution of available incentives, which is particularly relevant in the case that the available budget is not sufficient to cover the operating expenses of the unprofitable P recovery processes. In this section, the minimum necessary incentives for all P recovery systems in the studied area to reach the economical neutrality (i.e., no economic profits or losses are obtained) is firstly determined. In a second stage, a fairness-guided distribution of incentives among CAFOs is studied when the available incentives are lower than the monetary amount determined, i.e., they are not sufficient to cover the operating expenses of unprofitable processes. Due to the marginal benefits obtained by installing AD processes, as described in Section 6.3.2, the implementation of only P recovery systems is assumed in both studies, and therefore only incentives for P recovery are considered.

The minimum cost of incentives necessary for covering the economic losses of unprofitable processes, estimated in 222.6 million USD, is determined through the formulation of an optimization problem. The objective function of this problem minimizes the incentives used, Eq. 6.3a, subject to achieve the economical neutrality, Eq. 6.3b. Here, \mathcal{C} denotes the set of CAFOs studied, I_c the incentives allocated, and $OPEX_c$ and R_c the operating expenses and revenues of the P recovery system installed in each CAFO c respectively.

$$\min \sum_{c \in \mathcal{C}} I_c \quad (6.3a)$$

$$\text{s.t. } I_c + R_c - OPEX_c \geq 0 \quad (6.3b)$$

The results obtained, shown in Figure 6.7, reveal the crucial role of the economies of scale in the amount of incentives that must be deployed to cover the economic losses of P recovery systems. We note that the discrepancies of incentives for CAFOs of similar size that can be observed in the figure are due to different technology installed. The selection of different P recovery processes for CAFOs of similar size is based on the eutrophication risk of each watershed, as described in **Tool**. It can also be observed the 99.9% of CAFOs require incentives below the P releasing cost to the environment. A correlation to estimate the amount of incentives

needed to cover the operating expenses as a function of CAFOs capacities is proposed in Eq. 6.4 , where AU_c denotes the animal units of CAFO c .

$$I_c \left(\frac{\text{USD}}{\text{kg P}} \right) = \frac{3.383 \cdot 10^6}{1 + (AU_c \cdot 2.223 \cdot 10^5)^{0.647}} \quad (6.4)$$

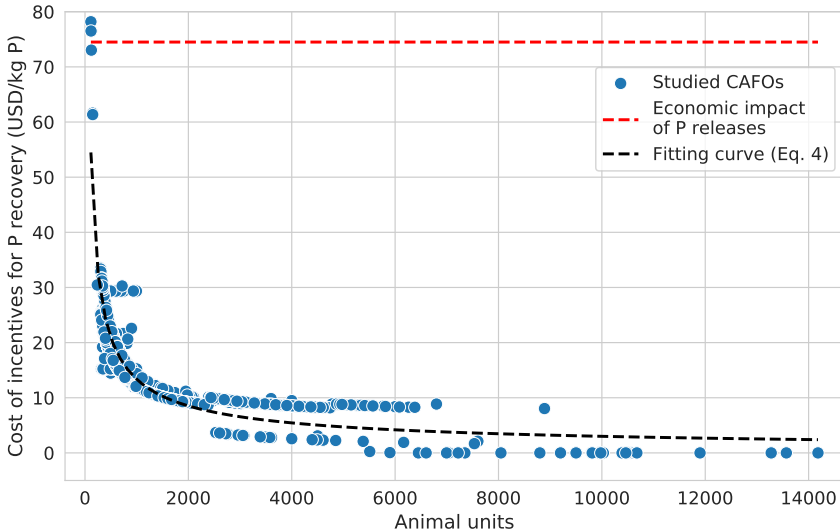


Figure 6.7: Allocation of incentives for achieving the economic neutrality of nutrient recovery systems minimizing the total cost of incentives.

The fair allocation of incentives when the monetary amount available is not sufficient to cover the expenses of all P recovery processes has been addressed by using the Nash allocation scheme. The Nash approach has been selected because this scheme is able to capture the scales of the different stakeholders (CAFO facilities) in order to achieve a fair distribution of a certain resource (incentives), as it was demonstrated by **sampat2019fairness**. This scheme is formulated in Eqs. 6.5a-6.5b, where $I_{\text{available}}$ denotes the available incentives.

$$\max \sum_{c \in \mathcal{C}} \ln (I_c + R_c - OPEX_c) \quad (6.5a)$$

$$\text{s.t. } \sum_{c \in \mathcal{C}} I_c \leq I_{\text{available}} \quad (6.5b)$$

Figure 6.8a illustrates the distribution of incentives as a function of the net revenues of the P recovery system installed in each CAFO c before any incentive is applied, Eq 6.6.

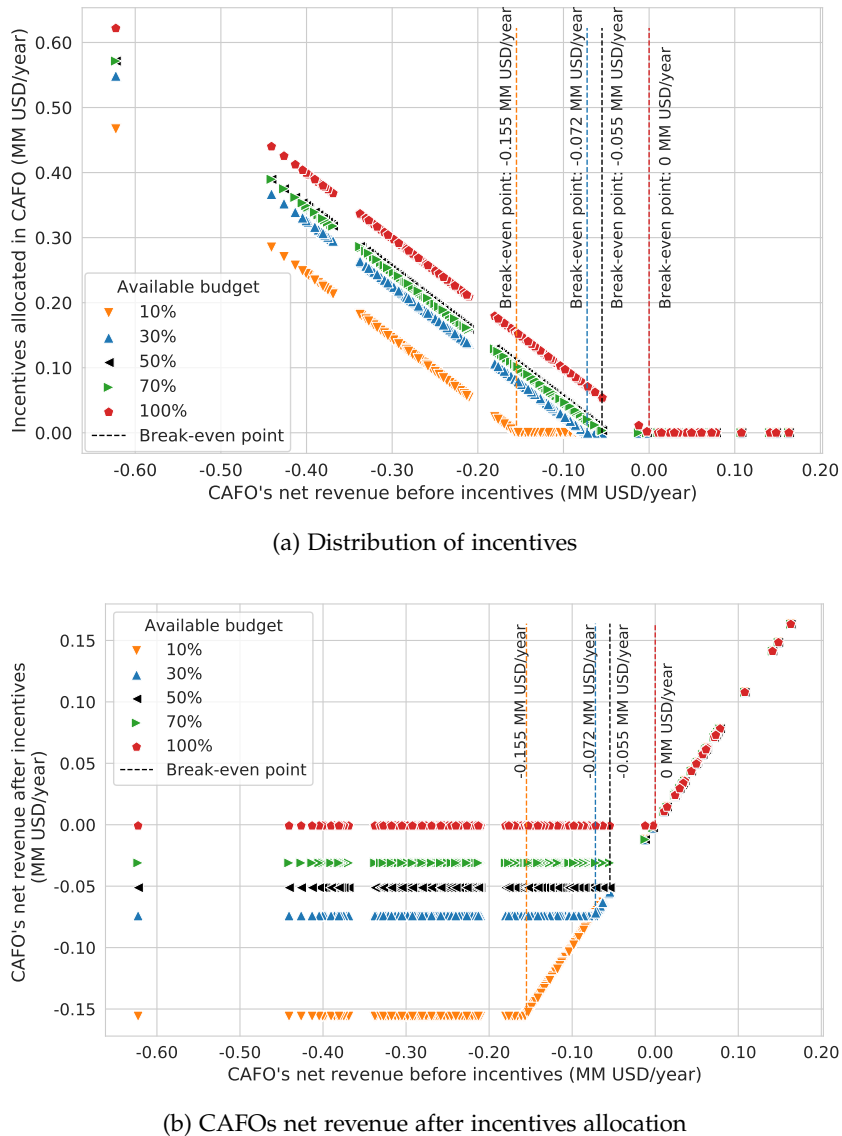


Figure 6.8: Distribution of incentives considering the Nash allocation scheme. Scenarios assuming available incentives equal to the 10%, 30%, 50%, 70%, and 100% of the incentives needed to cover the economic losses of unprofitable P recovery systems in the Great Lakes area are illustrated.

$$\text{Net revenue before incentives}_c \left(\frac{\text{USD}}{\text{year}} \right) = R_c - OPEX_c \quad (6.6)$$

The cases where the available budget are the 10%, 30%, 50%, 70%, and 100% of the incentives needed to cover the economic losses of unprofitable

CAFOs are analyzed (22.3, 66.8, 111.3, 155.8 and 222.6 MM USD respectively). The last case is equivalent to the scenario studied above. It can be observed that the available incentives are allocated accordingly to the net revenues of each CAFO, promoting the allocation of larger incentives to the less profitable P recovery processes. Since the available incentives are limited, a break-even point determining the profitability level of the P recovery systems below which the incentives should be allocated is set for each scenario. As a result, the fewer incentives available, the more restrictive the break-even point is. Additionally, it can be observed that the displacement of the break-even points is progressively reduced as the available incentives increase, resulting in a marginal improvement between the scenarios considering the 50% and 70% of the economic resources needed to guarantee the economic neutrality of the nutrient management systems. In Figure 6.8b we observe that, for each case evaluated, the allocation of limited incentives under the Nash scheme result in a uniform net revenue for those CAFOs receiving incentives. Additionally, we note that the economic losses have been mitigated in these facilities by the allocation of incentives. However, they are unable to be profitable due to the limited budget available. In addition, a correlation to estimate the fairness point as a function of available incentives has been developed based on these results, Eq. 6.7.

$$\text{Break-even point}_c \left(\frac{\text{USD}}{\text{year}} \right) = -2.482 \cdot 10^5 \cdot (0.955^{(I_{\text{available}}(\%))}) \quad (6.7)$$

6.4 CONCLUSIONS

The application of different incentives to promote the implementation of nutrient management systems at CAFOs is studied in this work, including the potential integration of phosphorus recovery technologies with the production of renewable electricity from biogas.

The results reveal that the recovery of phosphorus is more economically feasible in the largest CAFOs due to the economies of scale. The deployment of phosphorus recovery processes is self-profitable through struvite sales only for the largest P recovery processes, which represent less than the 5 % over the total CAFOs in all the studied states. However, the application of P credits increases the fraction of profitable processes around to 100% in the states with large-size CAFOs (Michigan, Ohio and Wisconsin), and up to 80% for the states with medium-size CAFOs (Indiana and Pennsylvania). The integration of phosphorus recovery technologies with anaerobic digestion and biogas upgrading processes does not result

in any practical improvement in terms of economic performance unless incentives for phosphorus recovery are considered, since the revenues from electricity sales can not cover the investment and operating cost of these processes given current market values.

The total cost of phosphorus recovery, including the investment amortization, operating costs, and total cost of incentives is lower than the long-term economic losses due to phosphorus pollution for all the evaluated states and policies, proving that sustainable nutrient management systems are economically and environmentally beneficial. Correlations to estimate the incentives necessary for P recovery systems to achieve economic neutrality has been also proposed. Additionally, the fair distribution of limited incentives has been studied, determining the break-even point for the allocation of monetary resources based on the availability of incentives.

Future work is aimed at assessing the effect of biomethane production in the economy of the waste treatment systems, and the integration within a logistics network model for the developing of nutrient pollution and ecosystem integrated responses at regional spatial resolution.

ACKNOWLEDGMENTS

This research was supported in part by an appointment for E.M.H. to the Research Participation Program for the Office of Research and Development, US EPA, administered by the Oak Ridge Institute for Science and Education through Interagency Agreement No. DW-89-92433001 between the US Department of Energy and the US Environmental Protection Agency. E.M.H. and M.M. acknowledge funding from Junta de Castilla y León, Spain, under grant SA026G18 and grant EDU/556/2019. Y.H. and V.M.Z. acknowledge funding from the U.S. Department of Agriculture, National Institute of Food and Agriculture, under grant number 2017-67003-26055.

Disclaimer: The views expressed in this article are those of the authors and do not necessarily reflect the views or policies of the U.S. EPA. Mention of trade names, products, or services does not convey, and should not be interpreted as conveying, official U.S. EPA approval, endorsement, or recommendation.

BIBLIOGRAPHY

Part II

NITROGEN MANAGEMENT AND RECOVERY

MULTI-SCALE TECHNO-ECONOMIC ASSESSMENT OF NITROGEN RECOVERY SYSTEMS FOR SWINE OPERATIONS

ABSTRACT

Intensive swine farming generates vast amounts of organic waste, which are an important source of nitrogen releases. Nitrogen released from farming activities contributes to multiple environmental problems, such as ecosystem fertilization, eutrophication of water systems, and greenhouse gases emissions. Nitrogen recovery is technically feasible, and there exists a number of processes for the processing of livestock waste recovering nitrogen in the form of different products. In this work, a multi-scale techno-economic assessment of six systems for nitrogen recovery from swine waste, i.e., transmembrane chemisorption, ammonia evaporation and scrubbing, striping in packed tower, MAPHEX, and struvite production, is performed. Additionally, the material flows from waste collection to final treatment are analyzed to determine the recovery efficiency and nitrogen losses for each process. The results show that transmembrane chemisorption is the process with the lowest recovery cost, from 10.4 to 3.4 USD per kilogram of nitrogen recovered. Moreover, considering that economic losses due to the harmful effects of nitrogen into the environment are estimated at 32-35 USD per kilogram of nitrogen released, nitrogen recovery by processing swine waste through three technologies, i.e., transmembrane chemisorption, MAPHEX, and stripping in packed bed, reveals to be economically beneficial. This work estimates the cost of nitrogen recovery at swine operations, and it is intended to be a starting point for designing and evaluating regulations and incentives for the transition to a more sustainable paradigm for food production.

Keywords: Organic Waste; Nitrogen Recovery; Nutrient Pollution; Livestock Industry; Techno-economic assessment

RESUMEN

La cría intensiva de cerdos genera grandes cantidades de residuos orgánicos, que son una importante fuente de liberación de nitrógeno. El nitrógeno liberado por las actividades ganaderas contribuye a múltiples problemas medioambientales, como la fertilización de los ecosistemas, la eutrofización de los sistemas acuáticos y las emisiones de gases de efecto invernadero. La recuperación de nitrógeno es técnicamente factible, y existen varios procesos para el tratamiento de residuos ganaderos que recuperan el nitrógeno en forma de diferentes productos. En este trabajo se realiza una evaluación tecno-económica a escala múltiple de seis sistemas para la recuperación de nitrógeno a partir de residuos porcinos: quimisorción transmembrana, evaporación y lavado de amoníaco, stripping en lecho empaquetado, MAPHEX y producción de estruvita. Además, se analizan los flujos de material desde la recogida de residuos hasta el tratamiento final para determinar la eficiencia de recuperación y las pérdidas de nitrógeno de cada proceso. Los resultados muestran que la quimisorción transmembrana es el proceso con menor coste de recuperación, de 10,4 a 3,4 USD por kilogramo de nitrógeno recuperado. Además, teniendo en cuenta que las pérdidas económicas debidas a los efectos nocivos del nitrógeno en el medio ambiente se estiman en 32-35 USD por kilogramo de nitrógeno emitido, la recuperación de nitrógeno mediante el procesamiento de los residuos porcinos a través de tres tecnologías, quimisorción transmembrana, MAPHEX y stripping en lecho empaquetado, se revela económicamente beneficiosa. Este trabajo estima el coste de la recuperación de nitrógeno en las explotaciones porcinas y pretende ser un punto de partida para el diseño y la evaluación de normativas e incentivos para la transición a un paradigma más sostenible de la producción de alimentos.

Palabras clave: Residuos orgánicos; Recuperación de nitrógeno; Contaminación por nutrientes; Industria ganadera; Análisis tecnoeconómico

7.1 INTRODUCTION

The agricultural sector has experienced an industrialization process since the XIX century, pursuing the intensification of the agri-products and food production, i.e., increasing the agricultural production per unit of input resources, including land, labor and feed among others (**FAOethics2004**). During the last decades, the agricultural intensification is driven by a sustained increase in the population, the average income growth in both developed and developing countries, and the trade liberalization and logistics advancements leading the transnational trade of products (**baker2014trends**). As a result of this intensification process, the largest quantity and variety of agri-products in the human history is produced and distributed nowadays. However, multiple environmental challenges must be faced as a consequence of the industrialization of the agriculture and farming activities: soil depletion of nutrients and organic matter as consequence of mono-cropping, excessive and inefficient use of synthetic fertilizers to maintain high cropping yields, spatial concentration and inappropriate management of livestock manure, biodiversity loss, etc. Focusing in the context of nutrient management, the use of synthetic fertilizers, and the detachment of arable lands and livestock facilities decoupled the previous link where the organic waste from livestock activities were used as nutrient and organic matter supply for crops (**bouwman2009human**). This decoupling has created a dependency on mineral (phosphorus) and synthetic (nitrogen) fertilizers, and the adequate management of animal manure has become a serious problem for concentrated animal feeding operations (CAFOs). Therefore, there is disconnection between localized areas with large concentrations of organic waste containing nutrients, such as the intensive livestock facilities, and croplands demanding nitrogen and phosphorus relying in synthetic and mineral fertilizers to keep high yield rates. Due to the sparse location of the facilities and the high density of organic wastes, including manure and digestate, the transportation of these wastes for nutrients redistribution is challenging and expensive (**sampat2018technologies**). Therefore, the implementation of technologies and processes for the recovery of nutrients in a form suitable for easy transport and use in croplands is of utmost importance, restoring the circularity of agricultural nutrients usage disrupted by industrial practices. However, the selection of the most suitable technology for an individual facility is not a trivial process, but involves multiple dimensions, including the recovery efficiency, the effect of the scale on the economic performance of the process, and the environmental footprint of the different technologies. Some previous works assessing and comparing technologies have been performed, but they do not capture the effect of the economies of scale (**munasinghe2020nitrogen**;

(de2019resource), or they are limited to a few number of technologies (bolzonella2018nutrients). beckinghausen2020removal reports a lack of techno-economic analyses for nitrogen recovery techniques to identify the most suitable process according to the characteristics of each facility. In addition, the previous studies do not capture the effects of integrating these processes with anaerobic digestion systems for energy recovery.

In this work, six state-of-the-art technologies for nitrogen recovery from livestock waste, i.e., transmembrane chemisorption, ammonia evaporation and scrubbing, striping in packed tower, MAPHEX, and struvite production, are systematically assessed and compared. Each system is evaluated performing a material flow analysis (MFA) of the whole process, from waste collection to the final treatment, and a techno-economic analysis (TEA) capturing the effect of the economies of scale on the cost of nitrogen recovery. The objective is to determine the most adequate technologies to close the nutrients loop from livestock to crops, and the optimal conditions for the implementation of these systems. The processes for livestock waste treatment studied involve all stages from waste collection to the production of the nutrient-rich final product: manure preconditioning, optional biogas production valorization, solid-liquid separation of manure or digestate, and nutrients recovery. The assessment of such technologies is performed through detailed mathematical models of the processes based on first principles and experimental data, resulting in a flexible framework able to analyze different combinations and scales of technologies for the treatment of swine waste. The information obtained from the techno-economic assessment of nitrogen recovery technologies is key for the further development of policies to promote nutrient recovery and to mitigate the environmental footprint of swine farming activities.

7.2 METHODS

7.2.1 Livestock waste

Swine manure generated by animals at different life stages have different composition, as well as a different waste generation ratio, i.e., waste mass generated per animal per day. Data reported by the US Department of Agriculture (USDAWaste; Kellog2000) is used to determine the waste flow and composition as a function of the number of animals in a facility and their type, as listed in Table 7.1. AU denotes animal units, which is defined as 1000 pounds (453.6 kg) of live animal (**animal_unit_definition**).

Table 7.1: Swine waste characterization. Adapted from **USDAWaste; Kellogg2000**.

Components	Units	Sow Gestating	Sow Lactating	Boar	Piglets Nursery	Piglets Grow to Finish
Animals:AU	ratio	2.67	2.67	2.67	9.09	9.09
Weight	kg/d AU	11.34	26.76	8.62	39.92	29.48
Volume	m ³ /d AU	0.012	0.027	0.0085	0.040	0.031
Moisture	%wt	90	90	90	90	90
TS	kg/d AU	1.13	2.68	0.86	4.54	2.95
VS	kg/d AU	1.04	2.45	0.77	3.99	2.45
N	kg/d AU	0.073	0.20	0.064	0.42	0.24
P	kg/d AU	0.023	0.059	0.023	0.068	0.041
K	kg/d AU	0.050	0.13	0.041	0.16	0.11
N _{inorganic} :N _{total}	ratio	0.61	0.61	0.61	0.61	0.61
N _{organic} :N _{total}	ratio	0.39	0.39	0.39	0.39	0.39
P _{inorganic} :P _{total}	ratio	0.58	0.58	0.58	0.58	0.58
P _{organic} :P _{total}	ratio	0.42	0.42	0.42	0.42	0.42

AU: Animal units.

TS: Total solids.

VS: Volatile solids.

N: Nitrogen.

P: Phosphorus.

K: Potassium.

7.2.2 Nitrogen management systems assessment framework

Swine manure processing involves several stages from manure collection to resources recovery, as shown in Figure 7.1. In this section the modeling details of each stage are drawn.

7.2.2.1 Anaerobic digestion

Swine manure can be processed in an anaerobic digestion (AD) unit for the production of biogas and digestate. These materials can be further processed to recover valuable resources, such as electricity and thermal energy from biogas, and nutrients from digestate. As a result of the digestion process, the organic and inorganic fractions of nutrients (i.e., nitrogen and phosphorus) vary due to the partial mineralization of the organic fraction of nitrogen and phosphorus. Therefore, the amount of inorganic nutrients in the digestate is larger than in raw manure, as shown in Table 7.2 ([fangueiro2020available](#)). In addition, the amount of total solids decreases as a consequence of the transformation of volatile solids into biogas. AD process is typically carried out either at mesophilic (25

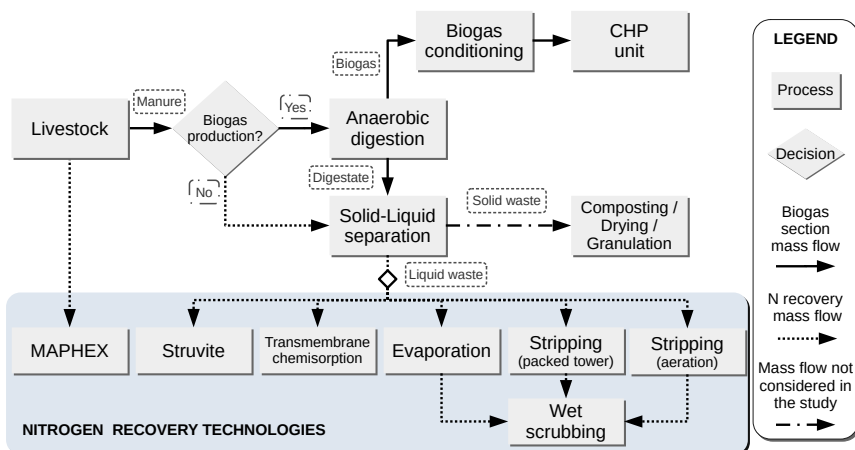


Figure 7.1: Flowchart of the processes assessed for the processing of livestock waste

and 45 °C) and thermophilic (45 and 50 °C) temperatures and atmospheric pressure, with retention times between 30-40 and 15-20 days respectively. There also exist low temperature digestion at psychrophilic conditions (< 25 °C), although it involves longer retention times between 70 and 80 days. The higher the temperature, the shorter the retention time (**Seadi2008**). A digestion temperature of 40 °C and a retention time (HRT_{AD}) of 21 days have been assumed in this work (**bolzonella2018nutrients**).

Table 7.2: Variation of the inorganic fraction of nutrients biogas generation after anaerobic digestion of swine waste. Adapted from [fangueiro2020available](#).

Parameter	Variation (%)
TS	-45
VS	-52.5
$N_{inorganic}$	45
$P_{inorganic}$	16

TS: Total solids.

VS: Volatile solids.

N: Nitrogen.

P: Phosphorus .

The composition of biogas produced is based on data reported by **Ciborowski**. The energy requirements of the AD unit ($Q_{digester}$), described in Eq 7.1, comprise the energy required for substrate warming up from ambient temperature (assumed to be 12 °C) (Q_{waste}) to the digestion temperature (40 °C), and the energy supplied to offset the digester heat losses

(Q_{losses}). The details of the energy balance to the AD unit can be found in the Supplementary Material, Eqs. D.1 to D.8. A maximum digester size ($n_{\text{AD}, \text{max}}$) of 6000 m³ is assumed (**ADSize**).

$$Q_{\text{digester}} = Q_{\text{waste}} + Q_{\text{losses}} \quad (7.1)$$

Correlations for capital expenditures (CAPEX) and operating expenses (OPEX) estimation as a function of animal units have been developed based on data reported by the USDA (**USDAOM**), as shown in Eqs. 7.2-7.4 and Figure D.1 of the Supplementary Material, where $\dot{m}_{\text{digestate}}$ denotes the digestate flow and AU the number of animal units. It should be noted that operating and management (O&M) cost does not include the capital cost amortization.

$$n_{\text{AD}} = \left\lceil \frac{\dot{m}_{\text{digestate}} \cdot HRT_{\text{AD}}}{n_{\text{AD}, \text{max}}} \right\rceil \quad (7.2)$$

$$\begin{aligned} \text{CAPEX (MM USD (2019))} &= \\ \left(2.9069 \cdot 10^{-4} \cdot AU + 0.01625 \right) \cdot 1.216 \end{aligned} \quad (7.3)$$

$$\begin{aligned} \text{OPEX} \left(\frac{\text{MM USD (2019)}}{\text{year}} \right) &= \\ \left(\frac{15.858 \cdot 10^3}{1 + (AU \cdot 13.917)^{1.461}} \right) \cdot \text{CAPEX} \end{aligned} \quad (7.4)$$

7.2.2.2 Biogas conditioning

The raw biogas generated is conditioned to remove its impurities. Most of moisture is removed through condensation by compressing and cooling down the biogas stream. H₂S is removed by using a fixed bed of Fe₂O₃, capturing the hydrogen sulfur as Fe₂S₃. The bed can be regenerated using the oxygen contained in air, leading to the formation of elementary sulfur ([ryckebosch2011techniques](#)). Ammonia and remaining moisture are removed through a pressure swing adsorption (PSA) system. For both processes, two adsorption units are typically installed in-parallel arrangement, so that one unit is in operation while the other bed is undergoing regeneration. Removal yields of 100% have been assumed. More details can be found in Section D.1.2 of the Supplementary Material.

7.2.2.3 Combined heat and power generation

Biogas is valorized using a combined heat and power (CHP) unit to produce electricity and heat, which can be used to cover the thermal energy demand of the AD unit, and also for the nitrogen recovery processes if a source of heat is needed, e.g., ammonia evaporation. The energy recovered from biogas is estimated through its low heating value (LHV). LHV of biogas is a function of methane content, and it can be estimated using Eq. 7.5 (**BiogasLHV**), where x_{CH_4} refers to the methane mass fraction. Biogas combustion in the CHP unit is performed considering a 20% air excess.

$$\begin{aligned} LHV_{\text{biogas}} \text{ (J/m}^3\text{)} = & \\ - 46.26 \cdot 10^6 \cdot x_{\text{CH}_4}^2 + 70.87 \cdot 10^6 \cdot x_{\text{CH}_4} + 2.29 \cdot 10^6 & \end{aligned} \quad (7.5)$$

Based on data reported by manufacturers, the electricity and thermal efficiencies assumed are 40% and 50% respectively (**ClarkeEnergy**). The heat produced can be classified in high grade heat (HGH), which is recovered from the exhaust gases of combustion at 450 °C, and low grade heat (LGH) recovered from other points of the equipment at lower temperature. HGH and LGH account for 62% and 38% of total heat energy respectively. LGH is used to cover the energy demand of AD units, while HGH is used for heat-intensive processes such as ammonia evaporation. If LGH from the CHP unit is not enough to cover the energy requirements of AD process, a fraction of HGH can be used to supplement the thermal energy supply.

7.2.2.4 Digestate solid-liquid separation

Nutrients contained in manure or digestate form organic and inorganic compounds. On the one hand, organic nutrients are in the form of carbon-based solid compounds, and therefore are mostly contained in the solid phase of waste. The nutrients bonded to organic compounds are not available for plants immediately, but they have to undergo a mineralization process to be transformed into inorganic nutrients (**USDAWaste**). On the other hand, inorganic nutrients are those forming inorganic compounds. Since they are water soluble, inorganic nutrients are mostly present in the liquid phase of waste.

The inorganic fraction of nutrients is recovered through a solid-liquid separation stage. The liquid fraction, containing most of inorganic nutrients, will be further processed for nutrient recovery. The solid phase of waste can be composted, promoting the mineralization of a fraction of the organic nutrients. The compost obtained can be used as a nutrient supplementation for crops. A screw press unit is considered for waste

liquid-solid phases separation in this study (**MollerSL**). The partition coefficients for the different components, CAPEX estimation, and electricity consumption considering the discretization of equipment size due to the commercial sizes available, are shown in the Section D.1.3 of the Supplementary Material.

7.2.2.5 Nitrogen recovery systems

The technologies for nitrogen recovery assessed in this work, illustrated in Figure 7.2, are described in this section, as well as their main modeling details.

Struvite production (Multiform system): Struvite is a mineral comprised by magnesium, ammonium, and phosphate that can be formed from different organic wastes by the chemical reaction shown in Eq. 7.6. The formation of struvite is a process that can be used for ammonia and phosphorus recovery by precipitation (**martin2020m**). MgCl₂ is supplied to the reactor at a phosphorus to magnesium molar ratio of 2 to increase struvite supersaturation (**bhuiyan2008phosphorus**). However, since phosphorus concentration in manure is lower than nitrogen concentration, phosphorus acts as the limiting reactant for struvite formation, and in turn, for nitrogen recovery. In this study, pH is adjusted to 9 for optimal struvite formation using sodium hydroxide (**Tao**).



Ammonium, phosphate, and other relevant compounds for struvite formation, such as carbonates competing for phosphate ions to form calcium-based precipitates, are part of chemical systems controlled by thermodynamic equilibrium. Therefore, a thermodynamic model for the formation of struvite and calcium precipitates accounting the variability of elements concentration in manure has been developed in a previous work (**martin2020m**). The chemical systems considered in the model for estimating struvite formation are included in Tables 1S and 2S of the Supplementary Material. Particularly, we note that calcium ions compete with magnesium ions for the phosphate ions, hindrance the formation of struvite. Therefore, a correlation to estimate the formation of struvite through the fraction of phosphorus recovered as struvite ($x_{\text{struvite}(\text{PO}_4^{3-})}$) as a function of calcium concentration in the waste has been used in this work, Eq. 7.7 (**martin2020m**). $x_{\text{Ca}^{2+}:\text{PO}_4^{3-}}$ denotes the molar calcium-phosphate ratio, while \dot{m}_i and MW_i refer to the mass flow and molecular weight of the component i respectively. We note that this correlation is valid for

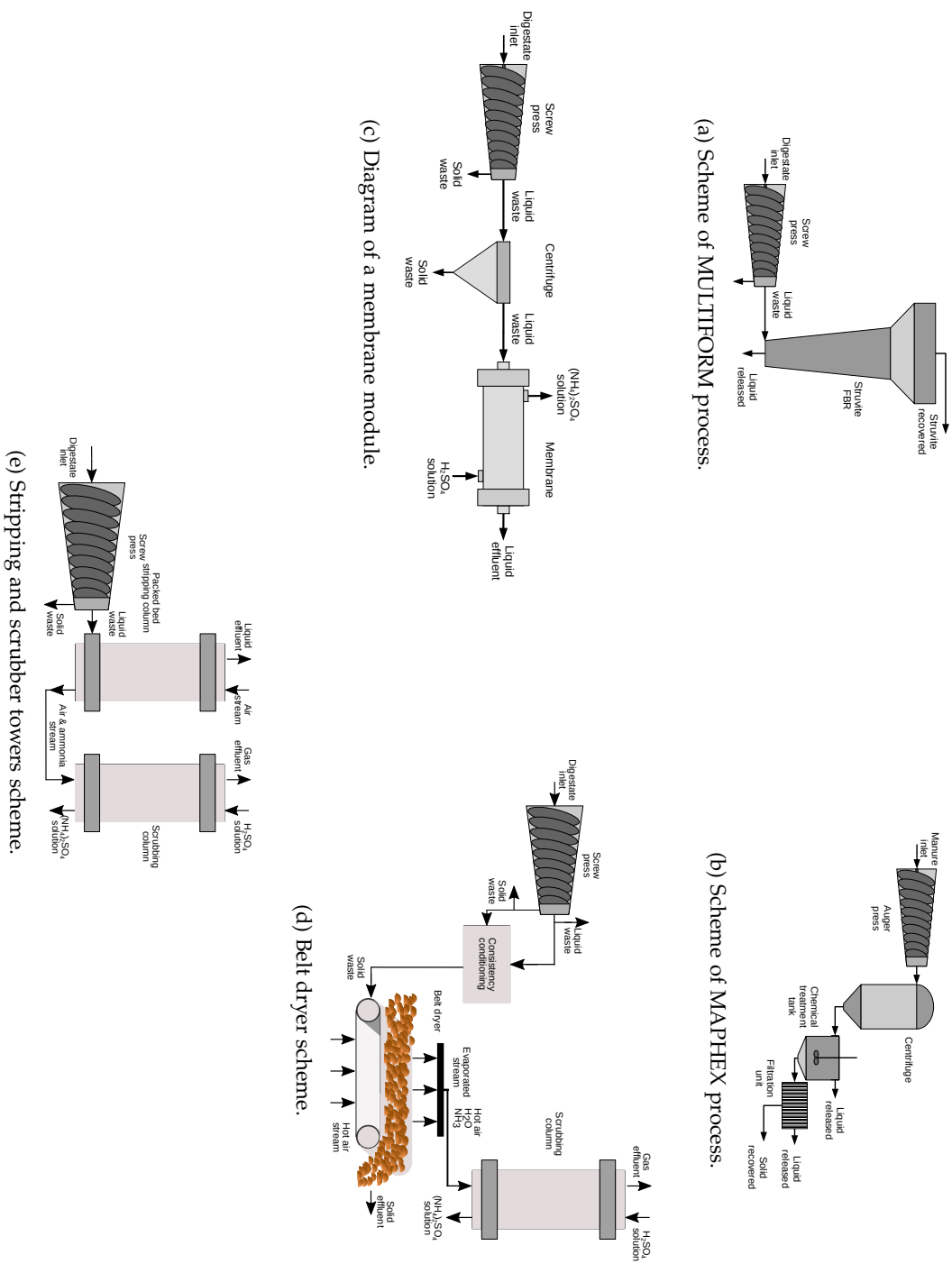


Figure 7.2: Nitrogen recovery systems assessed in the technoeconomic assessment.

estimating struvite formation at a pH of 9. Based on this correlation, the amount of nitrogen recovered is estimated through Eq. 7.9.

$$x_{\text{struvite}}(\text{PO}_4^{3-}) = \frac{0.798}{1 + (x_{\text{Ca}^{2+}:\text{PO}_4^{3-}} \cdot 0.576)^{2.113}} \quad (7.7)$$

$$\dot{m}_{\text{struvite recovered}} = \dot{m}_{\text{P in}} \cdot x_{\text{struvite}}(\text{PO}_4^{3-}) \cdot \frac{MW_{\text{struvite}}}{MW_{\text{P}}} \quad (7.8)$$

$$\dot{m}_{\text{N recovered}} = \dot{m}_{\text{struvite recovered}} \cdot \frac{MW_{\text{N}}}{MW_{\text{struvite}}} \quad (7.9)$$

Multiform Harvest is a commercial-level technology selected for the production of struvite from swine waste, since a previous work (**martin2021geospatial**) found this system as the most cost-effective struvite production process in a wide range of capacities for waste processing. This technology is based on a single pass fluidized bed reactor (FBR), with no recirculation, and conical design, as shown in Fig. 7.2a. The organic waste is pumped to the bottom of the reactor, as well as the magnesium supplement. The struvite particles grow, increasing their size, until their mass overcomes the drag force of the uplift stream. The conical design of the reactor keeps the small and lighter particles on the large diameter section at the top of the reactor, where the superficial velocity is slower. As the particles increase their mass, they settle gradually to lower levels of the reactor, where the diameter is smaller and the superficial velocity and drag force larger, until they are finally settled on the bottom of the reactor. The liquid phase exits the reactor from the top, where the cross-section is the widest, to ensure the retention of struvite fines.

The techno-economic model for the Multiform process considers a unique size able to process up to 48,000 kg of digestate per day, with an associated capital cost of 625,000 USD per each Multiform unit, plus 420,000 USD for the struvite dryer that serves all Multiform units. The operating cost for the Multiform system unit is 0.012 USD per kg of digestate processed (AMPC). Revenues by struvite sales of 0.85 USD/kg are also assumed (**molinos2011economic**).

MAPHEX: MAPHEX is a nutrient recovery system based on physico-chemical separations developed by Penn State University and the USDA, Fig. 7.2b. It is conceived as a mobile modular system which can be set in two interconnected truck trailers (**church_novel_2016**). MAPHEX involves three stages: liquid-solid separation with a screw press and a centrifuge, addition of iron sulfate to improve nutrients retention, and filtration with diatomaceous earth as filter media. Mass balances for MAPHEX, Eqs. D.15-D.19, are based on experimental data for full-scale modular units reported

by church_versatility_2018. The organic solid obtained contains the 93 % of the total solids in the raw waste, with a moisture content of 75%. The 90% of both nitrogen and phosphorus ($\eta_{MAPHEX}^{nutrients}$) is recovered in this solid material. This combination of processes results in a liquid effluent mostly composed of water with a low content of nutrients, while the nutrients are recovered in a solid stream mainly composed of organic matter. This organic solid has a lower density in nitrogen and phosphorus than other recovered products, such as ammonium sulphate or struvite, resulting in a low market value of this product and hindering the transportation and redistribution of the recovered nitrogen to nutrient-deficient areas.

Each MAPHEX unit is able to process up to 38 ton of manure per day with an associated operation cost of 0.054 USD per kilogram of manure processed. Capital cost of a MAPHEX unit is 291,000 USD (church_versatility_2018; church_novel_2016).

Transmembrane chemisorption: Transmembrane chemisorption is a process based on the separation of gaseous species contained in a liquid stream by using a hydrofobic membrane. An acid stripping solution circulates on the lumen side of the membrane to capture the recovered gaseous components. For the case of ammonia recovery, a solution of sulfuric acid is commonly used, resulting in the formation of ammonium sulfate, Eq 7.11. A 10% acid sulfuric solution is considered in this work as stripping fluid (darestani2017hollow). Ammonia recovery efficiency is improved by displacing ammonia-ammonium equilibrium, as shown in Eq. 7.10, to forming of gaseous ammonia raising the pH level up to 11 by adding sodium hydroxide.



Transmembrane chemisorption has been modeled adapting the model proposed by rongwong2020, considering mass transfer resistances on digestate liquid, membrane, and permeate phases, species distribution of the ammonia system, and the degree of membrane wetting. Mass transfer resistances on the permeate are considered negligible due to ammonia is rapidly converted into ammonium sulfate as a consequence of the excess concentration of sulfuric acid in this stream.

Membrane size is a function of the digestate flow to be treated. Liquid-Cel™ Extra Flow membranes (LiquidCelData) have been considered for ammonia recovery since their use for this purpose has been widely reported in the literature (darestani2017hollow; rongwong2020; linstrom2001). Membrane characteristics are reported in Table D.7 of the Supplementary Mate-

rial. Their sizes and costs are collected in Table 7.3. In case the capacity of the largest membrane module is not enough for the treatment of digestate, the installation of several parallel units is considered, as shown in Eq. 7.12. All membrane modules cost have been taken from values reported by manufacturers (**SGProjects; DPCWaterSolutions**), except for the Liquid-Cel™ 14x40 module, which price has been estimated based on the cost of the remaining modules, as illustrated in Figure D.3 of the Supplementary Material.

$$n_{\text{parallel}} = \begin{cases} 1 & \text{if } \dot{V}_{\text{digestate}} \leq 125 \frac{\text{m}^3}{\text{h}} \\ \left\lceil \frac{\dot{V}_{\text{digestate}} \left(\frac{\text{m}^3}{\text{h}} \right)}{125} \right\rceil & \text{if } \dot{V}_{\text{digestate}} > 125 \frac{\text{m}^3}{\text{h}} \end{cases} \quad (7.12)$$

Table 7.3: Liquid-Cel™ membranes size and cost (**LiquidCelData; SGProjects; DPCWaterSolutions**).

Membrane model	Flow capacity (m ³ /h)	Diameter (m)	Length (m)	Cost (USD)
2.5x8	0.1 - 0.7	0.067	0.200	5,000
4x13	0.5 - 3.4	0.116	0.242	5,700
8x20	1 - 11	0.219	0.406	14,150
10x28	10 - 48	0.279	0.683	17,000
14x40	16 - 125	0.356	1.129	24,300

Membrane sizing is performed through the membrane mass balances, Eqs. D.20-D.53. They are based on the distribution of ammonia species within the digestate, mass transfer on the digestate, wetted membrane, and non-wetted membrane phases, and the diffusion of ammonia through the membrane. Ammonia diffusion through the membrane is driven by bulk and Knudsen diffusivities, which consider the mean free path of molecules and the pore diameter respectively. Therefore, the cross-sectional area of the lumen and shell sides, as well as the length of the membrane are estimated based on mass balances, as shown in Eqs. D.24, D.25, and D.54 of the Supplementary Material respectively.

One or multiple membrane modules can be needed to achieve the total membrane length (z) needed to reach a certain efficiency, as shown in Eq. 7.13. n_{series} denotes the necessary number of membrane units of length L_{module} in-series arrangement to achieve the desired recovery efficiency. The length of the different membrane units is reported in Table 7.3. n_{parallel} refers to the number of membrane units in-parallel arrangement required to process the waste flow generated at the livestock facility under study

based on the processing capacities reported in Table 7.3. Membrane modules CAPEX is estimated through Eq. 7.14, assuming a membrane lifetime (t_{module}) of 10 years (verrecht2010cost), and a plant lifetime (t_{plant}) of 20 years. The use of sulfuric acid as stripping fluid and membrane cleaning is the main contributor to membrane OPEX, as shown in Eq. 7.15. Membrane cleaning cost (c_{cleaning}) is reported to be between 2% and 25% of the operating costs (yu2020performance; verrecht2010cost), for which we assume an average value of 13.5%. Additionally, the cost of the pumps needed for driving the digestate and stripping fluid streams through the membrane modules is considered. Cost estimation of pumps is collected in Eqs. D.55 to D.59 of the Supplementary Material.

$$n_{\text{series}} = \left\lceil \frac{z}{L_{\text{module}}} \right\rceil \quad (7.13)$$

$$\text{CAPEX}_{\text{membranes}} \text{ (2019 USD)} = (n_{\text{series}} \cdot n_{\text{parallel}}) \cdot \\ \text{Cost}_{\text{module}} \left(\frac{\text{USD}}{\text{module}} \right) \cdot \frac{t_{\text{plant}}}{t_{\text{module}}} \quad (7.14)$$

$$\text{OPEX}_{\text{membranes}} \left(\frac{2019 \text{ USD}}{\text{year}} \right) = \\ \frac{\dot{m}_{\text{H}_2\text{SO}_4} \left(\frac{\text{kg}}{\text{s}} \right)}{\rho_{\text{H}_2\text{SO}_4} \left(\frac{\text{kg}}{\text{m}^3} \right)} \cdot \text{Price}_{\text{H}_2\text{SO}_4} \left(\frac{\text{USD}}{\text{m}^3} \right) \cdot \frac{1}{1 - \frac{c_{\text{cleaning}}}{100}} \quad (7.15)$$

Total capital and operating expenses for the recovery of nitrogen from livestock digestate using a transmembrane chemisorption process result from the sum of membrane and pump costs are described in Eqs 7.16 and 7.17.

$$\text{CAPEX}_{\text{transmembrane}} = \text{CAPEX}_{\text{membranes}} + \sum_{i \in \{\text{shellside}, \text{lumenside}\}} \text{CAPEX}_{\text{pumps}_i} \quad (7.16)$$

$$\text{OPEX}_{\text{transmembrane}} = \text{OPEX}_{\text{membranes}} + \text{OPEX}_{\text{pumps}} \quad (7.17)$$

Ammonia evaporation: Nitrogen can be recovered by ammonia evaporation through digestate drying in a belt dryer unit. The operation of a belt dryer unit requires a minimum concentration of solids of 10% - 12% (bolzonella2018nutrients). Therefore, the liquid and solid outlet streams from the solid-liquid separation stage are combined to obtain a stream with the desired solids content. After solids content adjustment, digestate is dried in the belt drier, as shown in Fig 7.2d. This unit dries the digestate

over the belt with a stream of hot air crossing the belt through orifices on it. Heat (sensible and latent) is transferred from the hot air to the digestate on the belt to increase temperature and evaporate ammonia and a fraction of moisture.

The belt dryer model assumes the evaporation of two components in no equilibrium with a continuous extraction of the vapour phase ([treybal1980mass](#)). Since the amount of ammonia in digestate is significantly lower than moisture, air saturation with water vapor is considered the evaporation limit. It must be noted that the moisture carrying capacity of air (i.e., the saturation point) is a function of temperature. This requires to solve the mass and energy balances simultaneously, which are reported in the Supplementary Material Eqs. shown in Eqs. [D.60-D.72](#). An ammonia removal efficiency ($\eta_{\text{belt dryer}}$) of 80% has been assumed for mass balances calculation ([awiszus2018ammonia](#)). The assumptions for the modeling of ammonia evaporation by digestate drying are collected in the Section [D.1.7](#) of the Supplementary Material. Gaseous ammonia is further recovered through acidic scrubbing, as described in Section [D.1.9](#).

Capital expenses estimation for belt dryer units is based on the energy required for ammonia evaporation. A drying efficiency ($\eta_{\text{belt dryer}}$) of 0.6 has been assumed from the experimental work reported by [awiszus2018utilization](#). Belt dryer scale-up is based on the correlation proposed by [towler2012chemical](#), as shown in Eq. [7.21](#). The reference values and scale factor used in this correlation are taken from costs and capacities reported by [turley2016assessment](#), as well as the maximum belt dryer capacity used to compute the number of dryer units needed ($n_{\text{belt dryer}}$), as shown in Eq. [7.19](#). These data are also used to estimate the scale-up factor, which is estimated equal to 0.7. Belt dryer operating costs are due to electrical consumption, which has been estimated in 0.099 kW of electricity per kW of thermal energy used by the unit, as shown in Eq. [7.22](#) ([awiszus2018utilization](#)).

$$\dot{Q}_{\text{belt dryer}}^{\text{real}} = \frac{\dot{Q}_{\text{belt dryer}} (\text{kW})}{\eta_{\text{belt dryer}}} \quad (7.18)$$

$$n_{\text{belt dryer}} = \left\lceil \frac{\dot{Q}_{\text{belt dryer}}^{\text{real}} (\text{kW})}{1000} \right\rceil \quad (7.19)$$

$$\dot{Q}_{\text{belt dryer}}^{\text{design}} = \frac{\dot{Q}_{\text{belt dryer}}^{\text{real}}}{n_{\text{belt dryer}}} \quad (7.20)$$

$$CAPEX_{\text{belt dryer}} (\text{2019 USD}) = \quad (7.21)$$

$$\left(n_{\text{belt dryer}} \cdot 214,997 \cdot \left(\frac{\dot{Q}_{\text{belt dryer}}^{\text{design}} (\text{kW})}{500} \right)^{0.7} \right) \cdot 1.216$$

$$OPEX_{\text{belt dryer}} \left(\frac{\text{2019 USD}}{\text{year}} \right) = \quad (7.22)$$

$$n_{\text{belt dryer}} \cdot \dot{Q}_{\text{belt dryer}}^{\text{design}} (\text{kW}) \cdot 0.099 \left(\frac{\text{kW}_e}{\text{kW}_t} \right) \cdot t_{\text{operation}} (\text{s}) \cdot 3600 \cdot$$

$$Price_{\text{electricity}} \left(\frac{\text{USD}}{\text{kWh}} \right)$$

Stripping in packed tower: Nitrogen recovery by stripping of the liquid digestate is a widely used technique based on the transfer of ammonia from liquid digestate to an air stream. This operation can be performed in packed towers. Gaseous ammonia is further recovered through acidic scrubbing, as described in Section D.1.9.

Nitrogen recovery using packed tower stripping, illustrated in Figure 7.2e, has been modeled using the number of transfer units (NTU) method (**Metcalf**). The pressure drop of tower packing is estimated through the correlation proposed by **kister1991predict**, as shown in Eq. 7.23.

$$P \left(\frac{\text{inch water}}{\text{ft}} \right) = 0.115 \cdot \left(F_P \left(\text{ft}^{-1} \right) \right)^{0.7} \quad (7.23)$$

The tower diameter is calculated through the tower flooding capacity. A tower flooding capacity correlation considering the packing pressure drop is developed using ALAMO (**wilson2017alamo**) based on the flooding curves developed by **strigle1994packed**, as shown in Eq. 7.24 and Figure 7.3. Two-inch (0.051 m) Intalox packing is considered (**strigle1994packed**), which packing factor (F_P) is assumed to be 18 ft^{-1} (59 m^{-1}) (**geankoplis2003transport**). The operating line considered, defined as the ratio of gas and liquid volumetric flows, can be computed through Eqs. 7.24 to 7.27, where v_G denotes

the superficial gas velocity in $(\frac{\text{ft}}{\text{s}})$, ρ_G the gas density in $(\frac{\text{lb}}{\text{ft}^3})$, ρ_L the liquid density in $(\frac{\text{lb}}{\text{ft}^3})$, ν the kinematic viscosity in (censtokes), G_G the gas mass velocity in $(\frac{\text{lb}}{\text{ft}^2 \cdot \text{s}})$, and G_L the liquid mass velocity in $(\frac{\text{lb}}{\text{ft}^2 \cdot \text{s}})$ (strigle1994packed).

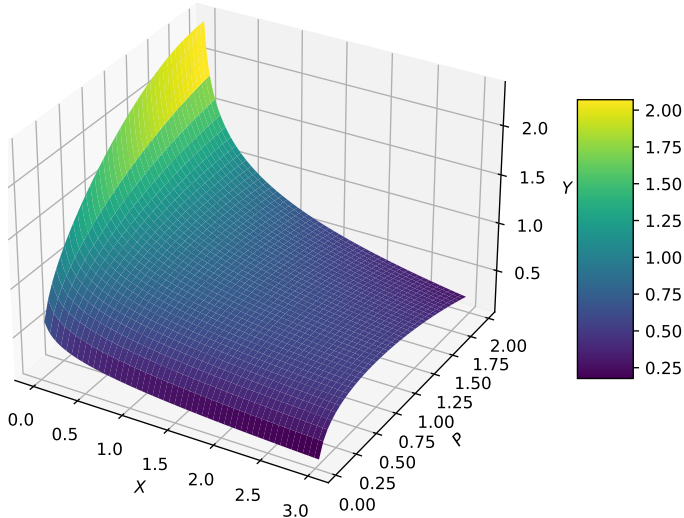


Figure 7.3: Tower flooding capacity correlation considering packing pressure drop.

$$\begin{aligned} Y = & -0.25 \cdot X + 0.22 \cdot \ln(P) - 0.78 \cdot 10^{-1} \cdot P^2 + 0.19 \cdot 10^{-1} \cdot X^3 \\ & - 0.39 \cdot X \cdot P + 0.49 \cdot 10^{-2} \cdot (X \cdot P)^3 + 0.89 \end{aligned} \quad (7.24)$$

$$Y = v_G \left(\frac{\rho_G}{\rho_L - \rho_G} \right)^{0.5} F_P^{0.5} \nu^{0.05} \quad (7.25)$$

$$X = \log_{10} \left(\frac{G_L}{G_G} \left(\frac{\rho_G}{\rho_L} \right)^{0.5} \right) \quad (7.26)$$

$$\frac{\dot{V}_G}{\dot{V}_L} = 2688 \frac{m_{\text{gas}}^3}{m_{\text{liquid}}^3} \quad (7.27)$$

$$G_{G_{\text{design}}} = 0.7 G_G = 0.7 \cdot v_G \cdot \rho_G \quad (7.28)$$

The liquid mass velocity is a known parameter since it corresponds to the digestate being processed. The gas velocity is estimated by combining Eqs. 7.23, 7.24, and 7.27. The design gas mass velocity considered is 0.7 time the theoretical gas mass velocity, Eq. 7.28, while the liquid design mass velocity is computed by combining Eqs. 7.28 and 7.27. Design restrictions reported by Branan have been considered in the sizing of the packed tower.

The tower height is estimated through the height and number of transfer units (**Metcalf**), as described in the Supplementary Material, Eqs. D.79 to D.84.

The number of stripping units needed ($n_{\text{stripping tower}}$) is calculated as the product of the number stripping units in-series arrangement to satisfy the packed towers height limit ($n_{\text{stripping tower}}^{\text{series}}$) and the number stripping units in-parallel arrangement to process the amount of waste generated in the livestock facility under evaluation ($n_{\text{stripping tower}}^{\text{parallel}}$), as shown in Eq. 7.29. CAPEX of stripping packed towers is estimated based on the columns volume using a correlation based on data from CAPCOST (CAPCOST), as shown Eq. 7.30. Additionally, capital expenses of compressor units are estimated based on the correlation reported by **almena2016technoeconomic**, Eq. 7.32. Operating expenses of scrubbing are mainly due to the compression cost, Eq. 7.33.

$$n_{\text{stripping tower}} = n_{\text{stripping tower}}^{\text{series}} \cdot n_{\text{stripping tower}}^{\text{parallel}} \quad (7.29)$$

$$\text{CAPEX}_{\text{stripping tower}} \text{ (2019 USD)} = 1.216 \cdot n_{\text{stripping tower}} \cdot \quad (7.30)$$

$$\left(-6.157 \cdot (V_{\text{stripping tower}} \text{ (m}^3\text{)})^2 + 1276.035 \cdot V_{\text{scrubber}} \text{ (m}^3\text{)} + 4007.619 \right) \\ V_{\text{stripping tower}} = \frac{(D_{\text{stripping tower}}^{\text{design}})^2 \cdot \pi}{4} \cdot H_{\text{stripping tower}} \quad (7.31)$$

$$\text{CAPEX}_{\text{compressor}} \text{ (2019 USD)} = 1.216 \cdot \\ (335.27 \cdot \dot{W}_{\text{compressor}} \text{ (kW)} + 36211) \quad (7.32)$$

$$\text{OPEX}_{\text{compressor}} \left(\frac{2019 \text{ USD}}{\text{year}} \right) = \\ \dot{W}_{\text{compressor}} \text{ (kW)} \cdot t_{\text{operation}} \text{ (s)} \cdot 3600 \cdot \text{Price}_{\text{electricity}} \left(\frac{\text{USD}}{\text{kWh}} \right) \quad (7.33)$$

Acidic scrubbing: Ammonia contained in the gaseous streams from ammonia evaporation and stripping in packed bed can be recovered in an acidic scrubbing stage using a solution of sulfuric acid in water, as described in Fig. 7.2e. Ammonia is trapped by the liquid stream, reacting with the sulfuric acid to form ammonium sulfate. Mass balances for the scrubber unit consider the water transferred to the gas stream, assuming that saturation is reached, Eq. D.86. Ammonia recovery efficiency ($\eta_{\text{scrubber}}^{\text{NH}_3}$) of full-scale ammonia scrubbers has been reported in the range of 40% to 99% (**melse2005**). A typical $\eta_{\text{scrubber}}^{\text{NH}_3}$ of 96% has been selected based on the work of **melse2005**.

$$\frac{P_{\text{water}}}{Pv_{\text{water}}} = 1 \quad (7.34)$$

$$Pv_{\text{water}} = \frac{\frac{\dot{m}_{\text{water out}}^{\text{gas stream}}}{MW_{\text{water}}}}{\sum_j \frac{\dot{m}_j^{\text{gas stream}}}{MW_j}} \cdot P_{in}^{\text{gas stream}} \quad (7.35)$$

$$\dot{m}_{\text{NH}_3 \text{ out}}^{\text{gas stream}} = \dot{m}_{\text{NH}_3 \text{ in}}^{\text{gas stream}} \cdot (1 - \eta_{\text{scrubber}}^{\text{NH}_3}) \quad (7.36)$$

The water flow needed to perform the scrubbing operation is computed from the operation line of the unit (L/G), Eq. D.88. Following the rules of thumb for scrubbing units, the design operation line has been assumed as twice the minimum operation line, Eq. D.89. Y_{NH_3} and X_{NH_3} denote the ammonia free basis molar fractions in gas and liquid streams respectively. The amount of sulfuric acid supplied to make-up the sulfate used for ammonium sulfate formation, Eq. D.91, is slightly larger than the stoichiometric amount of the precipitation reaction, 3.5 kg_{H₂SO₄} per kg_{NH₃} recovered (**bolzonella2018nutrients**).

$$(L/G)_{\min} = \frac{Y_{\text{NH}_3 \text{ in}} - Y_{\text{NH}_3 \text{ out}}}{X_{\text{NH}_3 \text{ out}} - X_{\text{NH}_3 \text{ in}}} \quad (7.37)$$

$$(L/G) = (L/G)_{\min} \cdot 2 \quad (7.38)$$

$$\dot{m}_{\text{water in}}^{\text{liquid stream}} = ((L/G) \cdot \dot{n}_{\text{total in}}^{\text{liquid stream}} - \dot{n}_{\text{NH}_3 \text{ in}}^{\text{liquid stream}}) \cdot MW_{\text{water}} \quad (7.39)$$

$$\dot{m}_{\text{H}_2\text{SO}_4 \text{ in}}^{\text{liquid stream}} = \dot{m}_{\text{NH}_3 \text{ in}}^{\text{gas stream}} \cdot \eta_{\text{scrubber}}^{\text{NH}_3} \cdot 3.5 \quad (7.40)$$

$$\dot{m}_{(\text{NH}_4)_2\text{SO}_4 \text{ out}}^{\text{liquid stream}} = \frac{\dot{m}_{\text{NH}_3 \text{ in}}^{\text{gas stream}} \cdot \eta_{\text{scrubber}}^{\text{NH}_3}}{MW_{\text{NH}_3}} \cdot MW_{(\text{NH}_4)_2\text{SO}_4 \text{ out}} \quad (7.41)$$

Scrubbing CAPEX is estimated through a preliminary design and sizing of the scrubbing units. As shown in the Section D.1.9 of the Supplementary Material, the estimation of the scrubber diameter is based on the gas velocity in the equipment (**melse2005**). The number of units is set by the maximum diameter of scrubbers, Eq. D.95, which is assumed equal to 1.2 m accordingly to the rules of thumb for packed columns (**Branan**). Similarly to the case of stripping columns, the height of scrubbing towers is computed through the transfer units method, as described by **copper2005chemical**. This method is shown in Eqs. D.96-D.101 of the Supplementary Material.

CAPEX of scrubber units is estimated through the column's volume by using the correlation described in Eq. 7.30. The cost of the compressor is estimated through Eq. 7.32. Operating expenses of scrubbing are mainly

related to the use of sulfuric acid, Eq. 7.42, and the compression cost, Eq. 7.43.

$$OPEX_{\text{scrubbers}} \left(\frac{\text{2019 USD}}{\text{year}} \right) = \frac{\dot{m}_{\text{H}_2\text{SO}_4} \left(\frac{\text{kg}}{\text{s}} \right)}{\rho_{\text{H}_2\text{SO}_4} \left(\frac{\text{kg}}{\text{m}^3} \right)} \cdot Price_{\text{H}_2\text{SO}_4} \left(\frac{\text{USD}}{\text{m}^3} \right) \quad (7.42)$$

$$OPEX_{\text{compressor}} \left(\frac{\text{2019 USD}}{\text{year}} \right) = \dot{W}_{\text{compressor}} (\text{kW}) \cdot t_{\text{operation}} (\text{s}) \cdot 3600 \cdot Price_{\text{electricity}} \left(\frac{\text{USD}}{\text{kWh}} \right) \quad (7.43)$$

7.2.3 Economic assessment

The total costs of nitrogen recovery and waste processing have been estimated for each nitrogen management system evaluated. These are defined in Eqs. 7.44 and 7.45 respectively for each evaluated technology i , where k represents the possible products obtained, i denotes the discount rate (assumed to be 7%), and n_{plant} represents the process lifetime, which is assumed to be 20 years. Cost estimation includes OPEX and CAPEX amortization of all equipment involved in the processing of swine waste, as well as incomes from the sale of recovered products for those processes producing struvite (Multiform) or ammonium sulphate (digestate drying, stripping in packed tower, and membrane system). The selling prices considered are 0.85 USD per kilogram of struvite (**molinos2011economic**), and 0.12 USD per kilogram of ammonium sulphate (**AmmoniumSulphatePrice**). Conversely, the liquid and organic solid effluents containing low concentrations of nitrogen, such as the products obtained from the MAPHEX system, as well as some streams recovered from other systems such as ammonia evaporation or struvite production, are considered products with no market value. This assumption is based in the fact that, although they can be used for nutrient supplementation in croplands, they are too bulky for being economically transported to nutrient deficient areas. Therefore, similarly to manure, they can just be applied locally, hindering their use as a bio-based substitute of synthetic nitrogen fertilizers.

$$\begin{aligned} Cost_j^{\text{recovery}} \left(\frac{\text{USD}}{\text{kg}_N \text{ recovered}} \right) = \\ \frac{OPEX_j + CAPEX_j \cdot \frac{i \cdot ((1+i)^n_{\text{plant}})}{((1+i)^n_{\text{plant}} - 1)} - \sum_k \dot{m}_{j,k} \cdot Price_k}{\dot{m}_{N_{\text{recovered}}}} \end{aligned} \quad (7.44)$$

$$\begin{aligned} Cost_j^{\text{processing}} \left(\frac{\text{USD}}{\text{kg}_{\text{Waste processed}}} \right) = \\ \frac{OPEX_j + CAPEX_j \cdot \frac{i \cdot ((1+i)^n_{\text{plant}})}{((1+i)^n_{\text{plant}} - 1)} - \sum_k \dot{m}_{j,k} \cdot Price_k}{\dot{m}_{\text{Waste}_{\text{processed}}}} \end{aligned} \quad (7.45)$$

7.3 RESULTS AND DISCUSSION

7.3.1 Nitrogen flows and recovery efficiency

The nitrogen flows of the evaluated systems have been analyzed to determine the fraction of nitrogen recovered as inorganic products, either in the form of ammonium sulphate solution or as struvite, the the nitrogen recovered within the organic solid fraction of the waste, and the fraction of nitrogen that it is not recovered and is released into the environment, as shown in Figure 7.4. The nitrogen flows have been analyzed considering the entire recovery systems for waste treatment, including the pretreatment and N recovery processes.

It can be observed that the ammonia evaporation process requires a waste stream with a high solids content for the ammonia evaporation in the belt dryer unit. Therefore, a solid adjustment must be performed, discarding a large fraction of the liquid phase of digestate, which contains most of the inorganic nitrogen. As a result, a significant fraction of nitrogen (79 %) is released in a liquid stream. Nitrogen recovery by stripping in packed tower and membrane systems results in a fraction of nitrogen recovered in the organic solid fraction of the waste as a consequence of liquid-solid separation stages, in addition to the nitrogen recovered as a solution of ammonium sulphate, as illustrated in Figures 7.4d and 7.4e.

Multiform system show a low efficiency of nitrogen recovered as struvite. This is due to the fact that phosphate is the limiting factor for stuvite production, since this compound is in much lower concentrations than nitrogen in swine waste, as reported in Table 7.1. As a result, a significant fraction of nitrogen is not recovered but released in a liquid stream,

similarly to ammonia evaporation process, as observed in 7.4b. Finally, since MAPHEX is a manure processing system that integrates all the stages from the feed of raw manure to the recovery of the final products, no pre-treatment stages are considered for this system. The nitrogen is recovered within a organic solid material, as shown in Figure 7.4c.

7.3.2 Economic assessment and scale-up

The total costs of nitrogen recovery and waste processing for each nitrogen management system evaluated estimated are through Eqs. 7.44 and 7.45, and shown in Figure 7.5. Correlations to estimate the processing cost of the evaluated technologies as a function of animal units are shown in Table 7.4. Significant differences on the processing cost of technologies are observed depending on the reference considered for comparison. Considering the cost per kilogram of swine waste, illustrated in Figure 7.5a, we observe that Multiform and membrane systems are the processes with the lowest processing cost, 0.13 to 0.02 USD per kg of swine waste processed.

This approach accounts for operating and amortized capital expenses, as well as for the incomes from the sales of recovered products, as shown in Eq. 7.45. This is a common metric used to measure and compare the processing costs of nitrogen recovery processes (**de2019resource; bolzonella2018nutrients**). However, it does not include the nitrogen recovery efficiency of each process, which can lead to the selection of processes with low waste treatment cost, and low nitrogen recovery efficiency. Therefore, we consider that measuring the processing cost as a function of the recovered nitrogen, as shown in Figure 7.5b, is a more accurate metric for comparing different systems. Accordingly to this approach, the economic performance of Multiform dramatically decreases as a result of the low nitrogen recovery efficiency of this technology. Conversely, MAPHEX is revealed as more competitive process when the nitrogen recovered is considered. Since MAPHEX is a single size modular technology, its recovery cost shows a linear behavior, slightly affected by adding extra in-parallel modules to process large amounts of waste. Membrane system is the process with the lowest nitrogen recovery cost, from 10.4 to 3.4 USD per kilogram of nitrogen recovered, depending on the waste processing capacity of the system.

We note that the cost of anaerobic digestion stage represents a large fraction of capital expenses. However, this technology might be already implemented in some swine operations. Therefore, the impact of AD in the CAPEX, OPEX and processing costs has been analyzed. Figures 7.5 and 1S show these costs including AD stages, and Figures 2S and 3S illustrate the costs of nitrogen recovery systems excluding AD. It can be observed that

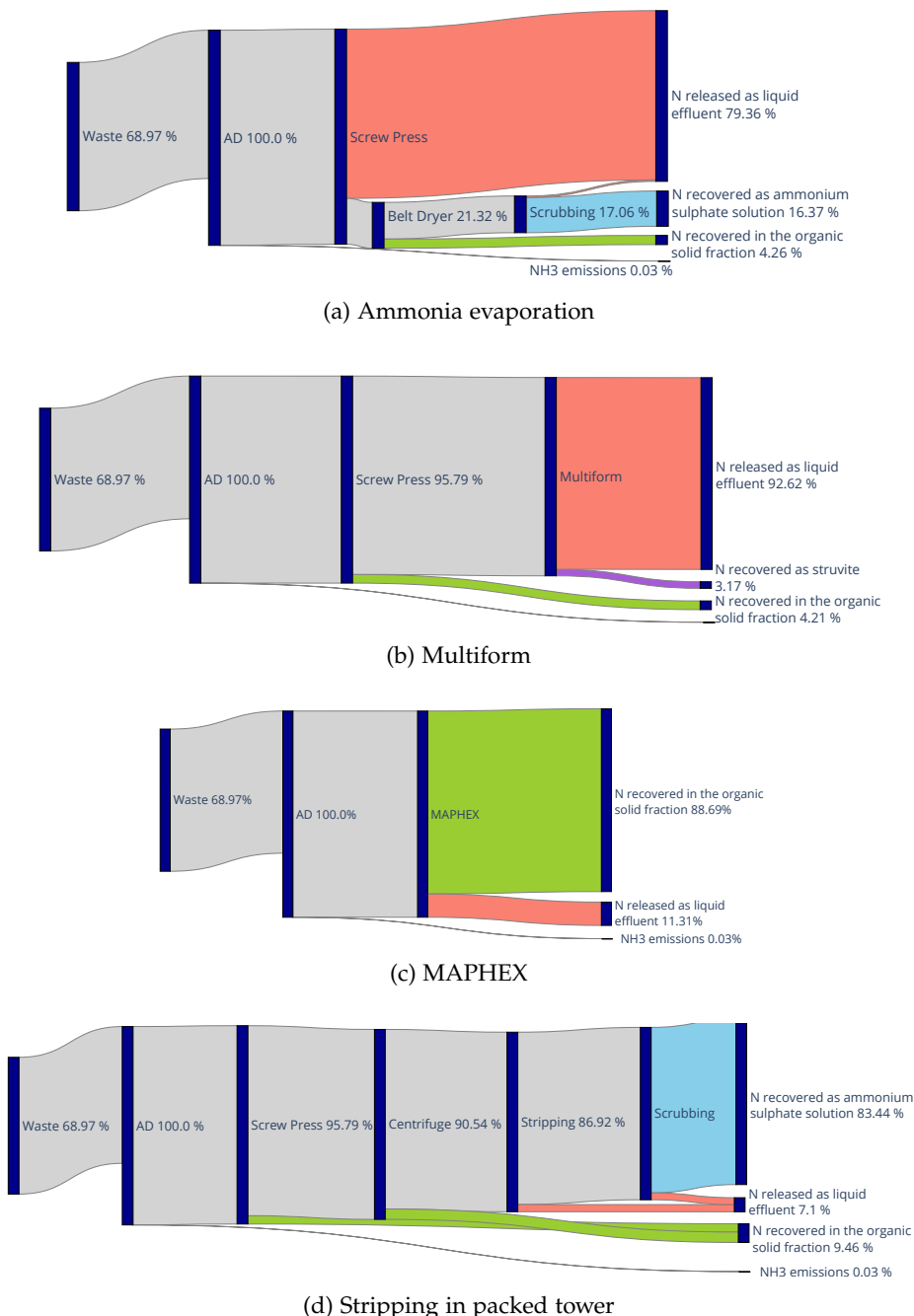
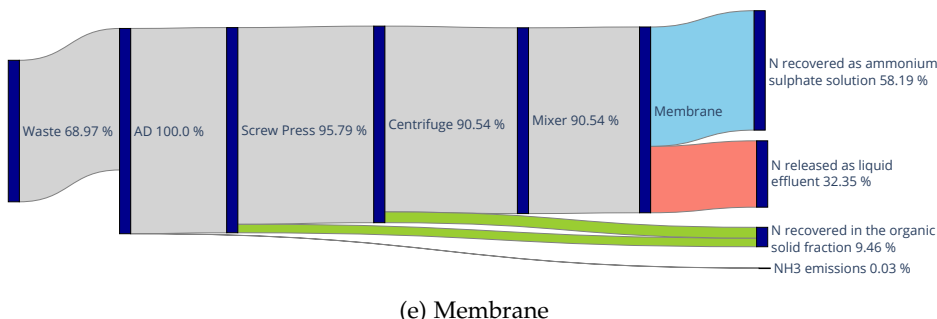


Figure 7.4: Relative flows of inorganic nitrogen in the studied processes. Since a fraction of organic nitrogen in swine manure is mineralized after the anaerobic digestion of the waste, the 100% refers to the inorganic nitrogen in digestate.



(e) Membrane

Figure 7.4: Relative flows of inorganic nitrogen in the studied processes. Since a fraction of organic nitrogen in swine manure is mineralized after the anaerobic digestion of the waste, the 100% refers to the inorganic nitrogen in digestate.

CAPEX costs are significantly higher when AD is considered. This turns into a decrease of processing costs when AD is not considered. Additional correlations for cost estimation are reported in Table 1S.

Additionally, the cost of releasing nitrogen to the environment is illustrated in Figure 7.5b in order to determine the processes for which nitrogen recovery is more economically beneficial than nitrogen release. The releasing cost of nitrogen is estimated based on the environmental and social cost of atmospheric NH₃ releases, and land, freshwater, and groundwater nitrogen loading. The cost of nitrogen release considering these damages reported by **sobota2015cost** and **compton2017assessing** are 32.5 and 35.15 USD/kg_N released respectively. We note that the recovery of nitrogen by using membrane systems, MAPHEX, and stripping in packed tower result in economic savings with respect to nitrogen release to the environment. This information can be a driver for the deployment of swine waste treatment processes for nitrogen recovery. However, a debate can be raised regarding what stakeholders should cover the cost of nitrogen recovery from swine industry. On the one hand, if nitrogen recovery is not performed at swine facilities, nitrogen releases result in environmental remediation costs in the long-term. These costs are usually covered by national and regional governments, which are ultimately funded by taxpayers. As a result, the environmental impact is covered by all citizens, whether or not they benefit from such businesses. On the other hand, the implementation of nutrient recovery systems could impact the economy of swine farms, which in turn could result in the raise of swine products cost, impacting the final consumers. This approach might seem fairer, since it only involves producers and consumers of swine products. However, it would lead to comparative disadvantages between different swine farms as a result of the savings in

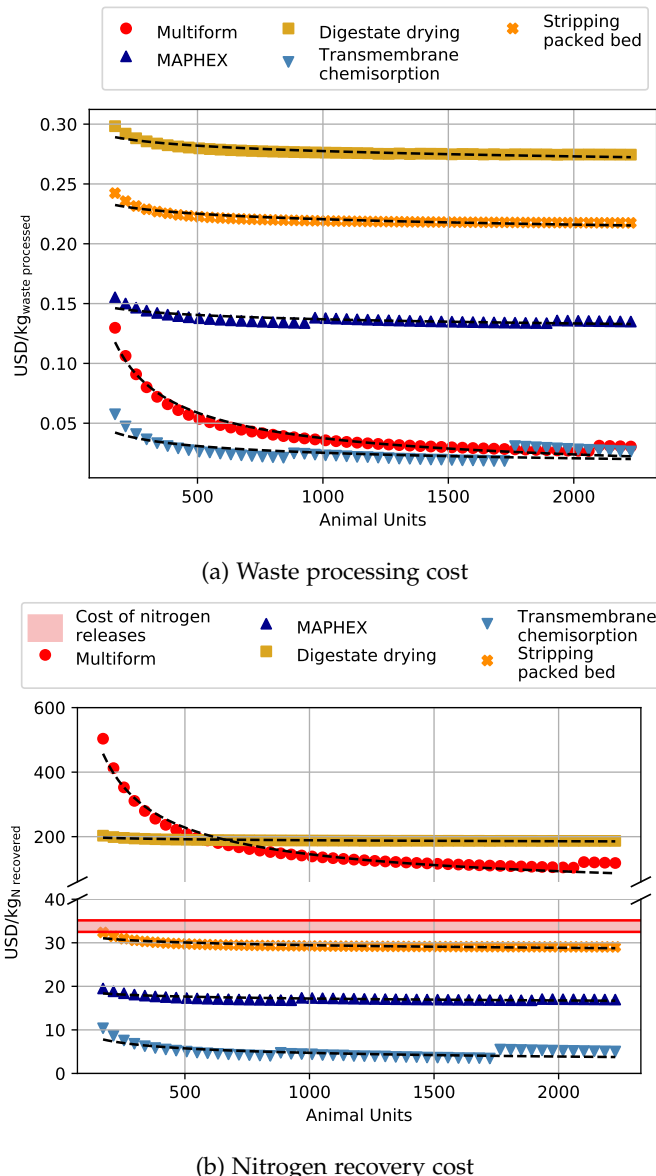


Figure 7.5: Processing cost for different livestock facility sizes, including the cost of pretreatment and AD stages.

nitrogen recovery costs due to the economies of scale, as shown in Figure 7.5a. Consequently, small facilities would be more affected by nitrogen recovery than large farms. Therefore, alternative economic schemes should be developed to mitigate the economic impact of the implementation of nitrogen recovery systems at swine facilities. In this regard, previous efforts developed for phosphorus recovery at livestock facilities can be adapted for

Table 7.4: Correlations to estimate the processing cost of the evaluated technologies as a function of animal units (*AU*), including the cost of AD stage.

System	Correlation	Waste processing cost	Total nitrogen recovery cost
		(USD/kg _{waste processed})	(USD/kg _{N recovered})
		Parameters	Parameters
Ammonia evaporation		$a=0.326$ $b=-0.0233$	$a=221.805$ $b=-0.0233$
Multiform		$a=3.308$ $b=-0.648$	$a=12837.477$ $b=-0.648$
MAPHEX	$C = a \cdot AU^b$	$a=0.177$ $b=-0.0372$	$a=22.240$ $b=-0.0372$
Stripping in packed tower		$a=0.271$ $b=-0.0298$	$a=36.181$ $b=-0.0298$
Membrane		$a=0.188$ $b=-0.290$	$a=33.612$ $b=-0.284$

nitrogen recovery. For instance, the development of a market for trading emissions allowances has been proposed for phosphorus releases from livestock farms (**Sampat2**). This scheme can also be explored for nitrogen releases. Additionally, **Policies** have studied several incentive policies for the implementation of phosphorus recovery systems in livestock facilities, including the fair allocation of limited incentive budgets, which could be adapted to the case of nitrogen recovery.

7.4 CONCLUSIONS

Intensive swine operations generate vast amounts of organic waste that it is a source of nitrogen releases into the environment. Since these releases are a significant contributor to the eutrophication of waterbodies, and they can result in harmful environmental impacts such as algal bloom episodes, the recovery of nitrogen at livestock facilities is a desirable measure to reduce the environmental footprint of the food production system.

Several processes have been developed for nitrogen recovery from organic waste, and therefore the selection of the most suitable process has to be addressed considering multiple dimensions, including the nitrogen recovery efficiency, the capital and operating expenses, and the impact of

the economies of scale in the final cost of nitrogen recovery. A multi-scale techno-economic study has been performed in order to determine the most suitable nitrogen recovery system based on the waste treatment capacity. The mass flows throughout all stages from manure collection to the final treatments have been analyzed in order to determine the nitrogen flows throughout each studied system. Two metrics have been considered to measure the operating cost of each technology, the waste treatment cost (USD/kg_{waste processed}), that it is a metric widely used in literature, and the nitrogen recovery cost (USD/kg_{N recovered}). Since the first metric does not account for the nitrogen recovery efficiency of each system, significant differences on the relative performance among the different technologies are found. This is because some technologies that result in low waste treatment costs show low nitrogen recovery efficiencies, resulting in comparatively large nitrogen recovery costs. However, transmembrane chemisorption is revealed as the most cost-effective nitrogen recovery technology, resulting in costs of 0.02-0.06 USD/kg_{waste processed}, and 3.4-10.4 USD/kg_{N recovered}. Moreover, comparing the negative economic impact of nitrogen releases into the environment, estimated between 32.5 and 35.15 USD/kg_{N released} with the cost of nitrogen recovery, three technologies reveal to be economically advantageous, transmembrane chemisorption, MAPHEX, and stripping in packed bed.

Future research is needed to discuss what stakeholders in the production and consumption cycle should assume the costs associated with nitrogen recovery. Additionally, further studies have to be addressed to design and evaluate incentive policies for the effective deployment of nitrogen recovery systems at intensive swine operations.

ACKNOWLEDGMENTS

The authors acknowledge funding from the Junta de Castilla y León, Spain, under grant EDU/556/2019.

Disclaimer: The views expressed in this article are those of the authors and do not necessarily reflect the views or policies of the U.S. Environmental Protection Agency. Mention of trade names, products, or services does not convey, and should not be interpreted as conveying, official U.S. EPA approval, endorsement, or recommendation.

BIBLIOGRAPHY

Part III

INTEGRATION OF ANAEROBIC DIGESTION AND NUTRIENT MANAGEMENT SYSTEMS

OPTIMAL TECHNOLOGY SELECTION FOR THE BIOGAS UPGRADING TO BIOMETHANE

ABSTRACT

A systematic approach is developed for the conceptual optimal design of biomethane production via carbon capture. A hybrid heuristic-mathematical procedure is proposed to determine the optimal technology and operating conditions. The heuristic step consists of a literature-based screening of the available technologies. After the prescreening stage, the technologies selected are amine absorption, pressure swing adsorption (PSA), and membrane separation. The mathematical stage is composed of two steps. First, different alternatives for each technology are modelled based on first principles and rules of thumb. These models are used to select the optimal configuration for each process considered. Second, a superstructure model for biomethane production is developed integrating the pre-selected upgrading technologies to select the optimal process, as well as to determine the optimal operating conditions. Four waste sources are analyzed: cattle manure, swine manure, municipal food waste, and sludge. The results suggest that the best amine is diethanolamine (DEA), the best membrane material is the polyimide, and the suggested zeolite is 13X among the ones studied. Finally, among the three technologies, the overall results show that carbon capture using a PSA system using zeolite 13X results in lower production and investment costs, but very close to the use of membranes. The results indicate that food waste shows the lowest production cost for biomethane 0.36 €/Nm³, due to the largest organic matter content, whereas the investment costs are 67 M€, considering a biogas production rate of 0.035 kg of biomethane per kg of waste and the processing of 311 kt/yr of food waste. Credits or incentives are still needed for biomethane to be competitive with fossil natural gas.

Keywords: Renewable energy; Biogas; Biomethane; Upgrading; Process design; Mathematical optimization

RESUMEN

Se ha desarrolla un enfoque sistemático para el diseño conceptual óptimo de la producción de biometano mediante la captura de carbono. Se propone un procedimiento híbrido heurístico-matemático para determinar la tecnología y las condiciones de funcionamiento óptimas. La etapa heurística consiste en un cribado bibliográfico de las tecnologías disponibles. Tras la etapa de preselección, las tecnologías seleccionadas son la absorción por aminas, la adsorción por oscilación de presión (PSA) y la separación por membranas. La etapa matemática se compone de dos pasos. En primer lugar, se modelizan las distintas alternativas de cada tecnología basándose en los primeros principios y en reglas empíricas. Estos modelos se utilizan para seleccionar la configuración óptima para cada proceso considerado. En segundo lugar, se desarrolla un modelo de superestructura para la producción de biometano que integra las tecnologías de mejora preseleccionadas para seleccionar el proceso óptimo, así como para determinar las condiciones óptimas de funcionamiento. Se analizan cuatro fuentes de residuos: estiércol bovino, estiércol porcino, residuos alimentarios municipales y lodos. Los resultados sugieren que la mejor amina es la dietanolamina (DEA), el mejor material de membrana es la poliimida, y la zeolita seleccionada de entre las estudiadas es la 13X. Por último, entre las tres tecnologías, los resultados globales muestran que la captura de carbono mediante sistemas PSA con zeolitas 13X tiene unos costes de producción e inversión menores, pero muy cercanos al uso de membranas. Los resultados indican que los residuos alimentarios presentan el menor coste de producción de biometano 0,36 €/Nm³, debido al mayor contenido de materia orgánica, mientras que los costes de inversión son de 67 M€, considerando una tasa de producción de biogás de 0,035 kg de biometano por kg de residuos y el procesamiento de 311 kt/año de residuos alimentarios. Todavía se necesitan créditos o incentivos para que el biometano sea competitivo con el gas natural fósil.

Palabras clave: Energía renovable; Biogás; Biometano; Purificación; Diseño de procesos; Optimización matemática

8.1 INTRODUCTION

Modern societies are characterized by the generation of large amounts of waste, arising from the manufacturing and production of goods and services to satisfy social demands. The traditional manufacturing model is one-way linear, starting with the extraction of the raw material from the environment, the manufacturing process, the use of the manufactured goods, and the final disposal of these goods, discarding the residues generated along the linear path. In addition, each of these stages involves energy consumption. According to the **WCED1987**, the one-way linear manufacturing process is an unsustainable production model, depleting natural resources and degrading the environment. The large amount of residues generated is a challenge in terms of treatment, but at the same time, it presents an opportunity towards the production of sustainable resources and energy through the development of circular economies around them (**WorldEnergyCouncil2016**). Therefore, waste-to-energy initiatives have gained support towards sustainability (**korhonen2018circular**). Among the treatment technologies for organic waste, anaerobic digestion is deemed promising as a renewable source of CH₄ and CO₂ for the production of biogas. Several studies have evaluated the use of the biogas for different purposes, including the production of chemicals. However, since the production cost of chemicals from biogas is high, the biogas is typically used as energy source.

Biogas can be used directly in gas turbines (**somehsaraei2014performance**), or in generators (**reddy2016investigation**). However, the large infrastructure available for the transport and use of natural gas in Europe (**Entsog**) and the United States (**EIAPIPelines**) suggests the purification of the biogas, also referred to as upgrading, into a composition similar to natural gas. The amount of residues available provides the capability of substituting non-renewable natural gas with biomethane in large regions, such as in Castile and Leon (Spain), where the amount of municipal solid wastes (MSW) available can cover the regional demand for natural gas (**taifouris2018multiscale**). There are several technologies to achieve this purpose, including hydrogenation or CO₂ removal.

On the one hand, it is possible to hydrogenate the CO₂ contained in biogas into methane (**stangeland2017co2**). However, the main issue is the high cost of producing hydrogen from renewable energy sources, such as wind (**davis2014optimala**) or solar energy (**davis2014optimalb**), resulting in non-competitive costs of biomethane (**curto2019renewable**) but in particular regions of high availability of solar or wind (**de2016characterization**). Alternatively, direct methanation of CO₂ within the digester has also been studied at laboratory scale (**Tynjala**).

On the other hand, several CO₂ capture technologies can be used to remove the carbon dioxide within the biogas obtaining high purity biomethane. A number of reviews have been published describing different CO₂ capture processes, including general perspectives (**adamu2020process**), specific reviews for pre and postcombustion gases (**macdowell2010overview**) and biogas upgrading processes (**adnan2019technologies; miltner2017review**). Techno-economic assessments and life cycle analysis for different technologies have been performed including membranes processes (**fang2018life**), adsorption and its comparison with membranes (**giordano2018life**), chemical absorption (**morero2017evaluation**), and biogas methanation (**curto2019renewable**), even comparing amine with ex-situ methanation (**v02018techno**). Furthermore, the liquefaction of biomethane has attracted the interest of researchers since, similar to liquefied conventional natural gas, it can be easily transported (**qyyum2020biogas**). However, the selection of the optimal technology for CO₂ capture has only been addressed in the context of post-combustion processes where membranes (**gassner2009integrated**), chemical absorption (**hasan2012modelinga**), or PSA (**hasan2012modelingb**) have been evaluated individually, or within a process design problem from the economic point of view (**klemevs2007techno**). Additionally, comparisons among different materials/solvents for the same capturing technology to determine the optimal configuration are also available, such as different membrane configurations based on simulation (**makaruk2010membrane**) and optimization (**gilassi2019optimizing**) approaches, or different solvents (**lee2013comparisons**). Nonetheless, recently a few recent works carried out systematic comparisons of different processes, such as the work of **pellegrini2018biogas**, where a comparison of cryogenic and amine scrubbing technologies is presented. However, this work extends the comparison to all mature CO₂ capture technologies within the context of an entire facility for production and upgrading of biogas. Therefore, there exists a gap in the literature regarding the determination of the optimal technology for biomethane production. It should be noted that, while biomethane upgrading technologies are similar to post-combustion capture processes, the CO₂ concentration in biogas is higher. Therefore, the results of the studies developed for post-combustion gases cannot be directly extrapolated to the biogas case.

This work presents a systematic framework to evaluate different technologies for biogas upgrading from a conceptual point of view, focusing on CO₂ capture processes. A hybrid heuristic-mathematical modelling approach has been developed to consider different technology configurations. In addition, an economic analysis for the production of biomethane considering four wastes (cattle manure, swine manure, municipal food waste, and sludge) has been carried out to evaluate the economic feasibility

of these processes. The selection of these waste is based on the large availability and amount produced by society that constitute a challenge in waste management. The rest of the paper is organized as follows: Section 8.2 presents the methodology for technology selection. Section 8.3 describes the modelling of the alternative upgrading technologies. Section 8.4 shows the results of the analysis, including the specifications for the optimal technology selected for biogas upgrading, as well as the economic evaluation results. Additionally, carbon dioxide capture will be compared with the hydrogenation of CO₂ for further reference on the cleaner process for biomethane production. Finally, Section 8.5 draws the conclusions.

8.2 METHODOLOGY FOR PROCESS DESIGN

The entire facility for the production and upgrading of biogas is comprised of three stages: the anaerobic digestion stage, where the organic matter fraction of the waste treated is decomposed producing biogas, the initial biogas conditioning stage, where H₂S and ammonia are removed, and the purification step that removes the CO₂ to reach enough purity to be injected into the grid. Therefore, the lower limit specified for the final purity of the biomethane is a CH₄ concentration equal to 98% in order to ensure compliance with current regulations **SpanishMinistryofIndustry**.

Anaerobic digestion transforms the organic matter into biogas and a residue, digestate. Digestate is a material rich in nutrients **leon2016optimal**, particularly nitrogen and phosphorus, that can be further used as fertilizers. Biogas is a mixture of CO₂ and methane, including smaller quantities of impurities such as ammonia, nitrogen, hydrogen sulphide, and water. These impurities are removed from the biogas using reactive beds for the H₂S, adsorption for ammonia and nitrogen and condensation for water removal. Finally, a set of technologies for the removal of carbon dioxide are evaluated using a hybrid heuristic-mathematical optimization methodology. This methodology, as shown in Fig. 8.1, starts with a screening stage based on information and data reported in literature, selecting the CO₂ capture technologies, and their technical configurations regarding different solvents, adsorbent media and membrane materials, which are more feasible to adapt to the biomethane production process. Secondly, a mathematical optimization stage determines the optimal configuration among the alternatives available for each technology. Finally, a superstructure model joining the models of biogas production, purification, and the different upgrading processes is formulated as a nonlinear programming problem (NLP) problem **trespalacios2014review** to select the optimal upgrading process. Once the optimal biogas upgrading is determined, a

rigorous simulation should be performed for the selected process before plant design. However, the scope of this work is limited to the selection of the optimal upgrading technology for bio-methane production from biogas.

This process will be evaluated for four waste sources: cattle and swine manure, municipal food waste, and sludge. The CO₂ captured, even if it may need further purification, is to be used within the context of carbon capture and utilization for the production of chemicals or in other industries. Table 8.1 shows the average composition of the four waste types analyzed.

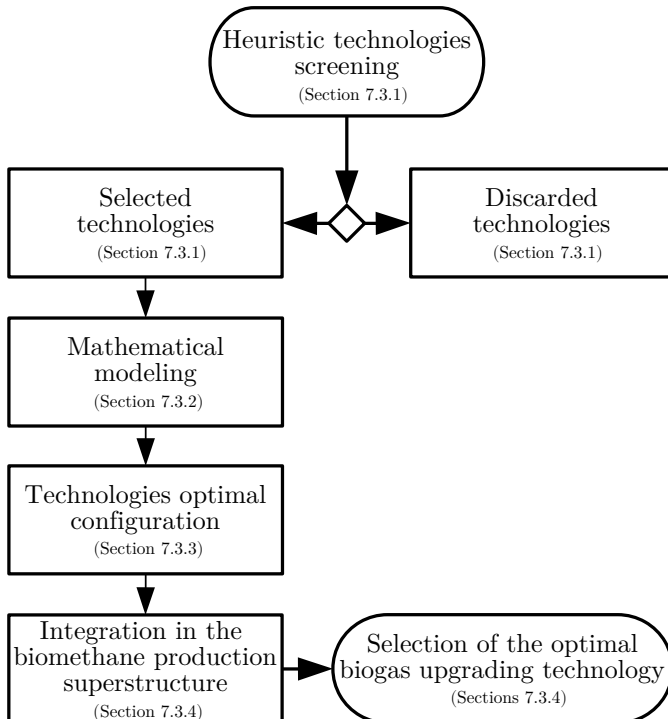


Figure 8.1: Scheme of the methodology followed to determine the optimal biogas upgrading technology.

8.3 PROCESS DESIGN

8.3.1 Technology screening

The technologies for CO₂ capture considered in the model are presented in Table 8.2. The technologies selected after the heuristic stage are chemical absorption, PSA, and membrane separation systems. Water scrubbing is a limiting case of the use of amine solutions, where amine

Table 8.1: Characteristics of the four waste types evaluated.

	Cattle manure ¹	Pig manure ^{1,2}	Sludge (wastewater) ¹	Urban food waste ¹
V _{biogas} (m ³ /kg)	0.25	0.38	0.35	0.44
w _{DM} (% wt)	0.25	0.25	0.17	0.31
w _{VS} (% dry wt)	0.80	0.75	0.4	0.85
w _N (% dry wt)	0.004	0.006	0.17	0.001
w _{N_{org}} (% dry wt)	0.020	0.022	0.0015	0.031
w _P (% dry wt)	0.006	0.010	0.035	0.005
w _K (% dry wt)	0.027	0.027	0.011	0.009
R _{CN}	20	15	15	15

¹

EuropeanCommission4953_2_11768_1

²

DanishEnvironmentalProtectionAgency2018

concentration would be zero. According to the literature the use of water scrubbing is more energy demanding, 3:1, than the use of amines (**Pellegrini2015**). Therefore, among scrubbing only amines will be considered. CO₂ hydrogenation is not actually a technology based on the removal of the sour gas, but a transformation process that can be compared outside of the framework used in this work for the CO₂ capture processes (**curto2019renewable**). Finally, cryogenic separation is still under development and the costs are high (**adnan2019technologies**). Each of the preselected technologies shows different configurations to be selected upon:

- In the case of amine scrubbing, three different amines are considered: monoethanolamine (MEA), diethanolamine (DEA), and methyl diethanolamine (MDEA) (**2004gpsa**).
- Pressure swing adsorption (PSA) systems can use different solid beds. Activated carbon presented a capture capacity about 25% lower than zeolites 13X and 4A (**hauchhum2014carbon**). The material cost being similar, and the lower adsorption of methane in the activated carbon (**ferella2017separation**), results in the preselection of the zeolites beds over activated carbon.
- Regarding the membrane systems, there are two variables to be considered, the configuration of the membrane units, and the material of the membranes. Among the possible configurations for the mem-

brane units, single-stage or multi-stage arrangements can be found. Multiple stage results in larger methane recovery and lower costs (**deng2010techno**). Among the multiple membrane stage systems, configurations with one compression stage (**makaruk2010membrane**) or multiple compression stages (**molino2013biogas**) are available. According to the literature, dual-stage membrane systems with single compression stage, considering only compression before the membrane system with no recompression stage between membrane units, have been deemed as the most economic under a wide range of feed compositions (**kim2017optimization**). Finally, the membrane materials are defined by the permeability of the gases. Lists of membrane materials for the separation of CO₂ from CH₄ can be found in several reviews (**zhang2013modeling**; **chen2015membrane**; **vrbova2017upgrading**). Among the common materials with larger permeabilities, cellulose acetate, polyimide, and polycarbonate are considered.

Table 8.2: CO₂ capture technologies considered in the study.

CO ₂ capture technology	Result after heuristic screening
Water scrubbing	Discarded
Amines scrubbing	Preselected
Pressure Swing Adsorption	Preselected
Membranes	Preselected
CO ₂ hydrogenation	Discarded
Cryogenic	Discarded

8.3.2 Mathematical modelling

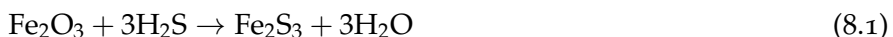
In this section the mathematical optimization stage of the procedure is presented and the models for the different units involved in biogas upgrading via CO₂ capture are described. For a more detailed description of the mathematical modelling, the reader is referred to the Supplementary Material, section E.2.

8.3.2.1 Biogas production and conditioning

The modelling of the biogas production and conditioning has been developed based on first principles in previous works **leon2016optimal**,

and therefore no further details are provided here. Anaerobic digestion is modelled based on mass and energy balances and yield data from the literature. For economic evaluation purposes, a standard digester size of 6,000 m³ is considered (**rohstoffe2010guia**). The biogas composition must be within the typical ratios for each of the raw materials. However, we consider it to be a variable that can be adjusted depending on its final use (**leon2016optimal**).

The compressors are modelled assuming polytropic behaviour, with a polytropic coefficient of 1.4, and an efficiency equal to 0.85 (Moran and Shapiro, 2003). Regarding the biogas conditioning stage, a bed of Fe₂O₃ is used for H₂S removal through the reaction described below. Experimental data shows almost 100% removal yield for H₂S using a fixed bed of Fe₂O₃.



Finally, ammonia and water are removed using a PSA system, considering removal yields equal to 100% (**Nexant2006; 2004gpsa**).

8.3.2.2 Absorption: amines

The amine scrubbing systems consist of an absorption column where the amine solution is put into contact with the biogas. The amine rich in CO₂ is heated up before being fed to the stripping column where the CO₂ is desorbed from the amine, which is recycled to the first column. The fresh amine used for making-up the losses of amine is mixed with the recycle stream from the regeneration column at the same temperature. The systems using amines typically operate at low temperatures, around 25-30 °C, and partial pressures of CO₂ above 0.05 bar, reaching removal yields of 90%-95% (**zhang2013modeling**). In contrast to post-combustion gases, which contain large amounts of nitrogen, biogas is composed mainly of methane and CO₂, resulting in higher carbon dioxide partial pressures requiring lower operating pressures. CO₂ partial pressures above 0.1 bar have been assumed to secure high removal yields (**zhang2013modeling**), resulting in the need to operate at total pressures around 1-1.5 bar to secure the appropriate CO₂ partial pressures (**movagharnejad2011simulation; xue2017comparative**).

Each unit is modelled based on first principles using industrial data (**2012gpsa**). To compute the flow of fresh amines, the CO₂ pickup rate and the column efficiency are used from industrial data. The energy balance to the preheater, the condenser and the reboiler of the CO₂ desorption column and the cooler are computed also using industrial rules of thumb. For the complete model see the Supplementary Material.

The model for the selection of the amine absorption is formulated as an NLP problem including the units described in sections 8.3.2.1 and E.2.1 of the Supplementary Material.

8.3.2.3 PSA

The stream of gases passes through the bed of zeolites and the carbon dioxide is captured by adsorption. The system consists of the compression train and the zeolite beds. The models for each of the units are based on the thermodynamics of gas compression and solid-gas Langmuir adsorption. The details can be seen in the Supplementary Material.

The adsorption capacity of the zeolites is directly related to the partial pressure of the CO₂. Therefore, the feed pressure is an operating variable adjusted using a system of compressors with intercooling. Each compression stage is modelled assumed polytropic behaviour and a compression efficiency of 0.85. The heat exchangers are modelled using mass and energy balances so that the gas temperature is from 25 to 60 °C entering the adsorption bed. The removal yield is assumed to be 98%, so that the exit gas contains less than 2% CO₂ ([ferella2017separation](#)). The mass of zeolite depends on the adsorption capacity that is computed as a function of the operating pressure and temperature using Langmuir adsorption models for the three materials. The operating time before regeneration must be below 20 min for the product gas to contain only traces of CO₂ ([hauchhum2014carbon](#)). Thus, two beds operate in parallel, one in adsorption, one in desorption mode. In addition, the adsorption capacity decays cycle after cycle until it stabilizes around 65% of the initial capacity given by Langmuir adoption isotherm. Therefore, the adsorption capacity is corrected to compute the amount of zeolite used in the PSA system. Furthermore, a lifetime of the zeolites bed of 5 years has been considered based on data reported by ([Xiao2013](#)).

The process is modelled as an NLP optimization problem including the models described in sections 8.3.2.1 and E.2.2 of the Supplementary Material.

8.3.2.4 Membranes

A dual-stage membrane system with single compression stage before the membrane module and no recompression stage between modules is considered since it has been deemed as the most economic arrangement under a wide range of feed compositions ([kim2017optimization](#)). The compressor is modelled as discussed above, assuming polytropic compression of the gas, see Supplementary Material for further details. Each

membrane module is modelled using mass balances considering the permeate and retentate streams, the flux of the gases across the membrane, that is a function of the concentration gradient between both sides of the membrane (**FernandesRodriguesMsc**). The flux is the parameter which allows computing the area of the membrane, based on the permeability of the membrane. As the driving force in the membrane separation process is the concentration gradient, the removal of CO₂ results in a change in the composition of the stream along the membrane, leading to a change in the driving force which controls the process. Therefore, an average molar fraction between the feed and the retentate composition is used to compute the separation driving force. Three different membrane materials are selected aiming at large CO₂ permeability, low methane permeability, and therefore, high selectivity; cellulose acetate, polyamide, and polycarbonate (**vrbova2017upgrading**). The solution of the optimization problem will yield intermediate conditions to assure natural gas composition of the biomethane.

The process model is formulated as an NLP problem, including the models described in sections [8.3.2.1](#) and [E.2.3](#) of the Supplementary Material, where the main decision variables are the operating pressure of the membrane, their areas and the flux across the membrane.

8.3.3 Selection of optimal configurations

8.3.3.1 Absorption: amines

Eq. [8.2](#) and the objective function shown in Eq. [8.3](#) are added to the model described in section [8.3.2.2](#) for determining the optimal amine for biogas upgrading. The first term, BioCH₄, presents the profit from the biomethane generated using the price of the natural gas given by the **EIAPrices**, and the second term corresponds to the operation considering the amortization of the investment costs of the amines purification systems, calculated in Eq. [8.3](#), where the investment cost is annualized with K equal to 3 (**douglas1988conceptual**).

$$Profit_{Amine\ system} = BioCH_4 - Cost_{Amine\ system} \quad (8.2)$$

$$Cost_{Amine\ system} =$$

$$C_{Steam} \sum_i \frac{Q_i}{\lambda} \cdot \tau_{year} + \frac{1}{K} C_{Amine} \cdot f c_{Amine} \cdot \tau_{year} \quad (8.3)$$

The cost of each amine is taken to be 1.3 USD/kg for MEA, 1.32 USD/kg for DEA, and 3.09 USD/kg for MDEA, based on **nuchitprasittichai2013optimization**.

The cost of high pressure steam (42 bar) is assumed to be 0.019 USD/kg (**perez2019superstructure**). The NLP problem consists of 288 equations and 953 variables per amine evaluated and is solved using a multistart initialization approach with CONOPT as the preferred solver where the main decision variables are the pressures temperatures and flow rates.

8.3.3.2 PSA

The main decision variables to select among the zeolite materials are the operating pressure and temperature at the PSA bed and the size of the zeolites bed. To estimate the cost of the PSA system, Eqs. 8.4 and 8.5 are included in the model described in section 8.3.2.3, assuming that the zeolite bed loses efficiency over time, resulting in a lifetime of 5 years before it needs to be replaced (**Xiao2013**). As the plant life is considered to be 20 years, the zeolites bed must be replaced 4 times during the plant life, N_{Cycle} . The cost of the zeolites considered is 5 USD/kg for both, zeolite 13 X and zeolite 4A (**Xiao2013**).

$$Profit_{PSA\ system} = BioCH_4 - Cost_{PSA\ system} \quad (8.4)$$

$$Cost_{PSA\ system} = \quad (8.5)$$

$$C_{Electricity} \cdot W_{Compressor} + \frac{1}{K} M_{Zeolite} \cdot C_{Zeolite} \cdot N_{Cycle}$$

The NLP problems, consisting 283 equations and 828 variables per adsorbent material, are solved similarly as in the case of the selection of amines.

8.3.3.3 Membranes

The selection of membrane material is carried out using the model described in 8.3.2.4, and an objective function considering the cost of the gas compression and the amortization of the investment costs of the membranes, Eqs. 8.6 and 8.7.

$$Profit_{Membrane\ system} = BioCH_4 - Cost_{Membrane\ system} \quad (8.6)$$

$$Cost_{Membrane\ system} = \quad (8.7)$$

$$C_{Electricity} \cdot W_{Compressor} + \frac{1}{K} \cdot C_{Membrane} \cdot \frac{1}{Lf} \\ \cdot N_{Membranes} \left(\sum_{i \in stages} Area_i \right)$$

A value of 50 USD/m² will be used based on the literature (**kim2017optimization**). Considering the plant life equal to 20 years, the membranes with a typical lifetime of 4 years must be replaced 5 times during the plant life, $N_{Membranes}$ (**scholz2015structural**). Each NLP consists of 299 equations and 869 variables and it is solved as the ones formulated for the previous cases.

8.3.4 Superstructure configuration

Once the best configuration from each technology is selected, the superstructure containing all the technologies evaluated is built considering only the best amine, membrane material and adsorbent bed, see Fig. 8.2. The superstructure includes the models presented in sections 8.3.2.1 to 8.3.2.4 and described in the Supplementary Material, section E.2. The superstructure is optimized evaluating all the processes simultaneously, for each waste raw material selecting only one technology, using as objective function Eq. 8.8.

$$Profit = \quad (8.8)$$

$$BioCH_4 - Cost_{Membrane\ system} - Cost_{PSA\ system} - Cost_{Amine\ system}$$

The superstructure model consists of 383 equations and 1367 variables, resulting in an NLP problem solved using a multistart optimization procedure with CONOPT as the preferred solver. The main decision variables are operating conditions including flows, temperatures, pressures, whereas the value for the variables of the non-selected technologies is null, including the mass flow. Binary variables per technology are not needed for the selection among the technologies since the costs are related to the flow processed per each technology.

8.3.5 Economic evaluation

Finally, a detailed economic evaluation for biomethane production from different wastes is performed. The production and investment costs are

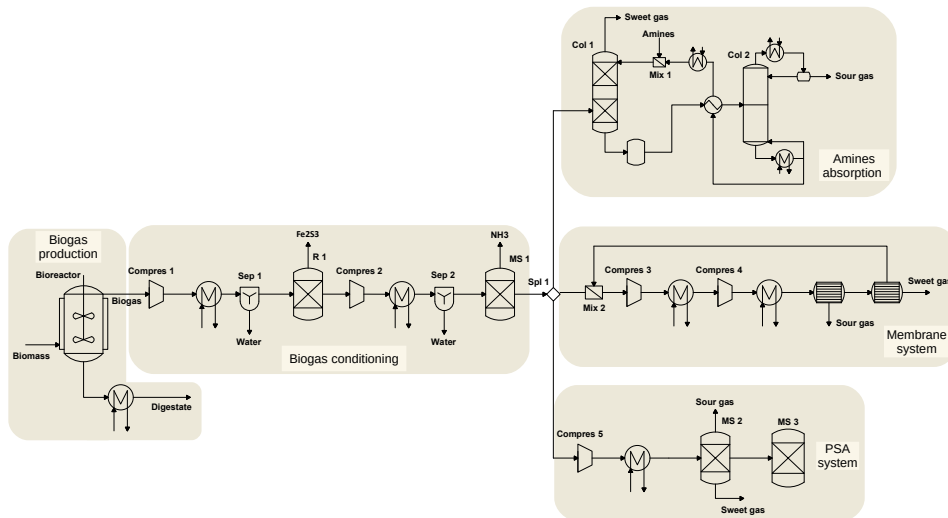


Figure 8.2: Scheme of the proposed superstructure for biogas upgrading into biomethane.

estimated using the factorial method presented in [towler2009chemical](#). It is based on the estimation of the unit costs, using the same factors as presented in [davis2014optimala](#); [davis2014optimalb](#) for further comparison with other renewable based methane production processes. The details on the method and correlations used for the economic assessment can be seen in the Supplementary Material, section E.3.

8.4 RESULTS

This section draws the results for the composition of the biogas obtained, technology selection, economic evaluation, the comparison of different technologies beyond biogas upgrading for the production of biomethane, and a scale-up study.

8.4.1 Biogas composition

The amount of each component of biogas is not fixed, but limited by upper and lower bounds for each component, as a range of values provided by the literature. The model aims at the composition of biogas that optimizes the production of methane, resulting in the same composition for all wastes, shown in Table 8.3.

Table 8.3: Raw biogas composition.

	CH ₄	CO ₂	H ₄ S	NH ₃	N ₂	O ₂	H ₂ O
Biogas composition (% mol)	56.8	25.2	≤0.2	≤ 7.6 · 10 ⁻³	1.7	0.4	15.7

8.4.2 Selection of technology

This section is divided into the selection of the best configuration per preselected technology and the optimization of the operating conditions where an economic objective function has been considered.

8.4.2.1 Selection of the optimal configuration

The selection of the optimal configuration of each technology, amines, PSA and membranes is carried out in a first optimization stage. Since the composition turned out to be the same for all wastes, the selection of technologies was also the same for the four wastes. In the case of the amines, DEA is the best among the amines. Note that the prices for the different amines change, but the recycle of the amines is such that the largest share of the cost comes from the energy involved in the regeneration column. Regarding adsorbent beds, zeolite 13 X shows the largest adsorption capacity. Finally, polyimide results as the best membrane material.

8.4.2.2 Selection of the optimal technology and operating conditions

The selection of technology for biogas upgrading was performed for four different wastes: cattle and swine manure, municipal food waste and sludge. The biogas upgrading technology selected for all residues is pressure swing adsorption. The results of the optimization problem formulated returns the optimal operating conditions of the biomethanation production facility for the wastes evaluated, as shown in Table 8.4. Regarding the wastes studied, food waste is the most promising one for biomethane production due to the larger organic matter content.

8.4.3 Estimation of production and investment costs

Table 8.5 shows the summary of the results of the economic evaluation considering the best upgrading technology for the different raw materials evaluated, and Fig. 8.3 presents the break-down of the production costs. Food waste is the most competitive residue for biomethane production,

Table 8.4: Main process parameters for the selected technology, pressure swing adsorption.

	Food waste	Cattle manure	Pig manure	Sludge
Waste flow (kg/s)	9.795	9.795	9.795	9.795
kg methane/kg feed	0.0355	0.00826	0.00449	0.00929
Methane produced (10^{-6} Nm ³ /yr)	15.132	3.521	1.914	3.960
P _{PSA} (atm)	2	2	2	2
T _{PSA} (°C)	25	25	25	25
M _{Zeolite} (kg)	6835	1583	856	1781
Steam (MW)	4.2	3.7	3.3	4.9
Cooling (MW)	3.3	0.7	0.4	1.0
Power (kW)	223	51.2	28	58.0
NPK ratio	1.1/0.9/0.47	1.1/1.1/0.6	0.8/2.5/1.3	0.0/4.6/2.4
R _{CN}	13.7	21.0	7.8	14.8

resulting in a production cost of 0.36 EUR/Nm³. On the other hand, the low organic load in manure results in production costs from 3 to 5 times larger than the production cost of biomethane from food waste. In all cases, the production cost is higher than current natural gas costs (0.18 EUR/Nm³) ([EIAPrices](#)) by at least a factor of 2. Therefore, the NPV or the ROI would be negative resulting in the need for additional income to balance the production costs obtaining credit from the nutrients contained within digestate, or through the application of incentive policies resulting in competitive market prices for biomethane. Considering the first alternative, food waste based biomethane, the most favourable case, becomes competitive if a credit of 0.022 EUR per kilogram of the fertilizer is obtained considering a methane market value of 5 EUR/MMBTU (0.18 EUR/Nm³), while the more expensive biomethane, obtained from swine manure, can be competitive at the cost of 0.116 EUR/kg of fertilizer. Considering a feed-in premium (FiP) incentive scheme, where bonuses are paid above the benchmark market price to subsidize the biomethane production, a range of bonus values between the 100% and 1000% of the methane market value are needed to reach a competitive selling price.

Regarding investment costs, the processing of larger flows of biogas for the processing of food waste results in up to 25% larger investment costs, from 49 M EUR to 66 M EUR, although as the flows of raw waste are similar for the different residues evaluated the number of digesters required is the same.

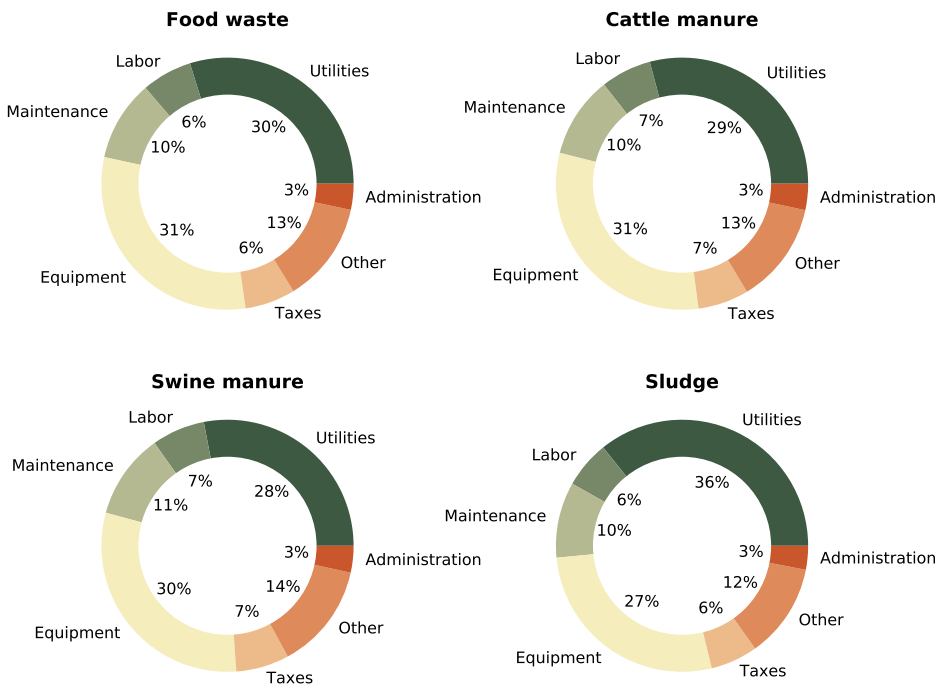


Figure 8.3: Breakdown of biomethane production costs for each residue analyzed.

For the most promising waste towards biomethane production, food municipal waste, the production and investment costs are computed in detail for the selected technologies, namely, PSA, membranes and amines, as shown in Table 8.6. It is possible to see that membranes and PSA show similar economic results, slightly in favour of the first technology. Membrane systems require 3 times more power than PSA units, resulting in a slightly more expensive alternative than the PSA. The optimal operating pressure of membranes is 65 bar, in the order of that presented by **kim2017optimization**, while the pressure of the PSA system is 2.05 bar, according with the results reported in (**ferella2017separation**) for biogas upgrading, and in the lower bound of the operating conditions reported by **santos2011pressure**. Amines scrubbing results the most expensive upgrading technology resulting in a cost 10% higher, mainly due to the larger consumption of utilities in the form of steam for the regeneration of the solvent. In all cases, with a reasonable credit from the fertilizer it would be possible to produce biomethane at a competitive cost, while the FiP bonus are between 100% and 117% of the methane market value.

Table 8.5: Summary of the cost estimation for biomethane production considering the optimal biogas upgrading technology, PSA system.

	Food Waste	Cattle Manure	Pig Manure	Sludge
Nºof digesters	6	6	6	6
Investment cost (M EUR)	66.4	54.4	48.7	51.3
Production cost (M EUR/yr)	5.1	4.0	3.6	4.2
Production cost (no credit)	0.36 $\frac{\text{EUR}}{\text{Nm}^3}$ 10.0 $\frac{\text{EUR}}{\text{MMBTU}}$	1.24 $\frac{\text{EUR}}{\text{Nm}^3}$ 33.5 $\frac{\text{EUR}}{\text{MMBTU}}$	2.00 $\frac{\text{EUR}}{\text{Nm}^3}$ 55.4 $\frac{\text{EUR}}{\text{MMBTU}}$	1.15 $\frac{\text{EUR}}{\text{Nm}^3}$ 31.8 $\frac{\text{EUR}}{\text{MMBTU}}$
EUR/kg fertilizer to achieve 5 EUR/MMBTU	0.022	0.048	0.116	0.041
EUR/Nm ³ FiP bonus to achieve 5 EUR/MMBTU	0.18	1.029	1.819	0.97

8.4.4 Comparison with renewable-based hydrogenation processes

The results presented in this work are compared with two different technologies for renewable methane production, the hydrogenation of the CO₂ contained in the biogas, reported by **curto2019renewable**, and synthetic methane produced from CO₂ hydrogenation, as presented by **davis2014optimala**; **davis2014optimalb**. In both cases, renewable energy is used to produce hydrogen, resulting in a high dependency between the methane production cost and the local availability of the renewable energy sources, i.e. solar irradiance and wind.

For the hydrogenation of the CO₂ within the biogas, the production costs depend on the mode of operation, continuum production or variable with the availability of solar energy. Considering a facility for food waste processing, with a production capacity of 0.67 kg/s of biomethane, a range of production costs of 0.57-0.27 EUR/Nm³ for CO₂ hydrogenation under steady and varying conditions respectively is found, with investment costs of 229 M EUR and 116 M EUR for the same two operating modes in Spain (**curto2019renewable**).

Alternatively, direct hydrogenation of CO₂ also allows the production of methane. For a facility with a methane production capacity of 0.78 kg/s, considering wind-based energy located in the most favourable allocation in Spain an investment of 375 M EUR is required. The production cost of synthetic methane is 0.48 EUR/Nm³, equivalent to 13.1 EUR/MMBTU (Davis and Martín, 2014a). On the other hand, if solar is used as source of renewable energy, the investment and production costs are reduced to 240 M EUR and 0.33 EUR/m³ (9.2 EUR/MMBTU) respectively in normal climate conditions **davis2014optimalb**.

Table 8.6: Detailed analysis for production of biomethane from food waste comparing technologies.

Food Waste	PSA	Membranes	Amines
Waste flow (kg/s)	9.795	9.795	9.795
Kg Methane/kg feed	0.0355	0.0355	0.0355
Nºof digesters	6	6	6
Steam (MW)	4.2	4.2	6.1
Cooling (MW)	3.3	3.4	5.0
Power (kW)	223	665	145
Investment cost (M EUR)	66.4	65.2	67.1
Production cost (M EUR/yr)	5.1	5.3	5.7
Production cost (no credit)	0.36 $\frac{\text{EUR}}{\text{Nm}^3}$ 10.0 $\frac{\text{EUR}}{\text{MMBTU}}$	0.38 $\frac{\text{EUR}}{\text{Nm}^3}$ 10.5 $\frac{\text{EUR}}{\text{MMBTU}}$	0.39 $\frac{\text{EUR}}{\text{Nm}^3}$ 10.7 $\frac{\text{EUR}}{\text{MMBTU}}$
EUR/kg fertilizer to achieve 5 EUR/MMBTU	0.022	0.023	0.026
EUR/Nm ³ FiP bonus to achieve 5 EUR/MMBTU	0.18	0.20	0.21

However, the comparison is not straightforward due to two reasons: the economies of scale and the effect of the credits obtained from digestate. The comparison can be carried out based on the feed flowrate, as in all cases a flow of waste of 10 kg/s is considered. Alternatively, the facility presented in this work is scaled-up to reach a similar methane production capacity. However, the difficulty of determining the correct credit obtained from the digestate makes difficult the direct comparison of biomethane/methane production costs.

8.4.4.1 Comparison based on feed flowrate

By comparing facilities that process the same waste flowrate, see Table 8.6, to the ones reported in the previous two paragraphs, the investment costs are lower in case of biogas upgrading using carbon capture technologies. The production of biomethane via CO₂ capture can be more competitive than the processes based on hydrogenation of CO₂ within the biogas except if the production rate is allowed to follow the availability of renewable energy. In addition, CO₂ capture is more attractive than the direct hydrogenation of CO₂ using wind as energy source for the production of the hydrogen, and only slightly more expensive than using solar

energy. However, the biomethane production capacity is the lowest of all three processes. Furthermore, note that allocations with favourable wind and solar based hydrogen production were selected.

8.4.4.2 Comparison based on production capacity

By scaling up the facility presented in this work, just for food residues and the best technology, the PSA, the production capacity is doubled reaching 0.72 kg/s of methane for comparison with previous work. This production capacity is between the two alternatives presented above (**curto2019renewable**; **davis2014optimala**; **davis2014optimalb**). The economic results for the scale-up of the carbon capture facility processing food are shown in Table 8.7 where it can be observed that the investment cost is in between the value obtained for continuum operation and the value obtained for variable hydrogenation of the CO₂ within the biogas. The production cost of the scaled-up facility is promising, 0.30 EUR/Nm³. Comparing this value with the ones from biogas hydrogenation or direct CO₂ hydrogenation, it is possible to observe that the production costs are competitive, and can be even lower than those of both technologies if a credit from the digestate can be obtained. The one drawback of the facility that uses carbon capture technologies is the need to find a use to the captured CO₂. The advantage is that it does not require additional power to produce renewable hydrogen.

Therefore, the recommendation among biogas upgrading via CO₂ capture, via CO₂ hydrogenation or synthetic methane production, would depend on the availability of solar or wind energy. Considering the case of Spain, the use of variable production of methane with the solar energy by direct hydrogenation of the CO₂ contained in the biogas is the best alternative (**curto2019renewable**). However, this is only competitive in the south of the country. Renewable methane can be the alternative when the power is produced in regions of high wind velocity (**de2016characterization**). Otherwise, the use of CO₂ capture technologies is preferred.

8.4.5 Plant scale-up study

Economies of scale play an important role in the chemical industry, reducing the cost as the facilities are larger. Because of the distributed availability of the residues and the difficulty of transport, it is relevant to evaluate the effect of the scale on the process economics. Two of the four residues, food waste and cattle manure, are considered for further analysis due to the large amounts of wastes produced and the environmental concerns involved. In the first case the aim is to evaluate the cost for the

Table 8.7: Operating conditions and economic parameter for the scaled-up plant from food waste.

Food Waste	
kg Methane/kg feed	0.72/20
N°of digesters	12
Investment cost (M EUR)	124.5
Production cost (M EUR/yr)	8.6
Credit digestate (M EUR/yr)	38.3
Production cost (no credit)	0.30 $\frac{\text{EUR}}{\text{Nm}^3}$ 8.21 $\frac{\text{EUR}}{\text{MMBTU}}$
EUR/kg fertilizer to achieve 5 EUR/MMBTU	0.014

biomethane for different city sizes as a function of the residues that they collect. Cities from 50 k to 5 million habitants are considered using the waste production rates of Spain, as shown in Fig. 8.4. Similar relationship between population and food waste generated can be expected for other countries or regions with a similar development level, although the results can be slightly affected by variations of some parameters, such as the amount of waste generated per person per year and the distribution of the population between urban and rural areas. The second case of study corresponds to cattle manure, assessing the biomethane production cost as a function of the size of concentrated animal feeding operations (CAFOs), considering facilities up to 16.000 cows. For a detailed description of the procedure followed in the scale-up study we refer the reader to the section S4 of the Supplementary Material. The cost of each unit is modelled as a function of the size, which is related to the mass or energy flow, as presented in the section E.4 of the Supplementary Material. The investment and production costs are estimated as described in section 8.3.5. Fig. 8.5 shows the production and investment costs as a function of the city size, and Fig. 8.6 shows the scale-up for cattle manure.

The results show that large cities above 1 million inhabitants are able to produce biomethane at competitive prices, even more if credit is obtained from the digestate. However, the lower concentration of organic matter in cattle manure results in non-competitive prices for the biomethane produced even for the largest CAFOs considered. Therefore, manure digestion can be a way to self-produce energy, particularly in isolated places, but at larger cost. After the scale-up study we correlated the

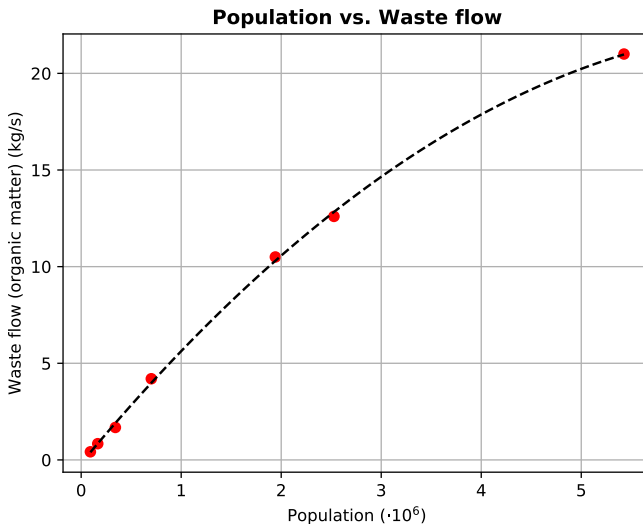


Figure 8.4: Relation between population and food waste produced in Spain.

investment and production costs of biomethane as a function of the plant size. The fitting parameters for the correlations can be found in Table 8.8.

Table 8.8: Scale-up correlations for investment and production costs for food waste and cattle manure.

Correlation	Food Waste		Cattle
	$V = \text{Population} \cdot 10^{-6}$	$V = \text{Number of animals} \cdot 10^{-6}$	
Waste flow (kg/s)	$F = a \cdot V^2 + b \cdot V + c$	$a = -0.430$ $b = 6.231$ $c = -0.175$	
Investment (MV)	$I = a \cdot V^2 + b \cdot V + c$	$a = -2.173$ $b = 24.485$ $c = 34.325$	$a = 0$ $b = 0.003$ $c = 16.769$
Production costs (EUR/Nm ³)	$C = a \cdot V^b$	$a = 0.546$ $b = -0.771$	$a = 220.023$ $b = -0.553$

8.5 CONCLUSIONS

In this work the upgrading of the biogas produced from different waste sources is studied comparing different carbon capture technologies following a systematic framework. A hybrid heuristic-mathematical approach is developed for the systematic process design. The heuristic screening stage

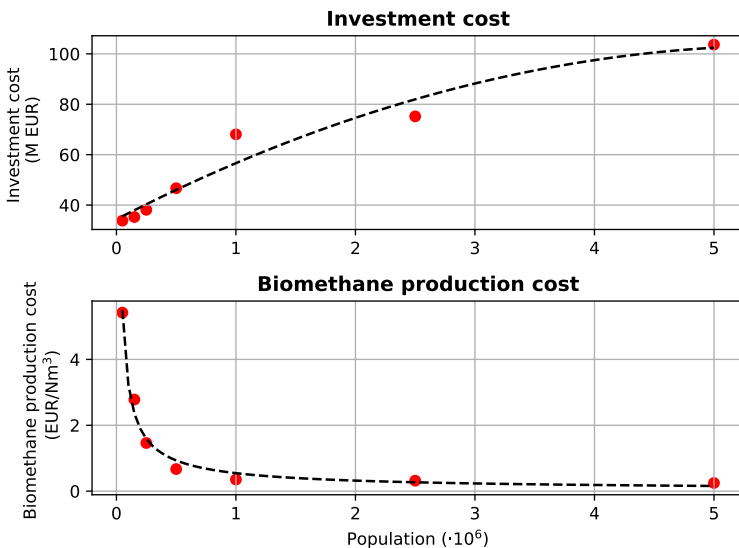


Figure 8.5: Scale-up in the investment costs for municipal food waste.

based on literature data is used to narrow the search. Next, a mathematical optimization approach is used to compare the most promising technologies and determine their operating conditions from an economic point of view. The framework is flexible to include more alternatives and compare novel technologies for different wastes, but relies on the prediction capacity of the models. The study evaluated swine and cattle manure, food solid waste and sludge.

The heuristic screening suggests the use of amine scrubbing, PSA adsorption, and membrane separation systems. Within each one of them, different configurations are evaluated, focusing on the study of different amines, including MEA, DEA, and MDEA, different membranes, including polycarbonate, polyimide, and cellulose acetate, and two types of zeolites for PSA systems, 13X and 4A. The selection of the best configuration for each technology is carried out formulating and solving an optimization problem for each technology. DEA, zeolite 13X and polyimide are the alternative selected. Next, a superstructure is formulated as an optimization problem for the processing of food waste, cattle manure, swine manure, and sludge, assessing the upgrading technologies for the production of high purity biomethane. The optimal technology for CO₂ capture for all residues studied is PSA systems with zeolite 13X as adsorbent material, although the use of membranes is just slightly more expensive. A detailed economic evaluation is performed for the entire biomethane production plant, yielding the production and investment costs for the production of biomethane. Food waste is the most promising waste due to the largest organic matter,

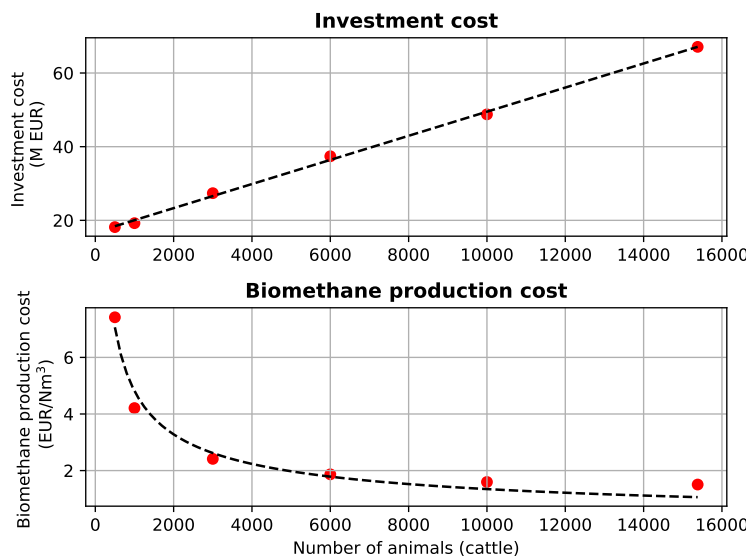


Figure 8.6: Scale-up in the investment costs for cattle manure.

resulting in an investment cost of 67 M EUR and a production cost of 0.36 EUR/Nm³ for the processing of 10 kg/s of waste. Finally, the upgrading of biogas using CO₂ capture is compared to direct CO₂ hydrogenation and direct production of synthetic methane. The comparison is in favour of the direct hydrogenation of CO₂, although this result is highly dependent on the availability of solar or wind energy. For low availabilities of these resources, biomethane production through CO₂ capture is suggested.

This framework is of general use of the systematic evaluation of technologies and can be extended for comparison of newly developed materials and technologies as well as the evaluation of different wastes. Life cycle assessment (LCA) can be added for a multiobjective kind of optimization beyond the production cost aiming at the most sustainable production of biomethane.

NOMENCLATURE

Variables

A	Antoine equation coefficient
$A_{membrane}$	Area of membrane (m ²)
B	Antoine equation coefficient
$BioCH_4$	Biomethane produced benefit (EUR/year)
C	Antoine equation coefficient

$CO_{2_{eff}}$	Removal efficiency of CO ₂
C_i	Cost of element i (EUR/unit or EUR/year)
D_c	Diameter of the amine contactor (in)
D_r	Diameter of the regeneration column (in)
F	Total flow (kmol/s)
F_{amine}	Flow of amine (gal/min)
F_{gas}	Flow of gas (MMscfd)
$GPSA$	Correction factor
I	Investment cost (M EUR)
J_i	Flux of component i (kmol/m ² s)
K	Coefficient in Langmuir correlation
L_f	Membranes cycles for costing purposes
MW_i	Molecular weight of component i (kg/kmol)
NPK	Mass ratio of nitrogen, phosphorus and potassium
PC	Production costs (EUR/Nm ³)
P_i	Vapor pressure of component i (mmHg)
P_{unit}	Pressure at $unit$ (mmHg)
$Perm_i$	Permeability of component i (kmol/(kPa·m))
$Profit$	Profit (EUR/year)
Q_{unit}	Thermal energy involved in $unit$ (kW)
R	Universal gas constant, (kJ/kmol·K)
R_{CN}	Mass carbon to nitrogen ratio
T_{unit}	Operating temperature at unit (K)
V_{biogas}	Biogas produced per mass unit of waste (m ³ /kg)
WF	Waste flow (kg/s)
W_{unit}	Electrical energy of $unit$ (kW)
Y	Specific humidity
ΔH_{reac}	Heat of reaction (kJ/kg)
δ	Membrane thickness
ϵ_i	Permeance of component i (kmol/(kPa·m ²))
η	CO ₂ removal yield for the PSA system
η_c	Compressor efficiency
λ_i	Vaporization latent heat of specie i (kJ/kg)
τ	Cycle time at the PSA (s)

τ_{year}	Annual time operation (s)
fc_i	Flow of component i (kg/s)
$m_{zeolites}$	Amount of zeolites (kg)
q	Adsorption capacity (mol/g)
q_m	Maximum adsorption capacity (mol/g)
$q_{unit,amine}$	Experimental value of the thermal energy consumed in amine processing <i>unit</i> ((BTU/h)/(gal/min))
w_C	Carbon (% dry wt)
w_{DM}	Dry matter (% wt)
w_K	Potassium (% dry wt)
$w_{N_{org}}$	Organic nitrogen (% dry wt)
w_N	Inorganic nitrogen (% dry wt)
w_P	Phosphorous (% dry wt)
w_{VS}	Volatile matter (% dry wt)
y_i	Molar fraction of component i
z	Polytropic coefficient

Units

CD	Condensation vessel
Col	Column
Compress	Compressor
Cond	Condenser
Feed	Distillation column feed
HX	Heat exchanger
MEM	Membrane
Mix	Mixer
MS	Molecular sieve
Reb	Reboiler
Sep	Decanter
Src	Source

Subscripts

Amine	Amine adsorption system
Electricity	Electricity

Membrane	Membrane system
PSA	PSA system
Sat	Saturated

Acronyms

CAFO	Concentrated animal feeding operation
DEA	Diethanolamine
MDEA	Methyl diethanolamine
MEA	Monoethanolamine
NLP	Non-linear programming
PSA	Pressure swing adsorption

ACKNOWLEDGMENTS

Authors thank funding from Junta de Castilla y León, Spain, under grant SA026G18 and grant EDU/556/2019, and PSEM3 research group for software licenses.

BIBLIOGRAPHY

CONTRIBUTIONS AND FUTURE DIRECTIONS

9.1 CONTRIBUTIONS

The key contribution of this work is the assessment of waste treatment processes and management strategies for the effective recovery of nutrients (i.e., phosphorus and nitrogen) at livestock facilities in order to abate their nutrient releases and mitigate the impact of this industry in the nutrient pollution of waterbodies. Therefore, we seek to promote the transition to a more sustainable paradigm for food production with this work. In this context, the following specific contributions can be drawn:

- 1. Techno-economic assessment of phosphorus and nitrogen recovery technologies for livestock facilities.** In Chapter 3, the different processes for phosphorus and nitrogen recovery at livestock facilities have been systematically evaluated and compared by means of techno-economic assessment. The recovery of phosphorus by struvite precipitation emerges as one of the most cost-effective processes due to the high value of the product recovered. This study is extended in Chapter 5 by assessing the available commercial technologies for struvite production. From an economic perspective, Multiform is the most suitable technology for CAFOs with sizes up to 5,000 animal units, NuReSys can be selected for CAFOs with a size between 2,000 and 5,000 animal units, and Crystalactor is the optimal technology for CAFOs larger than 5,000 animal units. For the case of nitrogen recovery, transmembrane chemisorption is revealed as the most cost-effective nitrogen recovery technology in a multi-scale techno-economic assessment of nitrogen recovery processes performed in Chapter 7.
- 2. Geospatial evaluation of phosphorus recovery at livestock facilities.** Since struvite precipitation is revealed as one of the most promising alternatives for phosphorus recovery at CAFOs, in Chapter 4 we perform a study to determine the impact of phosphorus recovery in the watersheds of the contiguous United States by deploying commercial struvite production systems in the livestock facilities of this region. Since livestock leachate presents some characteristics that hinder struvite precipitation (such as the presence of significant

amounts of calcium), a tailored thermodynamic model for precipitates formation from cattle waste is used to develop surrogate models for predicting the formation of struvite and calcium precipitates from cattle waste. In addition, the variability in the composition of manure is captured through a probability framework based on the Monte Carlo method embedded in the thermodynamic model. The results show that, from a thermodynamic perspective, phosphate recovery efficiencies up to 80% can be achieved. Therefore, struvite production has large potential for reducing the phosphorus losses from livestock facilities. Considering only struvite formation from intensive cattle operations, reductions between 22% and 36% of the total phosphorus releases from the agricultural sector (including the releases from farming activities and fertilizer application) in the contiguous United States can be achieved.

- 3. Development of a decision-making support tool for the implementation of phosphorus recovery system at CAFOs.** In Chapter 5, we present a decision-making support tool called COW2NUTRIENT (Cattle Organic Waste to NUTRIent and ENergy Technologies) for the selection of the most suitable phosphorus recovery system for each CAFOs under evaluation. Environmental and techno-economical criteria are combined in a multi-criteria decision analysis (MCDA) model to aid in the process selection. The environmental vulnerability to nutrient pollution is determined through a geographic information system (GIS)-based model at subbasin level, whereas economic information of each phosphorus recovery technology is obtained from their techno-economic assessment. As a result, a flexible framework able to balance the phosphorus recovery cost and recovery efficiency as a function of the environmental vulnerability to eutrophication of each region is obtained. As a result, the minimization of operating costs is prioritized in regions with low eutrophication risk, while the efficiency of P recovery is the most relevant criteria in regions affected by nutrient pollution.
- 4. Design and assessment of incentive policies for the implementation of phosphorus recovery technologies at CAFOs, including the fair allocation of monetary resources in limited-budget scenarios.** In Chapter 6, the COW2NUTRIENT framework is used to design and analyze incentive policies to promote the deployment of phosphorus recovery systems at CAFOs. Since P recovery systems can be implemented either as standalone systems or integrated with biogas production and upgrading processes, the combination of incentives for the recovery of both phosphorus and electricity has also been

considered. The results reveal that phosphorus recovery is more economically viable in the largest CAFOs due to economies of scale, although they also represent the largest eutrophication threats. For small and medium-scale CAFOs, the implementation of phosphorus credits progressively improve the profitability of nutrient management systems. The integration of biogas production does not improve the economic performance of phosphorus recovery systems at most of CAFOs, as they lack enough size to be cost-effective. However, we note that phosphorus recovery proves to be economically beneficial by comparing the total phosphorus recovery costs with the negative economic impact derived from phosphorus releases. Additionally, the fair distribution of incentives in limited budget scenarios is studied using a Nash allocation scheme, determining the break-even point for allocating monetary resources based on the availability of incentives. This information can be used to raise the debate on which stakeholders and by how much should cover the cost of phosphorus recovery from the livestock industry; and from a broader perspective, the cost of environmental remediation derived from the different environmental impacts caused by this sector.

5. **Potential integration of biogas production and nutrient recovery processes.** In Chapter 8, a systematic study of different processes for biogas upgrading to biomethane is performed to identify the optimal upgrading technology considering the particular characteristics of the biogas produced from livestock manure. A mathematical optimization approach is used to compare the technologies under evaluation using a non-linear programming (NLP) model. Pressure swing adsorption emerges as the most cost-effective technology for producing biomethane from raw biogas. Moreover, in Chapter 6 the integration of biogas production and phosphorus recovery processes in real CAFOs is studied. The results show that the combination of phosphorus recovery technologies with anaerobic digestion and biogas upgrading processes does not result in any practical improvement in terms of economic performance unless incentives for phosphorus recovery are considered, since the revenues from electricity sales can not cover the investment and operating cost of these processes given current market values.

9.2 DIRECTIONS FOR FUTURE WORK

Multiple directions for future research can be established to achieve effective nutrient management practices and to restore nutrient circularity. Some future lines of work are drawn below:

- 1. Assessment, routing, and scheduling of modular nutrient recovery systems for the treatment of organic waste in distributed networks.** In Chapter 6, the results show that the economies of scale play a major role in the feasibility of phosphorus recovery at CAFOs by using on-site processes. The development of modular and transportable processes allow the use of a single system for the processing of the waste generated in multiple livestock facilities. However, further research in the economic viability of these systems, as well as their optimal routing and scheduling, is needed.
- 2. Nutrient redistribution to nutrient deficient regions.** Intensive livestock operations result in the release of large amounts of nutrients in a particular location. In this work, the study of phosphorus and nitrogen recovery in the form of products with high nutrients density has been addressed. However, further studies regarding the feasibility of transporting this products to nutrient deficient regions must be addressed. In this regard, it would be particularly interesting to determine the maximum economically viable distances for the transportation of nutrient products.
- 3. Assessment of the economic impact derived from the variability of the phosphorus-based commercial materials prices in nutrient recovery.** Since phosphorus is a limited, non-renewable material, prices of phosphorus-based commercial materials can be expected to increase in the mid to long term. Further economic studies could determine the impact of rising phosphorus fertilizer prices on the food production system, and how the phosphorus recovered from organic waste may mitigate this impact.
- 4. Optimal funding schemes for phosphorus recovery incentives.** In this work, we have evaluated different incentive policies to promote the installation of phosphorus recovery processes. However, further economic studies are needed to determine the funding sources for these incentives. For instance, if the budget for these incentives is provided by national or regional administrations, taxpayers are the ultimate funders of these incentives. As a result, the environmental impact is covered by all citizens, whether or not they benefit from

such businesses. This approach is particularly unfair for those tax-payers unrelated with the livestock industry. On the other hand, the implementation of specific taxes to livestock products could result in the raise of swine products cost, impacting the final consumers. This approach might seem fairer, since it only involves producers and consumers of livestock products. However, it would lead to comparative disadvantages between different farms as a result of the savings in nitrogen recovery costs due to the economies of scale. Additionally, they can lead to the rise of the livestock product prices, discouraging consumers demand, business profitability, and outsourcing. Therefore, rigorous economic studies are needed in order to determine a fair and resource-efficient funding scheme for nutrient recovery incentives.

Part IV
APPENDIX

A

APPENDIX A: SUPPLEMENTARY INFORMATION OF CHAPTER 3

All the units involved in the flowsheet are modeled using mass and energy balances, thermodynamic relationships, chemical and vapor-liquid equilibria, and product yield calculations. Therefore, the variables of the equation oriented framework comprise the total mass flows, component mass flows, component mass fractions, temperatures and pressures of the streams in the process network. The components that are tracked in our calculations belong to the following set:

{Wa, CO₂, CO, O₂, N₂, H₂S, NH₃, CH₄, SO₂, C, H, O, N, N_{org}, P, K, S, Rest, Cattle slurry, Pig slurry, Poultry slurry, P₂O₅, CaCO₃, FeCl₃, Antifoam, Fe₂(SO₄)₃, Al₂(SO₄)₃, AlCl₃, MgCl₂, NaOH, Struvite seeds, Mg, Cl, Struvite, K-Struvite, MgCl₂ CSTR, NaOH CSTR, Mg CSTR, Cl CSTR, Struvite CSTR, KStruvite CSTR, FeCl₃ Coag}

In the following subsections we briefly present the main equations used to characterize the operation of the different units. Simpler balances based on removal efficiency or stoichiometry, or the equations that connect two units are omitted and only the conversion, the chemical reactions, and the removal efficiency are presented.

The decision on the technology to use to process the digestate requires the evaluation of the cost. Its estimation uses the factorial method based on the equipment units costs **rk1999coulson**. The total physical plant cost involving equipment erection, piping instrumentation, electrical, buildings, utilities, storages, site development, and ancillary buildings is 3.15 times the total equipment cost for processes which uses fluids and solids. On the other hand, the fixed cost, which includes design and engineering, contractor's fee, and contingency items is determined as 1.4 times the total physical plant cost for fluid and solid processes. In the subsequent cost estimation, these parameters are designed as f_i for the total physical plant parameter and f_j for the fixed cost parameter.

A.1 BIOGAS PRODUCTION

The anaerobic fermentation of different types of manure generates biogas, methane and carbon dioxide, through a series of reactions such as hydrolysis, acidogenesis, acetogenesis and methanogenesis (AlSeadi2008). The biogas produced shows a variable composition in methane and CO₂ depending on the composition of the manure processed and the operating conditions. The lower the temperature, the longer the retention time. We operate at 55 °C for 20 days. A part from methane and CO₂, nitrogen, H₂S, and NH₃ are produced (kaparaju2013generation). Thus, in order to compute the biogas composition a mass balance is performed considering the composition of the different manure sources:

$$MW_{dry\text{-}biogas} = \sum_{a'} Y_{a'/biogas-dry} \cdot MW_{a'} \quad (\text{A.1})$$

where the typical composition, Y_i , of the biogas is given by the following bounds:

$$\begin{aligned} 0.7 &\leq Y_{CH_4} \leq 0.5 \\ 0.3 &\leq Y_{CO_2} \leq 0.5 \\ 0.02 &\leq Y_{N_2} \leq 0.06 \\ 0.005 &\leq Y_{O_2} \leq 0.16 \\ Y_{H_2S} &\leq 0.002 \\ 9 \cdot 10^{-5} &\leq Y_{NH_3} \leq 1 \cdot 10^{-4} \end{aligned} \quad (\text{A.2})$$

The contact between biogas and the liquid residue results in biogas saturated with water. Gas moisture is computed using Antoine correlation as per Eq. A.3. The flow of dry biogas is determined using Eq A.4. To compute the power in the compressor, we need to determine the molar mass of the biogas as in Eq. A.5. The mass flow rate of each component is computed from its molecular weight and the total mass flow rate, Eqs. A.6-A.7.

$$y_{biogas} = \frac{MW_{H_2O}}{MW_{biogas-dry}} \frac{Pv(T)}{P - Pv(T)} \quad (\text{A.3})$$

$$F_{biogas} = \rho_{biogas} \sum_{Waste} w'_{SV/Waste} \cdot w_{MS/Waste} \cdot F_{Waste} \cdot V_{biogas/Waste} \quad (\text{A.4})$$

$$fc_{H_2O}^{biogas} = y_{biogas} \cdot \sum_{a'} fc_{a'}^{biogas} \quad (\text{A.5})$$

$$\frac{fc_{a'}^{Bioreactor, Compress1}}{MW_{a'}} = \frac{Y_{a'/biogas-dry}}{MW_{biogas-dry}} \left(F^{Bioreactor, Compress1} - fc_{H_2O}^{Bioreactor, Compress1} \right) \quad (\text{A.6})$$

$$MW_{biogas} \sum_a \frac{x_{a/biogas}}{MW_a} = \sum_a x_{a/biogas} \quad (\text{A.7})$$

The lower and upper limits for the generation of biogas are given by Eq. A.8 (**AlSeadi2008**):

$$\begin{aligned} 0.20 &\leq V_{biogas/Waste} \leq 0.50 \\ 0.10 &\leq w_{MS/Waste} \leq 0.20 \\ 0.50 &\leq w_{VS/Waste} \leq 0.80 \end{aligned} \quad (\text{A.8})$$

The mass of waste that does not leave as biogas constitutes the digestate as follows (**AlSeadi2008**):

$$w'_{C/k} = R_{C-N/k} \left(w'_{N_{org}/k} + w'_{N_{NH_3}/k} \right) \quad (\text{A.9})$$

Each manure type has its own composition (**DEFRA**).

$$\begin{aligned} 6 &\leq R_{C-N/Waste} \leq 20 \\ 0.005 &\leq w_{N/Waste} \leq 0.047 \\ 0.005 &\leq w_{N_{org}/Waste} \leq 0.036 \\ 0.008 &\leq w_{P/Waste} \leq 0.013 \\ 0.033 &\leq w_{K/Waste} \leq 0.1 \end{aligned} \quad (\text{A.10})$$

$$\begin{aligned} w_{C/Waste} + w_{N_{org}/Waste} + w_{N_{NH_3}/Waste} + w_{P/Waste} + \\ w_{K/Waste} + w_{Rest/Waste} = 1 \end{aligned} \quad (\text{A.11})$$

Atom mass balances are performed to compute the products of the reactors. We consider balances for carbon, organic nitrogen (N_{org}), inorganic

nitrogen (N), phosphate and potassium. The carbon either leaves in the form of CO_2 or CH_4 with the gas or as part of the waste in the digestate, Eq. A.12. The organic nitrogen in the digestate is given by the fraction of organic nitrogen in the digestate minus the nitrogen released as gas, Eq A.13. Similarly, the inorganic nitrogen that is not used to produce ammonia that accompanies the gas or is left as residue is computed using the values above, Eq. A.14. P and K directly leave the reactor as part of the digestate, Eqs. A.15-A.16. The rest that is not accounted for is assumed to be a residual part leaving the reactor with the digestate.

$$fc_C^{digestate} = w'_C \cdot w_{MS} \cdot F_{Waste} - fc_{\text{CH}_4} \frac{MW_C}{MW_{\text{CH}_4}} - fc_{\text{CO}_2} \frac{MW_C}{MW_{\text{CO}_2}} \quad (\text{A.12})$$

$$fc_{N_{\text{org}}}^{digestate} = w'_{N_{\text{org}}/\text{Waste}} \cdot w_{MS/\text{Waste}} \cdot F_{Waste} - fc_{\text{N}_2} \frac{MW_N}{MW_{\text{N}_2}} \quad (\text{A.13})$$

$$fc_N^{digestate} = w'_{N/\text{Waste}} \cdot w_{MS/\text{Waste}} \cdot F_{Waste} - fc_{\text{NH}_3} \frac{MW_N}{MW_{\text{NH}_3}} \quad (\text{A.14})$$

$$fc_P^{digestate} = w'_{P/\text{Waste}} \cdot w_{MS/\text{Waste}} \cdot F_{Waste} \quad (\text{A.15})$$

$$fc_K^{digestate} = w'_{K/\text{Waste}} \cdot w_{MS/\text{Waste}} \cdot F_{Waste} \quad (\text{A.16})$$

$$\begin{aligned} fc_{\text{Rest}}^{digestate} &= w'_{\text{Rest}/\text{Waste}} \cdot w_{MS/\text{Waste}} \cdot F_{Waste} + \\ &fc_{\text{CH}_4}^{\text{biogas}} \cdot \frac{4 \cdot MW_H}{MW_{\text{CH}_4}} - fc_{\text{CO}_2}^{\text{biogas}} \cdot \frac{2 \cdot MW_O}{MW_{\text{CO}_2}} - \\ &fc_{\text{NH}_3}^{\text{biogas}} \cdot \frac{3 \cdot MW_H}{MW_{\text{NH}_3}} - fc_{\text{H}_2\text{S}}^{\text{biogas}} - fc_{\text{O}_2}^{\text{biogas}} \end{aligned} \quad (\text{A.17})$$

$$fc_{\text{H}_2\text{O}}^{digestate} = (1 - w_{MS/\text{Waste}}) \cdot F_{Waste} - fc_{\text{H}_2\text{O}}^{\text{biogas}} \quad (\text{A.18})$$

The energy balance to the digester is as follows:

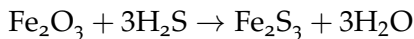
$$Q_{\text{digester}} = \Delta H_{\text{reaction}} - F \cdot c_p \cdot (T_{\text{digester}} - T_{in}) \quad (\text{A.19})$$

$$\Delta H_{\text{reaction}} = \sum_{\text{products}} \Delta H_{\text{comb}} - \sum_{\text{reactants}} \Delta H_{\text{comb}}$$

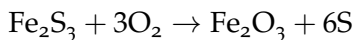
The digestate is further conditioned.

A.2 H₂S REMOVAL

Since biogas is burned for power production, any sulfur compound would potentially produce SO₂. We can avoid it by removing the H₂S. A reactive bed of Fe₂O₃ that operates at 25-50 °C is used. The actual removal is carried out following the chemical reaction below ([ryckebosch2011techniques](#)).



Thus, the model of this unit is based on a mass balance based on the stoichiometry of the reaction assuming 100% conversion. The bed can be regenerated using oxygen ([ryckebosch2011techniques](#)).



A.3 CO₂, NH₃ AND H₂O REMOVAL (PSA)

The flue gas from the gas turbine is to be used as heat source to produce steam for the steam turbine. Therefore, it is interesting that the stream has high temperature. CO₂ is removed from biogas using a packed bed of zeolite 5A operating at 25 °C and 4.5 bar. To secure continuous operation, two adsorbent beds operate in parallel so that while one is in adsorbent mode, the second one is under regeneration. We assume a recovery of 100% for NH₃ and H₂O (because of their low total quantities in the biogas, in general), 95% for CO₂ and 0% for any other gas of the mixture ([russell2004gpsa](#); [Nexant2006](#)).

A.4 BRAYTON CYCLE

The process consists of a three stage polytropic compressor with intercooling. Each compressor is modelled assuming polytropic behavior using Eqs. [A.20](#) - [A.21](#) to compute the exit temperature and the power required for each stage. After each compression stage, intercooling is used to reduce the power input. The polytropic coefficient, *k*, is taken to be 1.4 based on an offline simulation using CHEMCAD®. The efficiency of the compressor is assumed to be 85% ([Moran2003](#)). A maximum compression ratio of 40 for air is used, based on typical achievements ([Jane1997](#)). The intercooling stage is modeled as simple energy balance to compute the cooling required to cool down the gas to the initial temperature of the previous compressor.

$$T_{out/compressor} = \quad \quad \quad (A.20)$$

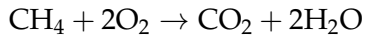
$$T_{in/compressor} + T_{in/compressor} \left(\left(\frac{P_{out/compressor}}{P_{in/compressor}} \right)^{\frac{z-1}{z}} - 1 \right) \frac{1}{\eta_c}$$

Eq21

$$W_{compressor} = \quad \quad \quad (A.21)$$

$$(F) \cdot \frac{R \cdot z \cdot (T_{in/compressor})}{((MW) \cdot (z - 1))} \frac{1}{\eta_c} \left(\left(\frac{P_{out/compressor}}{P_{in/compressor}} \right)^{\frac{z-1}{z}} - 1 \right)$$

The combustion of the biogas, see reactions below, heats up the mixture. We use an excess of 20% of air with respect to the stoichiometry and assume 100% conversion of the reaction.



The material balance is based on the stoichiometry of the chemical reaction stated above and an energy balance is used to compute temperature of the gases exiting the gas turbine as given by Eq. A.22:

$$Q_{Furnace} = \sum_h \Delta H_{f,h}^{Furnace, GasTurb}(T) - \quad \quad \quad (A.22)$$

$$\sum_h \Delta H_{f,h}^{Compres2,Furnace}(T) - \sum_h \Delta H_{f,h}^{Compres3,Furnace}(T)$$

The hot flue gas is expanded in the gas turbine to generate power. Eq. A.21 is used to model the performance of the gas turbine. The polytropic coefficient is taken to be 1.3, also based on an offline simulation using CHEMCAD ®, with an efficiency of 85% (Moran2003). Finally, the exhaust gas is cooled down and used to generate high pressure steam to be fed to the Rankine cycle.

A.5 RANKINE CYCLE

The steam is generated in a system of heat exchangers. Two alternatives are evaluated:

1. Only a fraction of the flue gas from the gas turbine is used to produce the high pressure steam fed to the steam turbine. The rest of the gas is used for the regeneration step.

2. The entire flue gas is used to heat up the saturated steam before feeding it to the high pressure turbine. Next, it is used to reheat the expanded steam before feeding it to the medium pressure turbine.

In the second body of the turbine, part of the steam is extracted at a medium pressure and it is used to heat up the condensate. The rest of the steam is finally expanded to an exhaust pressure, condensed and recycled. The flue gas is used for heating up and evaporating this stream. Due to the size of the plants and their typical location, a farm, it is expected that a lagoon is used to condensate the working fluid. Each unit is modeled using mass and energy balances as well as thermodynamic properties ([martin2013optimal](#); [vidal2015optimal](#)).

The enthalpy and entropy of steam as a function of the temperature and pressure are correlated as in previous work ([martin2013optimal](#); [vidal2015optimal](#)). The equations can be found in the appendix below. Therefore, the stream exiting the first body can be calculated using Eqs. A.23-A.28, assuming an isentropic efficiency, η_s , of 0.9.

$$\eta_s = \frac{H_{steam}^{Turb1,HX5} - H_{steam,HX4,Turb1}}{H_{steam,isoentropy} - H_{steam}^{HX4,Turb1}} \quad (\text{A.23})$$

where:

$$H_{steam,isoentropy} = f(p_{Turb1,HX5}, T^*_{Turb1,HX5}) \quad (\text{A.24})$$

T^* represents the isentropic temperature after the expansion computed as follows:

$$s_{steam}^{HX4,Turb1} = \\ f(p_{HX4,Turb1}, T_{HX4,Turb1}) = f(p_{Turb1,HX5}, T^*_{Turb1,HX5}) \quad (\text{A.25})$$

We make sure that the output of the turbine is superheated steam by maintaining its temperature above the one that corresponds to saturation for the pressure of the stream.

$$p_{turb,2} \cdot 760 = e^{\left(A_{H_2O} - \frac{B_{H_2O}}{(C_{H_2O} \cdot T_{turb,1,min})} \right)} \quad (\text{A.26})$$

$$T_{Turb,1,HX5} > T_{turb,1,min} \quad (\text{A.27})$$

The energy that is obtained in the steam expansion in the first turbine is given by Eq. A.28:

$$W_{Turbine1} = fc_{H2O}^{HX4,Turb1} \cdot (H_{steam}^{HX4,Turb1} - H_{steam}^{Turb1,HX5}) \quad (\text{A.28})$$

The stream, as superheated vapor, is heated up again in HX5 using a fraction of the exhaust gas from the gas turbine, Eq. A.29, or the entire flow depending on the flowsheet configuration, Eq. A.30. Next, the superheated steam is fed to a second turbine. HX5 is modeled using Eq. A.29-A.31.

$$Q_{HX5} = fc_{H2O}^{Turb1,HX5} \cdot (H_{steam}^{HX5,Turb2} - H_{steam}^{Turb1,HX5}) \quad (\text{A.29})$$

$$Q_{HX5} = -F_{Sp1,HX5}^{Spl1,HX5} \cdot \int_{T_{Sp1,HX5}}^{T_{HX5,Mix1}} Cp_{sat} dT \quad (\text{A.30})$$

$$Q_{HX5} = -F_{HX4,HX5}^{HX4,HX5} \cdot \int_{T_{(HX4,HX5)}}^{T_{HX5,Mix1}} Cp_{sat} dT \quad (\text{A.31})$$

In the second turbine there is another expansion to a lower pressure. Part of the stream will be sent to HX7, while the rest is used in the third body of the turbine, where it is expanded to a pressure below atmosphere, see Eq. A.32; this pressure ranges from 0.05 bar to 0.31 bar in the literature ([vidal2015optimal](#)). The second and third bodies of the turbine are calculated similarly to the first one, assuming 0.9 isentropic efficiency in all stages.

$$fc_{H2O}^{HX5,Turb2} = fc_{H2O}^{Turb2,HX7} + fc_{H2O}^{Turb2,Turb3} \quad (\text{A.32})$$

The stream extracted from the medium pressure turbine is sent to HX7, where it will be used to reheat the liquid obtained after condensing the exhaust of the third body of the turbine. The exhaust of the low pressure turbine is assumed to be saturated vapor. This stream is condensed in HX6:

$$Q_{(HX6)} = fc_{H2O}^{Turb3,HX6} \cdot (H_{liq}^{HX6,HX7} - H_{steam}^{Turb3,HX6}) \quad (\text{A.33})$$

This energy must be removed in the cooling system. We assume that a lagoon is used to cool down the water used to condense the saturated steam before reuse. This part is not included in the model. When mixing the exhaust of the second turbine with the compressed liquid from HX6, we must bear in mind that the outlet should be liquid since it is going to be compressed and heated up as a liquid in HX8. Eq. A.34 ensures this fact:

$$T_{HX7,HX8} \leq T_{turb,2,min} \quad (\text{A.34})$$

BIBLIOGRAPHY

B

APPENDIX B: SUPPLEMENTARY INFORMATION OF CHAPTER 4

B.1 CATTLE ORGANIC WASTE COMPOSITION

To calculate the distribution functions of the different compounds of the cattle organic waste, 37 data sets for cattle organic waste compositions from 20 bibliographic references were evaluated. Table B.1 collects the main statistical parameters of the data, and Table B.2 shown the data obtained from literature.

B.2 DISTRIBUTION FUNCTIONS OF ELEMENTS FROM CATTLE WASTE

The kernel density estimation (KDE) method is used to fit the probability function to data distribution and to determine the probability density distributions of calcium, nitrogen, phosphorus, potassium, ammonia/total nitrogen, and phosphate/total phosphorus. As histograms, KDE is a non-parametric way to estimate the probability density function of a random variable. However, in the KDE method, kernels are functions associated with each data set. Thus, the unknown density function can be computed as the weighted sum of these functions (**Duong**).

The calculation procedure is divided into three steps. First, cattle organic waste composition data are collected from the literature. Second, the KDEs of all compounds are estimated, and finally, distribution functions are fitted, using the kernel density estimations to validate the chosen distribution. The probability density distributions which best fit the data distribution are normal distribution functions for the distribution of nitrogen as in Figure B.1a, ammonia/total nitrogen molar ratio as observed in Figure B.1b, and phosphorus as shown in Figure B.1c. Lognormal distribution functions are the best fit for phosphate/total phosphorus molar ratio as in Figure B.1d, calcium, as shown in Figure B.1e, and potassium as observed in Figure B.1f.

Table B.1: Statistical summary of cattle organic waste composition. Data from (Albuquerque; Bolzonella; Seppala; Gell; Normak; Sorensen; Tampere; Moset; Zheng; Xia; Moller; WRAP; ADAS; Risberg; Ledda; Kirchmann; Mollerz; Walsh; Loes; Martinz).

	DM (% mass)	C (% mass)	Ca (% mass)	K (% mass)	N (% mass)	P (% mass)	$\frac{\text{Ca}^{2+}}{\text{Total Ca}}$	$\frac{\text{K}^+}{\text{Total K}}$	$\frac{\text{N-NH}_4^+}{\text{Total N}}$	$\frac{\text{P-PO}_4^{3-}}{\text{Total P}}$
count	36	6	9	12	35	24	1	1	31	13
mean	5.858	2.478	0.117	0.253	0.384	0.059	0.154	1.000	0.590	0.541
std	1.778	0.946	0.027	0.158	0.133	0.038	NaN	NaN	0.117	0.159
min	2.624	1.200	0.080	0.084	0.114	0.005	0.154	1.000	0.348	0.216
25.00%	4.610	1.719	0.100	0.148	0.299	0.032	0.154	1.000	0.516	0.421
50.00%	5.668	2.788	0.110	0.223	0.399	0.048	0.154	1.000	0.616	0.597
75.00%	7.362	3.194	0.129	0.276	0.449	0.080	0.154	1.000	0.666	0.671
max	9.200	3.400	0.165	0.635	0.789	0.164	0.154	1.000	0.820	0.700

Table B.2: Data obtained from literature.

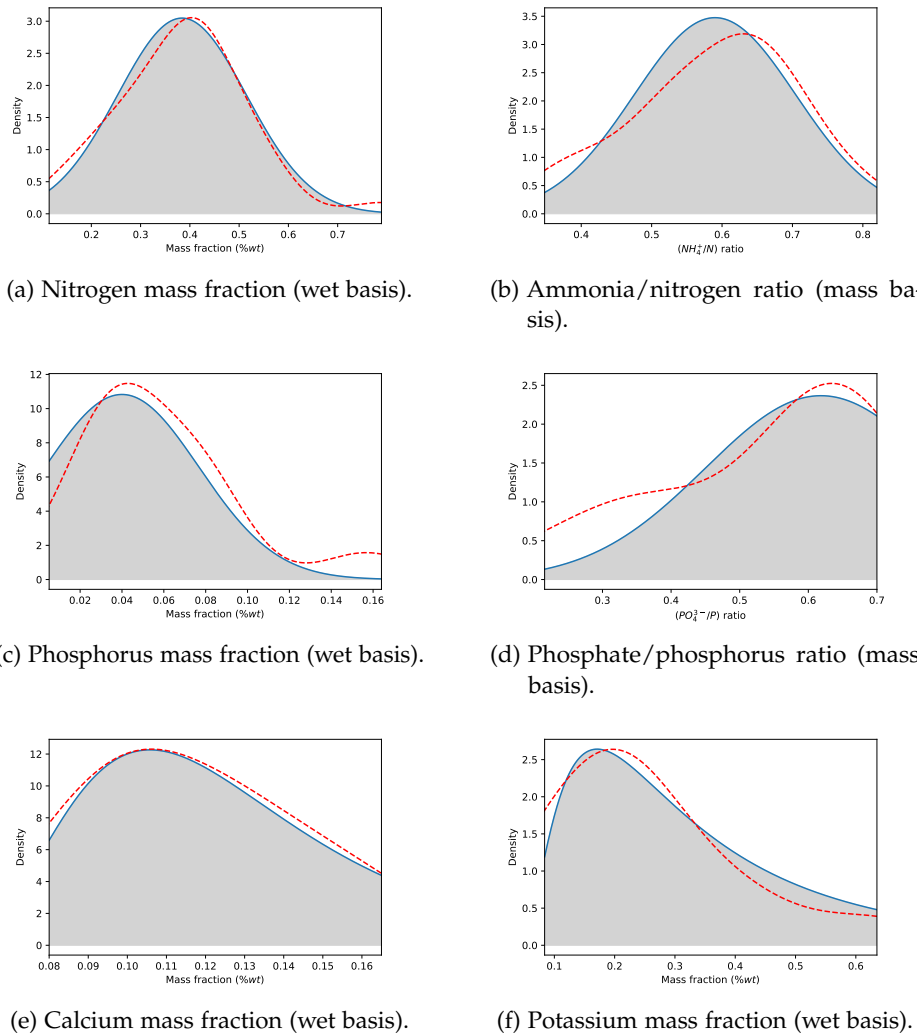


Figure B.1: Kernel density estimation (red dashed line) and probability density distribution (blue solid line) for the evaluated components in cattle organic waste.

B.3 THERMODYNAMIC MODELING OF THE CARBONATES SYSTEM

To calculate the total carbonate content, the concept of defining alkalinity will be used. The formal definition of total alkalinity is the capacity of a solution to buffer changes in pH that would make the solution more acidic. From the perspective of charge balance, total alkalinity can be considered as a measure of the number of protons that can be accepted by the proton acceptors present in the dissolution. Therefore, total alkalinity, TA , is calculated as the excess of proton acceptors over donors with respect to a chosen zero level of protons, as in Eq. B.1:

$$TA = \text{proton acceptors} - \text{proton donors} \quad (\text{B.1})$$

Note that the distribution of different species for various systems, such as carbonic acid and phosphoric acid, depend on pH, and the contribution of each species to alkalinity, is a function of its electrical charge. For our case, the chemical systems considered are water, carbonic acid, phosphoric acid, and ammonia systems

A zero level of protons is a reference system defined by choosing a certain chemical compound for each system at a certain pH selected arbitrarily. This reference chemical is the dominant species at the selected pH. The chemical species above this zero level of protons will be proton acceptors while species below this level will be proton donors in a determined chemical system. There is a standard defined by **Dickson**, where the reference pH value is set to 4.5 and chosen as the zero level of protons. For a more detailed discussion about alkalinity, we refer to **WolfGladrow**. The dominant chemical substances for each system at the reference pH of 4.5 are H_2O , H_2CO_3 , $H_2PO_4^-$ and NH_4^+ . With these considerations, the proton donors and acceptors for each system are collected in Table B.3:

Table B.3: Proton donors and acceptors for each chemical system.

Chemical system	Proton donors	Proton acceptors
Water	$\{H^+\}$	$\{OH^-\}$
Carbonic acid	$\{H^+\}$	$\{HCO_3^-\}$, $2 \cdot \{CO_3^{2-}\}$
Phosphoric acid	$\{H_3PO_4\}$, $\{H^+\}$	$\{HPO_4^{2-}\}$, $2 \cdot \{PO_4^{3-}\}$
Ammonia system	$\{H^+\}$	$\{NH_3\}$

Therefore, the alkalinity due to carbonates, called carbonate alkalinity (Alk_{carb}), as described in Eq. B.2, can be calculated from total alkalinity value minus the alkalinity contribution of the other compounds, Eq. B.4. The activities of the chemical species from water, phosphoric acid, and am-

monia systems are obtained by solving the equilibrium and mass balance equations described previously.

The formulation of the alkalinity problem is described next. First, the alkalinity given in milligrams of CaCO_3 per liter is transformed into equivalents per liter by Eq. B.3 and the carbonate alkalinity is calculated through Eq. B.4.

$$\text{Alk}_{\text{carb}} = \{\text{HCO}_3^-\} + 2\{\text{CO}_3^{2-}\} \quad (\text{B.2})$$

$$\text{Alk} \left(\frac{\text{Eq}}{\text{L}} \right) = \frac{\text{mg}_{\text{CaCO}_3}}{\text{L}} \cdot \frac{1 \text{ g}}{1000 \text{ mg}} \cdot \frac{1 \text{ Eq}}{50 \text{ g}} \quad (\text{B.3})$$

$$\begin{aligned} \text{Alk}_{\text{carb}} = & \text{Alk} - \{\text{OH}^-\} - \{\text{HPO}_4^{2-}\} - 2\{\text{PO}_4^{3-}\} \\ & - \{\text{NH}_3\} + \{\text{H}_3\text{PO}_4\} + \{\text{H}^+\} \end{aligned} \quad (\text{B.4})$$

To compute the distribution of carbonate species, the fractions of each compound (α_{CO_2} , $\alpha_{\text{HCO}_3^-}$ and $\alpha_{\text{CO}_3^{2-}}$), which only depend on the pH, are calculated by employing Eqs. B.5 - B.7 (WolfGladrow). As only HCO_3^- , and CO_3^{2-} contribute to alkalinity, the first one with one equivalent and the second one with two equivalents, as shown in Eq. B.2, it is necessary to add Eq. B.8. Because cattle waste has basic pH and the major species are HCO_3^- and CO_3^{2-} , it has been considered that total carbonates calculated in Eq. B.8, are equal to the sum of all carbonate species in the organic waste.

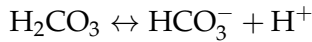
$$\alpha_{\text{CO}_2} = \frac{\{\text{H}^+\}^2}{\{\text{H}^+\}^2 + \{\text{H}^+\} K_{\text{sp}_{\text{H}_2\text{CO}_3}} + K_{\text{sp}_{\text{H}_2\text{CO}_3}} K_{\text{sp}_{\text{HCO}_3^-}}} \quad (\text{B.5})$$

$$\alpha_{\text{HCO}_3^-} = \frac{\{\text{H}^+\} K_{\text{sp}_{\text{H}_2\text{CO}_3}}}{\{\text{H}^+\}^2 + \{\text{H}^+\} K_{\text{sp}_{\text{H}_2\text{CO}_3}} + K_{\text{sp}_{\text{H}_2\text{CO}_3}} K_{\text{sp}_{\text{HCO}_3^-}}} \quad (\text{B.6})$$

$$\alpha_{\text{CO}_3^{2-}} = \frac{K_{\text{sp}_{\text{H}_2\text{CO}_3}} K_{\text{sp}_{\text{HCO}_3^-}}}{\{\text{H}^+\}^2 + \{\text{H}^+\} K_{\text{sp}_{\text{H}_2\text{CO}_3}} + K_{\text{sp}_{\text{H}_2\text{CO}_3}} K_{\text{sp}_{\text{HCO}_3^-}}} \quad (\text{B.7})$$

$$\text{Total carbonates} = \frac{\text{Alk}_{\text{carb}}}{\alpha_{\text{HCO}_3^-} + 2\alpha_{\text{CO}_3^{2-}}} \quad (\text{B.8})$$

Once the total carbonates concentration is known, the thermodynamic models for carbonate species existing in aqueous phase can be defined for the following species



Two elements are necessary to define the thermodynamic models for carbante species, the therodynamic equilibria defined by the Eq. B.9, computed using activity coefficients, and mass balance defined by Eq. B.11. Finally, solving the equations 2 to 11 the concentrations of the different carbonate species are determined. pK_{sp} values for all systems evaluated in this work are collected in Table B.4.

$$K_{sp} = \frac{\prod \{Products\}}{\prod \{Reactants\}} \quad (\text{B.9})$$

$$[i]_{initial} = \sum_{products} [i]_{products} \quad (\text{B.10})$$

$$i \in \{\text{CO}_3^{2-}\}$$

$$\text{Total carbonates} = [\text{H}_2\text{CO}_3] + [\text{HCO}_3^-] + [\text{CO}_3^{2-}] \quad (\text{B.11})$$

Table B.4: pK_{sp} values for the considered aqueous phase chemical systems.

Name	Chemical system	pK_{sp}	Source
Ammonia	$\text{NH}_4^+ \leftrightarrow \text{NH}_3 + \text{H}^+$	9.2	Bates
Water	$\text{H}_2\text{O} \leftrightarrow \text{OH}^- + \text{H}^+$	14	Skoog
Phosphoric acid	$\text{H}_3\text{PO}_4 \leftrightarrow \text{H}_2\text{PO}_4^- + \text{H}^+$	2.1	Ohlinger
	$\text{H}_2\text{PO}_4^- \leftrightarrow \text{HPO}_4^{2-} + \text{H}^+$	7.2	Ohlinger
Carbonic acid	$\text{HPO}_4^{2-} \leftrightarrow \text{PO}_4^{3-} + \text{H}^+$	12.35	Ohlinger
	$\text{H}_2\text{CO}_3 \leftrightarrow \text{HCO}_3^- + \text{H}^+$	6.35	Skoog
	$\text{HCO}_3^- \leftrightarrow \text{CO}_3^{2-} + \text{H}^+$	10.33	Skoog

B.4 SURROGATE MODELS TO ESTIMATE PRECIPITATES FORMATION FROM LIVESTOCK WASTE

B.4.1 Influence of magnesium

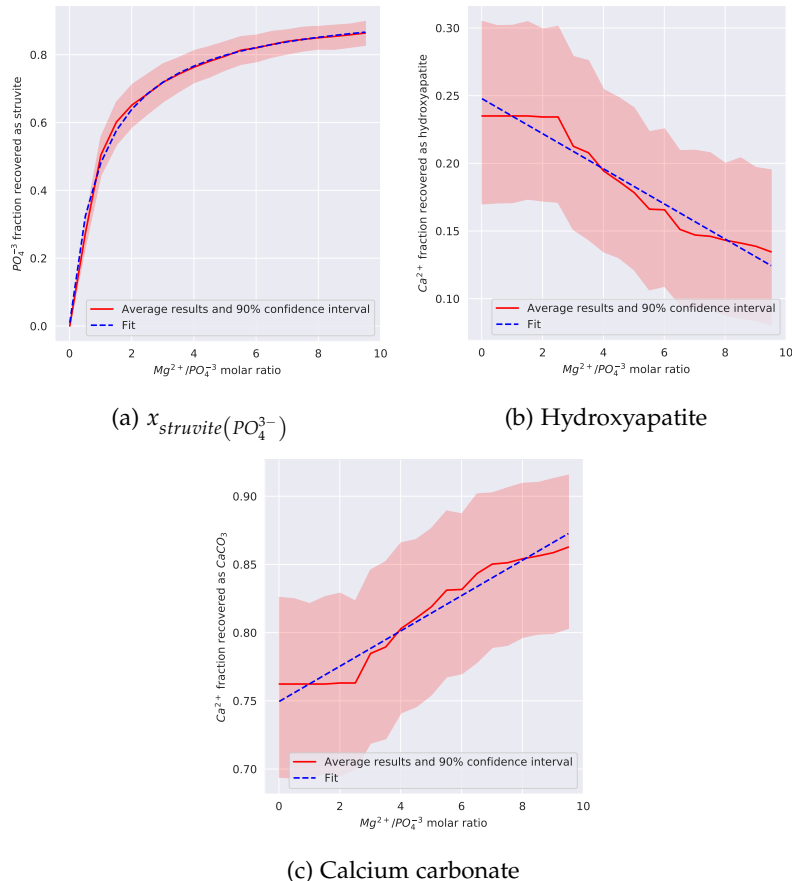


Figure B.2: Evolution phosphorus as phosphate fraction recovered as struvite and calcium fraction recovered as precipitates along Mg^{2+}/PO_4^{3-} molar ratio values considering 50 different composition data sets.

B.4.1.1 Influence of calcium

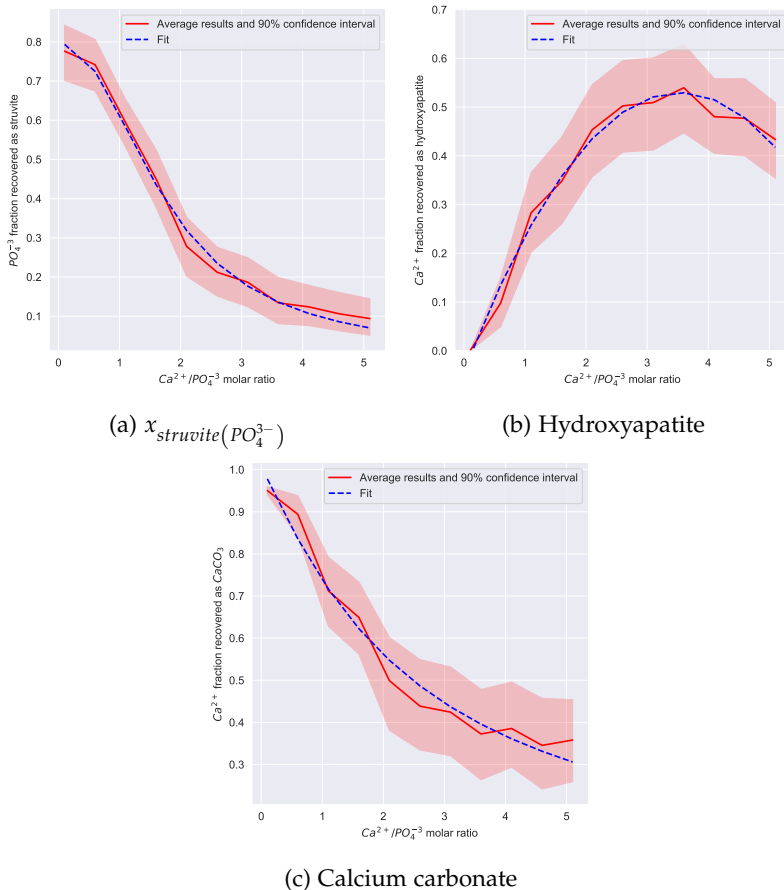


Figure B.3: Evolution of phosphorus as phosphate fraction recovered as struvite and calcium fraction recovered as precipitates along $\text{Ca}^{2+}/\text{PO}_4^{3-}$ molar ratio values considering 50 different composition data sets.

B.4.1.2 Influence of alkalinity

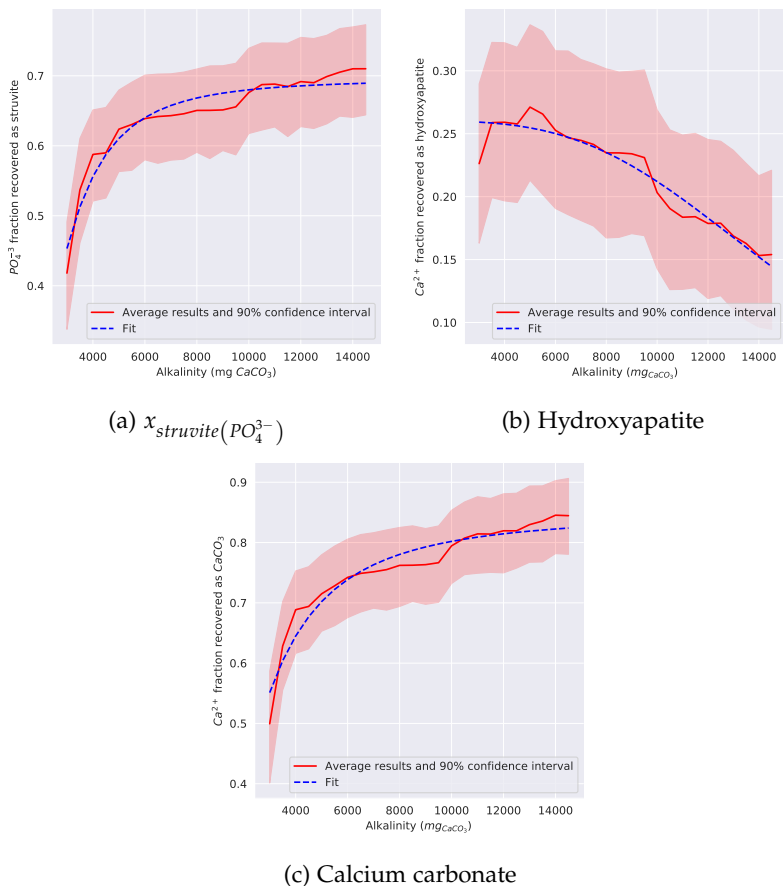


Figure B.4: Evolution of phosphorus as phosphate fraction recovered as struvite and calcium fraction recovered as precipitates among alkalinity values considering 50 different composition data sets.

BIBLIOGRAPHY

C

APPENDIX C: SUPPLEMENTARY INFORMATION OF CHAPTER 5

C.1 ENVIRONMENTAL GEOGRAPHIC INFORMATION MODEL

C.1.1 *Trophic State Index*

[carlson_trophic_1977](#) proposed the Trophic State Index (TSI) as a metric to determine the trophic status of waterbodies. This is used by the U.S. Environmental Protection Agency (US EPA) ([QAPP2012](#)). This index can be calculated using three parameters: concentration of chlorophyll- α (chl- α), concentration of total phosphorus, and water turbidity measured through the Secchi depth. Only the two first methods has been used in this work since they are less affected to exogenous phenomena (such as atmospheric conditions, or variations in the flow of water streams). Correlations to compute the TSI from these parameters are shown in Eq. [C.1](#) and [C.2](#), where Clh denotes the concentration of chlorophyll- α , and TP denotes the concentration of total phosphorus in mg/m^3 ([carlson_trophic_1977](#)).

The TSI of a waterbody is scored in a range from zero to one hundred, which can be correlated with the oligotrophic, mesotrophic, eutrophic and hypereutrophic classes as shown in Table [C.1](#). Oligotrophic and mesotrophic denote low and intermediate biomass productivities, while eutrophic and hypereutrophic are referred to waterbodies with high biological productivity and frequent algal blooms. Combined data for chl- α and total phosphorus concentrations retrieved from the National Lakes Assessments (NLA) carried out by the US EPA in the years 2007 and 2012 ([NLA2012](#); [NLA2007](#)) is used to determine the Trophic State Index of lentic waters in the contiguous U.S, as shown in Fig. [??](#). No TSI values are assigned to the watersheds without reported data.

$$TSI_{chl-\alpha} = 10 \cdot \left(6 - \frac{2.04 - 0.68 \cdot \ln(Clh)}{(2)} \right) \quad (C.1)$$

$$TSI_{TP} = 10 \cdot \left(6 - \frac{\ln(\frac{48}{TP})}{(2)} \right) \quad (C.2)$$

Table C.1: Relation between TSI value and trophic class.

TSI	<40	40-50	50-70	>70
Trophic Class	Oligotrophic	Mesotrophic	Eutrophic	Hypereutrophic

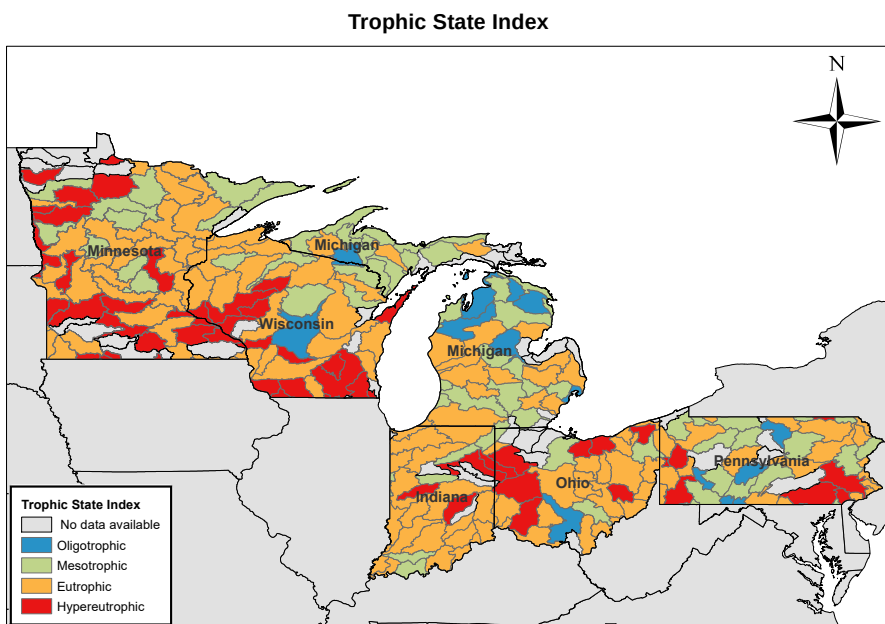


Figure C.1: Trophic State Index in the contiguous US HUC8 watersheds

C.1.2 Balance of anthropogenic phosphorus releases

Agricultural releases are a main source of human-based phosphorus releases due to the excessive use of synthetic fertilizers and livestock waste for nutrient supplementation in croplands (**Dzombak**). Since this work is limited to the assessment of agricultural phosphorus releases, other possible sources of phosphorus releases are not considered. Agricultural phosphorus releases have been estimated from data reported by the Nutrient Use Geographic Information System (NuGIS) project. Further information about the methodology used for the estimation of human-based phosphorus releases can be found in **NuGIS**.

The anthropogenic phosphorus uptakes considered are those due to the crops grown in each watershed. In addition, phosphorus retained by wetlands is considered. Data from **USDAWaste** is used to estimate the phosphorus uptakes of different crops, attending to their different phosphorus requirements and yield rates. To determine the crops grown in each watershed, the land cover uses are first determined using data from

the US EPA EnviroAtlas database for the most recent year available (2011), differentiating between croplands, pasturelands, wetlands, and developed areas (urban areas) (**EnviroAtlas**). To estimate the distribution of crops in croplands, including corn, soybeans, small grains, cotton, rice, vegetables, orchards, greenhouse and other crops (i.e., fruits, sugar crops, and oil crops) (**2017 Census of Agriculture**), data from the 2017 U.S. Census of Agriculture is used. In case of two or more crops were harvested from the same land during the year (double cropping), the area was counted for each crop. Since the data from the 2017 U.S. Census of Agriculture are published at HUC6 resolution, they have been reconciled to HUC8 level by the fraction of occupied area by each HUC8 watershed in the corresponding HUC6 watershed. The wetlands phosphorus uptake value assessed is $0.77 \text{ gP m}^{-2} \text{ year}^{-1}$, based on data reported by **Kadlec**.

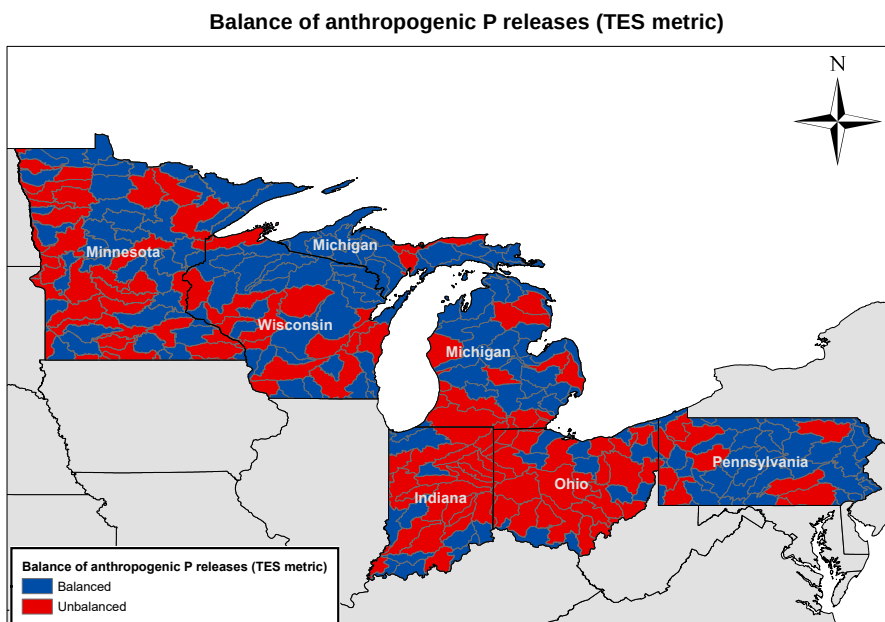


Figure C.2: Balance of anthropogenic phosphorus releases in the contiguous US at a HUC8 spatial resolution

C.1.3 Phosphorus in soils

Phosphorus concentration in soils is considered to evaluate the legacy phosphorous continuously builds-up in soils. However, only a fraction of phosphorus is available for plants. To measure this phosphorus fraction available for plants, several standardized phosphorus soil tests have been proposed, including Olsen, Bray 1 and Mehlich 3 tests. Among them,

Mehlich 3 (M₃P) has been selected as a measure of the concentration of P in soils since it is a widely used metric, and it is the P soil test least affected by changes in soil pH. To estimate the fraction of phosphorus available for plants from total phosphorus concentration data, a correlation developed by AllenMallarino2006 has been used, Eq. C.3. However, this correlation has been developed for agricultural soils in Iowa. Due to the lack of wider studies in this regard, the M₃P estimations calculated for the contiguous U.S. must be considered as an exploratory effort to determine the phosphorus saturation in soils across the the contiguous U.S. in an attempt to select the most suitable nutrients management technology according to the geographic environmental indicators. Datasets for samples from the soil A horizon published by the U.S. Geological Survey (USGS) in the "Geochemical and Mineralogical Data for Soils of the Conterminous United States" report were used to evaluate the concentration of total phosphorus along the contiguous U.S. (**SoilsUSGS**).

$$M_3P \text{ (% over TP)} = \frac{4.698 \cdot 10^{-1}}{1 + (\text{TotalP (mg/kg)} \cdot 1.336 \cdot 10^{-3})^{-2.148}} \quad (C.3)$$

The relationship between M₃P test value and the quality of soil is shown in Table C.2. Soil fertility levels below optimum indicate that nutrient supplementation is needed to enhance the yield of crops, optimum values indicates that no nutrient supplementation is needed, and excessive soil fertility level indicate over-saturation of phosphorus in soil that can reach waterbodies by runoff (**Espinoza2006**).

Table C.2: Relation between Mehlich 3 phosphorus and soil fertility level (**Espinoza2006**).

Soil Fertility Level	M ₃ P soil phosphorus concentration (ppm)
Very Low	<16
Low	16-25
Medium	26-35
Optimum	36-50
Excessive	>50

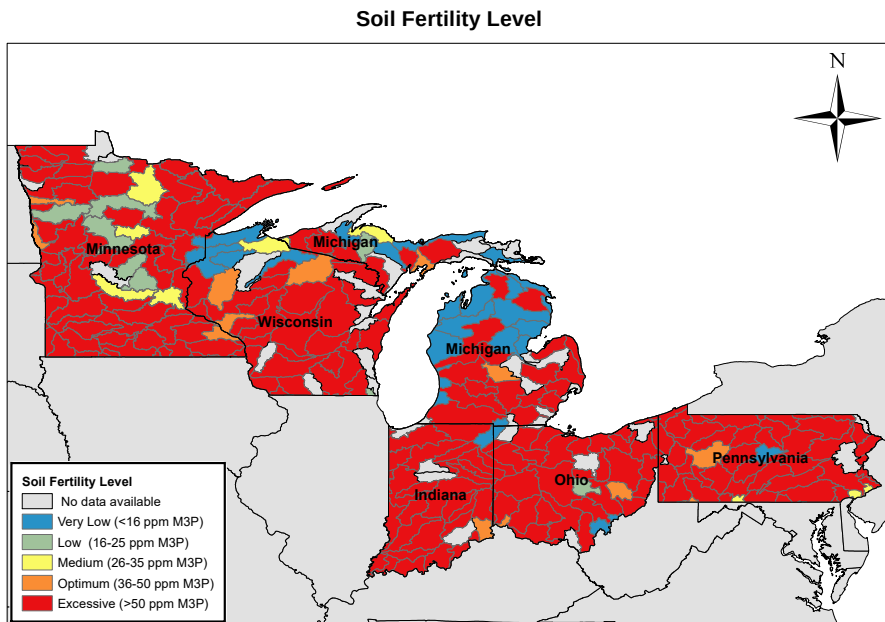


Figure C.3: Soil Fertility Level in the contiguous US at a HUC8 spatial resolution

Table C.3: Livestock waste composition and generation rates for different types of animals (**Kellogg2010; USDAHandbook**).

Livestock type	Water (%wt)	Organic matter (%wt)	Total N (%wt)	Total P (%wt)	Total Ca (%wt)	Total K (%wt)	Generation rate (kg/day)	Animal unit equivalence
Dairy cow	87	10,98	0,59	0,08	0,12	0,20	37,88	0,74
Dairy heifer	83	13,04	0,48	0,09	0,12	0,21	29,95	0,94
Dairy calf	83	9,28	0,51	0,06	0,12	0,13	29,95	4,00
Beef cow	88	10,58	0,34	0,08	0,12	0,24	28,58	1,00
Beef calf	88	10,00	0,58	0,10	0,12	0,38	28,14	4,00

C.2 FRAMEWORK DEVELOPMENT

C.2.1 Data entry

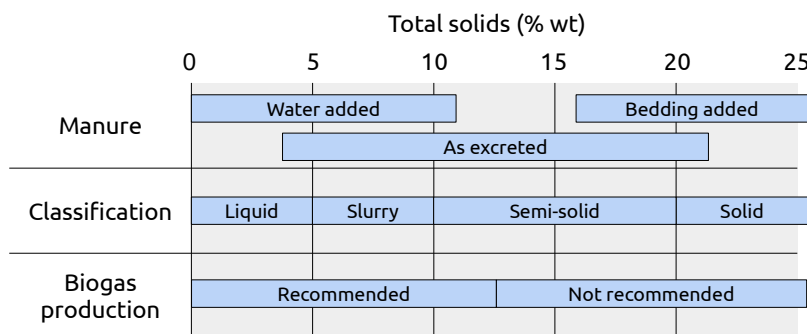
C.2.2 Techno-economic model

C.2.2.1 Manure conditioning model

U.S. EPA determines that the content of total solids in manure should be less than 15%, as shown in Fig. C.4 (AgSTARHandbook). Therefore, additional water may be added to reduce the solids content in manure before the anaerobic digestion stage.

Table C.4: Predefined economic parameters.

Parameter	Value
Discount rate (%)	7
Phosphorus credits (USD / kg P recovered)	22
Electricity price (Renewable Energy Certificates) (USD/MWh)	60
Bio-methane price (Renewable Identification Number) (USD/kg)	1.25
Capital cost incentive (% over total capital cost)	0

Figure C.4: Adequate manure properties for anaerobic digestion. Adapted from **AgSTARHandbook**.

C.2.2.2 Anaerobic digestion model

Correlations to estimate the capital cost, Eq. C.4, and operating and management costs (O&M), Eq. C.5, as a function of the animal population of CAFOs were developed using data from the US EPA AgSTAR program (**AgSTAR2003**) and the USDA (**USDA_OM**) respectively, as shown in Figure C.5. It should be noted that O&M cost does not include the capital cost amortization. Therefore, to estimate the total production cost, the annualized equipment cost has been added to the O&M costs, Eq. C.6. The assumed equipment lifetime is 20 years.

Table C.5: Statistical summary of nutrients composition for cattle manure before and after anaerobic digestion (AD). All concentrations are reported in mg/L. TKN is referred to total Kjeldahl nitrogen, and TP to total phosphorus. Data from **ADAS; Martinz; Alburquerque; Sorensen**.

	TKN before AD	TKN after AD	NH ₄ before AD	NH ₄ after AD	TP before AD	NH ₄ after AD	P-PO ₄ before AD	P-PO ₄ after AD
count	10.00	10.0	10.00	10.00	5.00	5.00	5.00	5.00
mean	3856.10	3967.1	1845.90	2340.10	1442.60	1449.60	811.40	946.40
std	847.41	942.9	354.59	387.34	467.14	485.29	277.67	331.88
min	2920.00	2800.0	1300.00	1810.00	813.00	838.00	457.00	562.00
25%	3050.00	3152.5	1607.50	2047.50	1170.00	1170.00	590.00	670.00
50%	3660.00	3855.0	1825.00	2340.00	1450.00	1360.00	880.00	950.00
75%	4630.75	4882.5	2159.75	2590.00	1860.00	1920.00	1050.00	1260.00
max	4960.00	5290.0	2300.00	2881.00	1920.00	1960.00	1080.00	1290.00

$$\text{Installation cost (MM USD (2019))} = (4.271 \cdot 10^{-4} \cdot N_{\text{animals}} + 0.127) \cdot 1.511 \quad (\text{C.4})$$

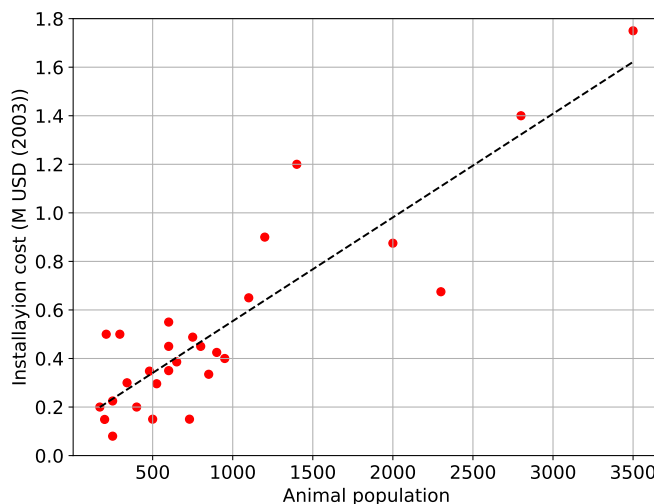
$$\frac{\text{O&M}}{\text{Installation cost}} \text{ ratio} = \frac{15.858 \cdot 10^3}{(1 + (N_{\text{animals}} \cdot 13.917)^{1.461})} \quad (\text{C.5})$$

$$\text{Operating cost} = \text{O&M costs} + \frac{\text{Investment cost}}{\text{Plant lifetime}} \quad (\text{C.6})$$

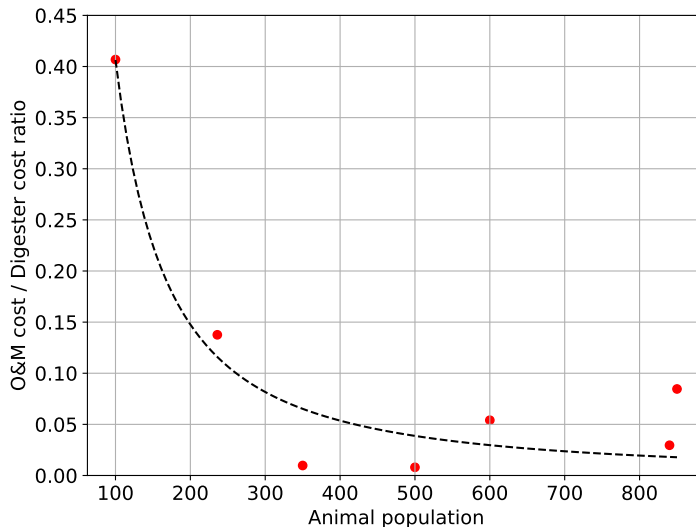
C.2.2.3 Solid-liquid separation model

Based on the evaluation reported by **MollerSLsep**, a screw press is the technology selected to carry out the solid-liquid separation stage since it is the most cost efficient liquid-solid equipment. The partition coefficients for the different components are shown in Table C.6.

To determine the commercial sizes and number of units necessary as a function of the flow to be treated, data from commercial manufacturers is considered (**PWTech**). The feasible configurations in terms of screw press diameter and number of units as a function of the waste flow treated are shown in Table C.7. Data reported by **Matches** for this type of equipment is used to relate the unit diameter and cost, while the operating costs are calculated assuming power consumption reported by the manufacturer for each model, as shown in Fig. C.6 and Table C.8.



(a) Cost of AD units as a function of the number of animals (cattle). Data from AgSTAR2003.



(b) O&M costs as a function of the number of animals (cattle). Data from USDA_OM

Figure C.5: Correlations between AD capital and O&M costs, and the number of cattle in the livestock facility.

C.2.2.4 Nutrient recovery model

Specific correlations for livestock waste to estimate the molar fraction of PO_4^{3-} and Ca^{2+} recovered as struvite as a function of the amount of calcium contained in the waste were developed in a previous work

Table C.6: Partition coefficients for solid-liquid manure separation using a screw press unit (**MollerSLsep**)

Element	Solid fraction	Liquid fraction
Total mass	0.08	0.92
Dry matter	0.31	0.69
Org. N	0.09	0.91
Org. P	0.22	0.78

Table C.7: Sizing estimated for screw press units based commercial on data (**PWTech**)

Load capacity $(\frac{m^3}{day})$	Number of units			
	$\varnothing(m) 0.23$	$\varnothing(m) 0.35$	$\varnothing(m) 0.42$	$\varnothing(m) 0.56$
< 43	1	-	-	-
43 - 81	-	1	-	-
81 - 190	-	-	1	-
190 - 381	-	-	2	-
381 - 572	-	-	3	-
572 - 708	-	-	-	2
708 - 1090	-	-	-	3
1090 - 1444	-	-	-	4
> 1444	-	-	-	$\left[\frac{\text{Flow } (m^3/day)}{\text{Load Capacity } \varnothing 0.56 \text{ m unit}} \right]$

(**MartinStruvite**), Eqs. C.7 to C.9, where $x_{Ca^{2+};PO_4^{3-}}$ refers to the Ca^{2+}/PO_4^{3-} molar ratio $x_{struvite(PO_4^{3-})}$ is the fraction of phosphorus as phosphate recovered as struvite, and $x_{HAP(Ca^{2+})}$ and $x_{CaCO_3(Ca^{2+})}$ are the fraction of calcium recovered as hydroxyapatite and calcium carbonate respectively.

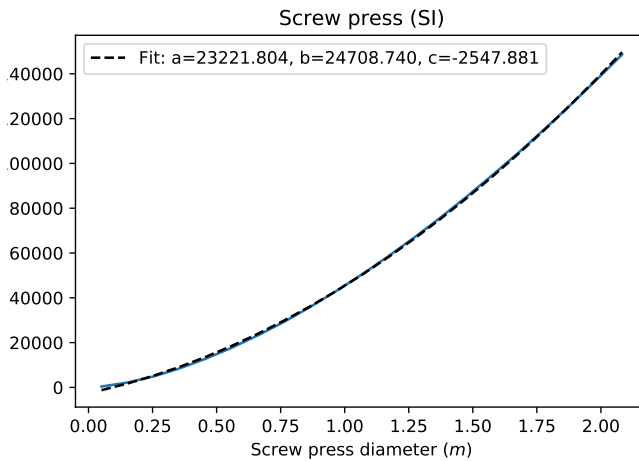


Figure C.6: Estimated screw press investment costs (USD) as a function of the size.

Table C.8: Electrical power of screw press units (**PWTech**)

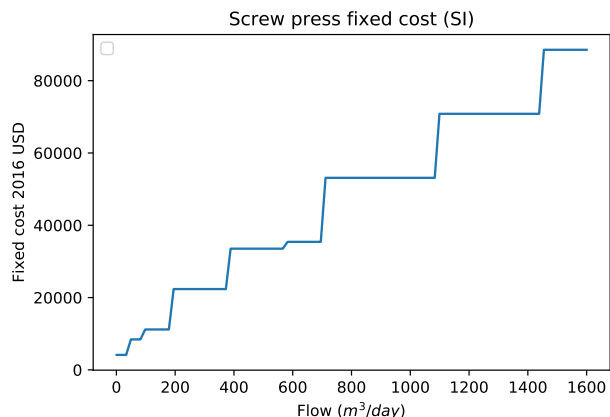
Number of units	Electrical power (kW)			
	$\varnothing(m)$ 0.23	$\varnothing(m)$ 0.35	$\varnothing(m)$ 0.42	$\varnothing(m)$ 0.56
1	0.3	0.45	0.9	-
2	-	-	1.27	3.88
3	-	-	2.01	6.34
4	-	-	-	7.83

$$x_{Struvite} = \frac{0.798}{1 + (x_{Ca^{2+}:PO_4^{3-}} \cdot 0.576)}^{2.113} \cdot 100 \quad (C.7)$$

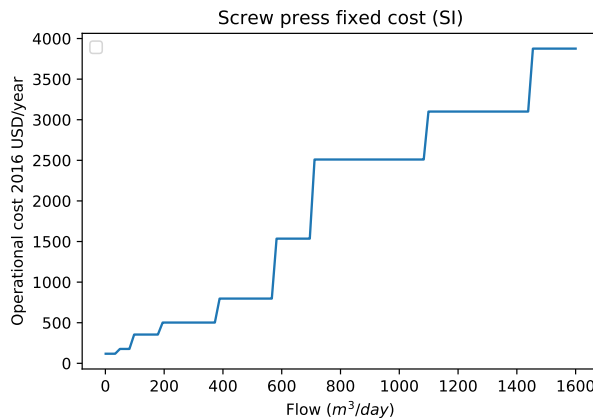
$$x_{HAP} = (-4.321 \cdot 10^{-2} \cdot x_{Ca^{2+}:PO_4^{3-}}^2 + 0.313 \cdot x_{Ca^{2+}:PO_4^{3-}} - 3.619 \cdot 10^{-2}) \cdot 100 \quad (C.8)$$

$$x_{CaCO_3} = \frac{1.020}{1 + (x_{Ca^{2+}:PO_4^{3-}} \cdot 0.410)}^{1.029} \cdot 100 \quad (C.9)$$

PHOSPHORUS RECOVERY AS STRUVITE IN SINGLE PASS FBR REACTOR:
MULTIFORM HARVEST AND CRYSTALACTOR. Phosphorus can be re-



(a) Estimated investment costs for screw press units.



(b) Estimated operation costs for screw press units.

Figure C.7: Estimated capital and operating costs for screw press units.

covered in the form of struvite using single pass fluidized bed reactors (FBR). Multiform Harvest and Crystalactor are commercial technologies using this configuration, based on single pass fluidized bed reactors, with no recirculation and conical or cylindrical design respectively, where the organic waste is pumped, carrying out the struvite formation. The struvite particles grow, increasing their size, until their mass overcome the drag force of the uplift stream.

Multiform, Fig. C.8a, is a nutrient recovery system developed by the U.S. based company Multiform Harvest. It is a struvite-based process designed to be simple, robust, and fully automatized. Large struvite particles settle towards the reactor base, from where they are removed to be dried before obtaining the final product. $MgCl_2$ is supplied to the reactor for increasing

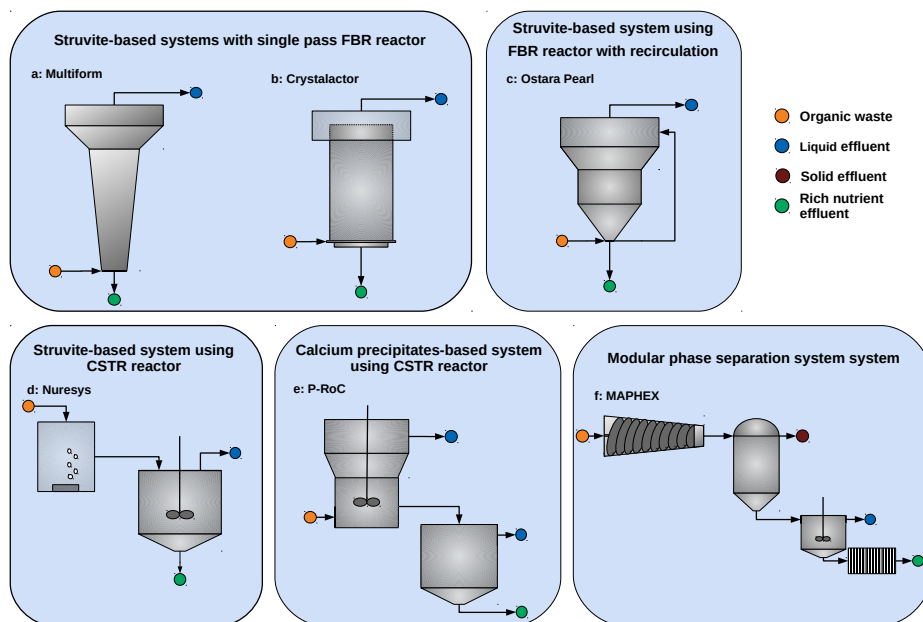


Figure C.8: Flowsheets of the nutrient recovery systems considered in the proposed framework. a: Multiform, b: Crystalactor, c: Ostara Pearl, d: Nuresys, e: P-RoC, f: MAPHEX.

struvite supersaturation, enhancing its precipitation. pH is adjusted using sodium hydroxide. The conical design of the reactor keeps the small and lighter particles on the large diameter section at the top of the reactor, where the superficial velocity is slower. As the particles increase their mass, they settle gradually to lower levels of the reactor, where the diameter is smaller and the superficial velocity and drag force larger, until they are finally settled on the bottom of the reactor. The liquid phase exits the reactor from the top, where the cross-section is the widest, to ensure the retention of struvite fines (**Pearl2Kcost2**). The techno-economic model for the Multiform process considers a unique size able to process up to 38.5 kg of phosphorus (P-PO_4) per day, with an associated capital cost of 625,000 USD per each Multiform unit, plus 420,000 USD for the struvite dryer that serves all Multiform units. The operating cost for the Multiform system unit is 15.419 USD per kg of P-PO_4 processed (**Pearl2Kcost2**).

Crystalactor is a nutrient recovery system created by the Dutch company Royal HaskoningDHV, Fig. C.8b. It is based on a fluidized bed reactor where phosphorus is recovered as precipitates. It can be configured to recover phosphate in the form of calcium phosphates or struvite, depending on the reactant supplied. The model included in the framework considers that the system is configured for struvite production since

struvite has a more consolidated market than calcium precipitates to sell the final product recovered. Under this configuration, the reactor is filled with small struvite particles playing the role of seeds to promote the precipitation process, and MgCl₂ is supplied to increase struvite supersaturation ([egle_phosphorus_2016](#)). It is considered that each unit is able to process up to 137.7 kg of P-PO₄ per day. The economy of scale for Crystalactor costs can be captured through the previous work developed by [egle_phosphorus_2016](#) using Eq. C.10, where $n_{\text{Crystalactor}}$ represents the number of Crystalactor units installed. Crystalactor operating cost assumed is 2.12 USD per kg of P-PO₄ processed ([egle_phosphorus_2016](#)).

$$\text{Capital cost}_{\text{Crystalactor}} = 2.3 \cdot 10^6 + 714,285.71 \cdot n_{\text{Crystalactor}} \quad (\text{C.10})$$

PHOSPHORUS RECOVERY AS STRUVITE IN A FBR REACTOR WITH RECIRCULATION: OSTARA PEARL. Pearl is a struvite-based nutrient recovery system developed by the Canadian company Ostara, Fig. C.8c. The system is based on a continuous operated fluidized bed reactor (FBR) reactor where the waste stream is in contact with struvite particles, which promotes the precipitation of struvite. To increase the supersaturation of struvite and enhance its precipitation, MgCl₂ is supplied to the reactor in a molar ratio of 2 mol of Mg per mol of phosphate. pH is adjusted using sodium hydroxide. In the reactor, the struvite particles grow until they reach a critical mass enough to overcome the drag force of the uplift liquid. To achieve different superficial velocities along the reactor, the diameter of the reactor increases with the height, providing sufficient superficial velocity in the bottom of the vessel to fluidize the struvite seeds, while the larger diameter in the top of the reactor reduces the liquid uplift velocity, allowing retention of fine crystal seed particles in the reactor. Large struvite particles sink towards the base of the reactor, from where they are periodically withdrawn. To increase the liquid flow in the reactor and achieve larger superficial velocities, an internal recirculation loop is used to recirculate liquid to the bottom of the reactor. A drying step is performed to remove the excess of moisture contained in the struvite particles obtained from the reactor. The liquid stream leaves the reactor at the top, where the cross-section has the largest diameter to ensure the retention of struvite fines.

Based on the information reported by Ostara ([Pearl2Kcost2](#)), standard equipment sizes for the Pearl system are divided in three different capacities, Pearl 500, Pearl 2K, and Pearl 10K, with a load capacities range from 65 to 1250 kg PO₄ per day, as shown in Table C.9. Investment and operation costs for the Ostara Pearl process, including the cost of the conveyor dryer included in the process, can be found in Table C.9

(**Pearl500cost1**; **Pearl2Kcost1**; **Pearl2Kcost2**; **Pearl10Kcost1**). A investment cost-equipment cost ratio of 1.9 has been considered (**Pearl2Kcost2**).

Table C.9: Sizing and equipment cost estimated for Ostara Pearl process

	Pearl 500	Pearl 2K	Pearl 10K
Load capacity $\left(\frac{\text{kg}_{\text{P-PO}_4}}{\text{day}} \right)$	65	250	1250
Capital cost (USD)	$2.3 \cdot 10^6$	$3.1 \cdot 10^6$	$10.0 \cdot 10^6$
Investment $\left(\frac{\text{USD}}{\frac{\text{kg}_{\text{P-PO}_4}}{\text{day}}} \right)$	35,385	12,252	8,000

PHOSPHORUS RECOVERY AS STRUVITE IN A CSTR REACTOR:

NURESYS. NuReSys, Fig. C.8d is a nutrient recovery technology developed in Belgium by Nutrients Recovery Systems. Struvite formation is carried out in a continuous stirred tank reactor (CSTR), equipped with a special impeller to minimize the breakage of struvite crystals. NuReSys process uses a stripper as pretreatment where air is injected in the organic waste, decomposing organic carbon and increasing the pH. If pH adjustment is needed, sodium hydroxide is added to the CSTR vessel. The liquid stream is fed into the CSTR reactor for struvite precipitation. Similar to other struvite-based processes, MgCl₂ is supplied to the reactor to increase struvite supersaturation. After struvite precipitation, both solid and liquid phases are extracted from the reactor in the same stream and it is injected in a settler where the separation of phases is carried out. Struvite fines are separated from the largest struvite particles through a hydrocyclone and they are recirculate to the process. The struvite particles are dried before their final collection (**Pearl2Kcost2**).

Considering the data available, it has been assumed that each NuReSys system unit is able to process up to 204 kg of P-PO₄ per day, with an associated capital cost of 1,380,655 USD. NuReSys operating cost is 6.22 USD per kg of P-PO₄ processed (**Pearl2Kcost2**).

PHOSPHORUS RECOVERY AS CALCIUM PRECIPITATES IN CSTR A REACTOR: P-ROC. P-RoC is a patented system by the Karlsruhe Institute of Technology (Germany) for phosphorus recovering as calcium precipitates, Fig. C.8e. P-RoC is based on a reactive substrate, calcium-silicate hydrate (CSH), which is the support on which phosphorus is deposited forming a calcium precipitate. The process is carried out in a CSTR reactor, where the precipitates are formed. Liquid and solid phases are separated by sedimentation in a settler, and the obtained particles are finally dried

in two consecutive steps composed by a belt filter and a conveyor dryer ([ehbrecht_p-recovery_2011](#)).

As P-RoC is not yet a fully commercial technology, the capital cost is estimated through a preliminary design of each equipment: CSTR reactor, settler, and belt dryer. The estimation of the investment of the CSTR reactor unit is the result of the sum of the vessel and the agitator costs. For design purposes, a maximum CSTR volume of 45 m³ is considered ([CAPCOST](#)). For larger volumes, multiple units installed in parallel are considered, Eq. [C.11](#). The vessel cost is based on data reported by CAPCOST ([CAPCOST](#)), from which the correlation shown in Fig. [C.9](#) has been developed.

$$\text{Number of CSTR} = \left\lceil \frac{\text{Total volume}}{\text{Max. size}} \right\rceil \quad (\text{C.11})$$

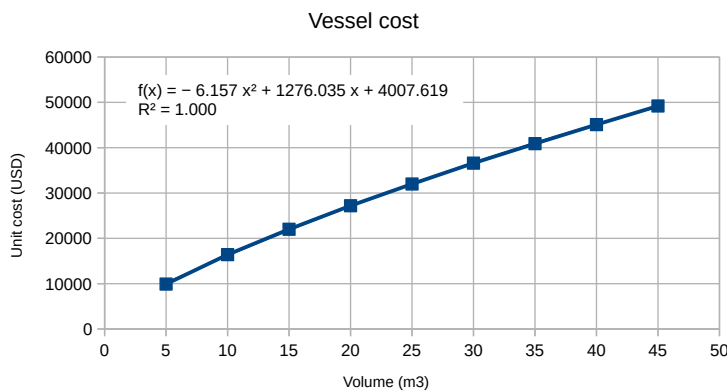


Figure C.9: Estimated investment costs for a non-jacketed vessel, based on data from CAPCOST ([CAPCOST](#)).

The clarifier cost has been estimated as a vessel, using the correlation shown in Fig. [C.9](#). The residence time assumed is 1 hour ([ehbrecht_p-recovery_2011](#)). A vacuum conveyor filter has been selected for struvite recovery from the outlet reactor stream since previous studies report the use of this equipment ([Matynia](#)). For design purposes, a filter rate of 0.011 kg/(m²·s) and a maximum area of 1,200 ft² are considered ([Walas](#)). The unit cost is based on the correlations reported in [Walas](#). This correlation is based on the area of the filter. Vacuum conveyor filter area and cost are collected in Eqs. [C.12](#) and [C.13](#). The final drying of struvite is achieved with a conveyor dryer. For design purposes, a drying time of 2,100 s and a dryer capacity of 20.85 kg/m² are assumed based on data reported on Table 12-21 of [Perry](#). The dryer loading and dryer area are estimated using Eqs. [C.14](#) and [C.15](#), respectively.

$$\text{Area}_{\text{filter}} \left(m^2 \right) = \frac{\text{Flow} \left(\frac{kg}{s} \right)}{\text{Rate}_{\text{filtration}} \left(\frac{kg}{m^2 \cdot s} \right)} \quad (\text{C.12})$$

$$\text{Filter cost (2009 USD)} = \frac{45506}{\text{Area}_{\text{filter}}^{0.5} \left(ft^2 \right)} \cdot \text{Area}_{\text{filter}} \left(ft^2 \right) \quad (\text{C.13})$$

$$\text{Loading}_{\text{dryer}} \left(kg \right) = \text{Flow} \left(\frac{kg}{s} \right) \cdot \text{time}_{\text{drying}} \left(s \right) \quad (\text{C.14})$$

$$\text{Area}_{\text{dryer}} \left(m^2 \right) = \frac{\text{Loading}_{\text{dryer}} \left(kg \right)}{\text{Capacity}_{\text{dryer}} \left(\frac{kg}{m^2} \right)} \quad (\text{C.15})$$

The cost estimation for a conveyor unit is based on data reported in Table 12-23 of Perry. The correlation developed, relating the unit cost and its area can be found in Fig. C.10. Additionally, based on these data, a maximum conveyor dryer size of 90 m² is assumed.

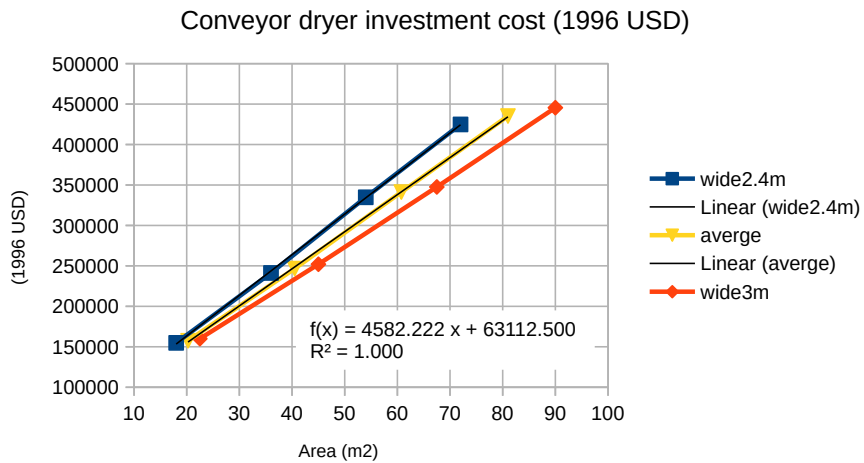


Figure C.10: Estimated investment costs for conveyor dryer unit.

Based on data reported by **egle_phosphorus_2016**, it has been considered that operation costs are variable as a function of the processed amount

of P-PO₄. as it is shown in Eq. C.16, where x_{P-PO_4} represents the kg of P-PO₄ processed per day

$$\text{Operation Cost}_{\text{P-RoC}} \left(\frac{\text{USD}}{\text{kg}_{P-PO_4}} \right) = \begin{cases} 115.5, & \text{if } x_{P-PO_4} < 135 \\ -0.09 \cdot x_{P-PO_4} + 127.19, & \text{if } 135 \geq x_{P-PO_4} \geq 662 \\ 67.9, & \text{if } x_{P-PO_4} > 662 \end{cases} \quad (\text{C.16})$$

PHOSPHORUS RECOVERY THROUGH A MODULAR PHASES SEPARATION SYSTEM: MAPHEX. MAPHEX is a nutrient recovery system based on physico-chemical separations developed by Penn State University and the USDA, Fig. C.8f. It involves three stages: liquid-solid separation with an screw press and a centrifuge, addition of iron sulfate to improve nutrients retention, and filtration with diatomaceous earth as filter media. It is conceived as a mobile modular system which can be set in two interconnected truck trailers ([church_novel_2016](#); [church_versatility_2018](#)). Each MAPHEX unit is able to process up to 18.54 kg of P-PO₄ fed per day, with an associated operation cost of 110.8 USD per kg of P-PO₄ processed. Capital cost of a MAPHEX unit is 291,000 USD ([church_novel_2016](#); [church_versatility_2018](#)).

C.3 MULTI-CRITERIA DECISION MODEL

In the SMAA method, the feasible space of each weight is explored through the Monte Carlo method ([tervonen_implementing_2007](#)), retrieving a set of weights for all criteria according to the assigned order. Fig. C.11 shows the feasible weight space for a problem with three criteria.

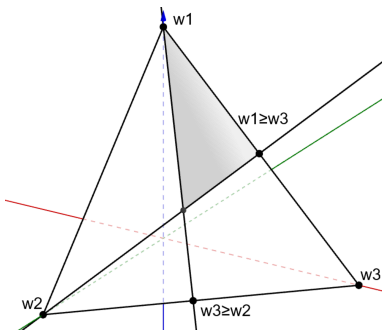


Figure C.11: Example of feasible weights space for a three criteria problem considering ranking of criteria. Figure adapted from [tervonen_implementing_2007](#)

C.4 DESCRIPTION OF THE GREAT LAKES AREA

Table C.10: Livestock residues and phosphorus releases by concentrated animal operation in the Great Lakes area, year 2019. (**Indiana_CAFOS**; **Ohio_CAFOS**; **Pennsylvania_CAFOS**; **Wisconsin_CAFOS**; **Minnesota_CAFOS**; **Michigan_CAFOS**)

	Pennsylvania	Ohio	Indiana	Michigan	Minnesota	Wisconsin
Total animal units	195,967	128,008	187,355	354,460	943,094	743,777
Manure generated (kg/year)	$2.60 \cdot 10^9$	$1.68 \cdot 10^9$	$2.48 \cdot 10^9$	$4.76 \cdot 10^9$	$1.13 \cdot 10^{10}$	$1.03 \cdot 10^{10}$
Phosphorus releases (kg/year)	$2.07 \cdot 10^6$	$1.34 \cdot 10^6$	$1.98 \cdot 10^6$	$3.80 \cdot 10^6$	$9.02 \cdot 10^6$	$8.20 \cdot 10^6$
Dairy Animal units	167,247	101,341	153,495	311,553	428,459	731,927
Manure generated from dairy cows (kg/year)	$2.29 \cdot 10^9$	$1.40 \cdot 10^9$	$2.12 \cdot 10^9$	$4.31 \cdot 10^9$	$5.95 \cdot 10^9$	$1.01 \cdot 10^{10}$
Phosphorus released from dairy cows(kg/year)	$1.83 \cdot 10^6$	$1.12 \cdot 10^6$	$1.70 \cdot 10^6$	$3.45 \cdot 10^6$	$4.76 \cdot 10^6$	$8.10 \cdot 10^6$
Beef animal units	29,370	26,667	33,860	42,907	51,4635	12,088
Manure generated from beef cows (kg/year)	$3.02 \cdot 10^8$	$2.78 \cdot 10^8$	$3.53 \cdot 10^8$	$4.48 \cdot 10^8$	$5.33 \cdot 10^9$	$1.26 \cdot 10^8$
Phosphorus released from beef cows(kg/year)	$2.42 \cdot 10^5$	$2.23 \cdot 10^5$	$2.83 \cdot 10^5$	$3.58 \cdot 10^5$	$4.26 \cdot 10^6$	$1.01 \cdot 10^5$

BIBLIOGRAPHY

D

APPENDIX D: SUPPLEMENTARY INFORMATION OF CHAPTER 7

D.1 MODELING DETAILS OF NITROGEN RECOVERY PROCESSES

D.1.1 *Anaerobic digestion*

The energy requirements of AD unit, described in Eq D.1, comprise the energy required for substrate warming from ambient temperature (considered equal to central Spain average annual temperature, 12 °C) to the digestion temperature (40 °C), Eq. D.2, and the energy supplied to offset the digester heat losses, Eq. D.3. The global heat transfer coefficients (U) for the different digester surfaces are collected in Table D.1. The area of different surfaces is estimated through preliminary equipment design, Eqs. D.4 to D.8, assuming a maximum digester of 6000 m³ (6000AD). The installation of multiple digestion units is considered if the waste flow exceeds this capacity.

$$Q_{\text{digester}} = Q_{\text{waste}} + Q_{\text{losses}} \quad (\text{D.1})$$

$$Q_{\text{waste}} = \dot{m}_{\text{waste}} \cdot c_p \cdot (T_{\text{digestion}} - T_{\text{ambient}}) \quad (\text{D.2})$$

$$Q_{\text{losses}} = \sum_i U_i A_i (T_{\text{digestion}} - T_{\text{ambient}}), \quad (\text{D.3})$$

$$\forall i \in \{\text{roof, walls, floor}\}$$

$$V_{\text{digester}} = \frac{\dot{m}_{\text{waste}}}{\rho_{\text{waste}}} \cdot HRT \cdot \left(1 + \frac{V_{\text{freeboard}}}{100} \right) \quad (\text{D.4})$$

$$V_{\text{digester}} = A_{\text{floor}} \cdot \frac{D_{\text{digester}}}{D_{\text{digester}} : H_{\text{digester}}} \quad (\text{D.5})$$

$$A_{\text{floor}} = \pi \cdot \frac{D_{\text{digester}}^2}{4} \quad (\text{D.6})$$

$$A_{\text{wall}} = 2\pi \cdot \frac{D_{\text{digester}}}{2} \cdot \frac{D_{\text{digester}}}{D_{\text{digester}} : H_{\text{digester}}} \quad (\text{D.7})$$

$$A_{\text{roof}} = A_{\text{floor}} \cdot (A_{\text{roof}} : A_{\text{floor}}) \quad (\text{D.8})$$

CAPEX and OPEX estimation as a function of animal units based on data reported by the USDA (**USDA_OM**) is shown in Figure D.1.

Table D.1: Anaerobic digester design parameters. (**ADPennState**).

Parameter	Unit	Value
U_{floor}	W/m ² K	2.85
U_{wall}	W/m ² K	0.39
U_{roof}	W/m ² K	0.3
V_{\max}	m ³	6000
$V_{\text{freeboard}}$	%	30
HRT	days	21
$D_{\text{digester}}:H_{\text{digester}}$	ratio	1.1
$A_{\text{roof}}:A_{\text{floor}}$	ratio	1.62

D.1.2 Biogas conditioning

D.1.2.1 Moisture removal

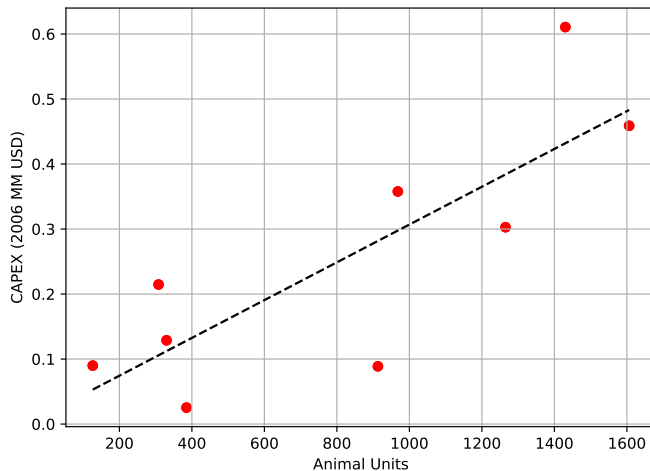
The biogas produced contains saturated water at operating temperature. The first stage for water removal is the moisture condensation, which can remove residual dust and oil as well. However, the biogas moisture can remain saturated at the cooled down temperature, and additional disecation stage can be needed, using adsorbent agents such as silica gel or zeolites in packed bed columns operating at pressures between 6 and 10 bar (**ryckebosch2011techniqu**).

D.1.2.2 H_2S removal

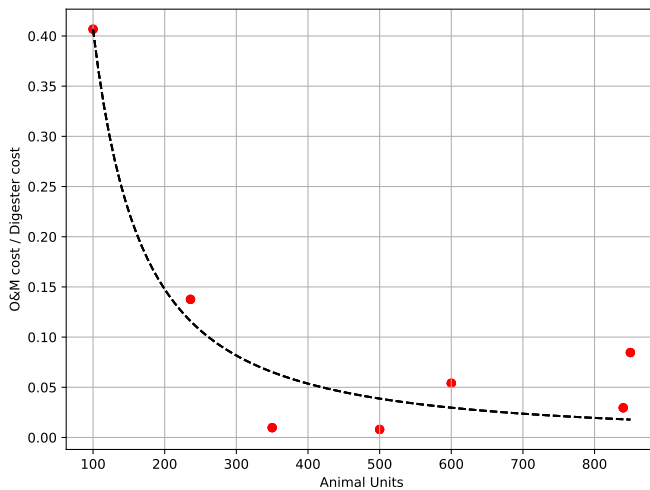
Hydrogen sulphide can be removed during the digestion step, or treating the biogas stream leaving the digestor. A review of H_2S can be found in **ryckebosch2011techniqu**. In this work, in-biogas hydrogen sulphide removal is considered by using a fixed absorbent bed of Fe_2O_3 , so that hydrogen sulphide is removed in the form of Fe_2S_3 , as shown in Eq D.9. This unit operates at 25-50 °C. Although is sensitive to the presence of water, it is a high efficient process. Therefore, the moisture removal must be previously performed.



The bed can be regenerated using oxygen (air), leading to the formation of elementary sulfur, Eq. D.10.



(a) Cost of AD units as a function of animal units.



(b) O&M costs as a function of animal units.

Figure D.1: Correlations between AD capital and O&M costs, and the number of cattle in the livestock facility. Data from **USDA_OM**.



D.1.2.3 Ammonia removal

Ammonia contained in biogas can be removed by using adsorption methods such as fixed beds of zeolites or activated carbon, as well as through water scrubbing processes.

D.1.3 Digestate solid-liquid separation

Nutrients contained in organic waste (manure or digestate, depending on whether AD is carried out or not) are present in both organic and inorganic forms. Organic nutrients are chemically bound to carbon, and they have to be converted into their inorganic forms through a mineralization process to be available for the vegetation to grow. Organic nutrients are mainly contained in the solid phase of organic waste. Inorganic nutrients are water soluble, and they are mostly present in the liquid phase, or bounded to soluble minerals. They are immediately available to plants, including algae involved in the occurrence of algal blooms. To recover the inorganic fraction of nutrients, a solid-liquid separation stage is implemented, keeping the inorganic nutrients in the liquid stage, which will be further processed, and the organic nutrients in the solid phase, which can be composted to mineralize nitrogen and phosphorus and be further used as fertilizers.

Based on the evaluation reported by **MollerSLsep**, a screw press is the technology selected to carry out the solid-liquid separation stage since it is the most cost efficient solid-liquid separation equipment. The experimental results reported in this study are used to determine the partition coefficients for the different elements, as shown in Table D.2.

Table D.2: Partition coefficients for solid-liquid manure separation using a screw press unit (**MollerSLsep**)

Element	Solid fraction	Liquid fraction
Total mass	0.08	0.92
Dry matter	0.31	0.69
Org. N	0.09	0.91
Org. P	0.22	0.78

To determine the commercial sizes and number of units necessary as a function of the flow to be treated, data from commercial manufacturers is considered (**PWTech**). The feasible configurations in terms of screw press diameter and number of units as a function of the waste flow treated are shown in Table 4 of the Supplementary Material. Data reported by **Matches** for this type of equipment is used to relate the unit diameter and cost, while the operating costs are calculated assuming power consumption reported by the manufacturer for each model, as shown in Fig. D.2 and Tables D.3 and D.4.

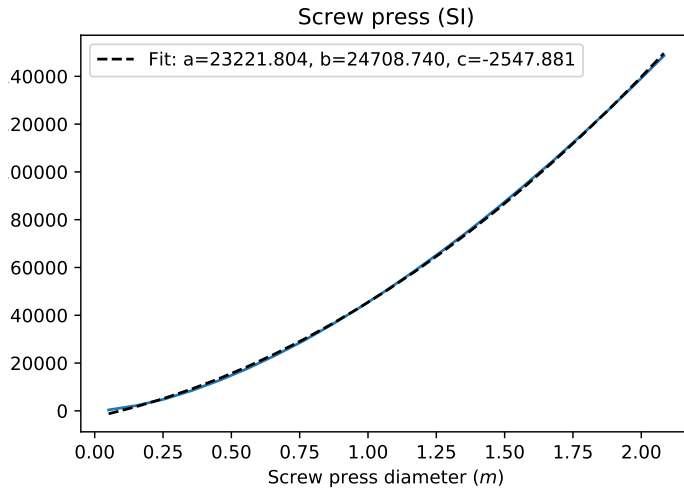


Figure D.2: Estimated screw press investment costs (USD) as a function of the size.

Table D.3: Sizing estimated for screw press units based on commercial data (PWTech)

Load capacity $\left(\frac{m^3}{day}\right)$	Number of units			
	$\varnothing(m)$ 0.23	$\varnothing(m)$ 0.35	$\varnothing(m)$ 0.42	$\varnothing(m)$ 0.56
< 43	1	-	-	-
43 - 81	-	1	-	-
81 - 190	-	-	1	-
190 - 381	-	-	2	-
381 - 572	-	-	3	-
572 - 708	-	-	-	2
708 - 1090	-	-	-	3
1090 - 1444	-	-	-	4
> 1444	-	-	-	$\left[\frac{\text{Flow } (m^3/day)}{\text{Load Capacity } \varnothing 0.56 \text{ unit}} \right]$

Assuming the discretization of units due to the commercial sizes available, the investment and operating costs for the screw press equipment are presented in Fig 4 of the Supplementary Material.

Table D.4: Electrical power of screw press units (**PWTech**)

Number of units	Electrical power (kW)			
	$\varnothing(m) 0.23$	$\varnothing(m) 0.35$	$\varnothing(m) 0.42$	$\varnothing(m) 0.56$
1	0.3	0.45	0.9	-
2	-	-	1.27	3.88
3	-	-	2.01	6.34
4	-	-	-	7.83

D.1.4 Struvite production: Multiform system

Struvite production from livestock waste has been estimated based on a detailed thermodynamic model for precipitates (struvite and calcium compounds) formation considering the main chemical systems involved in the formation of precipitates, shown in Tables D.5 and D.6. pK denotes the thermodynamic equilibrium constant, and pK_{sp} refers to the solubility product. The variability in the organic waste composition is also considered, obtaining surrogate models to predict the formation of struvite based on different waste parameters, including the concentration of magnesium, the concentration of calcium, and the alkalinity level ([martin2020model](#)). Based on previous studies, the supply of magnesium has been fixed at a Mg^{2+}/PO_4^{3-} molar ratio of 2, estimating the formation of struvite as a function of the concentration of Ca^{2+} ions, which compete for phosphate ions hindering the formation of struvite, shown in Eq. D.11. A comprehensive description of the thermodynamic model used for the development of the correlations to estimate the formation of struvite can be found in [martin2020model](#).

A correlation to estimate the formation of struvite through the fraction of phosphorus recovered as struvite ($x_{\text{struvite}(PO_4^{3-})}$) as a function of calcium concentration in the waste has been used in this work, Eq. D.11 ([martin2020model](#)). Based on the correlation shown in Eq. D.11, the amount of nitrogen recovered is estimated through Eq. D.13.

Table D.5: Aqueous phase chemical systems considered in the thermodynamic model for estimating the formation of struvite.

Name	Chemical system	pK	Source
Ammonia	$\text{NH}_4^+ \leftrightarrow \text{NH}_3 + \text{H}^+$	9.2	Bates
Water	$\text{H}_2\text{O} \leftrightarrow \text{OH}^- + \text{H}^+$	14	Skoog
	$\text{H}_3\text{PO}_4 \leftrightarrow \text{H}_2\text{PO}_4^- + \text{H}^+$	2.1	Ohlinger
Phosphoric acid	$\text{H}_2\text{PO}_4^- \leftrightarrow \text{HPO}_4^{2-} + \text{H}^+$	7.2	Ohlinger
	$\text{HPO}_4^{2-} \leftrightarrow \text{PO}_4^{3-} + \text{H}^+$	12.35	Ohlinger
Carbonic acid	$\text{H}_2\text{CO}_3 \leftrightarrow \text{HCO}_3^- + \text{H}^+$	6.35	Skoog
	$\text{HCO}_3^- \leftrightarrow \text{CO}_3^{2-} + \text{H}^+$	10.33	Skoog

Table D.6: Solids species considered in the thermodynamic model for estimating the formation of struvite.

Name	Chemical system	pK_{sp}	Source
Struvite	$\text{MgNH}_4\text{PO}_4 \cdot 6\text{H}_2\text{O} \leftrightarrow \text{Mg}^{2+} + \text{NH}_4^+ + \text{PO}_4^{3-}$	13.26	Ohlinger
K-struvite	$\text{MgKPO}_4 \cdot 6\text{H}_2\text{O} \leftrightarrow \text{Mg}^{2+} + \text{K}^+ + \text{PO}_4^{3-}$	10.6	TaylorAW
Hydroxyapatite	$\text{Ca}_5(\text{PO}_4)_3\text{OH} \leftrightarrow 5\text{Ca}^{2+} + 3\text{PO}_4^{3-} + \text{OH}^-$	44.33	Brezonik
Calcium carbonate	$\text{CaCO}_3 \leftrightarrow \text{Ca}^{2+} + \text{CO}_3^{2-}$	8.48	Morse
Tricalcium phosphate	$\text{Ca}_3(\text{PO}_4)_2 \leftrightarrow 3\text{Ca}^{2+} + 2\text{PO}_4^{3-}$	25.50	Fowler
Dicalcium phosphate	$\text{CaHPO}_4 \leftrightarrow \text{Ca}^{2+} + \text{HPO}_4^{2-}$	6.57	Gregory
Calcium hydroxide	$\text{Ca}(\text{OH})_2 \leftrightarrow \text{Ca}^{2+} + 2\text{OH}^-$	5.19	Skoog
Magnesium hydroxide	$\text{Mg}(\text{OH})_2 \leftrightarrow \text{Mg}^{2+} + 2\text{OH}^-$	11.15	Skoog

$$x_{\text{struvite}}(\text{PO}_4^{3-}) = \frac{0.798}{1 + \left(x_{\text{Ca}^{2+}:\text{PO}_4^{3-}} \cdot 0.576\right)^{2.113}} \quad (\text{D.11})$$

$$\dot{m}_{\text{struvite recovered}} = \dot{m}_{\text{P in}} \cdot x_{\text{struvite}}(\text{PO}_4^{3-}) \cdot \frac{MW_{\text{struvite}}}{MW_{\text{P}}} \quad (\text{D.12})$$

$$\dot{m}_{\text{N recovered}} = \dot{m}_{\text{struvite recovered}} \cdot \frac{MW_{\text{N}}}{MW_{\text{struvite}}} \quad (\text{D.13})$$

$$\dot{m}_{\text{N released}} = \dot{m}_{\text{N in}} - \dot{m}_{\text{struvite recovered}} \cdot \frac{MW_{\text{N}}}{MW_{\text{struvite}}} \quad (\text{D.14})$$

D.1.5 MAPHEX

The mass balances of MAPHEX process are shown in Eqs. D.15-D.19, based on experimental data for full-scale modular units reported by church_versatility2018.

$$\dot{m}_{\text{nutrients recovered}} = \dot{m}_{\text{nutrients, in}} \cdot \eta_{\text{MAPHEX}}^{\text{nutrients}}, \quad (\text{D.15})$$

$$\forall \text{ nutrients} \in \{\text{P, N}\}$$

$$\dot{m}_{\text{nutrients released}} = \dot{m}_{\text{nutrients, in}} \cdot \left(1 - \eta_{\text{MAPHEX}}^{\text{nutrients}}\right), \quad (\text{D.16})$$

$$\forall \text{ nutrients} \in \{\text{P, N}\}$$

$$\dot{m}_{\text{TS recovered}} = \dot{m}_{\text{TS,in}} \cdot 0.93 \quad (\text{D.17})$$

$$\dot{m}_{\text{water recovered}} = \frac{\dot{m}_{\text{TS recovered}}}{0.25} \cdot 0.75 \quad (\text{D.18})$$

$$\dot{m}_{\text{water released}} = \dot{m}_{\text{water,in}} - \dot{m}_{\text{water recovered}} \quad (\text{D.19})$$

D.1.6 Transmembrane chemisorption

Characteristics of Liquid-Cel™ Extra Flow membranes are shown in Table D.7. Membrane modules cost are illustrated in Figure D.3.

Table D.7: Main characteristics of Liquid-Cel™ membrane (rongwong2020modelin; ulbricht2013ammoni).

Membrane parameters	Unit	Variable	Values
Number of fibers	$\frac{\text{fibers}}{\text{m}^2_{\text{module}}}$	n_f	$2.13 \cdot 10^6$
Fiber outer diameter	m	d_o	$300 \cdot 10^{-6}$
Fiber inner diameter	m	d_i	$240 \cdot 10^{-6}$
Pore diameter	m	a	$0.04 \cdot 10^{-6}$
Porosity	-	ε	0.40
Tortuosity factor	-	τ	2.60
Pressure drop shell side	bar	$\Delta P_{\text{shell side}}$	0.3
Pressure drop lumen side	bar	$\Delta P_{\text{lumen side}}$	2

The main parameters for membrane modeling are collected in Eqs. D.20-D.33. Digestate density (ρ) and (μ) viscosity were assumed equal to those of water. Correlations to estimate these parameters are reported by hsu1997densities. Ammonia Henry's constant (H_{NH_3}) have been taken from linstrom2001nist.

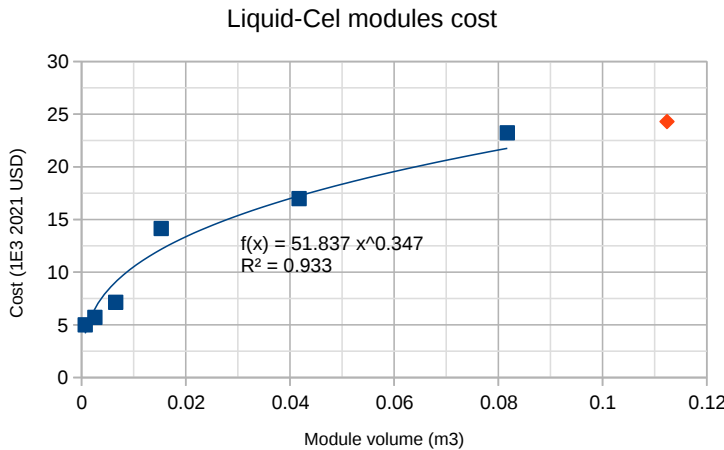


Figure D.3: Estimation of Liquid-CelTM 14x40 membrane module cost.

$$\rho_{\text{water}} \left(\frac{\text{kg}}{\text{m}^3} \right) = (10^3) \cdot (0.863559 + 1.21494 \cdot 10^{-3} \cdot T(\text{K}) - 2.5708 \cdot 10^{-6} \cdot T(\text{K})^2) \quad (\text{D.20})$$

$$\mu_{\text{water}} \left(\frac{\text{kg}}{\text{m} \cdot \text{s}} \right) = (10^{-6}) \cdot \left(\rho \cdot e^{-3.28285 + \frac{456.029}{T(\text{K}) - 154.576}} \right) \quad (\text{D.21})$$

$$H_{\text{NH}_3} \left(\frac{\text{kmol}}{\text{atm} \cdot \text{m}^3} \right) = 58 \cdot e^{4100 \cdot \left(\frac{1}{T(\text{K})} - \frac{1}{298.15} \right)} \quad (\text{D.22})$$

The cross-sectional area of the lumen area is calculated based on the transverse area of hollow fiber, and the number of fibers in the membrane module, Eq. D.24. Shell area is calculated as the difference between total and lumen side cross-sectional areas. Velocities of digestate and stripping fluid (i.e., sulfuric acid solution) are computed based on their respective volumetric flow and transverse areas.

$$n_{f_{\text{module}}} = A_{\text{module}} \cdot n_f \quad (\text{D.23})$$

$$A_{\text{lumen side}} \left(\text{m}^2 \right) = \frac{d_i^2}{4} \cdot \pi \cdot n_{f_{\text{module}}} \quad (\text{D.24})$$

$$A_{\text{shell side}} \left(\text{m}^2 \right) = \frac{D_{\text{module}}^2}{4} \cdot \pi - A_{\text{lumen side}} \quad (\text{D.25})$$

$$V_{\text{stripping fluid}} \left(\frac{\text{m}}{\text{s}} \right) = \frac{\dot{V}_{\text{stripping fluid}}}{A_{\text{lumen side}}} \quad (\text{D.26})$$

$$V_{\text{digestate}} \left(\frac{\text{m}}{\text{s}} \right) = \frac{\dot{V}_{\text{digestate}}}{A_{\text{shell side}}} \quad (\text{D.27})$$

Diffusion of ammonia through the membrane is driven by bulk and Knudsen diffusivities, which consider the mean free path of molecules and the pore diameter respectively. Bulk diffusivity of ammonia is calculated based on the kinetic theory, using Eq. D.29, while Knudsen diffusivity depends on the molecular velocity, Eq. D.28, and pore diameter, Eq. D.31 [agrahari2012model](#). Both contributions to ammonia transport are combined in an effective diffusion coefficient, Eq. D.32. Ammonia diffusion in liquid phase has been assumed equal to ammonia diffusion in water, which is calculated using Eq. D.33.

$$\bar{v} \left(\frac{\text{m}}{\text{s}} \right) = \left(\frac{8 \cdot R \left(\frac{\text{J}}{\text{mol} \cdot \text{K}} \right) \cdot T (\text{K})}{MW_{\text{NH}_3} \left(\frac{\text{kg}}{\text{mol}} \right) \cdot \pi} \right)^{1/2} \quad (\text{D.28})$$

$$D_{\text{NH}_3} \left(\frac{\text{m}^2}{\text{s}} \right) = \frac{1}{3} \cdot \lambda \cdot \bar{v} \quad (\text{D.29})$$

$$\lambda (\text{m}) = \frac{\kappa \left(\frac{\text{J}}{\text{K}} \right) \cdot T (\text{K})}{\pi \cdot \sigma_{\text{NH}_3}^2 (\text{m}^2) \cdot P (\text{Pa}) \cdot 2^{1/2}} \quad (\text{D.30})$$

$$D_{\text{NH}_3_{\text{Kn}}} \left(\frac{\text{m}^2}{\text{s}} \right) = \frac{d_{\text{pore}}}{3} \cdot \left(\frac{8 \cdot R \left(\frac{\text{J}}{\text{mol} \cdot \text{K}} \right) \cdot T (\text{K})}{\pi \cdot MW_{\text{NH}_3} \left(\frac{\text{kg}}{\text{mol}} \right)} \right)^{1/2} \quad (\text{D.31})$$

$$D_{\text{eff}} \left(\frac{\text{m}^2}{\text{s}} \right) = \frac{1}{\frac{1}{D_{\text{NH}_3_{\text{Kn}}}} + \frac{1}{D_{\text{NH}_3}}} \quad (\text{D.32})$$

$$D_{\text{NH}_3_{\text{water}}} \left(\frac{\text{m}^2}{\text{s}} \right) = 1.96 \cdot 10^{-9} \cdot \frac{\mu_{\text{water}_{T=298\text{K}}}}{\mu_{\text{water}_T}} \cdot \frac{T (\text{K})}{298} \quad (\text{D.33})$$

The distribution of ammonia species shown in Eq. 7.10 is calculated at initial conditions based on the pH of the digestate stream being fed through the tube side of the membrane module, which is assumed equal to 11, as shown in Eqs. D.34-D.38.

$$f_{\text{NH}_3} = \frac{1}{10^{(pK_{a_{\text{NH}_3}} - pH)} + 1} \quad (\text{D.34})$$

$$pK_{a_{\text{NH}_3}} \left(\frac{\text{kmol}}{\text{m}^3} \right) = 0.0901821 + \frac{2729.92}{T (\text{K})} \quad (\text{D.35})$$

$$[\text{NH}_3] = [\text{N}_{\text{inorg}}] \cdot f_{\text{NH}_3} \quad (\text{D.36})$$

$$[\text{NH}_4^+] = [\text{N}_{\text{inorg}}] \cdot (1 - f_{\text{NH}_3}) \quad (\text{D.37})$$

$$[\text{H}^+] = K_a \cdot \frac{[\text{NH}_4^+]}{[\text{NH}_3]} \quad (\text{D.38})$$

A modified Henry's constant considering the speciation of ammonia is used in the model proposed by [rongwong2020modelin](#) to evaluate the liquid-solid equilibrium of ammonia, Eq. D.39.

$$H_{\text{NH}_3}^* = H_{\text{NH}_3} \cdot \left(1 + \frac{K_a \cdot [\text{H}^+]}{K_w} \right) \quad (\text{D.39})$$

The mass transfer coefficient of the digestate flowing in the tube side, $k_{\text{digestate}}$, is calculated through the Sherwood number of this stream, Eq. D.40.

$$\begin{aligned} \text{Sh}_{\text{digestate}} &= \frac{k_{\text{digestate}} \cdot d_i}{D_{\text{NH}_3\text{water}}} = \\ &1.62 \cdot \left(\frac{d_i}{L} \cdot \text{Re}_{\text{digestate}} \cdot \text{Sc}_{\text{digestate}} \right)^{1/3} \end{aligned} \quad (\text{D.40})$$

$$\text{Re}_{\text{digestate}} = \frac{d_i \cdot \rho_{\text{digestate}} \cdot V_{\text{digestate}}}{\mu_{\text{digestate}}} \quad (\text{D.41})$$

$$\text{Sc}_{\text{digestate}} = \frac{\mu_{\text{digestate}}}{\rho_{\text{digestate}} \cdot D_{\text{NH}_3\text{water}}} \quad (\text{D.42})$$

The membrane phase can be divided into non-wetted and wetted membrane sections. Their mass transfers coefficients, k_M and k'_M respectively, are calculated based on the fraction of membrane wetted by the digestate. This is calculated based on a correlation reported by [rongwong2020modelin](#), shown in Eq. D.43. Eqs. D.45-D.46 and D.47-D.48 show the equations employed for the estimation of k_M and k'_M respectively.

$$w_{\text{membrane}} = \frac{0.368}{2.709 + e^{-17.486 \cdot (V_{\text{digestate}} - 0.25)}} \quad (\text{D.43})$$

$$d_{\text{interfacial}} (\text{m}) = d_i + w_{\text{membrane}} \cdot (d_o - d_i) \quad (\text{D.44})$$

$$k_M \left(\frac{\text{m}}{\text{s}} \right) = \frac{D_{\text{eff}} \cdot \varepsilon}{\tau \cdot \delta_{\text{non-wetted}}} \quad (\text{D.45})$$

$$\delta_{\text{non-wetted}} (\text{m}) = \frac{d_o - d_{\text{interfacial}}}{2} \quad (\text{D.46})$$

$$k'_M \left(\frac{\text{m}}{\text{s}} \right) = \frac{D_{\text{water}} \cdot \varepsilon}{\tau \cdot \delta_{\text{wetted}}} \quad (\text{D.47})$$

$$\delta_{\text{wetted}} (\text{m}) = \frac{d_{\text{interfacial}} - d_i}{2} \quad (\text{D.48})$$

The overall mass transfer coefficient is calculated based on the liquid, wetted membrane, and non-wetted membranes mass transfer coefficients, as shown in Eq. D.49. However, high ammonia concentrations result in a

decrease of the overall mass transfer (**zhu2005modified**). Therefore, K_{ov} is modified using a correction factor that consider the concentration of ammonia in digestate.

$$K_{ov} \left(\frac{\text{m}}{\text{s}} \right) = \frac{1}{\left(\frac{1}{k_{\text{digestate}} \cdot d_i} + \frac{1}{k'_M \cdot \delta_{\text{ln wetted}}} + \frac{R \left(\frac{\text{atm} \cdot \text{m}^3}{\text{kmol} \cdot \text{K}} \right) \cdot T(\text{K}) \cdot H_{\text{NH}_3}^*}{k_M \delta_{\text{ln non-wetted}}} \right) \cdot d_o} \quad (\text{D.49})$$

$$\delta_{\text{ln wetted}} = \frac{d_{\text{interfacial}} - d_i}{\ln \left(\frac{d_{\text{interfacial}}}{d_i} \right)} \quad (\text{D.50})$$

$$\delta_{\text{ln non-wetted}} = \frac{d_o - d_{\text{interfacial}}}{\ln \left(\frac{d_o}{d_{\text{interfacial}}} \right)} \quad (\text{D.51})$$

$$K_{ov_{\text{corrected}}} \left(\frac{\text{m}}{\text{s}} \right) = K_{ov} \cdot \left(1 - \frac{0.002728 \cdot [\text{NH}_3] \left(\frac{\text{mg}}{\text{L}} \right)}{100} \right) \quad (\text{D.52})$$

The mass balance along the membrane can be performed considering the mass transfer in an infinitesimal element of the membrane, as shown in Eq. D.53. Due to the excess of sulfuric acid in the lumen side that lead to the formation of ammonium sulfate from the ammonia recovered, the concentration of ammonia in the lumen side is assumed negligible. This differential expression can be analytically integrated to estimate the total length of the membrane, Eq. D.54.

$$\begin{aligned} \frac{\dot{n}_{\text{NH}_3}}{dz} &= -n_{f_{\text{module}}} \cdot \pi \cdot d_o \cdot K_{ov_{\text{corrected}}} \cdot \left(\frac{\dot{n}_{\text{NH}_3}}{\dot{V}_{\text{digestate}}} - \frac{H_{\text{NH}_3}^* \cdot p_{\text{NH}_3}}{\dot{V}_{\text{digestate}}} \right) \\ &\approx -n_{f_{\text{module}}} \cdot \pi \cdot d_o \cdot K_{ov_{\text{corrected}}} \cdot \frac{\dot{n}_{\text{NH}_3}}{\dot{V}_{\text{digestate}}} \end{aligned} \quad (\text{D.53})$$

$$z \text{ (m)} = \ln \left(\frac{\dot{n}_{\text{NH}_3_{\text{final}}}}{\dot{n}_{\text{NH}_3_{\text{initial}}}} \right) \cdot \frac{\dot{V}_{\text{digestate}}}{-n_{f_{\text{module}}} \cdot \pi \cdot d_o \cdot K_{ov_{\text{corrected}}}} \quad (\text{D.54})$$

Pumps to drive the digestate and stripping fluid streams are needed. Their cost is estimated using Eqs. D.55 and D.56, assuming that the maximum capacity of one single pump ($\dot{V}_{\text{pump}_{\text{max}}}$) is $1 \text{ m}^3/\text{s}$ (**peters2003plant**). Pumps operating cost are estimated through Eqs. D.57 to D.59, calculating the energy needed to balance the pressure drop of the shell and lumen

sides of the membrane, Table D.7. Pump efficiencies (η_{pump_i}) of 0.8 are assumed.

$$n_{\text{pump}_i} = \left\lceil \frac{\dot{V}_i}{\dot{V}_{\text{pump}_{\max}}} \right\rceil \quad (\text{D.55})$$

$$\text{CAPEX}_{\text{pumps}_i} \text{ (2019 USD)} = \begin{cases} (-50.387 \cdot 10^6 \cdot \dot{V}_i^2 + 1.607 \cdot 10^6 \cdot \dot{V}_i \\ + 5.127 \cdot 10^3) \cdot n_{\text{pump}_i} \cdot 1.055 & \text{if } \dot{V}_i \leq 9 \cdot 10^{-3} \frac{\text{m}^3}{\text{s}} \\ (92.562 \cdot 10^3 \cdot \dot{V}_i^{0.381}) \cdot n_{\text{pump}_i} \cdot 1.055 & \text{if } \dot{V}_i > 9 \cdot 10^{-3} \frac{\text{m}^3}{\text{h}} \end{cases} \quad (\text{D.56})$$

$$H_i \text{ (m)} = \frac{\Delta P_i \text{ (Pa)}}{\rho \left(\frac{\text{kg}}{\text{m}^3} \right) g \left(\frac{\text{m}}{\text{s}^2} \right)} \quad (\text{D.57})$$

$$\dot{W}_{\text{pump}_i} \text{ (kW)} = \frac{g \left(\frac{\text{m}}{\text{s}^2} \right) \cdot H_i \text{ (m)} \cdot \rho \left(\frac{\text{kg}}{\text{m}^3} \right) \cdot \dot{V}_i \left(\frac{\text{m}^3}{\text{s}} \right)}{\eta_{\text{pump}_i}} \quad (\text{D.58})$$

$$\text{OPEX}_{\text{pumps}} \left(\frac{2019 \text{ USD}}{\text{year}} \right) = \sum_i \dot{W}_{\text{pump}_i} \text{ (kW)} \cdot t_{\text{operation}} \text{ (s)} \cdot 3600 \\ \cdot \text{Price}_{\text{electricity}} \left(\frac{\text{USD}}{\text{kWh}} \right) \forall i \in \{\text{shellside, lumenside}\} \quad (\text{D.59})$$

D.1.7 Ammonia evaporation

The following assumptions have been made for the modeling of digestate drying:

- $c_{p_{\text{digestate}_{\text{in}}}} \approx c_{p_{\text{water}}}$
- $P_{\text{water}} + P_{\text{NH}_3} \approx P_{\text{water}}$
- $T_{\text{out}_{\text{air}}} = T_{\text{out}_{\text{digestate}}}$
- $\alpha = \text{constant}$

The mass and energy balances for digestate drying in a belt dryer unit are shown in Eqs. D.60-D.62 and D.63-D.72 respectively

$$\dot{m}_{\text{NH}_3 \text{ evap}} = \dot{m}_{\text{NH}_3 \text{ in}} \cdot \eta_{\text{belt dryer}}^{\text{NH}_3} \quad (\text{D.60})$$

$$\frac{\dot{m}_{\text{water evap}}}{\sum_j \frac{\dot{m}_j}{MW_j}} \cdot P_{\text{total}} \leq Pv_{\text{water}}(T) \quad \forall j \in \{\text{air, H}_2\text{O, NH}_3\} \quad (\text{D.61})$$

$$\frac{\dot{m}_{\text{NH}_3 \text{ evap}}}{\sum_j \frac{\dot{m}_j}{MW_j}} \leq Pv_{\text{NH}_3}(T) \quad \forall j \in \{\text{air, H}_2\text{O, NH}_3\} \quad (\text{D.62})$$

$$\dot{Q}_{\text{Belt Dryer}} = \dot{H}_{\text{latent}} + \dot{H}_{\text{sensible}} = \dot{H}_{\text{air in}} - \dot{H}_{\text{air out}} \quad (\text{D.63})$$

$$\dot{H}_{\text{latent}} = \dot{m}_{\text{water evap}} \cdot \lambda_{\text{evap water}}(T) + \dot{m}_{\text{NH}_3 \text{ evap}} \cdot \lambda_{\text{evap NH}_3}(T) \quad (\text{D.64})$$

$$\dot{H}_{\text{sensible}} = \dot{H}_{\text{digestate out}} - \dot{H}_{\text{digestate in}} + \dot{H}_{\text{sensible gases}} \quad (\text{D.65})$$

$$\dot{H}_{\text{sensible gases}} = \left(\dot{m}_{\text{water evap}} + \dot{m}_{\text{NH}_3 \text{ evap}} \right) \cdot c_{p_{\text{water (liquid)}}} \cdot T_{\text{air out}} \quad (\text{D.66})$$

$$\dot{H}_{\text{digestate in}} = \dot{m}_{\text{digestate in}} \cdot c_{p_{\text{water}}} \cdot \Delta T_{\text{digestate in}} \quad (\text{D.67})$$

$$\dot{H}_{\text{digestate out}} = \dot{m}_{\text{digestate out}} \cdot c_{p_{\text{digestate}}} \cdot \Delta T_{\text{digestate out}} \quad (\text{D.68})$$

$$c_{p_{\text{digestate}}} \left(\frac{\text{kg}}{\text{kJ} \cdot \text{K}} \right) = 4.19 - 0.0275 \cdot \left(\frac{\dot{m}_{\text{TS out}}}{\dot{m}_{\text{digestate out}}} \cdot 100 \right) \quad (\text{D.69})$$

$$\dot{H}_{\text{air in}} = \dot{m}_{\text{air}} \cdot c_{p_{\text{air}}} \cdot \Delta T_{\text{air in}} \quad (\text{D.70})$$

$$\dot{H}_{\text{air out}} = \left(\dot{m}_{\text{air}} \cdot c_{p_{\text{air}}} + \dot{m}_{\text{water evap}} \cdot c_{p_{\text{water (gas)}}} + \dot{m}_{\text{NH}_3 \text{ evap}} \cdot c_{p_{\text{NH}_3 \text{ (gas)}}} \right) \cdot \Delta T_{\text{air out}} \quad (\text{D.71})$$

$$\Delta T_i = T_i - T_{\text{ref}} \quad \forall i \in \{\text{air in, air out, digestate in, digestate out}\} \quad (\text{D.72})$$

D.1.8 Stripping in packed tower

The liquid mass velocity is a known parameter since it corresponds to the digestate being processed. The gas velocity is estimated by combining Eqs. 7.23, 7.24 and 7.27. The design gas mass velocity considered is 0.7 time the gas mass velocity, Eq 7.28, while the liquid design mass velocity is computed by combining Eqs. 7.28 and 7.27. Tower diameter is computed based on the design liquid mass velocity and liquid mass flow. However, design restrictions reported by (Brana2005) have been considered in the sizing of the packed tower. Tower height is estimated through the height and number of transfer units, Eqs D.73 and D.74. Therefore, the design diameter is computed as shown in Eqs. D.75 to D.77. Additionally, the number of packed towers that have to be installed in-parallel arrangement is estimated through Eq. D.78.

$$D_{\text{design}} \leq 1.2 \text{ m} \quad (\text{D.73})$$

$$\frac{H_{\text{design}}}{D_{\text{design}}} \leq 30 \quad (\text{D.74})$$

$$A_{\text{stripping tower}} = \frac{\dot{m}_L}{G_{L_{\text{design}}}} \quad (\text{D.75})$$

$$D_{\text{stripping tower}} = \left(\frac{A_{\text{stripping tower}}}{\pi} \right)^{0.5} \quad (\text{D.76})$$

$$D_{\text{stripping tower}}^{\text{design}} \text{ (m)} = \begin{cases} D_{\text{stripping tower}} & \text{if } D_{\text{stripping tower}} \leq 1.2 \text{ m} \\ 1.2 & \text{if } D_{\text{scrubber}} > 1.2 \text{ m} \end{cases} \quad (\text{D.77})$$

$$n_{\text{stripping tower}}^{\text{parallel}} = \left\lceil \frac{D_{\text{stripping tower}}(\text{m})}{1.2} \right\rceil \quad (\text{D.78})$$

The height of the stripping packed towers is estimated through the height and number of transfer units, Eq. D.79 and D.80 respectively (**Metcalf2014**). The liquid overall mass transfer coefficient value assumed for the ammonia air system is 2 h^{-1} (**larsen2013so**). The design restriction shown in Eq. D.74 is considered to compute the design height of the stripping towers, and the number of units that must be installed in series, Eq. D.83.

$$HTU = \frac{\frac{\dot{m}_L}{n_{\text{stripping tower}}^{\text{parallel}} \cdot \rho_{\text{digestate}}}}{K_{La} \cdot \pi \cdot \left(\frac{D_{\text{stripping tower}}}{2} \right)^2} \quad (\text{D.79})$$

$$NTU = \frac{S}{S - 1} \ln \left(\frac{\frac{1}{1 - \eta_{\text{stripping tower}}/100} \cdot (S - 1) + 1}{S} \right) \quad (\text{D.80})$$

$$S = \frac{H_{\text{NH}_3}}{P_{\text{stripping tower}}} \cdot \frac{\dot{m}_G}{\dot{m}_L} \quad (\text{D.81})$$

$$H_{\text{stripping tower}} = NTU \cdot HTU \quad (\text{D.82})$$

$$n_{\text{stripping tower}}^{\text{series}} = \left\lceil \frac{\frac{H_{\text{stripping tower}}}{D_{\text{stripping tower}}^{\text{design}}}}{30} \right\rceil \quad (\text{D.83})$$

$$H_{\text{stripping tower}}^{\text{design}} \text{ (m)} = \begin{cases} H_{\text{stripping tower}} & \text{if } \frac{H_{\text{stripping tower}}}{D_{\text{stripping tower}}} \leq 30 \\ \frac{\frac{\dot{m}_L}{n_{\text{stripping tower}}^{\text{series}} \cdot n_{\text{stripping tower}}^{\text{parallel}} \cdot \rho_{\text{digestate}}}}{K_{La} \cdot \pi \cdot \left(\frac{D_{\text{stripping tower}}}{2} \right)^2} & \text{if } \frac{H_{\text{stripping tower}}}{D_{\text{stripping tower}}} \geq 30 \end{cases} \quad (\text{D.84})$$

D.1.9 Acidic scrubbing

Mass balances to scrubber unit consider the water transferred to the gas stream, assuming that saturation is reached, Eq. D.86. Ammonia recovery efficiency ($\eta_{scrubber}^{NH_3}$) of full-scale ammonia scrubbers has been reported in the range of 40% to 99% (melse2005air). A typical $\eta_{scrubber}^{NH_3}$ of 96% has been selected based on the work of melse2005air.

$$\frac{P_{water}}{Pv_{water}} = 1 \quad (D.85)$$

$$Pv_{water} = \frac{\frac{\dot{m}_{water_out}^{gas\ stream}}{MW_{water}}}{\sum_j \frac{\dot{m}_j^{gas\ stream}}{MW_j}} \cdot P_{in}^{gas\ stream} \quad (D.86)$$

$$\dot{m}_{NH_3\ out}^{gas\ stream} = \dot{m}_{NH_3\ in}^{gas\ stream} \cdot (1 - \eta_{scrubber}^{NH_3}) \quad (D.87)$$

The water flow needed to perform the scrubbing operation is computed from the operation line of the unit (L/G), Eq. D.88. Following the rules of thumb for scrubbing units, the design operation line has been assumed as twice the minimum operation line, Eq. D.89. Y_{NH_3} and X_{NH_3} denote the ammonia free basis molar fractions in gas and liquid streams respectively. The amount of sulfuric acid supplied to make-up the sulfate used for ammonium sulfate formation, Eq. D.91, is slightly larger than the stoichiometric amount of the precipitation reaction, 3.5 kg_{H₂SO₄} per kg_{NH₃} recovered (bolzonella2018nutr).

$$(L/G)_{min} = \frac{Y_{NH_3\ in} - Y_{NH_3\ out}}{X_{NH_3\ out} - X_{NH_3\ in}} \quad (D.88)$$

$$(L/G) = (L/G)_{min} \cdot 2 \quad (D.89)$$

$$\dot{m}_{water_in}^{liquid\ stream} = ((L/G) \cdot \dot{n}_{total,in}^{liquid\ stream} - \dot{n}_{NH_3\ in}^{liquid\ stream}) \cdot MW_{water} \quad (D.90)$$

$$\dot{m}_{H_2SO_4,in}^{liquid\ stream} = \dot{m}_{NH_3\ in}^{gas\ stream} \cdot \eta_{scrubber}^{NH_3} \cdot 3.5 \quad (D.91)$$

$$\dot{m}_{(NH_4)_2SO_4,out}^{liquid\ stream} = \frac{\dot{m}_{NH_3\ in}^{gas\ stream} \cdot \eta_{scrubber}^{NH_3}}{MW_{NH_3}} \cdot MW_{(NH_4)_2SO_4,out} \quad (D.92)$$

The scrubber diameter, Eq. D.94, is based on the gas velocity in the equipment, which is assumed equal to 1.75 m/s (melse2005air). The number of units is set by the maximum diameter of scrubbers, Eq. D.95, which is assumed equal to 1.2 m according to the rules of thumb for packed columns (Brana2005).

$$D_{\text{scrubber}} (\text{m}) = \frac{\dot{V}_{\text{gas stream}} \left(\frac{\text{m}^3}{\text{s}} \right)}{1.75 \left(\frac{\text{m}}{\text{s}} \right)} \quad (\text{D.93})$$

$$D_{\text{scrubber}}^{\text{design}} (\text{m}) = \begin{cases} D_{\text{scrubber}} & \text{if } D_{\text{scrubber}} \leq 1.2 \text{ m} \\ 1.2 & \text{if } D_{\text{scrubber}} > 1.2 \text{ m} \end{cases} \quad (\text{D.94})$$

$$n_{\text{scrubbers}} = \left\lceil \frac{\dot{V}_{\text{gas stream}} \left(\frac{\text{m}^3}{\text{s}} \right)}{1.75 \left(\frac{\text{m}}{\text{s}} \right) \cdot \frac{1.2^2(\text{m}^2)}{4} \pi} \right\rceil \quad (\text{D.95})$$

The height of scrubbing units is estimated through the height and number of transfer units, Eq. D.96, as described by **couper2005chem**. The number of transfer units is determined by the Kremser shortcut method, as shown in Eq. D.97 (**seader2004prod**), while the height of each transfer unit is calculated in Eq. D.101. The gas film overall mass transfer coefficient value for the ammonia air system is $272474.56 \frac{\text{mol}}{\text{h} \cdot \text{m}^3 \cdot \text{atm}}$ (**Branan2005**). The scrubbing operation involves the use of compressors for pumping the stripping gas stream. The energy required for compression is estimated though Eq. D.102, assuming a compressor efficiency ($\eta_{\text{compressor}}$) of 0.85 and a polytropic coefficient (k) of 1.4. The pressure drop of a typical scrubber for ammonia capture assumed is 200 Pa (**melse2005air**).

$$H_{\text{scrubber}} = NTU \cdot HTU \quad (\text{D.96})$$

$$NTU = \quad (\text{D.97})$$

$$\frac{\ln \left(\left(1 - m \cdot \frac{\dot{n}_{\text{gas stream}}}{\dot{n}_{\text{liquid stream}}} \right) \frac{x_{\text{NH}_3 \text{in}}^{\text{gas stream}} - x_{\text{NH}_3}^*}{x_{\text{NH}_3 \text{out}}^{\text{gas stream}} - x_{\text{NH}_3}^*} + m \cdot \frac{\dot{n}_{\text{gas stream}}}{\dot{n}_{\text{liquid stream}}} \right)}{\ln \left(m \cdot \frac{L}{V} \right)}$$

$$x_{\text{NH}_3 k}^{\text{gas stream}} = \frac{\dot{n}_{\text{NH}_3 k}^{\text{gas stream}}}{\dot{n}_{\text{gas stream}}}, \forall k \in \{\text{in}, \text{out}\} \quad (\text{D.98})$$

$$x_{\text{NH}_3}^* = 0 \quad (\text{D.99})$$

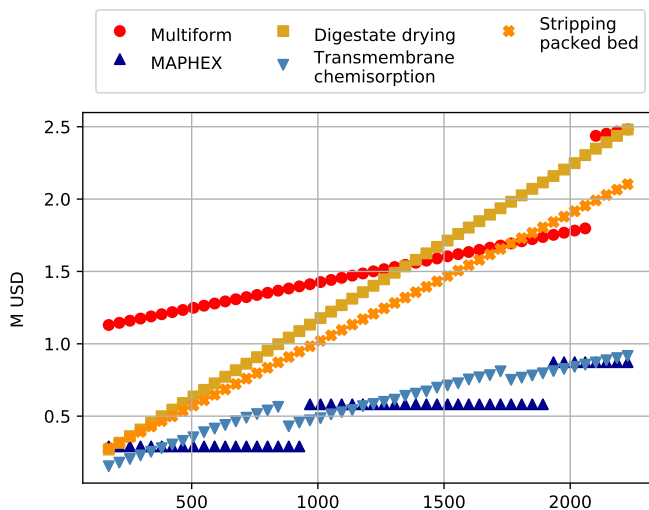
$$m = \frac{P_{\text{NH}_3}}{P} \quad (\text{D.100})$$

$$HTU = \frac{\dot{n}_{\text{gas stream}} \left(\frac{\text{mol}}{\text{h}} \right)}{\pi \cdot \frac{D_{\text{scrubber}}^{\text{design}}}{4} (\text{m}^2) \cdot k_{GA} \left(\frac{\text{mol}}{\text{h} \cdot \text{m}^3 \cdot \text{atm}} \right) \cdot P (\text{atm})} \quad (\text{D.101})$$

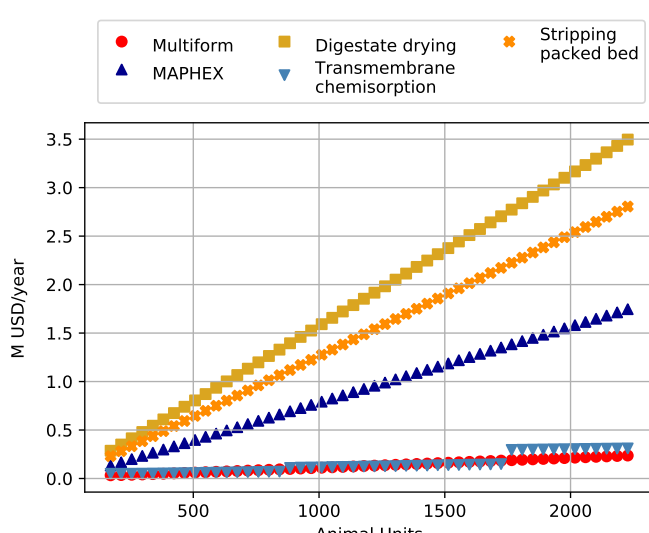
$$\dot{W}_{\text{compressor}} (\text{kW}) = \frac{k \cdot R \left(\frac{\text{J}}{\text{K} \cdot \text{kmol}} \right) \cdot T_{in}^{\text{gas stream}} (\text{K}) \cdot \dot{m}_{in}^{\text{gas stream}} \left(\frac{\text{kg}}{\text{s}} \right)}{\eta_{\text{compressor}} \cdot (k - 1) \cdot MW_{\text{gas}}}.$$

$$\left(\left(\frac{P_{in}^{\text{gas stream}}}{P_{out}^{\text{gas stream}}} \right)^{\frac{k-1}{k}} - 1 \right) \quad (\text{D.102})$$

D.2 CAPITAL AND OPERATING EXPENSES

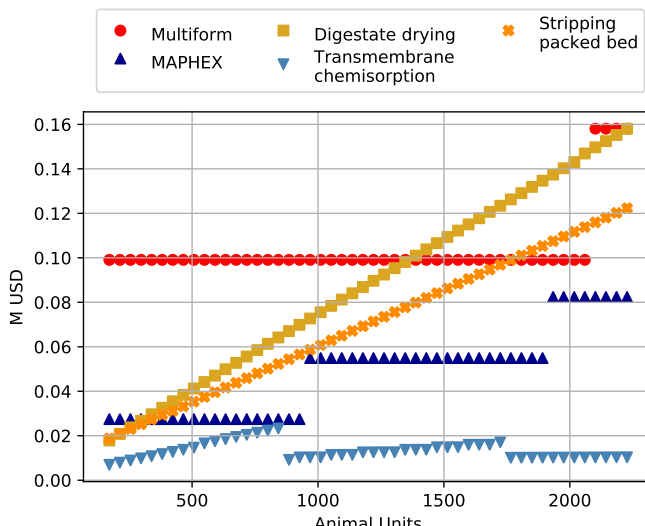


(a) CAPEX

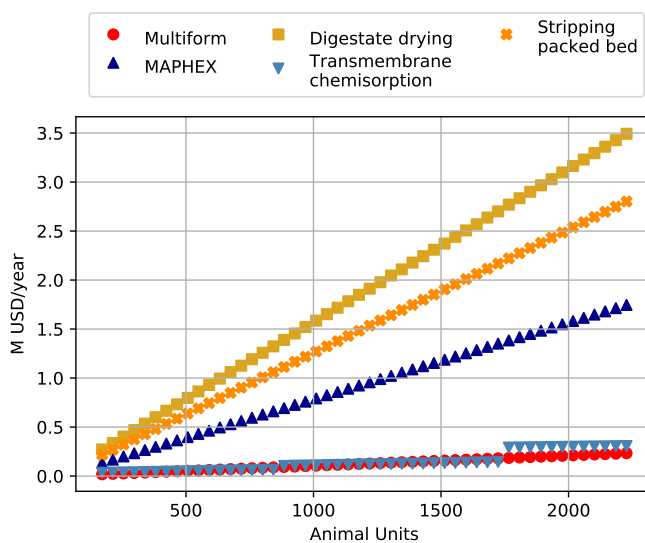


(b) OPEX

Figure D.4: CAPEX and OPEX of the assessed nitrogen recovery technologies, including the cost of anaerobic digestion stage.



(a) CAPEX



(b) OPEX

Figure D.5: CAPEX and OPEX of the assesed nitrogen recovery technologies, excluding the cost of anaerobic digestion stage.

D.3 PROCESSING COST

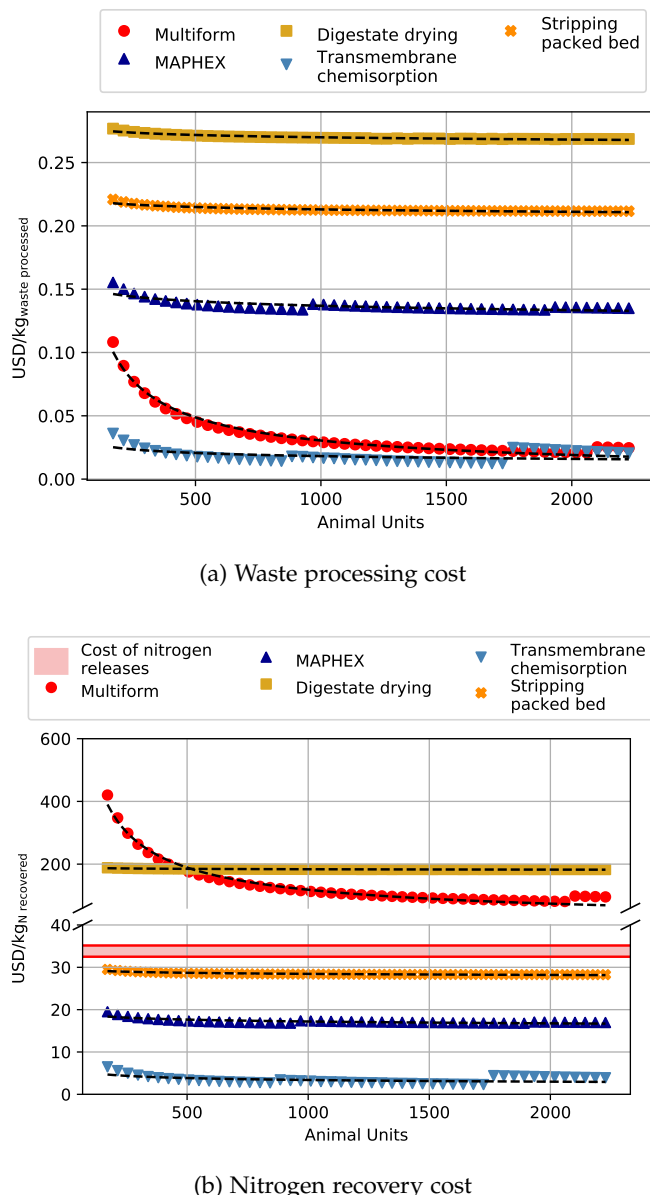


Figure D.6: Processing cost for different livestock facility sizes, excluding the cost of anaerobic digestion stage.

Table D.8: Correlations to estimate the processing cost of the evaluated technologies as a function of animal units (AU), excluding the cost of anaerobic digestion stage.

System	Waste processing cost		Total nitrogen recovery cost (USD/kg _N recovered)
	(USD/kg _{waste processed})	Parameters	
Correlation	Parameters	Parameters	
Digestate drying	$a=0.289$ $b=-0.00974$		$a=196.534$ $b=-0.00974$
Multiform	$a=3.261$ $b=-0.676$		$a=12660.077$ $b=-0.676$
MAPHEX	$C = a \cdot AU^b$	$a=0.177$ $b=-0.0372$	$a=22.240$ $b=-0.0372$
Stripping in packed tower		$a=0.233$ $b=-0.0128$	$a=31.089$ $b=-0.0128$
Membrane		$a=0.0410$ $b=-0.135$	$a=7.488$ $b=-0.132$

BIBLIOGRAPHY

E

APPENDIX E: SUPPLEMENTARY INFORMATION OF CHAPTER 8

E.1 LITERATURE REVIEW

The literature available referred to CO₂ capture is extensive, not only for combustion processes also for the particular case of biogas upgrading, there exists a lack of literature regarding the selection of the most appropriate biogas upgrading technology. It should be noted that the goal of this work it is not limited to the optimization the biogas production and upgrading processes, which it is implicitly done in the work, but the aim pursued is to determine the optimal biogas upgrading technology among the different feasible processes.

This lack in the literature was detected after a literature review, carried out with special emphasis in specific studies about biogas upgrading. On one hand, as a result of the literature review made, it could be concluded that the literature about reviews of biogas upgrading processes is extensive, even when only recent works are considered, as it is shown in Table E.1. On the other hand, just a few recent works are approaching to carry out a systematic comparison of the processes, such as the work of **collet2017techno**, where a comparison of several CO₂ capture technologies using experimental data from other studies is presented, but without integrating and optimizing the biogas production and upgrading processes, or the study of **vo2018techno**, where simulations of biogas upgrading processes limited to amine scrubbing and biological methanation are carried out, not including some essential upgrading technologies such as membranes or PSA. Other works, including but not limited to **capra2018biogas; curto2019renewable; gilassi2019optimizing**, determine the optimal biogas upgrading process but analyzing only one technology in each case (amines scrubbing, biogas methanation, and membrane separation). In the work presented, 5 technologies have been evaluated considering both heuristic and mathematical modelling stages (biogas methanation, water scrubbing, pressure swing adsorption systems, amines scrubbing, and membranes separation systems).

Table E.1: Relevant literature for biogas upgrading.

Author	Study performed
angelidakis2018biogas	Review of biogas upgrading technologies
awe2017review	Review of biogas upgrading technologies
bauer2013biogas	Review of biogas upgrading technologies
khan2017biogas	Review of biogas upgrading technologies
miltner2017review	Review of biogas upgrading technologies
sun2015selection	Review of biogas upgrading technologies
zhou2017alternative	Review of biogas upgrading technologies
collet2017techno	Techno-economic and life cycle assessment of biogas upgrading
ferella2019techno	Techno-economic assesment of strategic plans for biogas upgrading plants
toledo2017comparative	Comparison of photosynthetic and physico-chemical biogas upgrading processes
v2018techno	Simulation of amine scrubbing and biological methanation
capra2018biogas	Optimal selection of amine scrubbing process for biogas upgrading
curto2019renewable	Optimal selection of renewable biogas methanation processes
filipetto2019optimization	Optimal selection of membrane separation process for biogas upgrading
gilassi2019optimizing	Optimal selection of membrane separation process for biogas upgrading
morero2017evaluation	Optimal selection of amine scrubbing process for biogas upgrading

E.2 MODELLING APPROACH

E.2.1 Amines

The CO₂ absorption systems using amines typically operate at low temperatures, around 25-30 °C, and partial pressures above 0.05 bar, reaching removal yields of 90%-95% (**zhang2013modeling**). In contrast to postcombustion gases, which contains large amounts of nitrogen from air, biogas is composed mainly by methane and CO₂, resulting in higher carbon dioxide partial pressures and in the need for lower operating pressures. CO₂ partial pressures above 0.1 bar have been assumed to secure high removal yields (**zhang2013modeling**), resulting in the need to operate at total pressures around 1-1.5 bar to secure the appropriate CO₂ partial pressures (**movaghernajad2011simulation; xue2017comparative**).

The total amount of solution of amines needed to absorb the CO₂ from the gas stream is calculated as a function of the amount of sour gases eliminated, Eq. E.1. According to **2012gpsa**, the concentration of solution and the correction factor (GPSA) depend on the amine used, as is shown in Table E.2. The flow of the amine solutions depends on their solubility. Thus, for a fixed removal ratio, the amines solution flow required changes from one to another. It is considered there is no methane absorption in the amines flow, therefore all biomethane entering in the unit leaves the column and it is sent to storage.

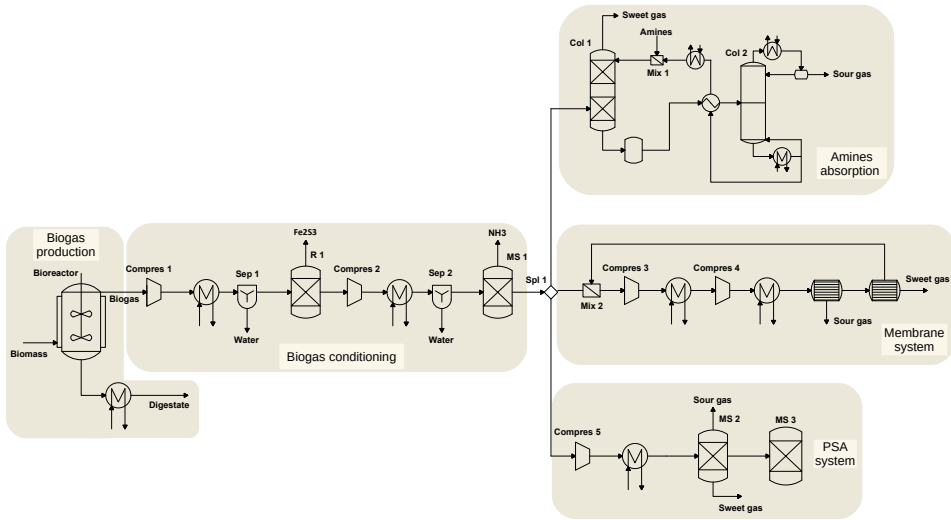


Figure E.1: Scheme of the proposed superstructure for biogas upgrading into biomethane.

$$fc_{amine} = \frac{MW_{amine}}{[amine]} \cdot \left(\frac{CO_{2eff} \cdot fc_{CO_2}}{MW_{CO_2}} \right) \cdot \left(\frac{1}{GPSA} \right) \quad (\text{E.1})$$

The solution of amine used in column 1 comes from two sources, as it shown in Eq. E.2, i.e., the amines from the regeneration column (column 2 in Figure 1), and some make-up solution to replace the amine losses with the gas outlet stream in the regeneration column. Additionally, to mix the two streams of amines at the same temperature, a heat exchanger is used to adjust the temperature of the amine flow stream which leaves the regeneration column to 25 °C.

$$fc_{amine} = fc_{recycled\ amine} + fc_{fresh\ amine} \quad (\text{E.2})$$

The mixing of the two amines streams is assumed to be adiabatic. The energy balance to the heat exchanger is as follows, Eq. E.3.

$$Q = F_{amine} \cdot q_{heat,amine} \quad (\text{E.3})$$

Where F_{amine} is referred to the total mass flow of the amines stream, and q_{amine} the heat flow ratio based on the rules of thumb reported by 2012gpsa. The values are collected in Table E.2.

The assumed CO₂ removal efficiency in the absorption column is 0.95, based on literature data (zhang2013modeling). The sour gas is absorbed

by the amines in the absorption column, being withdrawn from the gas phase. The absorption is an exothermic process. Therefore, this energy is to be refrigerated, and the operation of the column is isothermal, Eq. E.4. The heats of reaction are shown in Table E.3.

$$Q_{Col1} = \Delta H_{react,amine} \cdot CO_{2_{eff}} \cdot f c_{CO_2} \quad (\text{E.4})$$

The biomethane leaves the column and it is sent to storage. On the other hand, the amine with the CO₂ absorbed is sent to the regeneration column (column 2). The solution is heated up before being fed to column 2 through the heat transfer from the amines stream leaving the reboiler of the regeneration column with the aim of improving the desorption process. Rules of thumb reported in the literature are used to compute the energy involved in the heat exchanger using Eq. E.6, considering the corresponding values of qamine collected in Table E.3.

The operation of column 2 is also based on rules of thumb (2012gpsa; 2004gpsa) including the estimation of the energy consumption in the reboiler and the cooler refrigeration requirements. According to the literature, the inlet temperature to column 2, T_{Col2} , is equal to 93 °C, whereas the temperature of the outlet amines stream, T_{bottom} , is equal to 125 °C, while at the condenser, the temperature, T_{top} , is equal to 54 °C. Thus, the energy balances of the stream entering column 2 are described in Eq. E.5.

$$\begin{aligned} Q_{Cond} &= F_{Cond} \cdot q_{Cond,amine} \\ Q_{Reb} &= F_{Reb} \cdot q_{Reb,amine} \end{aligned} \quad (\text{E.5})$$

From the reboiler, the regenerated amine is cooled down heating up the feed to the column, Eq. E.6.

$$Q_{Cooling} = F_{Cooling} \cdot q_{Cooling,amine} \quad (\text{E.6})$$

The gas leaving the regeneration column is saturated with the amines aqueous solution, producing the losses of amines which have to be replaced before be recirculated to the absorption column. In order to calculate these losses, humidification models are used. First, the saturation pressure of the amine solution is calculated, Eq. E.7. Then, the specific humidity of the gaseous stream is computed to determine the amount of amines solution accompanying the CO₂ gaseous stream which leaves the regeneration column, Eq. E.8, where the operating pressure of the regeneration column, P_{Col2} , is equal to 1.7 bar (2004gpsa). As an approximation, it is assumed

that the amine solution behaves as water. The amount of amine lost with the sour gases is the one to be fed as fresh amine.

$$P_{\text{amines solution}} = \text{Exp} \left(A - \frac{B}{(C + T_{\text{top}})} \right) \quad (\text{E.7})$$

$$\gamma = \frac{MW_{Wa}}{MW_{\text{outlet gas}}} \cdot \frac{P_{\text{amines solution}}}{(P_{\text{Col2}} - P_{\text{amines solution}})} \quad (\text{E.8})$$

Three different amines are selected aiming a high selectivity, MEA, DEA, and MDEA. Table E.2 shows the parameters used in the amines absorption modelling for each amine considered (**2012gpsa**; **2004gpsa**).

Table E.2: Amine properties for CO₂ capture **2012gpsa**; **2004gpsa**.

	MEA	DEA	MDEA
Gas pickup (mol/mol _{amine})	0.35	0.35-0.65	0.2-0.55
Solution concentration (wt %)	20	35	45
Heat of reaction (BTU/lb CO ₂)	620-700	580-650	570-600
GPSA	0.35	0.50	0.38
Density	1.01	1.05	1.05
Cost (EUR/kg)	1.30	1.32	3.09
Molecular weight	61	105	119

Table E.3: Amine regeneration heat loads **2004gpsa**.

	Duty (BTU/hr)
Reboiler	72000 GPM
Condenser	30000 GPM
Amine feed to distillation	45000 GPM
Amine cooler	15000 GPM

The biomethane production model through amines scrubbing includes the units described in sections [8.3.2.1](#) and [E.2.1](#). The NLP problem consists of 288 equations and 953 variables per amine evaluated and is solved using a multistart initialization approach with CONOPT as the preferred solver where the main decision variable are the pressures temperatures and flow rates.

E.2.2 PSA

The stream of gases passes through the bed of zeolites and the carbon dioxide is captured by adsorption. The system consists of the compression train and the zeolite beds.

The adsorption capacity of the zeolites is directly related to the partial pressure of the CO₂. Therefore, a system of compressors with intermediate cooling is implemented to determine the optimal operating pressure. As it is described previously, the compressors are modelled assuming polytropic behavior, with a polytropic coefficient z of 1.4 and an efficiency of the compression stages of 0.85, Eq. E.10.

$$T_{out/compressor} = T_{in/compressor} + T_{in/compressor} \left(\left(\frac{P_{out/compressor}}{P_{in/compressor}} \right)^{\frac{z-1}{z}} - 1 \right) \frac{1}{\eta_c} \quad (\text{E.9})$$

$$W_{compressor} = (F) \cdot \frac{R \cdot z \cdot (T_{in/compressor})}{((Mw) \cdot (z-1))} \frac{1}{\eta_c} \left(\left(\frac{P_{out/compressor}}{P_{in/compressor}} \right)^{\frac{z-1}{z}} - 1 \right) \quad (\text{E.10})$$

The removal ratio is given by the breakthrough curve of the adsorbent bed. Based on experimental data (**hauchhum2014carbon**) for adsorption stages below 20 min, the CO₂ removal yield of the PSA system is assumed to be 98%, containing below 2% CO₂ at the outlet stream, (**ferella2017separation**). The mass balance at the bed is as shown in Eq. E.11.

CO₂ stream:

$$\begin{aligned} fc_{CO_2}|_{out} &= \eta fc_{CO_2}|_{in} \\ fc_{CH_4}|_{out} &= 0.02 \cdot fc_{CH_4}|_{in} \end{aligned} \quad (\text{E.11})$$

CH₄ stream:

$$\begin{aligned} fc_{CO_2}|_{out} &= (1 - \eta) fc_{CO_2}|_{in} \\ fc_{CH_4}|_{out} &= 0.98 \cdot fc_{CH_4}|_{in} \end{aligned}$$

To compute the mass of bed the adsorption capacity of the bed is evaluated. Based on experimental data, the Langmuir isotherm is the adsorption model considered for this process, Eq. E.12, since this is the one that best fits the performance of the zeolite 13X - CO₂ system (**hauchhum2014carbon**).

$$q = \frac{q_m \cdot K \cdot P_{CO_2}}{1 + K \cdot P_{CO_2}} \quad (\text{E.12})$$

Where the parameters q_m and K depend on the adsorbent material. Considering zeolite 13X, the effect of the operating temperature, within the range of 25 °C-60 °C, for both parameters can be correlated using data available in the literature, Eq. E.13a (**hauchhum2014carbon**).

$$\begin{aligned} q_m &= -3.15551 \cdot 10^{-2} T(\text{°C}) + 5.02915 \\ K &= (1.63070 \cdot 10^{-3} T(\text{°C}))^2 - 3.68662 \cdot 10^{-1} T(\text{°C}) + 27.3737 \end{aligned} \quad (\text{E.13a})$$

$$\begin{aligned} q_m &= -1.8235510^{-2} T(\text{°C}) + 3.72021 \\ K &= 1.6307010^{-3} T(\text{°C})^2 - 3.6866210^{-1} T(\text{°C}) + 27.3737 \end{aligned} \quad (\text{E.13b})$$

As result of the breakthrough curve for the zeolite 13X – carbon dioxide system, the operating time must be below 20 min so that the exit gas (methane) contains only traces of CO₂. Similarly, correlations are developed for zeolite 4A, Eq. E.13b. The operating time of zeolite 4A must be below 20 min (**hauchhum2014carbon**). Note that the expression for the computing of the constant K in the Langmuir correlation is the same for both adsorbents evaluated.

However, the adsorption capacity decays cycle after cycle until it stabilizes around 65% of the initial capacity computed by Eq. E.14 (**hauchhum2014carbon**). Therefore, a corrected value for q is applied to compute the amount of zeolite used in the PSA system, as it can be shown in Eq. 14, where the CO₂ removal yield of the PSA system, is assumed to be 98%, containing below 2% CO₂ at the outlet stream (**ferella2017separation**), and τ is equal to 20 min, based on the results of (**hauchhum2014carbon**). Furthermore, a lifetime of the zeolites bed of 5 years has been considered based on data reported by **Xiao2013**. Thus for the cost, we considered that over the 20 years life time of the plant, 5 beds will be used.

$$m_{\text{Zeolite}} = \frac{1}{q \cdot 0.65} \frac{f_{\text{CO}_2} \cdot 1000}{\text{MW}(\text{CO}_2)} \eta \cdot \tau \quad (\text{E.14})$$

In the case of the PSA system, the objective function is shown in Eq. E.15. To estimate the cost of the PSA system, Eq. E.16, it is assumed that the zeolite bed loses efficiency over time, resulting in a lifetime of 5 years before it needs to be replaced (**Xiao2013**). As the plant life is considered 20 years, the zeolites bed must be replaced 4 times during the plant life, N_{Cycle} .

$$\text{Profit} = \text{BioCH}_4 - \text{Cost}_{\text{Zeolite system}} \quad (\text{E.15})$$

$$\begin{aligned} \text{Cost}_{\text{Zeolite system}} = & \\ C_{\text{Electricity}} \cdot W_{\text{Compressor}} + \frac{1}{K} M_{\text{Zeolite}} \cdot C_{\text{Zeolite}} \cdot N_{\text{Cycle}} \end{aligned} \quad (\text{E.16})$$

The cost of the zeolites considered is 5 USD/kg for both zeolite 13 X and zeolite 4A (**Xiao2013**).

The production of biomethane through pressure swing adsorption includes the units described in sections [8.3.2.1](#) and [E.2.2](#) consisting of an NLP problem of 283 equations and 828 variables that is solved similarly as in the case of the selection of amines where the main decision variables are the operating pressure of the adsorption tower and the size of the bed.

E.2.3 Membranes

The membrane system considered is dual-stage membrane systems with single compression stage before the membrane system and no recompression stage between membrane units, have been deemed as the most economic under a wide range of feed compositions (**kim2017optimization**). The compressor is modelled as presented above, assuming polytropic compression of the gas, Eq. [E.10](#). Each membrane module is modelled using mass balances, considering the permeate and retentate streams, Eqs. [E.17](#) and [E.18](#), and the flux of the gases through the membrane, that is a function of the concentration gradient between both sides of the membrane, Eq. [E.20](#) (**FernandesRodriguesMsc**). The flux is the parameter which allows computing the area of the membrane, as it is shown in Eq. [E.19](#), based on the permeability of the membrane, Eq. [E.22](#). As the driving force in the membrane separation process is the concentration gradient, the removal of CO₂ results in a change in the composition of the stream along the membrane, leading to a change in the driving force which controls the process. Therefore, an average molar fraction between the feed and the retentate composition is used to compute the separation driving force, Eq. [E.21](#).

$$F_{\text{feed}} = F_{\text{permeate}} + F_{\text{retentate}} \quad (\text{E.17})$$

$$F_{\text{feed}} \cdot y_{i,\text{feed}} = F_{\text{permeate}} \cdot y_{i,\text{permeate}} + F_{\text{retentate}} \cdot y_{i,\text{retentate}}; i \in (\text{CO}_2, \text{CH}_4) \quad (\text{E.18})$$

$$J_i = \frac{F_{\text{permeate}} \cdot y_{i,\text{permeate}}}{A_{\text{membrane}}}; \quad i \in (CO_2, CH_4) \quad (\text{E.19})$$

$$J_i = \varepsilon_i [y_{\text{feedside}} \cdot P_{\text{feed}} - y_{i,\text{permeate}} \cdot P_{\text{Permeate}}]; \quad i \in (CO_2, CH_4) \quad (\text{E.20})$$

$$y_{\text{feedside}} = \frac{y_{i,\text{feed}} - y_{i,\text{retentate}}}{\ln \left(\frac{y_{i,\text{feed}}}{y_{i,\text{retentate}}} \right)}; \quad i \in (CO_2, CH_4) \quad (\text{E.21})$$

$$\varepsilon_i = \frac{Perm_i}{\delta}; \quad i \in (CO_2, CH_4) \quad (\text{E.22})$$

Where δ is the membrane thickness, and $Perm_i$ the permeability of the component i . The usual membrane thickness for industrial units is equal to 30 nm. Three different membrane materials are selected aiming a large CO_2 permeability, low methane permeability, and therefore, high selectivity; cellulose acetate, polyamide, and polycarbonate. Table E.4 shows the permeabilities for each membrane material considered in the model at 25 °C (**vrbova2017upgrading**). The solution of the optimization problem will yield intermediate conditions to assure natural gas composition of the biomethane.

Table E.4: Gases permeability **vrbova2017upgrading**.

Permeability (Barrer)		
Polymer	CH ₄	CO ₂
Cellulose acetate	0.21	6.30
Polycarbonate	0.13	4.23
Polyimide	0.25	10.7

Finally, the simplified profit objective function for the membrane separation system, Eq. E.23, considers cost of the gas compression and the amortization of the investment costs of the membranes, Eq. E.24.

$$Profit = BioCH_4 - Cost_{\text{Membrane system}} \quad (\text{E.23})$$

$$Cost_{Membrane\ system} = \quad (E.24)$$

$$C_{Electricity} \cdot W_{Compressor} + \frac{1}{K} \cdot C_{Membrane} \cdot \frac{1}{L_f} \cdot N_{Membranes} \left(\sum_{i \in stages} Area_i \right)$$

A value of 50 USD/m² will be used based on the literature (**kim2017optimization**). Considering the plant life equal to 20 years, the membranes with a typical lifetime of 4 years must be replaced 5 times during the plant life, $N_{Membranes}$ (**scholz2015structural**).

The biogas production and upgrading considering a membranes separation system is formulated as an NLP problem considering the units described in sections [8.3.2.1](#) and [E.2.3](#) consisting of 299 equations and 869 variables for each material evaluated where the major decision variables are the flows, operating pressures, temperatures and the area required by the membrane units.

E.3 ECONOMIC EVALUATION

The evaluation of the cost for biomethane production is also estimated from different wastes. The production and investment costs are estimated. The CAPEX, or investment cost, is estimated based on **towler2009chemical** that presents a factorial method. This method estimates the CAPEX usinf as reference the cost of all the major units of the flowsheet.

The sizing of all the units involved in the flowsheet, see Figure 2, is carried out following the method presented in **martin2011energy**, and updated by **almena2016technoeconomic**. However, the following considerations for some specific units have been assumed:

- For the digester cost, assumed to be 365 EUR/m³ (**taifouris2018multiscale**).
- The cost estimation of the columns for the amines is carried out using the rules reported in **2012gpsa**. The diameter for the amine contactor can be estimated as given in Eq. [E.25](#).

$$D_C = 44 \sqrt{\frac{F_{gas} (\text{MMscfd})}{P (\text{psia})}} \quad (E.25)$$

While the diameter of the regenerator column can be estimated as given in Eq. [E.26](#).

$$D_R = 3.0\sqrt{F_{amine}(\text{gal/min})} \quad (\text{E.26})$$

We use the same factors as presented in **davis2014optimala** to estimate the investment, CAPEX, of the facility for further comparison with other renewable based methane production processes. The costs for piping, isolation, instrumentation, and utilities infrastructure are estimated with respect to the equipment cost as 20%, 15%, 20% and 10% of its value respectively. Land and buildings costs are estimated to be 8 M EUR. These items add up to the fixed cost. The fees represent 1% of the fixed cost, other administrative expenses and overheads, and the plant layout represent 10% of the direct costs (fees plus fixed capital) and 5% of the fixed cost, respectively. Finally, the plant start-up cost represents 5% of the investment.

Furthermore, the production costs of biomethane are estimated using also the factorial method with the coefficients presented and validated in **davis2014optimala**. For the average annual cost, the labour costs (0.5% of investment), equipment maintenance and raw materials (1% of fix costs), amortization (linear with time in 20 years), taxes (0.5% of investment), overheads (1% of investment), and administration (5% of labour, equipment maintenance, amortization, taxes and overheads) are considered. The utilities, particularly cooling water, power, and steam, are taken from the mass and energy balances performed in the superstructure model. Heat integration is carried out to reduce the utilities consumption. The cost of electricity is 0.06 EUR/kWh. The hot compressed gas is used to evaporate the water and ammonia to prepare the digestate to be sold as fertilizer. However, the credit for the digestate to be used as fertilizer is difficult to be estimated. It depends on the market that typically is saturated. Although the cost is around 0.48 EUR/kg, only a fraction is typically obtained. To be conservative, a value of one third of this one is assumed to calculate the benefits received by the sold of the digestate produced (**leon2016optimal**). In addition, the cost of the digestate for the methane to be competitive with other resources, targeting 5 EUR/MMBTU (0.17 EUR/Nm³), is computed.

E.4 SCALING-UP STUDY

The scaling-up study, based on the previous work of **sanchez2018scale**, is performed in the following stages. Firstly, the capital cost of the different units is correlated as a function of a design variable, such as the membrane area for membranes systems or the column sizes in function of the flow processed. This variable will be denoted as scaling variable. The scaling variable of each equipment is directly related to the processing capacity

of the facility studied through the mass or energy flows involved in that particular unit. The limitations in the size of equipment are considered in the scaling-up study. When an equipment excess the size defined by the rules of thumb, that unit is duplicated, affecting to the cost estimation. In a second stage, after defined the scaling variables for all units and the relation between these units, the mass and energy flows and the processing capacity of the facility, different capacities are evaluated, calculating the mas and energy balances, and estimating the sizes of the equipment, and the number of units in case some equipment needs to be duplicated. In a third stage, the capital and operating costs are estimated considering the equipment sizes and number of unit of each equipment using the factorial method presented in **towler2009chemical** and the estimation of the unit costs presented in **almena2016technoeconomic**.

BIBLIOGRAPHY